Winter 12-22-2009

Sensorimotor Integration an a Small Motor Circuit

Nicholas D. DeLong
University of Pennsylvania, ndelong@mail.med.upenn.edu

Sensorimotor Integration an a Small Motor Circuit

Abstract
Rhythmic motor patterns, which underlie behaviors such as mastication, respiration and locomotion, are generated by specialized neural circuits called central pattern generators (CPGs). Although CPGs can generate their rhythmic motor output in the absence of rhythmic input, these motor patterns are modified by rhythmic sensory feedback in vivo. Furthermore, although the importance of sensory feedback in shaping CPG output is well known, most systems lack the experimental access needed to elucidate the mechanisms underlying sensorimotor integration at the cellular and synaptic level. I am therefore examining this issue using the gastric mill CPG, a circuit which generates the rhythmic retraction and protraction motor activity that drives chewing by the teeth in the gastric mill compartment of the crustacean stomach. The gastric mill CPG is well defined and very accessible at the cellular level. Specifically, I am examining the mechanism by which the gastropyloric receptor (GPR), a phasically active proprioceptor, selectively prolongs one phase (retraction) of the gastric mill rhythm in the isolated nervous system when it is activated in a pattern that mimics its in vivo activity. I first demonstrate that GPR regulation of the gastric mill rhythm relies on its presynaptic inhibition of modulatory commissural neuron 1 (MCN1), a projection neuron that activates and drives this rhythm. I also demonstrate that the GPR inhibition of MCN1 regulates the gastric mill rhythm by selectively regulating peptidergic cotransmission by MCN1. Lastly, I demonstrate that a peptide hormone (crustacean cardioactive peptide) that only modestly modifies the gastric mill rhythm, strongly gates the GPR regulation of this rhythm. Mechanistically, it acts not by influencing GPR or MCN1, but by activating the same excitatory current in the CPG neuron LG (lateral gastric) that is activated by MCN1-released peptide. This novel gating mechanism reduces GPR control over the amplitude of this excitatory current in LG. Thus, I have identified specific cellular mechanisms by which (a) phase-specific regulation of an ongoing motor pattern by a sensory input is accomplished, and (b) hormonal modulation gates that sensory input. These events are likely to reflect comparable ones occurring in the larger and less accessible vertebrate CNS.

Degree Type
Dissertation

Degree Name
Doctor of Philosophy (PhD)

Graduate Group
Neuroscience

First Advisor
Michael Nusbaum

Keywords
Neuromodulation, Sensory, Motor, Invertebrate, Central Pattern Generator, CPG

Subject Categories
Systems Neuroscience

SENSORIMOTOR INTEGRATION IN A SMALL MOTOR CIRCUIT

Nicholas David DeLong

A DISSERTATION

in

Neuroscience

Presented to the Faculties of the University of Pennsylvania

in

Partial Fulfillment of the Requirements for the Degree of

Doctor of Philosophy

2009

Michael P. Nusbaum, Ph. D.
Supervisor of Dissertation

Rita Balice-Gordon, Ph. D.
Graduate Group Chair

Dissertation Committee:
Marc Schmidt, Ph. D. (Committee Chair)
Joshua Gold, Ph. D.
Diego Contreras, Ph. D.
Farzan Nadim, Ph. D. (Rutgers University, Dept. of Biology)

Acknowledgements

The years I have spent completing this thesis work could not have been possible without a lot of help and support from a lot of people. I am very thankful to all of them.

Mikey: It has been a privilege to work with you. You taught me an incredible amount about science, writing, communication, presentation, problem solving and a lot of other things I'm probably not even aware of. I know that I could not have gotten that education anywhere else.

The Nusbaum Lab: Thanks Aaron, for talking science, movies, politics and stand-up comedy with me for the past 6 years. Dawn, for always being there to answer my questions about anything and everything. Rachel and Jason, for making the whole experience of grad school a lot more fun, and always being there to share a beer (or 3) at SFN and NerveNet.

My Family: Mom and Dad, I can't thank you enough for the amazing support over the last six years. There is simply no possible way I could have done it without you. Sue and Holly, for encouraging me to do well since I was too young to remember, and for never calling me a nerd (wait, forget that last part).

Madelyn: For always making me smile, no matter what, and for always being proud of her daddy.

Sara: For making me happy and keeping me sane for the last few years, and for never complaining when I show up late for dinner. I am truly lucky to have you.

Abstract

SENSORIMOTOR INTEGRATION IN A SMALL MOTOR CIRCUIT

Nicholas D. DeLong

Advisor: Michael P. Nusbaum, Ph. D.

Rhythmic motor patterns, which underlie behaviors such as mastication, respiration and locomotion, are generated by specialized neural circuits called central pattern generators (CPGs). Although CPGs can generate their rhythmic motor output in the absence of rhythmic input, these motor patterns are modified by rhythmic sensory feedback *in vivo*. Furthermore, although the importance of sensory feedback in shaping CPG output is well known, most systems lack the experimental access needed to elucidate the mechanisms underlying sensorimotor integration at the cellular and synaptic level. I am therefore examining this issue using the gastric mill CPG, a circuit which generates the rhythmic retraction and protraction motor activity that drives chewing by the teeth in the gastric mill compartment of the crustacean stomach. The gastric mill CPG is well defined and very accessible at the cellular level. Specifically, I am examining the mechanism by which the gastropyloric receptor (GPR), a phasically active proprioceptor, selectively prolongs one phase (retraction) of the gastric mill rhythm in the isolated nervous system when it is activated in a pattern that mimics its *in vivo* activity. I first demonstrate that GPR regulation of the

gastric mill rhythm relies on its presynaptic inhibition of modulatory commissural neuron 1 (MCN1), a projection neuron that activates and drives this rhythm. I also demonstrate that the GPR inhibition of MCN1 regulates the gastric mill rhythm by selectively regulating peptidergic cotransmission by MCN1. Lastly, I demonstrate that a peptide hormone (crustacean cardioactive peptide) that only modestly modifies the gastric mill rhythm, strongly gates the GPR regulation of this rhythm. Mechanistically, it acts not by influencing GPR or MCN1, but by activating the same excitatory current in the CPG neuron LG (lateral gastric) that is activated by MCN1-released peptide. This novel gating mechanism reduces GPR control over the amplitude of this excitatory current in LG. Thus, I have identified specific cellular mechanisms by which (a) phase-specific regulation of an ongoing motor pattern by a sensory input is accomplished, and (b) hormonal modulation gates that sensory input. These events are likely to reflect comparable ones occurring in the larger and less accessible vertebrate CNS.

TABLE OF CONTENTS

LIST OF TABLES

Chapter 3:

Chapter 5:

LIST OF FIGURES

Chapter 1:

Chapter 2:

Chapter 1

Introduction

The overall goal of my thesis is to elucidate the cellular mechanisms by which rhythmically active motor circuits are regulated by sensory feedback. Sensory feedback plays a key role in the expression of motor patterns, including its initiation, termination and the regulation of its ongoing timing and pattern (Di Prisco et al., 2000; Perrins et al., 2002; Beenhakker et al., 2004; Blitz et al., 2004; Yakovenko et al., 2005; Rossignol et al., 2006; Buschges et al., 2008; Pearson, 2008). Some insight has been gained regarding the functional impact of sensory feedback onto vertebrate motor circuits, such as those underlying locomotion (Yakovenko et al., 2005; Rossignol et al., 2006; Pearson, 2008), but in such systems the limited access to a cellular-level analysis has precluded a detailed understanding of the cellular mechanisms underlying sensorimotor integration.

I am therefore investigating the cellular basis of sensorimotor integration in a small motor system, the stomatogastric nervous system (STNS) of decapod crustaceans, where analysis at the cellular level is feasible. The STNS is an extension of the crustacean central nervous system (CNS) which generates a set of feeding-related motor patterns (Marder and Bucher, 2007). It includes four ganglia plus their connecting and peripheral nerves (Fig. 1). The ganglia are the paired commissural ganglia (CoGs), oesophageal ganglion (OG) and stomatogastric ganglion (STG).

My thesis focuses on the gastric mill rhythm in the Jonah crab, *Cancer borealis*. The gastric mill rhythm is a rhythmically active motor pattern which underlies the rhythmic movement of the paired lateral teeth and unpaired medial tooth during chewing. The teeth are located in the gastric mill stomach compartment. Chewing in the gastric mill is a biphasic, rhythmic repeating movement consisting of alternating protraction and retraction of the lateral and medial teeth (Turrigiano and Heinzel, 1992; Heinzel et al., 1993).

The gastric mill circuit is located in the STG. This circuit is a central pattern generator (CPG), meaning that the basic rhythmic motor pattern that it generates can be elicited in isolated, reduced preparations that include only the regions of the CNS that contain the relevant circuit elements (see below) (Marder and Bucher, 2001; Marder et al., 2005). In the case of the gastric mill rhythm, the basic motor pattern can be readily elicited in the completely isolated STNS, and in the even more reduced preparation in which the CoGs are removed (Coleman and Nusbaum, 1994; Coleman et al., 1995). The core CPG circuit that generates this rhythm is well-documented (Coleman and Nusbaum, 1994; Coleman et al., 1995; Beenhakker et al., 2004; Saideman et al., 2007b). Additionally, several identified sensory systems innervate the gastric mill circuit (Simmers and Moulins, 1988; Katz et al., 1989; Beenhakker et al., 2004). I have therefore taken advantage of the unique toolset available in this system to (1) elucidate features of the gastric mill circuit which influence its ability to be regulated by sensory feedback, and (2) characterize the cellular mechanisms by which a

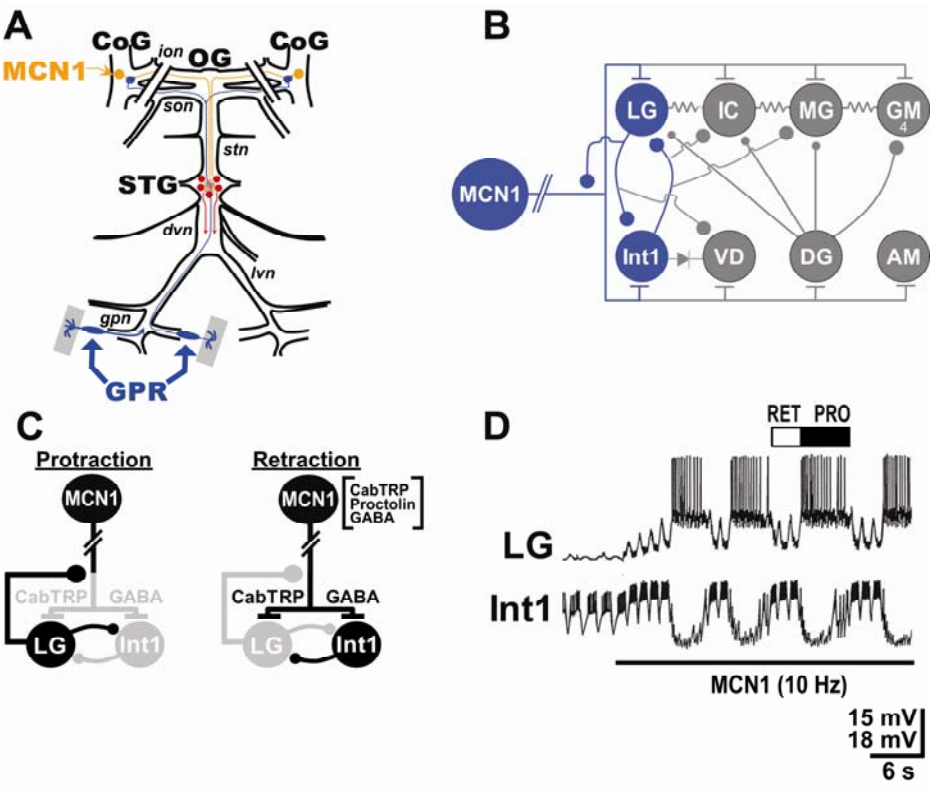

Figure 1. Schematic of the isolated STNS and the MCN1-elicited gastric mill rhythm. **(A)** In each CoG, there is a single copy of the projection neuron MCN1. MCN1 projects to the STG via the *ion* and *stn* nerves. Each GPR arborizes in the STG and each CoG. The paired diagonal bars through the *sons* and *ions* represent the transection of these nerves at the start of each experiment. Grey rectangles represent protractor muscles in which GPR dendrites arborize. Abbreviations: Ganglia: CoG, commissural ganglion; OG, oesophageal ganglion; STG, stomatogastric ganglion; Neurons: GPR, gastropyloric receptor; MCN1, modulatory commissural neuron 1; Nerves: *dvn*, dorsal ventricular nerve; *gpn*, gastropyloric n.; *ion*, inferior oesophageal n.; *lvn*, lateral ventricular n.; *son*, superior oesophageal n.; *stn*, stomatogastric n. **(B)** Gastric mill neurons and

their synaptic connections. Gray circles represent follower motor neurons, while blue circles represent neurons in the CPG. For synapses, filled circles represent synaptic inhibition, while T-bars represent synaptic excitation. Jagged lines connecting two neurons represent electrical coupling, and the directional line connecting Int1 and VD represents a rectifying (uni-directional) gap junction. **(C)** Core gastric mill CPG schematic during each phase (protraction, retraction) of the gastric mill rhythm. Paired diagonal bars through MCN1 axon represent additional distance between CoG and STG. All synapses shown are located in the STG neuropil. Gray somata and synapses represent silent neurons/synapses. Synapses drawn on somata or axons actually occur on small branches in the STG neuropil. Neurotransmitters listed in brackets next to MCN1 are the identified MCN1 cotransmitters. Note that MCN1 uses only CabTRP Ia to excite LG and only GABA to excite Int1. Symbols: Filled circles, synaptic inhibition; T-bars, synaptic excitation. Abbreviations: Neurons: Int1, interneuron 1; LG, lateral gastric. **(D)** The gastric mill rhythm elicited by tonic MCN1 stimulation. Before MCN1 activation, there is no gastric mill rhythm but there is a pyloric rhythm. At this time, Int1 is spontaneously active and exhibits a pyloric rhythm-timed pattern, while LG is silent. During MCN1 stimulation, LG (protraction: PRO) and Int1 (retraction: RET) burst in alternation. At the start of MCN1 stimulation, the retractor phase was initiated with a fast increase in Int1 activity while LG slowly depolarized. When LG reached burst threshold, it inhibited Int1 (and MCN1) and protraction commenced.

particular proprioceptor (the gastro-pyloric receptor, GPR) regulates gastric mill circuit output.

It is important to note that, in contrast to the work in several larger motor systems, the behavioral correlates of the gastric mill rhythm are not as carefully studied (Fleischer, 1981; Heinzel, 1988; Turrigiano and Heinzel, 1992; Heinzel et al., 1993). Historically, as well as in my thesis work, the STNS has not been used to study the particular behaviors it generates. Instead, similar to the way in which computational models are often used, this work seeks to understand the low-level mechanisms by which neurons can interact to generate network output in a real biological circuit. The ultimate goal is not to understand the gastric mill rhythm *per se*. Instead, the goal is to obtain a generalizable understanding of the network dynamics that can underlie sensorimotor integration, in much the same way as this system has historically been used to generate insights about other aspects of motor network operation (Nusbaum and Beenhakker, 2002; Marder and Bucher, 2007).

Central pattern generators

Central pattern generators (CPGs) are neural circuits that generate the neuronal activity patterns underlying most or all rhythmic movements, such as respiration, locomotion and mastication. The most essential feature common to all CPGs is that they generate rhythmic motor output in the absence of any rhythmic input (Marder and Calabrese, 1996; Marder and Bucher, 2001).

Therefore, all CPGs share the attribute that they can continue to generate their rhythmic output even when separated from the surrounding nervous system (Nusbaum and Beenhakker, 2002). For this reason, CPGs provide a convenient experimental subject for understanding neuronal network dynamics at the cellular and synaptic level. This convenience includes, in part, the fact that these circuits can be studied in an isolated preparation, dissected from the animal and pinned down in a Petri dish (Feldman and Gray, 2000; Marder and Bucher, 2001; Wenning et al., 2004; Kristan et al., 2005; Masino and Fetcho, 2005). Beyond convenience, CPGs represent an interesting and compelling model for neuronal networks in general, since many of them are based at least partly on the same set of basic principles and organizational schemes (Marder and Bucher, 2001; Nusbaum and Beenhakker, 2002).

The most basic requirement of any CPG is that it must produce a rhythmic output pattern consisting of multiple repeating network states, or phases. There are two basic mechanisms by which such rhythmicity can arise within a CPG. First, rhythmicity can be inherent in a single neuron or neuronal population within the circuit. Such neurons are called intrinsic or endogenous oscillators (Marder and Bucher, 2001). In the simplest version of this organizational scheme, only one neuron (or homogeneous population) is responsible for the actual generation of rhythmicity, and the control over the timing of each phase originates from the presence of membrane properties in the intrinsic oscillator and its synaptic outputs to the other circuit neurons (Harris-Warrick, 2002; Ramirez et al., 2004;

Doi and Ramirez, 2008). Alternatively, rhythmic CPG output can be produced by a so-called network oscillator, in which rhythmicity originates as an emergent property of synaptic interactions and intrinsic properties of the component neurons in the circuit, none of which are endogenous oscillators, rather than from the properties of any one neuron or class of neurons (Marder and Calabrese, 1996; Marder and Bucher, 2001; Kristan et al., 2005; Kiehn, 2006; Pirtle and Satterlie, 2006; Marder and Bucher, 2007) .

The gastric mill CPG, on which my thesis focuses, is an example of a network oscillator. None of the gastric mill CPG neurons are intrinsically rhythmic. Instead, the rhythmic, repeating alternation between the two gastric mill phases (protraction, retraction) originates from the synaptic interactions between CPG neurons. In the crab *C. borealis*, the core CPG for the gastric mill rhythm is composed of three different neurons (Coleman et al., 1995; Bartos et al., 1999) (see below).

Another basic feature of CPGs is their flexibility in response to modulation. Hormones, neurally released peptides and amines, as well as other substances can activate or modulate the synaptic and intrinsic membrane properties in CPG neurons, thereby modifying CPG output (Marder and Calabrese, 1996; Dickinson, 2006). Such modulation can allow the generation of distinct versions of a motor pattern by the same CPG. For example, in the mammalian respiratory system, substance P modulates the frequency and magnitude of rhythmic output by pacemaker neurons (Pena and Ramirez, 2004). In the same system, varying

oxygen levels can lead to the generation of two distinct motor patters – normal breathing and gasping – by the same motor circuit, apparently by modulating a persistent sodium current (Feldman and Gray, 2000; Paton et al., 2006). Similarly, in *Aplysia*, application of dopamine to the isolated ganglia containing the feeding CPG produced synchrony in a pair of bilaterally symmetrical, normally asynchronous motor neurons (Serrano and Miller, 2006), demonstrating a potential role for modulation in facilitating the coordination of CPG output.

Similarly, there are numerous examples of neuromodulation in the STNS (Marder and Calabrese, 1996; Nusbaum and Beenhakker, 2002; Dickinson, 2006; Marder and Bucher, 2007). In addition to several cases in which modulation allows a single CPG to produce multiple distinct outputs, the gastric mill CPG provides an example of the alternative role for neuromodulation of enabling similar motor patterns to be produced by distinct circuit mechanisms (Prinz et al., 2004; Saideman et al., 2007b). Until recently, each of the identified methods for eliciting the gastric mill rhythm in the crab included activating modulatory commissural neuron 1 (MCN1), a projection neuron that innervates the gastric mill CPG (Coleman et al., 1995; Beenhakker et al., 2004; Blitz et al., 2004; Blitz et al., 2008). However, there is also a version of the gastric mill rhythm that is elicited by bath applying the neuropeptide *Cancer borealis* pyrokinin peptide (CabPK) (Saideman et al., 2007a; Saideman et al., 2007b). MCN1 does not contain CabPK, nor is its activity necessary for the CabPK-activated gastric mill rhythm. The CabPK-elicited gastric mill rhythm is very

similar to the MCN1-elicited rhythm, but it is generated by a distinct circuit (Saideman et al., 2007b). Although the utility of generating the same rhythm via distinct mechanisms is unknown, one possibility is that the modified circuit dynamics which underlie the generation of this version of the gastric mill rhythm might allow it to be differently regulated by modulatory or sensory inputs. This possibility, in fact, is addressed in a related context in Chapter 6 of this Thesis.

Sensorimotor integration in CPGs

As the ability to produce rhythmic motor output in isolation is an essential feature of CPGs, rhythmic motor circuits are commonly studied in isolated preparations to achieve an understanding of the cellular and synaptic mechanisms underlying rhythm generation (Feldman and Gray, 2000; Nusbaum and Beenhakker, 2002; Wenning et al., 2004; Kristan et al., 2005; Marder et al., 2005; Masino and Fetcho, 2005; Grillner, 2006; Marder and Bucher, 2007; Doi and Ramirez, 2008). Indeed, in the STNS and other systems, this approach has yielded an abundance of cellular-level insights in the basic operation of CPGs, as well as the mechanisms by which their activity is modulated (see above). One drawback of this approach, however, is that studying CPGs in isolation explicitly removes sensory feedback. As a result, although sensory feedback is essential for shaping and coordinating CPG output (Buschges and El Manira, 1998; Pearson, 2004; Buschges, 2005; Rossignol et al., 2006), information regarding the cellular and synaptic mechanisms by which sensory feedback regulates CPG

output has lagged relative to our understanding the mechanisms underlying the basic generation of rhythmic motor activity.

Although a cellular-level understanding of how sensory systems influence CPGs is often unavailable, some insight has been gained into the functional roles of sensory input from studying CPGs *in vivo* or in semi-intact preparations. One such role is the initiation of motor pattern generation. In this scenario, a sensory input provides a mechanism for activating a CPG and thereby eliciting an appropriate behavior in response to some environmental stimulus. One well-known example of this role of sensory input is the escape swimming system in fish and leech, where auditory or mechanosensory neurons can elicit the escape swimming motor pattern (Korn and Faber, 2005; Kristan et al., 2005; Douglass et al., 2008). Similarly, in the gastric mill system, activation of a class of mechanoreceptors in the stomach wall, presumably in response to pressure exerted by food in the stomach, triggers the gastric mill rhythm to generate chewing behavior in the gastric mill stomach compartment (Beenhakker et al., 2004).

A key role for sensory feedback is to regulate the speed, timing and transition between phases of a motor pattern in response to feedback from the periphery. In this scenario, sensory systems such as proprioceptors enable modification of rhythmic motor output by a CPG in response to the position of muscles and/or limbs. For example, the locomotor CPG for the hindlimbs of spinal-transected or decerebrate cats can still adapt the speed of walking in

response to changing treadmill speed. This regulation of the locomotor CPG appears to rely on proprioceptors which sense hip flexion, as well as tendon organs which report ankle position (Pearson, 2004).

Sensory feedback can also facilitate the coordination between multiple CPG components, such as those controlling multiple body segments, or multiple segments of a jointed limb. For example, in the stick insect, which has a multi-jointed leg, individual CPGs control the rhythmic movement of each leg joint and can be active independently. Coordinated movement of the joints to produce walking is accomplished by sensory feedback to each individual CPG from muscle stretch organs as well as load sensors in the cuticle (Buschges, 2005). Similarly, in the leech, coordinated rhythmic movements of multiple body segments during swimming are facilitated by proprioceptor feedback (Yu et al., 1999; Kristan et al., 2005).

Sensory feedback thus has diverse roles in regulating CPG output. Although several of these roles are well understood at the level of functional output and behavior, a number of technical and experimental limitations have prevented the elucidation of the low-level mechanisms underlying the integration of sensory input in many systems. I have therefore used the gastric mill CPG, a small motor system with a number of distinct experimental advantages (see below) to examine this issue at the cellular level.

The gastric mill CPG

The gastric mill rhythm is a two-phase motor pattern which underlies the protraction and retraction of the teeth in the gastric mill stomach compartment. My thesis work has focused on studying this rhythm in an isolated preparation in which the STNS is dissected from the animal, including the muscles it innervates and the rest of the CNS, and pinned down in a Petri dish superfused with physiological saline (Marder and Bucher, 2007). All the neurons in the gastric mill circuit of *C. borealis* are physiologically identified, including those in the CPG and all follower motor neurons. This includes identification of the transmitters used by each neuron, their synaptic interactions and many of their intrinsic membrane properties. There are also several identified projection neurons and sensory systems which influence the gastric mill circuit.

The gastric mill system has several experimental advantages as a model system for understanding comparable events in the larger and less accessible vertebrate CPGs. For example, unlike most vertebrate CPGs which are composed of interneurons that drive motor neurons, all but one of the neurons in the gastric mill circuit are also motor neurons (Nusbaum and Beenhakker, 2002), simplifying the understanding of the circuit. In addition, all the gastric mill CPG neurons, as well as most follower motor neurons, occur as single copies. Thus, manipulating the activity of any specific circuit element is sufficient for understanding its role in motor pattern generation. Even those that exist as multiple copies occur as small populations (2-4). The entire gastric mill circuit consists of only ~15 neurons in total.

Another experimental advantage of this system is the fact that all CPG neurons are located within a single ganglion, which contains only 26 neurons in total (Kilman and Marder, 1996). In contrast, the vertebrate locomotor CPG consists of neurons which occur in large copy numbers, are distributed throughout the spinal cord and brainstem, and are interspersed with a large number of neurons that are not involved in locomotion (Kiehn, 2006). As a result, simultaneous intracellular recording and manipulation of multiple CPG neurons in the gastric mill CPG is routine, whereas it is often technically challenging or not feasible in other systems.

As a result of the above experimental advantages, considerable information is available regarding the neurons, synapses and intrinsic membrane properties underlying gastric mill rhythm generation (Fig. 1B) (Coleman et al., 1995; Marder et al., 1998; Nadim et al., 1998; Bartos et al., 1999; Beenhakker et al., 2005; DeLong et al., 2009). Multiple pathways and mechanisms for eliciting different versions of the gastric mill rhythm in this isolated preparation have been identified (Coleman et al., 1995; Beenhakker et al., 2004; Blitz et al., 2004; Saideman et al., 2007b; Blitz et al., 2008), but in my work the rhythm was always elicited by the tonic activation of modulatory commissural neuron 1 (MCN1) in preparations that excluded the CoGs.

The CPG for the MCN1-elicited version of the gastric mill rhythm consists of the reciprocally inhibitory lateral gastric (LG) protractor neuron and interneuron 1 (Int1), which is active during retraction, plus the STG axon terminals of MCN1

($MCN1_{STG}$) (Coleman et al., 1995) (Fig. 1C). In the absence of MCN1 activity, Int1 is active and LG is silent (Fig. 1D). During the gastric mill rhythm, MCN1 is tonically active and excites Int1 via a fast, ionotropic GABAergic synapse and excites LG via a slow, peptidergic (CabTRP Ia) synapse (Coleman et al., 1995; Wood and Nusbaum, 2002; Stein et al., 2007). During the gastric mill retractor phase (LG silent, Int1 active), MCN1 releases its cotransmitters to excite LG and Int1. Its slow excitation of LG enables LG to slowly overcome Int1 inhibition and fire a burst (Coleman et al., 1995; Beenhakker et al., 2005; Stein et al., 2007). During the protractor phase (LG active, Int1 silent), LG directly inhibits Int1 and its presynaptic inhibition of $MCN1_{STG}$ weakens CabTRP Ia release from MCN1, causing the excitation of LG to decay until the LG burst terminates and the next retractor phase commences (Coleman et al., 1995; Beenhakker et al., 2005; DeLong et al., 2009).

The STNS also contains several identified sensory systems which influence the gastric mill neurons (Simmers and Moulins, 1988; Katz et al., 1989; Beenhakker et al., 2004). Among these is the anterior gastric receptor (AGR), a muscle tendon receptor which influences gastric mill output via its actions in the CoGs, a pair of ganglia in the STNS which contain projection neurons that innervate the STG and drive gastric mill output. As mentioned above, a population of mechanoreceptors known as the ventral cardiac neurons (VCNs) are also identified. VCN activation triggers the gastric mill rhythm by activating two projection neurons (MCN1, CPN2) in the CoGs, presumably in response to

the presence of food in the stomach.

My thesis focuses largely on the gastropyloric receptor (GPR) neuron, a muscle stretch receptor that innervates a gastric mill protractor muscle which is stretched during the gastric mill retractor phase (Katz et al., 1989) (Fig. 2). GPR therefore is likely to be rhythmically active during the gastric mill rhythm *in vivo*, providing proprioceptor feedback to the gastric mill CPG. Much of my thesis work focuses on the consequences of this feedback, as well as the mechanisms by which it is integrated into gastric mill output.

As a result of the extensive knowledge available regarding the cellular and synaptic mechanisms underlying generation of the MCN1-elicited gastric mill rhythm, this system offers a unique experimental toolset not available in most other systems. For example, previous experimental insights were used to construct computational models which simulate various aspects of CPG dynamics (Marder et al., 1998; Manor et al., 1999; Beenhakker et al., 2005; Kintos et al., 2008). These models provided new insights into how this system operations, making predictions that were subsequently confirmed in the biological systems (Bartos et al., 1999; Beenhakker et al., 2005).

Building on these models, I have created models which include sensory input to the gastric mill circuit. Furthermore, I have tested the predictions of these models using the dynamic clamp, a technique originally developed in the STNS (Sharp et al., 1993). Using this technique, simulated versions of synaptic or intrinsic conductances that have produced a particular result in a model can be

injected into real biological neurons. Using this powerful combination of modeling and the dynamic clamp has yielded invaluable insight into the operation of the gastric mill system (Nadim et al., 1998; Bartos et al., 1999; Beenhakker et al., 2005).

Sensorimotor integration in a small motor circuit

Given the importance of sensory feedback in CPG systems, as well as the generally limited knowledge regarding the specific cellular and synaptic mechanisms which mediate sensorimotor integration in such systems, the primary goal of my thesis work has been to take advantage of the toolset available in the gastric mill CPG to expand on what is already known about sensorimotor integration into rhythmic motor output. The majority of my thesis work has focused on the mechanism by which GPR regulates the gastric mill rhythm. However, two of my thesis chapters do not directly relate to GPR, but instead elucidate features of the gastric mill circuit which influence its ability to be regulated by GPR, as well as other sensory inputs. For example, Chapter 2 examines the nature of the cotransmitter mechanisms used by MCN1 to activate and maintain the gastric mill rhythm. The divergent nature of this cotransmission turns out to be pivotal to the mechanism by which GPR regulates gastric mill output (Chapter 4). Similarly, Chapter 5 illustrates a novel mechanism by which a peptide hormone modulates the gastric mill rhythm, while Chapter 6 investigates how this same hormone-mediated mechanism modulates GPR input to the

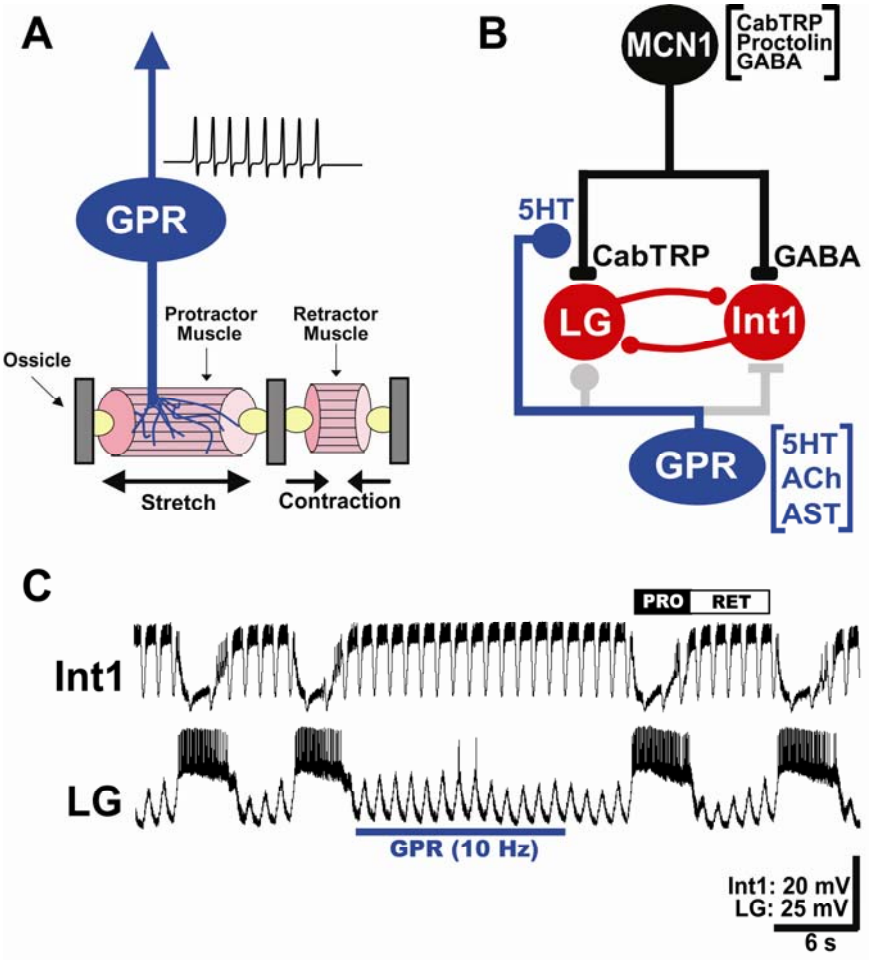

Figure 2: The gastropyloric receptor (GPR) is a muscle stretch receptor neuron which regulates the gastric mill rhythm. **(A)** GPR is activated during the gastric mill retractor phase by stretch of the protractor muscle in which its dendrites are embedded. The protractor muscle does not contract during the retractor phase. Instead, this muscle is stretched during retraction due to the contraction of the retractor muscle which shares an attachment point (ossicle) with the protractor muscle. This muscle stretch activates GPR spiking (Katz et al., 1989). **(B)** As shown in this thesis, GPR regulates the MCN1-elicited gastric mill rhythm by selectively inhibiting peptidergic transmission from MCN1 in the STG, via

serotonergic presynaptic inhibition. The GPR synapses onto on LG and Int1 are shown in gray because their actions are gated out during this gastric mill rhythm, as also shown in this thesis. Transmitters in brackets next to the GPR soma are the identified GPR cotransmitters. Symbols: Filled circles, synaptic inhibition; T-bars, synaptic excitation. **(C)** GPR activation during retraction (to mimic its *in vivo* activity) selectively prolongs the gastric mill retractor phase. Note that the duration of the retractor (LG silent, Int1 active) phase during GPR stimulation is longer than the same phase in the cycles immediately before or after GPR stimulation.

gastric mill CPG.

Cotransmission is a common feature of many neural circuits (Nusbaum et al., 2001; Seal and Edwards, 2006). Cotransmitter mechanisms may be convergent, with co-released transmitters converging onto the same neuron, or divergent, with different cotransmitters acting on different target neurons, often under different circumstances (Jan and Jan, 1982; Blitz and Nusbaum, 1999; Christie et al., 2004; Dugue et al., 2005; Nishimaru et al., 2005; Lu et al., 2008; Maher and Westbrook, 2008). In Chapter 2, we demonstrate that MCN1 uses divergent cotransmission for its actions on the gastric mill CPG. MCN1 contains three cotransmitters, including GABA, and the peptide transmitters proctolin and CabTRP Ia (Blitz et al., 1999). However, as indicated above, MCN1 uses only GABA and CabTRP Ia to activate the gastric mill CPG. All of the non-CPG neurons in the gastric mill circuit are also excited by MCN1, and in each case this excitation is mediated by proctolin and/or CabTRP Ia (Chapter 2: Stein et al., 2007). Therefore, MCN1 uses divergent cotransmitter actions to activate the gastric mill CPG, a fact which turns out to be pivotal for the GPR regulation of this gastric mill rhythm (see Chapter 4).

GPR is a muscle stretch receptor which is active during the gastric mill retractor phase (Katz et al., 1989) (Fig. 2A). In Chapter 3, we demonstrate that activation of GPR during the retractor phase selectively prolongs this phase, and that this GPR action appears to be mediated by GPR presynaptic inhibition of $MCN1_{STG}$. Although GPR also influences both LG and Int1, these actions are not

effective during the MCN1-gastric mill rhythm (Chapters 3 and 4). Thus, we concluded in Chapter 3 that the likely mechanism by which GPR selectively prolongs the gastric mill retractor phase is via its presynaptic inhibition of $MCN1_{STG}$ and the resulting reduction of MCN1 excitation of its synaptic targets in the gastric mill CPG.

In Chapter 4, we continue to investigate the mechanism of the GPR action on the gastric mill CPG by extending previous studies of GPR cotransmission. Specifically, although GPR contains three cotransmitters (5-HT, ACh, allatostatin – AST), we show that GPR exclusively uses 5-HT to regulate the gastric mill CPG. Furthermore, in support of the modeling results in Chapter 3, we document that the site of this 5-HT action is exclusively on $MCN1_{STG}$. We also demonstrate that the GPR inhibition of $MCN1_{STG}$ selectively reduces the peptidergic actions of MCN1, sparing its GABAergic excitation of Int1. Finally, we use our computational model and the dynamic clamp to demonstrate that this selective reduction in peptide transmission is pivotal to the actions of GPR on the gastric mill rhythm. Thus, the use of divergent cotransmission by MCN1 (Chapter 2) to activate the gastric mill rhythm provides a critical access point by which the gastric mill CPG is regulated by sensory input.

Hormonal modulation of sensorimotor integration

As described above, neuromodulation provides a key mechanism by which CPG output is adjusted by external stimuli (Nusbaum and Beenhakker,

2002; Dickinson, 2006). In Chapter 5, we examine a specific and novel mechanism by which the peptide hormone crustacean cardioactive peptide (CCAP) modulates the gastric mill rhythm. It was previously shown that CCAP selectively and only modestly (~20%) prolongs the protractor phase of the MCN1-elicited gastric mill rhythm (Kirby and Nusbaum, 2007). As a prelude for studying the impact of the presence of CCAP on GPR regulation of the gastric mill rhythm, in this Chapter we examined the mechanism underlying that CCAP action.

MCN1 activates the gastric mill rhythm primarily via CabTRP Ia-mediated excitation of LG, which enables LG to overcome inhibition from Int1 and fire a burst (Fig. 1). During each LG burst, LG presynaptic inhibition of MCN1 causes this CabTRP Ia-activated conductance to decay until the burst terminates (Coleman et al., 1995; Beenhakker et al., 2005). In Chapter 5 we demonstrate that CCAP activates the same modulator-activated inward conductance (G_{MI}) as MCN1-released CabTRP Ia. Using our computational model, we show that although the activated conductances are the same, the CCAP-activated component ($G_{MI\text{-}CCAP}$) is not subject to presynaptic inhibition-mediated decay during the protractor (LG-burst) phase, because it is independent of MCN1. The non-decaying nature of the $G_{MI\text{-}CCAP}$ during the LG burst is what prolongs LG activity and thus mediates the observed albeit modest prolonging of the protractor phase.

Finally, in Chapter 6 we show that, using a similar mechanism as the one

described above, CCAP gates the actions of GPR on the gastric mill rhythm. As shown in Chapters 3 and 4, GPR regulates the gastric mill retractor phase by its inhibition of $MCN1_{STG}$, weakening MCN1 excitation of LG. As described above, CCAP provides a parallel mechanism for activating the CabTRP Ia-activated $G_{MI-MCN1}$, namely $G_{MI-CCAP}$, in LG. As a result, a portion of the activated G_{MI} is not under the control MCN1, and thus cannot be reduced by GPR presynaptic inhibition. Thus, GPR is less effective at prolonging the retractor phase in the presence of CCAP.

Thus, in Chapter 6 we illustrate a novel mechanism for the gating of a sensory input. Specifically, although CCAP reduces the effectiveness of GPR, it does so without direct actions on GPR or on the synaptic target (MCN1) by which GPR regulates this rhythm. Furthermore, the actions of CCAP on the gastric mill rhythm itself are modest. Therefore, even when a neurmodulator has only a modest influence on CPG output, it can reconfigure network dynamics in such a way as to alter its response to external inputs.

Due to the depth of understanding of the mechanism by which the gastric mill CPG operates, I have had access to a unique toolset for studying both the gastric mill circuit and the mechanisms by which it is regulated by sensory and hormonal input. The wealth of information regarding the identity of the neurons and synapses which comprise the CPG has allowed me to construct informative computational models of the circuit. These models in turn have suggested experiments in the biological preparation, often using the dynamic clamp

technique. As a result, I have been able to gain insights at the level of individual neurons, synapses and membrane properties about how a sensory input can regulate motor output.

Past studies of the gastric mill CPG, along with other small system CPGs, have uncovered general principles that have proved common to many or all CPGs including those in vertebrates (Marder and Calabrese, 1996; Marder and Bucher, 2001; Nusbaum and Beenhakker, 2002). Similarly, I believe that my insights into mechanisms of sensorimotor integration may have a larger, more general application to CPGs in many systems. The gastric mill circuit is organized as a pair of reciprocally-inhibitory neurons (half-center oscillator) driven by external excitation from a projection neuron. This organizational scheme is common to many CPGs (Marder and Calabrese, 1996; Marder and Bucher, 2001; Kristan et al., 2005; Kiehn, 2006; Pirtle and Satterlie, 2006). It therefore stands to reason that insights gained about the general dynamics underlying the operation of such a circuit, as well as its regulation by external influences such as sensory inputs, are likely to be generally applicable to many different systems which share a similar organization.

One of the main advantages of the gastric mill CPG as model system is its accessibility to experimentation, owing largely to the small number of neurons of which it is composed. However, although every neuron and synapse in the circuit has been identified and characterized, a full understanding of the dynamics by which the circuit operates has not been achieved, particularly in the

presence of external inputs such as sensory feedback. This illustrates the point that even in a seemingly simple system composed of a small number of neurons, surprising complexity arises from the dynamic interaction between circuit neurons, their intrinsic and synaptic conductances, and external influences such as sensory inputs. This realization is humbling, particularly with regard to the pursuit of an understanding of the even more complex, vertebrate systems. However, it is likely this very dynamic complexity that endows even small neural circuits with the ability to generate critical and flexible behaviors will contribute to the comparable events in the larger, less accessible vertebrate systems.

Literature Cited

Bartos M, Manor Y, Nadim F, Marder E, Nusbaum MP (1999) Coordination of fast and slow rhythmic neuronal circuits. J Neurosci 19:6650-60.

Beenhakker MP, Blitz DM, Nusbaum MP (2004) Long-lasting activation of rhythmic neuronal activity by a novel mechanosensory system in the crustacean stomatogastric nervous system. J Neurophysiol 91:78-91.

Beenhakker MP, DeLong ND, Saideman SR, Nadim F, Nusbaum MP (2005) Proprioceptor regulation of motor circuit activity by presynaptic inhibition of a modulatory projection neuron. J Neurosci 25:8794-806.

Blitz DM, Beenhakker MP, Nusbaum MP (2004) Different sensory systems share projection neurons but elicit distinct motor patterns. J Neurosci 24:11381-90.

Blitz DM, Christie AE, Coleman MJ, Norris BJ, Marder E, Nusbaum MP (1999) Different proctolin neurons elicit distinct motor patterns from a multifunctional neuronal network. J Neurosci 19:5449-63.

Blitz DM, Nusbaum MP (1999) Distinct functions for cotransmitters mediating motor pattern selection. J Neurosci 19:6774-83.

Blitz DM, White RS, Saideman SR, Cook A, Christie AE, Nadim F, Nusbaum MP (2008) A newly identified extrinsic input triggers a distinct gastric mill rhythm via activation of modulatory projection neurons. J Exp Biol. 211:1000-11.

Buschges A (2005) Sensory control and organization of neural networks mediating coordination of multisegmental organs for locomotion. J Neurophysiol 93:1127-35.

Buschges A, Akay T, Gabriel JP, Schmidt J (2008) Organizing network action for

locomotion: insights from studying insect walking. Brain Res Rev 57:162-71.

Buschges A, El Manira A (1998) Sensory pathways and their modulation in the control of locomotion. Curr Opin Neurobiol 8:733-9.

Christie AE, Stein W, Quinlan JE, Beenhakker MP, Marder E, Nusbaum MP (2004) Actions of a histaminergic/peptidergic projection neuron on rhythmic motor patterns in the stomatogastric nervous system of the crab Cancer borealis. J Comp Neurol 469:153-69.

Coleman MJ, Meyrand P, Nusbaum MP (1995) A switch between two modes of synaptic transmission mediated by presynaptic inhibition. Nature 378:502-5.

Coleman MJ, Nusbaum MP (1994) Functional consequences of compartmentalization of synaptic input. J Neurosci 14:6544-52.

DeLong ND, Kirby MS, Blitz DM, Nusbaum MP (2009) Parallel Regulation of a Modulator-Activated Current Underlies Metamodulation of Motor Circuit Output. Submitted.

Di Prisco GV, Pearlstein E, Le Ray D, Robitaille R, Dubuc R (2000) A cellular mechanism for the transformation of a sensory input into a motor command. J Neurosci 20:8169-76.

Dickinson PS (2006) Neuromodulation of central pattern generators in invertebrates and vertebrates. Curr Opin Neurobiol 16:604-14.

Doi A, Ramirez JM (2008) Neuromodulation and the orchestration of the respiratory rhythm. Respir Physiol Neurobiol 164:96-104.

Douglass AD, Kraves S, Deisseroth K, Schier AF, Engert F (2008) Escape behavior elicited by single, channelrhodopsin-2-evoked spikes in zebrafish somatosensory neurons. Curr Biol 18:1133-7.

Dugue GP, Dumoulin A, Triller A, Dieudonne S (2005) Target-dependent use of co-released inhibitory transmitters at central synapses. J Neurosci 25:6490-8.

Feldman JL, Gray PA (2000) Sighs and gasps in a dish. Nat Neurosci 3:531-2.

Fleischer AG (1981) The effect of eyestalk hormones of the gastric mill in the intact lobster, *Panulirus interruptus*. J Comp Physiol 141:363-368.

Grillner S (2006) Neuronal networks in motion from ion channels to behaviour. An R Acad Nac Med (Madr) 123:297-8.

Harris-Warrick RM (2002) Voltage-sensitive ion channels in rhythmic motor systems. Curr Opin Neurobiol 12:646-51.

Heinzel HG (1988) Gastric mill activity in the lobster. I. Spontaneous modes of chewing. J Neurophysiol 59:528-50.

Heinzel HG, Weimann JM, Marder E (1993) The behavioral repertoire of the gastric mill in the crab, Cancer pagurus: an in situ endoscopic and electrophysiological examination. J Neurosci 13:1793-803.

Jan LY, Jan YN (1982) Peptidergic transmission in sympathetic ganglia of the frog. J Physiol 327:219-46.

Katz PS, Eigg MH, Harris-Warrick RM (1989) Serotonergic/cholinergic muscle receptor cells in the crab stomatogastric nervous system. I. Identification and characterization of the gastropyloric receptor cells. J Neurophysiol 62:558-70.

Kiehn O (2006) Locomotor circuits in the mammalian spinal cord. Annu Rev Neurosci 29:279-306.

Kilman VL, Marder E (1996) Ultrastructure of the stomatogastric ganglion neuropil of the crab, Cancer borealis. J Comp Neurol 374:362-75.

Kintos N, Nusbaum MP, Nadim F (2008) A modeling comparison of projection neuron-

and neuromodulator-elicited oscillations in a central pattern generating network. J Comput Neurosci 24:374-97.

Kirby MS, Nusbaum MP (2007) Peptide hormone modulation of a neuronally modulated motor circuit. J Neurophysiol 98:3206-20.

Korn H, Faber DS (2005) The Mauthner cell half a century later: a neurobiological model for decision-making? Neuron 47:13-28.

Kristan WB, Jr., Calabrese RL, Friesen WO (2005) Neuronal control of leech behavior. Prog Neurobiol 76:279-327.

Lu T, Rubio ME, Trussell LO (2008) Glycinergic transmission shaped by the corelease of GABA in a mammalian auditory synapse. Neuron 57:524-35.

Maher BJ, Westbrook GL (2008) Co-transmission of dopamine and GABA in periglomerular cells. J Neurophysiol 99:1559-64.

Manor Y, Nadim F, Epstein S, Ritt J, Marder E, Kopell N (1999) Network oscillations generated by balancing graded asymmetric reciprocal inhibition in passive neurons. J Neurosci 19:2765-79.

Marder E, Bucher D (2001) Central pattern generators and the control of rhythmic movements. Curr Biol 11:R986-96.

Marder E, Bucher D (2007) Understanding circuit dynamics using the stomatogastric nervous system of lobsters and crabs. Annu Rev Physiol. 69:291-316.

Marder E, Bucher D, Schulz DJ, Taylor AL (2005) Invertebrate central pattern generation moves along. Curr Biol 15:R685-99.

Marder E, Calabrese RL (1996) Principles of rhythmic motor pattern generation. Physiol Rev 76:687-717.

Marder E, Manor Y, Nadim F, Bartos M, Nusbaum MP (1998) Frequency control of a

slow oscillatory network by a fast rhythmic input: pyloric to gastric mill interactions in the crab stomatogastric nervous system. Ann N Y Acad Sci 860:226-38.

Masino MA, Fetcho JR (2005) Fictive swimming motor patterns in wild type and mutant larval zebrafish. J Neurophysiol 93:3177-88.

Nadim F, Manor Y, Nusbaum MP, Marder E (1998) Frequency regulation of a slow rhythm by a fast periodic input. J Neurosci 18:5053-67.

Nishimaru H, Restrepo CE, Ryge J, Yanagawa Y, Kiehn O (2005) Mammalian motor neurons corelease glutamate and acetylcholine at central synapses. Proc Natl Acad Sci U S A 102:5245-9.

Nusbaum MP, Beenhakker MP (2002) A small-systems approach to motor pattern generation. Nature 417:343-50.

Nusbaum MP, Blitz DM, Swensen AM, Wood D, Marder E (2001) The roles of co-transmission in neural network modulation. Trends Neurosci 24:146-54.

Paton JF, Abdala AP, Koizumi H, Smith JC, St-John WM (2006) Respiratory rhythm generation during gasping depends on persistent sodium current. Nat Neurosci 9:311-3.

Pearson KG (2004) Generating the walking gait: role of sensory feedback. Prog Brain Res 143:123-9.

Pearson KG (2008) Role of sensory feedback in the control of stance duration in walking cats. Brain Res Rev 57:222-7.

Pena F, Ramirez JM (2004) Substance P-mediated modulation of pacemaker properties in the mammalian respiratory network. J Neurosci 24:7549-56.

Perrins R, Walford A, Roberts A (2002) Sensory activation and role of inhibitory

reticulospinal neurons that stop swimming in hatchling frog tadpoles. J Neurosci 22:4229-40.

Pirtle TJ, Satterlie RA (2006) The contribution of the pleural type 12 interneuron to swim acceleration in Clione limacina. Invert Neurosci 6:161-8.

Prinz AA, Bucher D, Marder E (2004) Similar network activity from disparate circuit parameters. Nat Neurosci 7:1345-52.

Ramirez JM, Tryba AK, Pena F (2004) Pacemaker neurons and neuronal networks: an integrative view. Curr Opin Neurobiol 14:665-74.

Rossignol S, Dubuc R, Gossard JP (2006) Dynamic sensorimotor interactions in locomotion. Physiol Rev 86:89-154.

Saideman SR, Blitz DM, Nusbaum MP (2007b) Convergent motor patterns from divergent circuits. J Neurosci 27:6664-74.

Saideman SR, Ma M, Kutz-Naber KK, Cook A, Torfs P, Schoofs L, Li L, Nusbaum MP (2007a) Modulation of rhythmic motor activity by pyrokinin peptides. J Neurophysiol 97:579-95.

Seal RP, Edwards RH (2006) Functional implications of neurotransmitter co-release: glutamate and GABA share the load. Curr Opin Pharmacol 6:114-9.

Serrano GE, Miller MW (2006) Conditional rhythmicity and synchrony in a bilateral pair of bursting motor neurons in Aplysia. J Neurophysiol 96:2056-71.

Sharp AA, O'Neil MB, Abbott LF, Marder E (1993) The dynamic clamp: artificial conductances in biological neurons. Trends Neurosci 16:389-94.

Simmers J, Moulins M (1988) A disynaptic sensorimotor pathway in the lobster stomatogastric system. J Neurophysiol 59:740-56.

Stein W, DeLong ND, Wood DE, Nusbaum MP (2007) Divergent co-transmitter actions

underlie motor pattern activation by a modulatory projection neuron. Eur J Neurosci 26:1148-65.

Turrigiano GG, Heinzel HG (1992) Behavioral correlates of stomatogastric network function. In: Dynamic Biological Networks: The Stomatogastric Nervous System (eds: R. M. Harris-Warrick, E. Marder, A. I. Selverston and M. Moulins), pps 197-220. MIT Press: Cambridge, MA.

Wenning A, Hill AA, Calabrese RL (2004) Heartbeat control in leeches. II. Fictive motor pattern. J Neurophysiol 91:397-409.

Wood DE, Nusbaum MP (2002) Extracellular peptidase activity tunes motor pattern modulation. J Neurosci 22:4185-95.

Yakovenko S, McCrea DA, Stecina K, Prochazka A (2005) Control of locomotor cycle durations. J Neurophysiol 94:1057-65.

Yu X, Nguyen B, Friesen WO (1999) Sensory feedback can coordinate the swimming activity of the leech. J Neurosci 19:4634-43.

Chapter 2

Divergent Cotransmitter Actions Underlie Motor Pattern Activation by a Modulatory Projection Neuron

Wolfgang Stein

Nicholas D. DeLong

Debra E. Wood

Michael P. Nusbaum

Published:

European Journal of Neuroscience, 2007

26: 1148 - 1165

ABSTRACT

Cotransmission is a common means of neuronal communication, but its consequences for neuronal signaling within a defined neuronal circuit remain unknown in most systems. We are addressing this issue in the crab stomatogastric nervous system by characterizing how the identified modulatory projection neuron MCN1 uses its cotransmitters to activate the gastric mill (chewing) rhythm in the stomatogastric ganglion (STG). MCN1 contains GABA plus the peptides proctolin and CabTRP Ia, which it coreleases during the retractor phase of the gastric mill rhythm to influence both retractor and protractor neurons. By focally applying each MCN1 cotransmitter, and pharmacologically manipulating each cotransmitter action during MCN1 stimulation, we found that MCN1 has divergent cotransmitter actions on the gastric mill central pattern generator (CPG), which includes the neurons LG and Int1 plus the STG terminals of MCN1 ($MCN1_{STG}$). MCN1 used only CabTRP Ia to influence LG, while it used only GABA to influence Int1 and the contralateral $MCN1_{STG}$. These MCN1 actions caused a slow excitation of LG, a fast excitation of Int1 and a fast inhibition of $MCN1_{STG}$. MCN1-released proctolin had no direct influence on the gastric mill CPG, although it likely indirectly regulates this CPG via its influence on the pyloric rhythm. MCN1 appeared to have no ionotropic actions on the gastric mill follower motor neurons, but it did use proctolin and/or CabTRP Ia to excite them. Thus, a modulatory projection neuron can elicit rhythmic motor activity by using distinct cotransmitters, with different time courses of action, to simultaneously influence different CPG neurons.

INTRODUCTION

Cotransmission is prevalent throughout all nervous systems (Nusbaum et al., 2001; Burnstock, 2004; Seal & Edwards, 2006). Convergence of ionotropic and/or metabotropic cotransmitter actions onto single target neurons has been documented in several systems (Jan & Jan, 1982; Jonas et al., 1998; Vilim et al., 2000; Koh et al., 2003; Li et al., 2004; Dugue et al., 2005; Koh & Weiss, 2005; Nishimaru et al., 2005). A few divergent cotransmitter actions are also established, where different cotransmitters influence separate target neurons (Blitz & Nusbaum, 1999; Thirumalai & Marder, 2002; Sun et al., 2003). There remains, however, limited information available regarding the consequences of cotransmission in the regulation of neuronal circuit activity.

We are studying cotransmitter function within the stomatogastric nervous system (STNS) of *Cancer* crabs (Nusbaum & Beenhakker, 2002; Marder & Bucher, 2007). The STNS is an extension of the crab central nervous system that contains four interconnected ganglia, including the paired commissural ganglia (CoGs) and the unpaired oesophageal and stomatogastric (STG) ganglia. The STG contains the gastric mill (chewing) and pyloric (filtering of chewed food) central pattern generating (CPG) circuits. These circuits are modulated by projection neurons located primarily in the CoGs (Nusbaum et al., 2001). Several of these projection neurons, including modulatory commissural neuron 1 (MCN1), are identified (Beenhakker & Nusbaum, 2004).

MCN1 contains three cotransmitters, including GABA and the

neuropeptides proctolin and CabTRP Ia (Blitz et al., 1999). Selective activation of MCN1 elicits the gastric mill rhythm (GMR) and modulates the pyloric rhythm (Coleman & Nusbaum, 1994; Bartos & Nusbaum, 1997). The CabTRP Ia actions are necessary for MCN1 activation of the gastric mill rhythm, while both CabTRP Ia and proctolin contribute to MCN1 modulation of the pyloric rhythm (Wood et al., 2000; Wood & Nusbaum, 2002).

Here we determined how the set of cotransmitters used by MCN1 influences each gastric mill circuit neuron. We found that both divergence and convergence of MCN1 cotransmission contribute to its actions on this circuit. Divergence is key to MCN1 activation of the gastric mill CPG, while its actions on most gastric mill follower neurons result from convergent cotransmitter actions. The gastric mill CPG includes the reciprocally inhibitory lateral gastric (LG) neuron and interneuron 1 (Int1), plus the STG terminals of MCN1 ($MCN1_{STG}$) (Coleman et al., 1995). We showed previously that MCN1 elicits a slow excitation of LG, exclusively via CabTRP Ia (Wood et al., 2000). Here we show that MCN1 uses only GABA to influence Int1 and the contralateral $MCN1_{STG}$. Its GABAergic actions are fast excitation of Int1, but inhibition of the contralateral $MCN1_{STG}$. MCN1 appears to have only an indirect proctolinergic influence on the gastric mill CPG, by using proctolin (and CabTRP Ia) to excite the pyloric rhythm (Wood & Nusbaum, 2002). The pyloric rhythm regulates the speed of the gastric mill rhythm (Bartos et al., 1999). Several of the gastric mill follower motor neurons are excited by both MCN1-released peptides.

Some of this work has been published in abstract form (Stein et al., 2001).

MATERIALS & METHODS

Animals/preparation. Male crabs, *Cancer borealis* (Jonah crabs), were obtained from Commercial Lobster & Seafood Co. (Boston, MA, USA) and the Marine Biological Laboratory (Woods Hole, MA, USA). Brown crabs (*Cancer pagurus*) were purchased from Feinfisch GmbH (Neu-Ulm, Germany). The connectivity and the properties of the neurons in the STNS of *C. pagurus* and are similar to those in *C. borealis* (Heinzel et al., 1993, Stein et al., 2005). Crabs were housed in commercial tanks containing chilled, filtered and recirculated artificial seawater (10°C). Before dissection, each crab was anesthetized by packing in ice for at least 30 minutes. The foregut was removed and then transferred to a dissection dish containing saline (10-12°C) to enable dissection of the STNS from the foregut. The isolated STNS (Fig. 1A) was then transferred and pinned down in a silicone elastomer (Sylgard 184, KR Anderson, Santa Clara, CA, USA)-lined Petri dish filled with saline (10-12°C). All experiments were performed on preparations in which the CoGs were first removed, via transection of the superior- and inferior (*ions*) oesophageal nerves (Fig. 1A).

Solutions. During dissection and experimentation, the STNS was supplied with *C. borealis* saline (mM): 440 NaCl, 26 $MgCl_2$, 13 $CaCl_2$, 11 KCl, 10 Trizma base and 5 maleic acid (pH 7.4-7.6). In some experiments, transmitter release was suppressed by superfusing the preparation with saline containing 10-fold reduced

Ca^{2+} levels, substituted on an equimolar basis with Mn^{2+} ("low Ca^{2+} saline") (Blitz & Nusbaum, 1999). This saline contained (in mM): 440 NaCl, 26 $MgCl_2$, 1.3 $CaCl_2$, 11.7 $MnCl_2$, 11 KCl, 10 Trizma base and 5 maleic acid (pH 7.4-7.6). During the experiment, the STNS was continuously superfused with chilled (10-11^o C) saline (7-12 ml/min).

The tachykinin receptor antagonist spantide I was synthesized at the Cancer Research Center, University of Pennsylvania School of Medicine (Philadelphia, PA, USA) or obtained from Peninsula Laboratories (Belmont, CA) and Sigma Chemical Company (St. Louis, MO, USA). Spantide solutions were made by dissolving spantide I into *C. borealis* physiological saline. The peptidase inhibitors actinonin and phosphoramidon as well as the GABA/glutamate antagonist picrotoxin (PTX) were obtained from Sigma. Solutions of any one of these peptidase inhibitors were made by diluting frozen aliquots of stock solution into *C. borealis* saline. PTX saline was made fresh for each experiment. PTX applications were continued for at least 30 min before the first MCN1 stimulation. The effects of PTX (10^{-5} M) on the STG, when superfused for more than 15-20 minutes, persist for several hours after the start of washout with normal saline. Therefore, in most experiments we did not obtain post-PTX recordings. Each application of actinonin or phosphoramidon was continued for at least 10-15 min before MCN1 stimulation was begun. Preparations were washed by superfusing normal saline for at least 40-60 min before post-application control experiments were performed.

Transmitter applications. Transmitter applications were done either via focal pressure application onto the desheathed STG neuropil, using a Picospritzer II (General Valve Co., Fairfield, NJ, USA), or via superfusion. For focal applications, a blunt-tipped micropipette (tip resistance ~1MΩ) filled with CabTRP Ia (10^{-4} M), proctolin (10^{-3} M, 10^{-4} M) or GABA (10^{-2} M) was positioned over the STG neuropil only for the duration of an application. These pipettes were otherwise maintained at a distance from the STG, on the superfusion outflow side of the ganglion, to prevent the influence of any leak from the pipette.

Electrophysiology. STNS neurons were identified by their activity patterns, synaptic interactions with other identified neurons and extracellularly recorded axonal branching patterns, using intracellular and extracellular recording and stimulating methods that are standard for this system (Beenhakker & Nusbaum, 2004). Briefly, extracellular recordings from connecting and peripheral nerves were obtained by electrically isolating individual sections of these nerves from the bath with a petroleum jelly (Vaseline: Lab Safety Supply, Janesville, WI, USA)-based cylindrical compartment. To record action potentials propagating through a nerve, one of a pair of stainless steel electrode wires was placed within the isolated nerve compartment, with the second wire of the pair being placed in the bath as a reference electrode. The differential signal was recorded, filtered and

amplified, first through an amplifier from AM Systems (Model 1700, Carlsborg, WA, USA) and then through an amplifier from Brownlee Precision (Model 410, Santa Clara, CA, USA). Extracellular nerve stimulation was achieved by placing the two extracellular wires into a stimulus isolation unit (Astromed/Grass Instruments, Model SIU5, West Warwick, RI, USA) controlled by a stimulator (Astromed/Grass Instruments, Model S88).

Intracellular recordings of STNS somata were obtained with sharp glass microelectrodes (15-30 MΩ) filled with either 4 M potassium acetate plus 20 mM potassium chloride (KCl) or 0.6 M K_2SO_4 plus 20 mM KCl. To preserve neurotransmitter release from the STG terminals of projection neurons during intra-axonal recordings, we used an intracellular electrode solution of 1 M KCl (Coleman et al., 1995). All intracellular signals were amplified and filtered with Axoclamp 2B amplifiers (Molecular Devices, Sunnyvale, CA, USA), then further amplified with Brownlee Model 410 amplifiers. Intracellular current injections were performed in discontinuous current clamp mode with sampling rates of 2-3 KHz.

Selective stimulation of the projection neuron MCN1 was performed by extracellular stimulation of one or both of the transected *ion* nerves. This selective stimulation was possible because there are only two CoG projection neurons that innervate the STG via the ion, including MCN1 and modulatory commissural neuron 5 (MCN5), and MCN1 has the lower stimulus threshold (Coleman et al., 1992; Coleman & Nusbaum, 1994; Norris et al., 1996; Bartos &

Nusbaum, 1997).

Data Acquisition and Analysis. Data were acquired in parallel onto a chart recorder (MT-95000 or Everest Model, Astromed Corp., West Warwick, RI, USA), and by digitizing (~5 KHz) and storing the data on computer with data acquisition hardware/software (Spike2, Cambridge Electronic Design, Cambridge, England). Digitized data were analyzed with a homemade Spike2 program ('The Crab Analyzer', freely available at http://cuniculina.biologie.uni-ulm.de/wstein/spike2/The_Crab_Analyzer.s2s). Briefly, the burst duration of a neuron was defined as the elapsed time (sec) between the first and last action potential in an impulse burst. From each experiment we determined the average burst duration of ten consecutive bursts of action potentials. We also determined the mean intraburst firing frequency of individual gastric mill neurons to characterize their responses to applied transmitters. The intraburst firing frequency was calculated by dividing the number of action potentials minus one by the burst duration. In the presented plots of firing frequency, each successive data point (time increments were determined by sampling at 5 kHz) represents the mean firing frequency for the preceding time bin (bin width: 0.5s or 1s). Gastric mill cycle period was defined by the duration (sec) between the onsets of 2 successive impulse bursts in the LG neuron.

In some experiments, we depolarized each gastric mill neuron with

rhythmic current injections to ensure that they were sufficiently depolarized to exhibit a response, because peptidergic actions in the STG are voltage-dependent (Swensen & Marder, 2000). To determine the influence of a peptidase inhibitor (i.e., phosphoramidon or actinonin) on the actions of MCN1, we compared the response of the recorded neuron at a fixed duration (90 sec) after the termination of MCN1 stimulation during normal saline or peptidase inhibitor superfusion. Phosphoramidon and actinonin prolong the actions of CabTRP Ia and proctolin, respectively (Coleman et al., 1994; Wood et al., 2000).

The data are presented as mean ± SD. Statistical analyses (Student's unpaired *t*-test, paired-samples *t*-test) were performed with SigmaStat 3.0 (SPSS, Chicago, IL, USA), Excel (Microsoft, Seattle, WA, USA) or Plotit (Scientific Programming Enterprises, Haslet, MI, USA). Figures were made from Spike2 files incorporated in the Adobe Photoshop (Adobe, San Jose, CA, USA) and CorelDraw (Corel Corporation, Ottawa, Canada) graphics programs.

RESULTS

The MCN1-Elicited Gastric Mill Rhythm

Previous work identified the reciprocally inhibitory LG neuron and Int1, plus the STG terminals of MCN1 ($MCN1_{STG}$), as pivotal CPG neurons for the MCN1-elicited gastric mill rhythm (Fig. 1B) (Coleman et al., 1995; Bartos et al., 1999). Despite the fact that MCN1 is stimulated tonically to elicit the gastric mill rhythm, its STG terminals ($MCN1_{STG}$) release their cotransmitters rhythmically during the gastric mill rhythm, due to the inhibitory input to $MCN1_{STG}$ from the LG neuron (Fig. 1B) (Coleman & Nusbaum, 1994, Coleman et al., 1995). This MCN1 cotransmitter release pattern and its necessity for gastric mill rhythm generation supports the inclusion of MCN1 as a gastric mill CPG neuron, in addition to its role as an integrator of sensory inputs and activator of this rhythm (Coleman & Nusbaum, 1994; Beenhakker & Nusbaum, 2004; Blitz et al., 2004).

Three of the four protractor phase neurons and three of the four retractor phase neurons participate reliably in the MCN1-elicited gastric mill rhythm. This includes the protractor neurons LG, medial gastric (MG) and inferior cardiac (IC) and the retractor neurons Int1, dorsal gastric (DG) and ventricular dilator (VD) (Fig. 1C). In contrast, the gastric mill (GM) protractor neurons (n>50) and the anterior median (AM) retractor neuron (n>25) are at best weakly and intermittently active in this version of the gastric mill rhythm (see below). These two neurons do, however, participate reliably in other versions of this rhythm

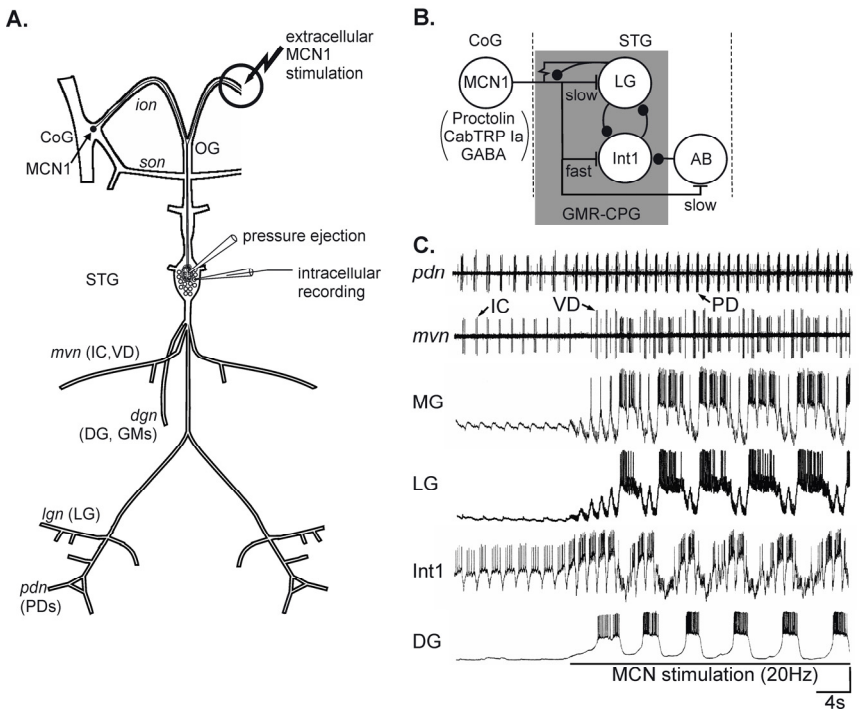

Figure 1. Selective stimulation of the projection neuron MCN1 elicits the gastric mill rhythm (GMR) in the isolated stomatogastric nervous system. **(A)** Schematic illustration of the stomatogastric nervous system including its ganglia and connecting and peripheral nerves. Note that there is a single MCN1 in each of the paired commissural ganglia (CoGs). MCN1 projects through the inferior oesophageal (*ion*; illustrated for the left *ion*) and stomatogastric nerves (*stn*) to innervate the stomatogastric ganglion (STG). In these experiments, both CoGs were cut away (illustrated for the right CoG) and MCN1 was stimulated via *ion* stimulation (see Methods). In the STG, focal pressure applications were made onto the desheathed STG neuropil. The STG somata form a single cell layer around the perimeter of the neuropil. The acronyms of identified STG neurons listed in parentheses next to each nerve acronym indicate the neurons whose

axons project through each of these nerves and therefore can be recorded extracellularly from them. **(B)** Summary schematic of the MCN1 actions on the gastric mill central pattern generator (CPG). The MCN1 cotransmitter identification is from Blitz et al. (1999). The MCN1 synaptic actions, including the presence of monosynaptic fast, unitary EPSPs in Int1 and a slow depolarization in LG, are from Coleman et al. (1995) and Bartos & Nusbaum (1997). Synapse symbols: t-bar, transmitter-mediated excitation; filled circle, transmitter-mediated inhibition; resistor, electrical coupling. Note that all of these synapses occur within the STG neuropil, and that there are no synapses onto the somata of the STG neurons. **(C)** Selective stimulation of MCN1 (see Methods) elicits the gastric mill rhythm. Action potential bursts in the protractor phase neurons LG, MG and IC alternate with bursts in the retractor phase neurons Int1, DG and VD. Note that MCN1 stimulation also increased the pyloric (PD) cycle frequency (Bartos and Nusbaum, 1997). Before MCN1 stimulation, there was an ongoing pyloric rhythm (PD, IC) and no gastric mill rhythm.

(Beenhakker & Nusbaum, 2004; Blitz et al., 2004). All but one of the gastric mill circuit neurons occurs as a single copy in each STG. The GM protractor neuron occurs instead as 4 apparently equivalent copies.

Commonly, in the isolated STG, the only gastric mill neurons that are spontaneously active in the absence of MCN1 activity are Int1 and IC (Fig. 1C). As is evident in Figure 1C from the timing of Int1 and IC activity relative to that of the pyloric dilator (PD) neuron, their rhythmic activity, as well as that of the MG and VD neurons, is time-locked with the pyloric rhythm as well as the gastric mill rhythm (see also Blitz & Nusbaum, 1997).

MCN1 Excites All Gastric Mill Follower Motor Neurons

MCN1 activates the gastric mill CPG via its fast excitation of Int1 and slow excitation of LG (Coleman et al., 1995) (Fig. 1B). We also showed previously that MCN1 excites the gastro/pyloric neurons IC and VD (Bartos & Nusbaum, 1997). Herein we document that there are associated excitatory actions of MCN1 on all other gastric mill motor neurons.

Protractor Neurons: During the MCN1-elicited gastric mill rhythm, MG neuron activity was either initiated or enhanced (pre-MCN1: 1.8 $\pm$ 2.6 Hz; during MCN1: 12.7 $\pm$ 4.4 Hz, n=7, $p<0.01$). At these times the MG activity pattern was pyloric-timed during the protractor (LG active) phase and either weaker or suppressed during the retractor (Int1 active) phase (n=6) (Fig. 1C). The

increased MG neuron activity during this rhythm appeared to be at least partly a consequence of direct MCN1 excitation because it persisted after the LG neuron (to which it is electrically coupled) was hyperpolarized (n=6) (not shown).

The activity of the protractor neuron GM was consistently, albeit weakly enhanced during the MCN1-elicited gastric mill rhythm (n=15/18). GM firing frequency increased, from 1.1 $\pm$ 1.0 Hz before MCN1 stimulation to 3.2 $\pm$ 1.9 Hz during stimulation (n=15, $p<0.01$). In 3 of these 18 recordings, only a subthreshold depolarization was evident. In 2 of these latter 3 recordings, depolarizing GM via a constant amplitude current injection to a level that was near or just above spike threshold (~-55 mV) enabled it to be activated during the subsequent MCN1-GMR. As is the case for the MG neuron, the GM neurons are electrically coupled to LG. Nevertheless, the MCN1 excitation of GM persisted when LG was hyperpolarized to hold it below spike threshold during MCN1 stimulation (n=6) (Fig. 2A).

Retractor Neurons: MCN1 stimulation either activated the AM neuron or enhanced its activity (n=9/11) (Fig. 2B). AM neuron firing frequency increased modestly but consistently, from 1.3 ± 1.4 Hz (pre-MCN1) to 4.6 ± 3.3 Hz: (during MCN1) (n=9, $p<0.05$). The AM neuron was also activated effectively when the LG neuron was hyperpolarized, preventing activation of the gastric mill rhythm (n=3) (Fig. 2B). Surprisingly, during the MCN1-elicited gastric mill rhythm the AM neuron activity was strongest during the protractor phase (Fig. 2B). In contrast, during other versions of the gastric mill rhythm the AM neuron is exclusively a

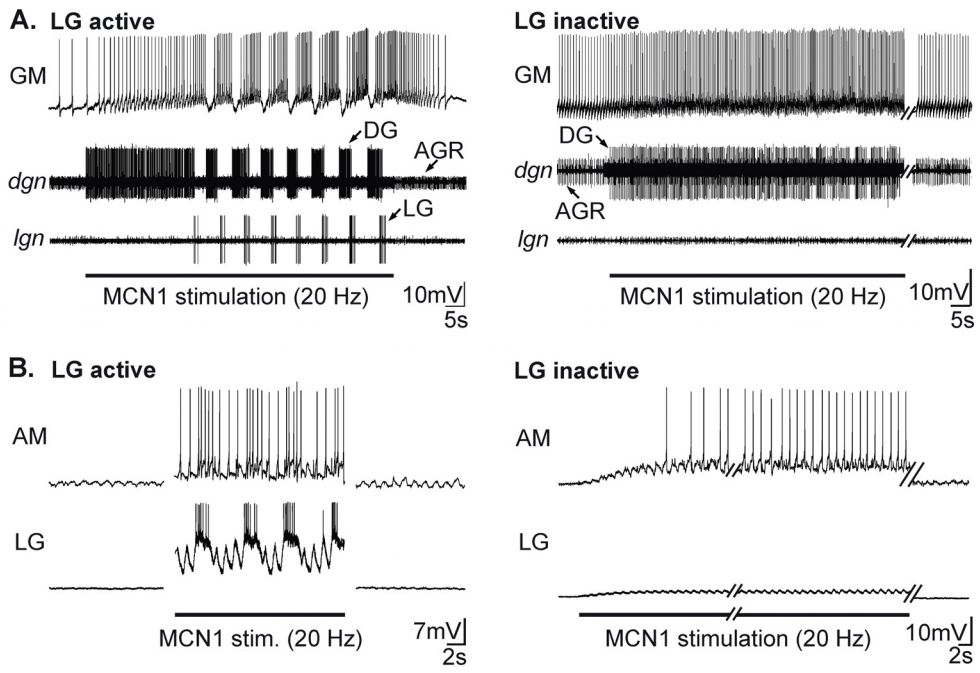

Figure 2. MCN1 stimulation excites the gastric mill neurons GM, AM and DG. **(A)** (Left) When the GM neuron is suprathreshold before MCN1 stimulation, its activity increases and exhibits protractor phase bursts (LG activity) that alternate with retractor phase bursts (DG neuron) during the ensuing gastric mill rhythm. (Right) When the LG neuron is held hyperpolarized by current injection (not shown), MCN1 stimulation does not elicit the gastric mill rhythm but it still excites the GM and DG neurons. The tonically active unit in the *dgn* is the anterior gastric receptor (AGR), a muscle tendon organ receptor that has no synaptic actions in the STG (Combes et al., 1995). Most hyperpolarized V_m: (Left) GM, -62 mV; (Right) GM, -56 mV. **(B)** (Left) MCN1 stimulation activates the AM neuron, which fires protractor phase bursts as well as pyloric-timed action potentials during the retractor phase. (Right) With LG neuron activity (and the gastric mill rhythm) suppressed by hyperpolarizing current, MCN1 stimulation still excited the

AM neuron. Panels A and B are from separate preparations. Most hyperpolarized V_m: (Left) AM, -63 mV; LG, -73 mV; (Right) AM, -60 mV; LG, -79 mV.

retractor phase neuron (Beenhakker & Nusbaum, 2004).

The DG neuron is also effectively activated by MCN1 stimulation, whether or not a gastric mill rhythm is generated (Coleman & Nusbaum, 1994). When the LG neuron was hyperpolarized to prevent activation of the gastric mill rhythm, MCN1 stimulation elicited either tonic firing from DG (Fig. 2A, right panel, at the start of MCN1 stimulation) or rhythmic bursting that was independent of all other STG neurons (Fig. 2A, right panel, towards the end of MCN1 stimulation; see also Coleman & Nusbaum, 1994).

MCN1 Cotransmitter Actions on Gastric Mill CPG Neurons

Effects on the LG neuron. MCN1 is the only source of CabTRP Ia in the STG (Christie et al., 1997; Blitz et al., 1999). It directly excites the LG neuron via a slow, CabTRP Ia-mediated excitation plus electrical EPSPs (eEPSPs) (Coleman et al., 1995; Wood et al., 2000). MCN1-released proctolin does not appear to contribute to the LG response (Wood et al., 2000).

It remained possible that LG was proctolin-sensitive but in a voltage-dependent manner. We therefore tested whether focally applied proctolin (pipette concentration: 10^{-3} M or 10^{-4} M) influenced the LG neuron when it was maintained at a depolarized level that was just above spike threshold. At these holding potentials, however, the LG neuron firing rate remained unaffected by proctolin application (pre-proct.: 1.9 $\pm$ 1.9 Hz; during proct.: 2.0 $\pm$ 1.9 Hz; n=7, $p>0.2$). In

contrast, as reported previously (Wood et al., 2000), LG activity consistently increased in response to CabTRP Ia applications (pre-CabTRP Ia: 0.5 $\pm$ 0.9 Hz; during CabTRP Ia: 4.0 $\pm$ 4.3 Hz; n=21, $p<0.01$).

Neuropeptide release sometimes requires a baseline firing frequency, while small molecule transmitters are effectively released even by single action potentials (Cazalis et al., 1985; Whim & Lloyd, 1989; Vilim et al., 2000). Because CabTRP Ia was the only MCN1-released cotransmitter that influenced the LG neuron, we assayed whether there was a CabTRP Ia-mediated depolarization of LG at MCN1 firing frequencies that were below the MCN1 threshold for activating the gastric mill rhythm. This threshold is generally higher than 5 Hz, and often closer to 10 Hz. Stimulating MCN1 at firing rates as low as 2 Hz consistently elicited a slow, subthreshold depolarization of the LG neuron that slowly decayed after MCN1 stimulation was terminated (n=6).

Although MCN1 affected the LG neuron only via CabTRP Ia, LG also exhibited a relatively fast onset and short-lasting hyperpolarizing response to GABA application (Fig. 3A) (Swensen et al., 2000). This response persisted in low Ca^{2+}-saline (n=6), indicating that GABA is likely to directly inhibit this gastric mill CPG neuron (Fig. 3B). Consistent with our spantide results, we found no evidence that GABA released from MCN1 affected LG. For example, we never recorded unitary, transmitter-mediated PSPs in LG that corresponded to MCN1 spike activity (n>50 animals). Additionally, in experiments where we hyperpolarized Int1 and stimulated MCN1, the LG neuron response was

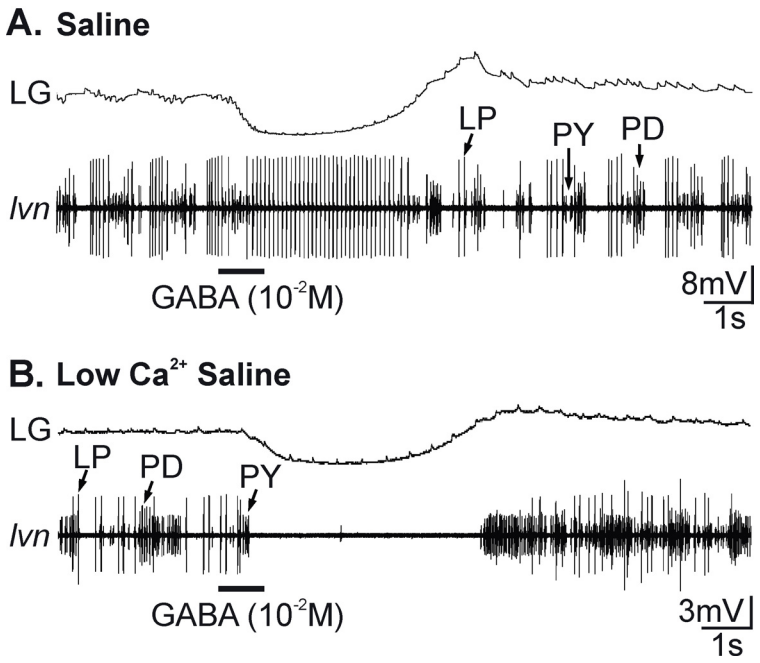

Figure 3. Focally applied GABA hyperpolarizes the LG neuron. **(A)** During normal saline superfusion, focal pressure application of GABA onto the desheathed STG neuropil reversibly hyperpolarized the LG neuron. Note that GABA also altered the activity of the extracellularly recorded pyloric neurons LP, PY and PD (Swensen et al., 2000). **(B)** GABA application directly hyperpolarizes the LG neuron. Focally applied GABA hyperpolarized the LG neuron when transmitter release was suppressed by low Ca^{2+} saline superfusion. Note that the GABA solution was also made with low Ca^{2+} saline. Most hyperpolarized V_m: (A) LG, -68 mV; (B) LG, -72 mV.

consistently depolarizing and excitatory (n=25). We also tested whether the latency to activation of the LG neuron by MCN1 stimulation would be reduced in the presence of picrotoxin (PTX: 10^{-5} M), which suppresses some GABA actions in this system (Blitz & Nusbaum, 1999; Swensen et al., 2000). An altered latency would support the presence of an underlying GABAergic action of MCN1 on the LG neuron. However, the delay between the start of the MCN1 stimulation and the first LG spike was not significantly different in saline and PTX (saline: 5.03 $\pm$ 1.8 s; PTX: 5.45 $\pm$ 1.0 s, n=8, p>0.2).

We also used the eEPSP as a measure of the LG neuron input resistance within its neuropilar branches to assess whether there might be a slowly developing GABAergic inhibitory action of MCN1. In these experiments, we again suppressed the actions of CabTRP Ia with spantide I (5 X 10^{-5} M) and compared the amplitude of the first MCN1-elicited ePSP with those occurring 1 s and 2 s after the start of tonic MCN1 stimulation. We anticipated that the presence of a GABA conductance would likely shunt these EPSPs, decreasing their amplitude. Such a shunt in the eEPSP did occur when we focally-applied GABA (pre-application: 4.3 $\pm$ 2.3mV; GABA: 2.6 $\pm$ 1.7mV; n=7; P<0.05), but not in its absence (1^{st} EPSP: 8.0 $\pm$ 3.0 mV; EPSP after 1s: 7.8 $\pm$ 2.9 mV; EPSP after 2s: 8.1 $\pm$ 3.1 mV; n=12, p>0.2). These experiments were performed in low Ca^{2+} saline, to selectively assess the direct actions of GABA on LG. Thus, the LG neuron GABA receptors are likely relevant only to GABAergic synapses from one or more other GABA-containing neurons.

Effects on Int1. MCN1 excitation of Int1 appeared to be at least partly ionotropic, because individual MCN1 action potentials elicit constant latency, short-lasting EPSPs in Int1 that are reversibly eliminated when transmitter release is suppressed (Coleman et al., 1995). During MCN1 stimulation, Int1 firing frequency consistently increased (pre-MCN1: 3.3 $\pm$ 3.5 Hz; during-MCN1: 13.6 $\pm$ 5.1 Hz; n=24, $p<0.01$) (Fig. 4A). In contrast, the Int1 firing frequency was unchanged by proctolin application (pre-proct.: 5.2 $\pm$ 2.6 Hz; during proct.: 5.2 $\pm$ 2.5 Hz; n=18, $p>0.2$), despite the ability of these proctolin applications to excite other STG neurons, such as the lateral pyloric (LP) neuron (Fig. 4B).

We observed variable Int1 responses to CabTRP Ia application. In 13 preparations we observed a small but consistent increase of Int1 firing frequency (saline: 5.8 $\pm$ 2.7 Hz; CabTRP Ia: 7.5 $\pm$ 2.6; n=13, $p<0.01$). In 19 other preparations, despite having the same control level of activity, there was no Int1 response to CabTRP Ia application (saline: 5.2 $\pm$ 3.0 Hz; CabTRP Ia: 5.1 $\pm$ 3.0 Hz; n=19, $p>0.2$) (Fig. 4C). In these latter experiments, CabTRP Ia still effectively excited other STG neurons, such as LP (Fig. 4C).

We confirmed that, as shown qualitatively in previous work (Swensen et al., 2000), Int1 was strongly excited by focally-applied GABA (n=14/14) (Fig. 4D). This response included a considerable increase in Int1 firing frequency (saline: 5.2 $\pm$ 3.8 Hz; GABA: 23.6 $\pm$ 8.2 Hz; n=18, $p<0.01$). This GABA-mediated

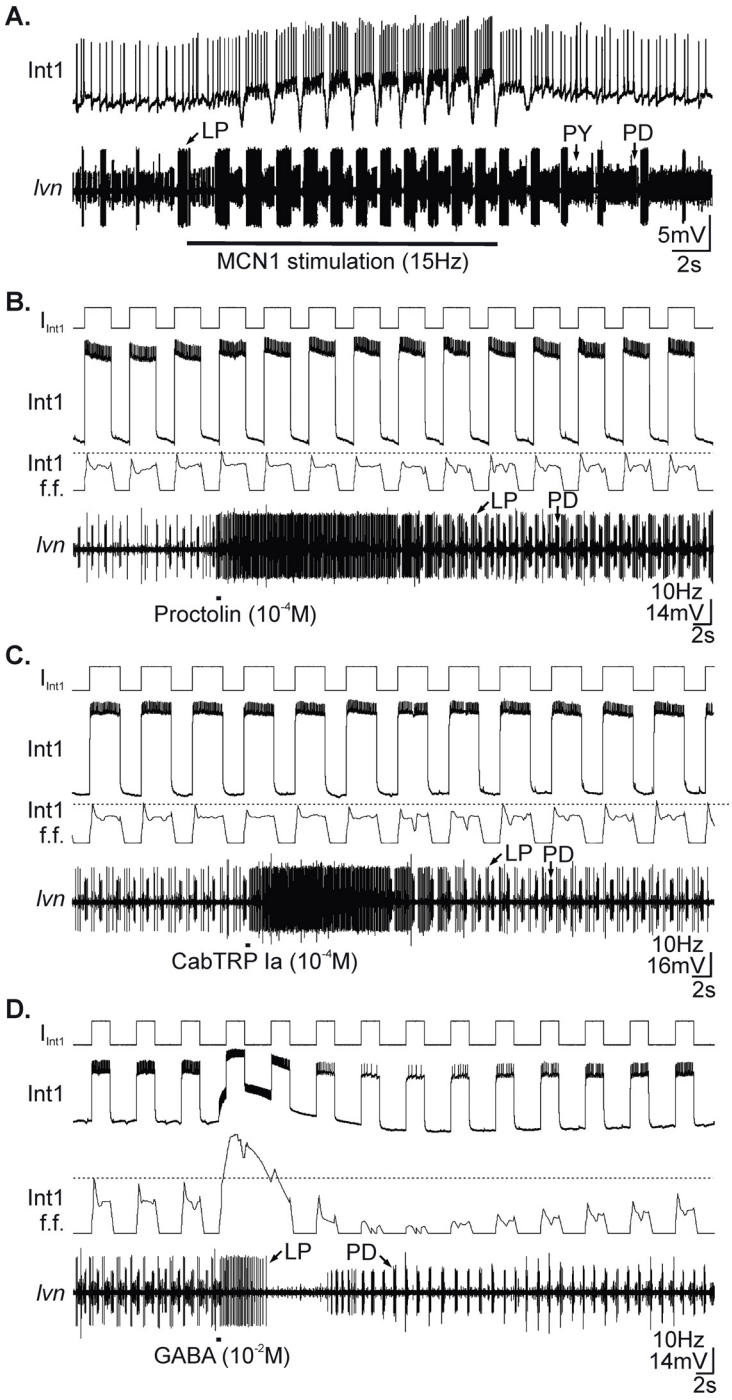

Figure 4. GABA is the only MCN1 cotransmitter to influence Int1. **(A)** Relatively brief MCN1 stimulation increases Int1 activity. Note that MCN1 stimulation also strengthened the ongoing pyloric rhythm (*lvn*). Most hyperpolarized V_m: Int1, -46

mV. **(B)** Focally applied proctolin did not alter Int1 activity, despite its strong excitatory action on the pyloric rhythm (*lvn*). Int1 was rhythmically depolarized and hyperpolarized by constant amplitude current injections (top trace: +1 nA, -0.5 nA) while its firing frequency (f.f.) was tracked continuously (third trace). Most hyperpolarized V_m: Int1, -68 mV. **(C)** Focally applied CabTRP Ia did not alter Int1 activity, despite its strong excitatory action on the pyloric rhythm (*lvn*). Most hyperpolarized V_m: Int1, -69 mV. **(D)** Focally applied GABA reversibly excited Int1 and increased its firing frequency, after which Int1 exhibited a long-term reduction in activity. In panels B-D, dotted lines indicate the maximum firing frequency before transmitter application. Most hyperpolarized V_m: Int1, -56 mV.

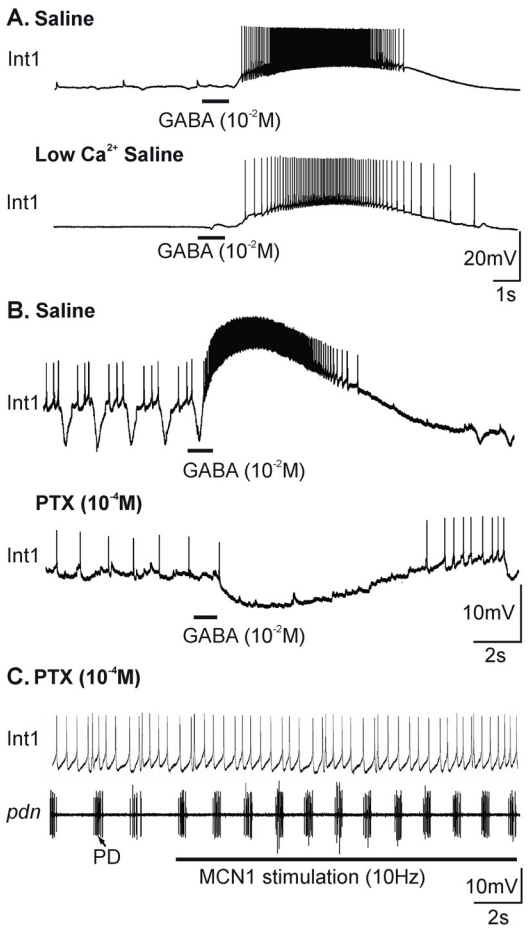

Figure 5. MCN1 elicits a direct, PTX-sensitive GABAergic excitation of Int 1. **(A)** Focally applied GABA reversibly excites Int1 in both normal saline and with transmitter release suppressed by low Ca^{2+} saline. Most hyperpolarized V_m: Saline, -47 mV; Low Ca^{2+} Saline, -56 mV. **(B)** GABA excitation of Int1 is PTX-sensitive. GABA excitation of Int1 during normal saline superfusion is eliminated during PTX superfusion, unmasking an underlying hyperpolarization. Most hyperpolarized V_m: Saline, -49 mV; PTX, -50 mV. **(C)** MCN1 stimulation during PTX superfusion did not increase Int1 activity. Note that the pyloric rhythm (*pdn*) was still excited by MCN1 stimulation in PTX. Most hyperpolarized V_m: -53 mV.

excitation of Int1 was apparently direct because it persisted when transmitter release was suppressed by low-Ca^{2+} saline (n=4) (Fig. 5A). Although Int1 was not spontaneously active in low-Ca^{2+} saline, GABA application in this condition again evoked a relatively high Int1 firing rate (20.0 $\pm$ 8.2 Hz; n=4).

PTX (10^{-5} M) application suppressed the GABA excitation of Int1 and unmasked an underlying hyperpolarizing response in Int1 (n=6) (Fig. 5B). Consistent with the presence of a direct GABAergic excitation of Int1 by MCN1, PTX either suppressed (n=3/8) or reduced (n=5/8) MCN1 excitation of Int1 (saline: pre-MCN1, 3.3 ± 3.4 Hz; during MCN1, 13.5 ± 5.1 Hz, n=24, $p<0.01$; PTX: pre-MCN1, 2.4 $\pm$ 1.5 Hz; during MCN1, 4.5 ± 2.8 Hz; n=8, $p<0.05$) (Fig. 5C**).**

To determine whether Int1 was also affected by MCN1-released CabTRP Ia, we additionally recorded the Int1 response to MCN1 stimulation in the presence of spantide I (5 X 10^{-5} M). Under this condition, the Int1 response to MCN1 stimulation was unchanged relative to saline controls (saline: 14.9 $\pm$ 5.5 Hz; spantide: 14.2 $\pm$ 4.1 Hz, n=5, $p>0.2$). It therefore seems likely that the modest increase in Int1 activity during some CabTRP Ia applications was an indirect consequence of the peptide actions on other STG neurons.

Effects on $MCN1_{STG}$. The STG terminals of MCN1 ($MCN1_{STG}$) are considered part of the gastric mill central pattern generator, due to the fact that it must

release its cotransmitters in a gastric mill-timed pattern for this rhythm to be generated (Coleman et al., 1995). We therefore assessed the influence of the MCN1 cotransmitters on its own axon terminals in the STG, by recording intra-axonally from the contralateral $MCN1_{STG}$ near the entrance to the STG neuropil (Coleman & Nusbaum, 1994; Beenhakker et al., 2005). Neither proctolin (n=7) nor CabTRP Ia (n=7) application influenced $MCN1_{STG}$, despite their ability to excite other STG neurons during those applications. This lack of influence on $MCN1_{STG}$ also occurred when depolarizing current was injected into $MCN1_{STG}$ to activate its STG spike initiation zone (Fig. 6A,B) (Coleman & Nusbaum, 1994; Beenhakker et al., 2005). Neither peptide altered the $MCN1_{STG}$ firing rate in response to depolarizing current injection (saline: 4.6 ± 0.5 Hz; CabTRP Ia: 4.6 ± 0.5 Hz; n=3, $p>0.2$; saline: 5.0 ± 0.8; proct.: 4.3 ± 1.0; n=3, $p>0.2$). In contrast, GABA application consistently hyperpolarized $MCN1_{STG}$ (n=7, Fig. 6C1).

It was possible that the MCN1 response to GABA application was an indirect consequence of GABA inhibition of LG, because $MCN1_{STG}$ is electrically coupled to LG (Coleman et al., 1995). However, GABA application still hyperpolarized $MCN1_{STG}$ at times when LG was sufficiently hyperpolarized by current injection that it exhibited a reversed, depolarizing response to GABA application (n=5) (Fig. 6C2). Similarly, MCN1 stimulation consistently hyperpolarized the contralateral $MCN1_{STG}$ (n=5) (Fig. 7A). As was the case for direct GABA applications (Fig. 6C2), the hyperpolarizing response of the contralateral $MCN1_{STG}$ persisted when the LG neuron was maintained at a

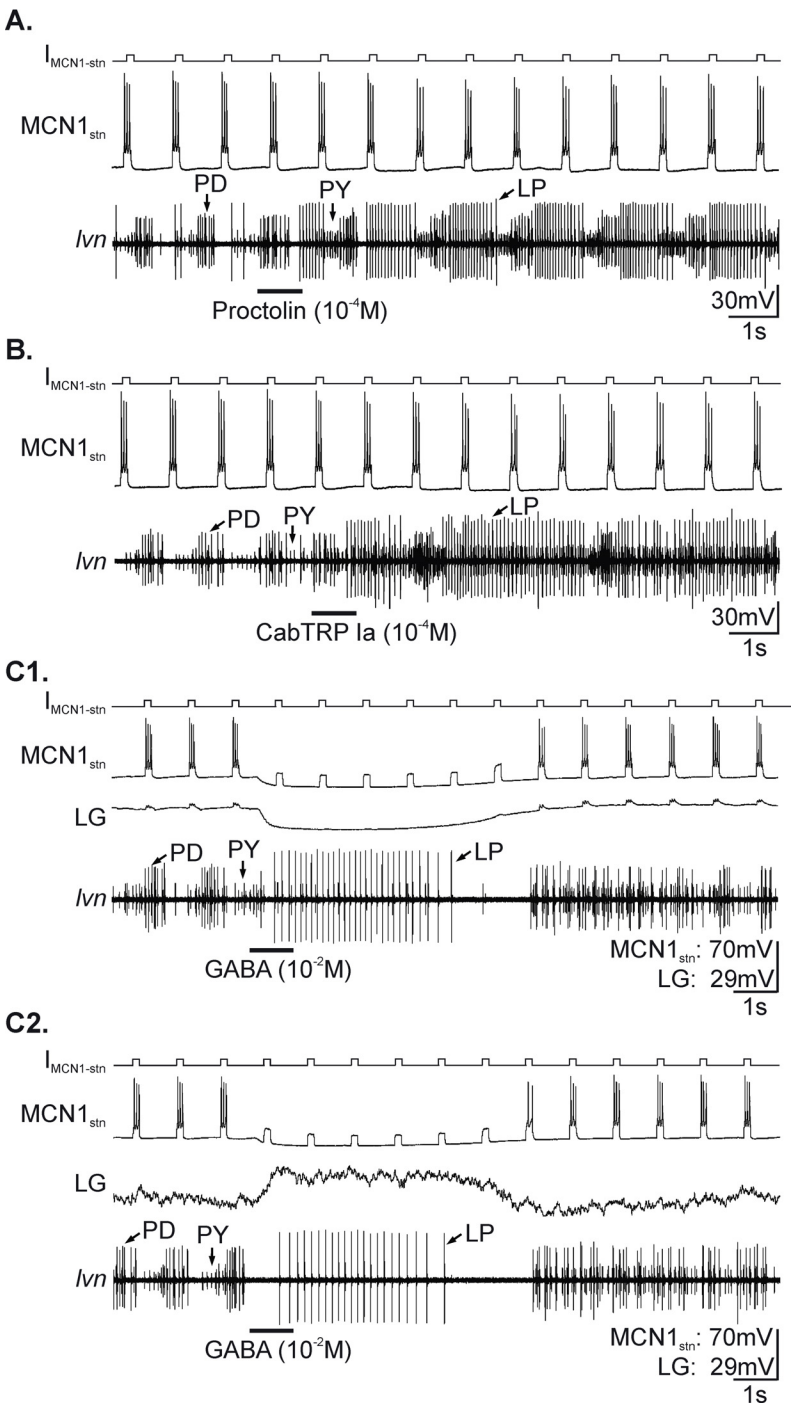

Figure 6. GABA is the only MCN1 cotransmitter to influence to STG terminals of MCN1 ($MCN1_{STG}$). Intra-axonal recording of MCN1 ($MCN1_{stn}$) near the entrance to the STG revealed no influence of either **(A)** proctolin or **(B)** CabTRP Ia on

$MCN1_{STG}$, despite their ability to influence the pyloric rhythm (*lvn*). Most hyperpolarized V_m: proctolin application, -53 mV; CabTRP Ia application, -53 mV. **(C)** Focal GABA application reversibly hyperpolarized $MCN1_{STG}$ and suppressed its rhythmic activation, independent of GABA inhibition of LG. Most hyperpolarized V_m: MCN1, -68 mV; LG, -84 mV. **(C1)** MCN1 and LG both hyperpolarized in response to GABA application. **(C2)** When the LG neuron was held, by constant amplitude current injection, at a membrane potential that was more hyperpolarized than the reversal potential for its GABA response, GABA application depolarized LG but still hyperpolarized MCN1. Most hyperpolarized V_m: MCN1, -67 mV; LG, -99 mV. In all panels, MCN1 was rhythmically activated by constant amplitude depolarizing current (top trace, +1 nA).

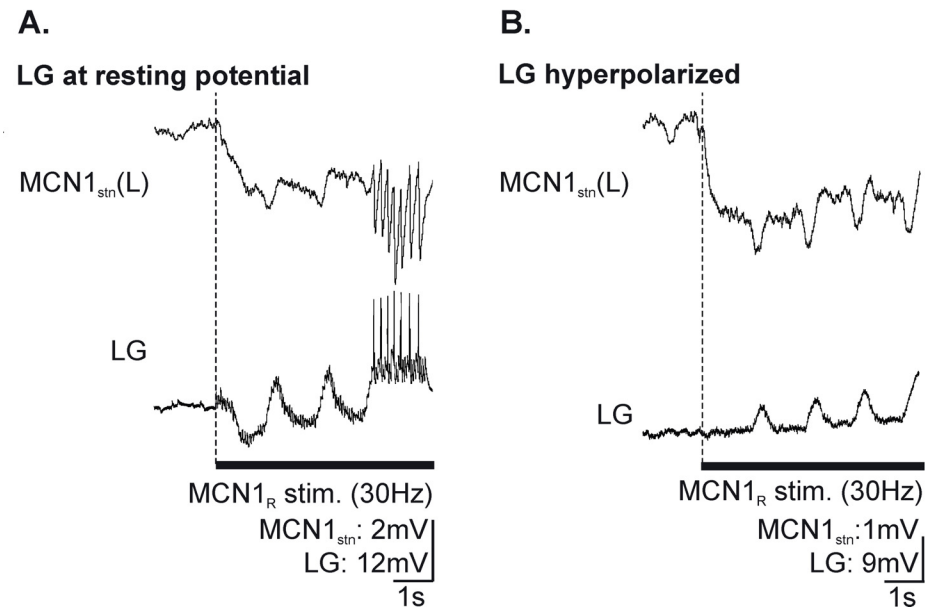

Figure 7. MCN1 stimulation hyperpolarizes the contralateral $MCN1_{STG}$. **(A)** At the start of $MCN1_{Right}$ stimulation, there was a hyperpolarization of both $MCN1_{STG\text{-}Left}$ and LG. The hyperpolarization in LG resulted from inhibitory input from Int1. Most hyperpolarized V_m: MCN1, -64 mV; LG, -77 mV. **(B)** With LG held close to the reversal potential for the Int1-mediated inhibition by constant amplitude hyperpolarizing current (-5 nA), $MCN1_{Right}$ stimulation did not hyperpolarize LG but $MCN1_{STG\text{-}Left}$ still hyperpolarized. Most hyperpolarized V_m: MCN1, -65 mV.

hyperpolarized membrane potential such that it did not hyperpolarize in response to MCN1 stimulation (n=3) (Fig. 7B).

Applied MCN1 Cotransmitter Actions on Gastric Mill Follower Neurons

Previous studies showed that proctolin and CabTRP Ia activate the same voltage-dependent current in all of their pyloric neuron targets, and that these two peptides have convergent actions on many of these targets (Swensen & Marder, 2000, 2001). However, the response of most gastric mill neurons to application of these peptides has not been determined. We therefore examined the response of all gastric mill follower motor neurons to focal application of proctolin and CabTRP Ia (see below). This included the MG and GM protractor motor neurons and the DG and AM retractor motor neurons. No gastric mill neurons responded to focal peptide applications onto their somata whereas, as reported below, neuropil applications consistently elicited responses to these peptides. Although there are no previous studies focused on the influence of proctolin and CabTRP Ia on these gastric mill neurons, the response of all gastric mill neurons to GABA application has been documented (Swensen et al., 2000). All of the gastric mill neurons except for Int1 respond to GABA application with a net hyperpolarizing response. As indicated above, Int1 is excited by GABA application.

As was the case during MCN1 stimulation (Fig. 2A), the protractor neuron GM was consistently excited by pressure application of proctolin, as long as it

was close to or above spike threshold (saline: 1.3 ± 1.2 Hz; proct.: 3.7 ± 1.9 Hz, n=23, $p<0.01$). GM also exhibited a consistent excitatory response to CabTRP Ia application (saline: 1.0 ± 1.0 Hz; CabTRP Ia: 2.9 ±1.6 Hz, n=25, $p<0.01$). In contrast, as shown previously (Swensen et al., 2000), GABA application hyperpolarized GM in 8/9 preparations. Each of these cotransmitter actions on GM persisted in low Ca^{2+} saline (proctolin, n=5; CabTRP Ia, n=6; GABA, n=8).

Unlike the GM neuron, the protractor neuron MG was responsive to CabTRP Ia and GABA but not to proctolin application (n=11) (Fig. 8). We tested the MG response to proctolin at both its resting potential (~-60 mV) and at membrane potentials well above spike threshold, either with constant amplitude or rhythmic depolarizing current injections. The latter approach was used to ensure that MG was sufficiently depolarized to exhibit a response, in case its responsiveness was only present at depolarized potentials (Swensen & Marder, 2000). In these latter experiments, proctolin application did not alter the MG firing frequency (saline: 2.9 ± 2.5 Hz; proct.: 2.9 ± 2.4 Hz; n=6, $p>0.2$). As is evident in Figure 8A, these proctolin applications effectively influenced the pyloric rhythm. The MG response to CabTRP Ia was considerably stronger than that of the GM neuron, and it also responded vigorously even when it was subthreshold before CabTRP Ia application (saline: 1.2 ± 2.5 Hz; CabTRP: 14.3 ± 6.2 Hz; n=12, $p<0.01$) (Fig. 8B). We also reaffirmed that MG exhibited a hyperpolarizing response to GABA (n=6) (Fig. 8C) (Swensen et al., 2000). The MG response to GABA persisted in low Ca^{2+} saline (n=3).

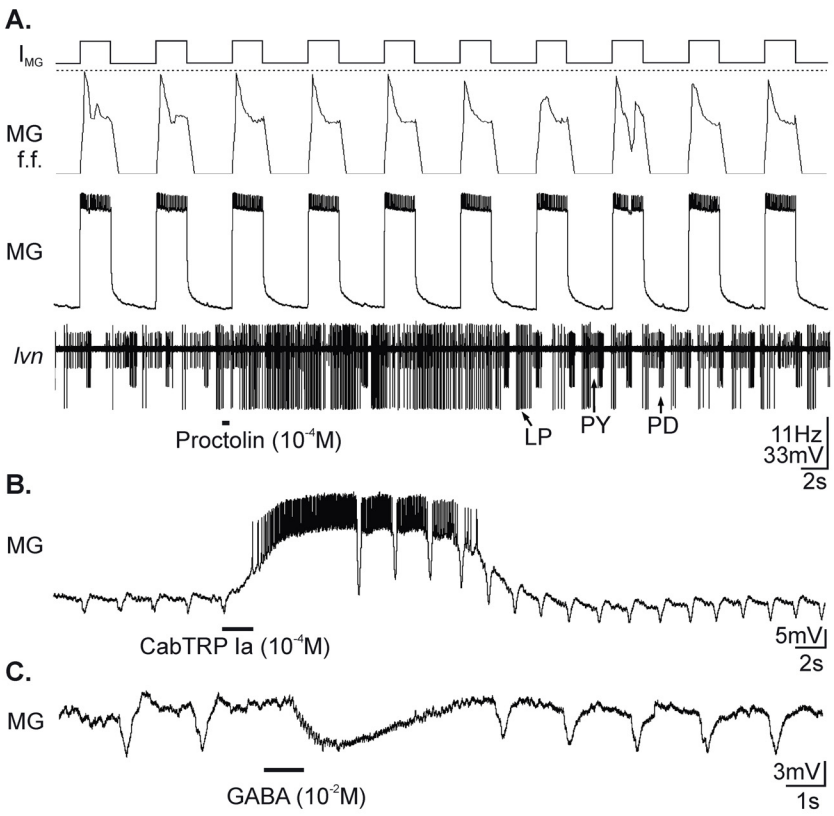

Figure 8. Focally applied CabTRP Ia and GABA, but not proctolin, influence the MG neuron. **(A)** Proctolin application did not alter MG neuron activity, despite its ability to influence the pyloric rhythm (*lvn*). MG was rhythmically depolarized and hyperpolarized by constant amplitude current (top trace: +1 nA; -1 nA) and its firing frequency was monitored continuously (second trace). Dotted line indicates the maximum firing frequency before proctolin application. Most hyperpolarized V_m: -80 mV. **(B)** CabTRP Ia application reversibly excited the MG neuron, eliciting a prolonged action potential burst. Most hyperpolarized V_m: -70 mV. **(C)** GABA application reversibly hyperpolarized MG. Most hyperpolarized V_m: -70 mV. Panels B and C are from the same preparation**.**

Because MG and LG are electrically coupled, it was possible that there was only a direct excitatory action of CabTRP Ia on one of these two neurons, which in turn activated the other neuron. To test this possibility, we maintained one or the other of these neurons at a hyperpolarized membrane potential (via intracellular current injection) while applying CabTRP Ia. At these times, the hyperpolarized neuron either exhibited a small amplitude, subthreshold depolarization or no response while the other neuron exhibited its usual strong bursting response (n=10). An example of this result during hyperpolarization of the MG neuron is shown in Figure 9.

As occurred during MCN1 stimulation (Fig. 2B), focal application of either proctolin or CabTRP Ia excited the retractor neuron AM (n=4 each) (Fig. 10A,B). During proctolin application, the AM firing frequency nearly doubled (saline: 3.3 $\pm$ 3.2 Hz; proct.: 6.1 $\pm$ 3.5 Hz; n=4, $p<0.05$). Similarly, it increased during CabTRP Ia application (saline: 2.2 $\pm$ 3.1 Hz; CabTRP Ia: 4.3 $\pm$ 3.3 Hz; n=5, $p<0.05$). Both of these responses persisted in low Ca^{2+} saline (proctolin, n=2; CabTRP Ia, n=3). As shown previously (Swensen et al., 2000), GABA application consistently hyperpolarized this neuron (n=3) (Fig. 10C).

The retractor neuron DG was modestly but consistently excited by proctolin application (saline: 3.5 $\pm$ 3.2 Hz; proct.: 4.3 $\pm$ 2.7 Hz; n=14, $p<0.01$). DG was also excited by CabTRP Ia application, albeit only when it was close to or above spike threshold (saline: 4.2 $\pm$ 4.3 Hz; CabTRP: 6.0 $\pm$ 4.1 Hz; n=12, $p<0.05$). As was the case with the other gastric mill follower neurons, GABA

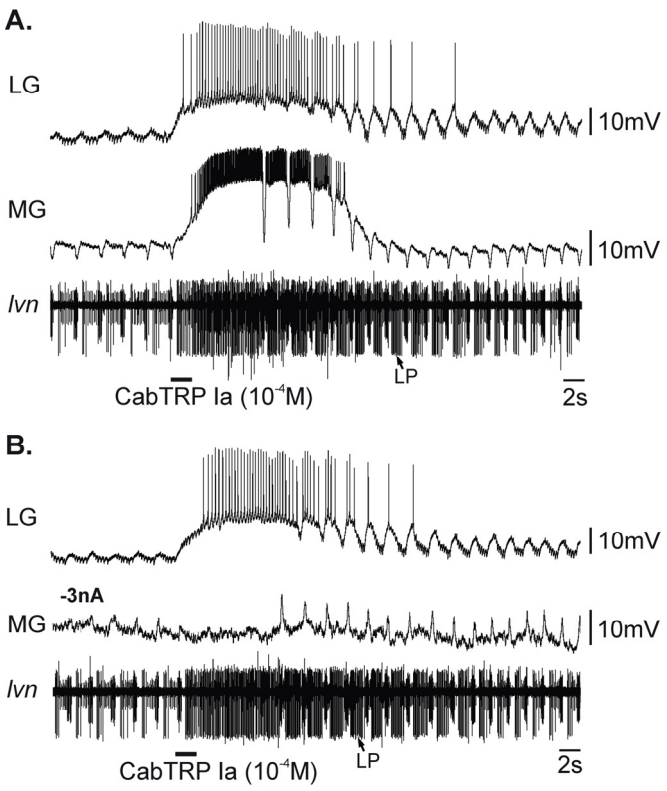

Figure 9. Focally applied CabTRP Ia activates the LG neuron independent of MG neuron activity. **(A)** CabTRP Ia application elicited action potential bursts in the LG and MG neurons, as well as exciting the pyloric rhythm (*lvn*). Most hyperpolarized V_m: LG, -55 mV; MG, -72 mV. **(B)** CabTRP Ia continued to excite the LG neuron, and the pyloric rhythm, when MG activity was suppressed by constant amplitude hyperpolarizing current. Most hyperpolarized V_m: LG, -55 mV; MG, -98 mV. Note that MG was sufficiently hyperpolarized that the normal pyloric-timed hyperpolarizations in this neuron became rhythmic depolarizations.

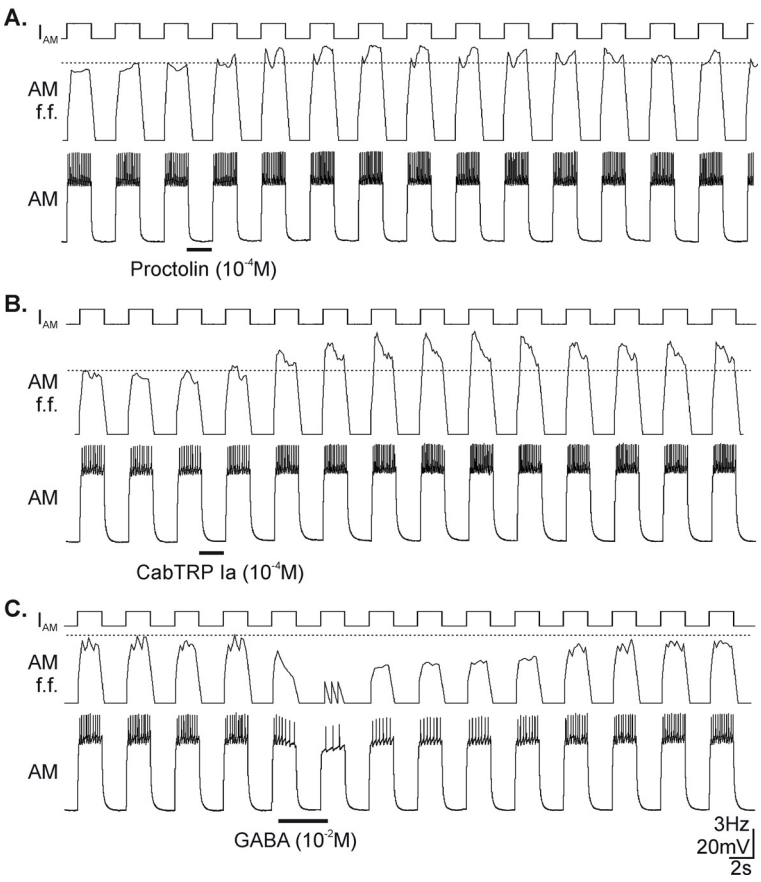

Figure 10. Focal application of each MCN1 cotransmitter influenced the AM neuron. Both **(A)** proctolin and **(B)** CabTRP Ia application increased AM neuron activity in response to constant amplitude depolarizing current pulses. Note the increase in firing frequency after each application (second trace). Dotted lines indicate the maximum firing frequency before transmitter application. **(C)** GABA application reversibly reduced AM activity. In all panels, AM was rhythmically activated by constant amplitude depolarizing current (top trace: +2nA). Most hyperpolarized V_m: (A) -67 mV; (B) -67 mV; (C) -68 mV.

application hyperpolarized DG (n=7) (Swensen et al., 2000).

MCN1-Released Cotransmitter Actions on Gastric Mill Follower Neurons

To determine the set of MCN1-released cotransmitters that influenced the gastric mill follower motor neurons, we stimulated MCN1 in the presence of agents that either suppressed or enhanced the actions of one of its cotransmitters. Specifically, we used the tachykinin receptor blocker spantide I (5 X 10^{-5} M) to suppress the actions of CabTRP Ia (Wood et al., 2000; Wood & Nusbaum, 2002), the endopeptidase inhibitor phosphoramidon (10^{-5} M) to prolong the actions of CabTRP Ia (Wood et al., 2000), the aminopeptidase inhibitor actinonin (10^{-4} M) to prolong proctolin actions (Coleman et al., 1994; Wood & Nusbaum, 2002) and PTX to suppress a subset of GABA actions (Blitz & Nusbaum, 1999; Swensen et al., 2000). Previous work showed that phosphoramidon does not influence proctolin actions (Wood et al., 2000). Actinonin also appears to not affect CabTRP Ia actions (see below). No receptor antagonist for proctolin has been identified.

The only MCN1 action on the gastric mill neurons that was altered by the presence of PTX was the aforementioned MCN1 excitation of Int1 (Fig. 5). Additionally, none of the gastric mill follower motor neurons exhibited transmitter-mediated PSPs in response to MCN1 stimulation (n>6 for each neuron), reducing the likelihood that MCN1 actions on these neurons was mediated by an

ionotropic GABAergic action.

We showed previously that, in the presence of spantide I, the retractor neuron DG response to MCN1 stimulation switched from rhythmic bursting to tonic firing (Wood et al., 2000). In our current experiments, we determined that the presence of spantide I also reduced the DG neuron firing frequency in response to MCN1 stimulation (saline, 13.3 ± 3.7 Hz; spantide I, 6.0 ± 2.0 Hz; $n=7$, $p<0.01$). In all 7 of these experiments, the DG neuron was not active before MCN1 was stimulated. We also assessed whether the remaining DG neuron response to MCN1 that persisted in the presence of spantide I was due to the action of proctolin. To this end, we determined whether this DG response was prolonged by the proctolin peptidase inhibitor actinonin. We found, however, that this was not the case (saline: 15.8 ± 13.5 sec; actinonin: 10.7 ± 6.2 sec; $n=4$, $p>0.05$). This lack of actinonin action on the DG response occurred despite the fact that actinonin consistently prolonged the MCN1 excitation of other gastric mill neurons (see below).

There was no evident GABAergic ionotropic or inhibitory metabotropic component to the DG response to MCN1 stimulation. First, as stated above, no unitary PSPs were recorded in DG during MCN1 stimulation ($n>30$). Second, DG never exhibited an initial hyperpolarizing response to these stimulations ($n>30$). Any such inhibitory action would be most evident during the first 5-10 sec of MCN1 stimulation because of the initially slow buildup of its peptidergic actions (Coleman et al., 1995; Wood et al., 2000). Third, there was not a depolarizing,

inhibitory GABAergic action on DG. We tested this possibility by stimulating MCN1 while holding DG at a depolarized membrane potential that was just suprathreshold (~-50 mV) and therefore was above the reversal potential for any possible inhibitory action. During this manipulation, there was no initial hyperpolarization (n=6). Fourth, there was no evident change in the DG response to MCN1 stimulation during PTX superfusion (saline: 13.9 ± 3.3 Hz; PTX: 12.0 ± 4.0; n=14, $p>0.05$). Fifth, no PTX-sensitive DG response to MCN1 stimulation was revealed by coapplying spantide I and PTX (spantide I: 6.0 ± 2.0 Hz; spantide I/PTX: 5.7 ± 1.5; n=7, $p>0.05$).

MCN1 excitation of the retractor AM neuron appeared to result from both CabTRP Ia and proctolin release. We assessed the influence of each MCN1-released peptide by determining whether MCN1 excitation of the AM neuron was prolonged when either CabTRP Ia or proctolin degradation was suppressed by the peptidase inhibitor phosphopramidon (Fig. 11) or actinonin (Fig. 12), respectively. During phosphoramidon superfusion, MCN1 excitation of AM was consistently prolonged after termination of MCN1 stimulation relative to saline superfusion (pre-phospho.: 25.2 ± 14.2 sec; phospho.: 227.4 ± 80.5 sec; post-phospho.: 38.9 ± 33.8 sec; n=6; $p<0.001$, pre-phospho. vs. phospho.). The MCN1 excitation of AM also persisted for longer than control values in the presence of actinonin (pre-actinonin: 26.2 ± 11.9 sec; actinonin: 203.8 ± 77.7 sec; post-actinonin: 52.5 ± 18.4 sec; n=5; $p<0.005$, pre-actinonin vs. actinonin).

Experiments with phosphoramidon and actinonin indicated that the

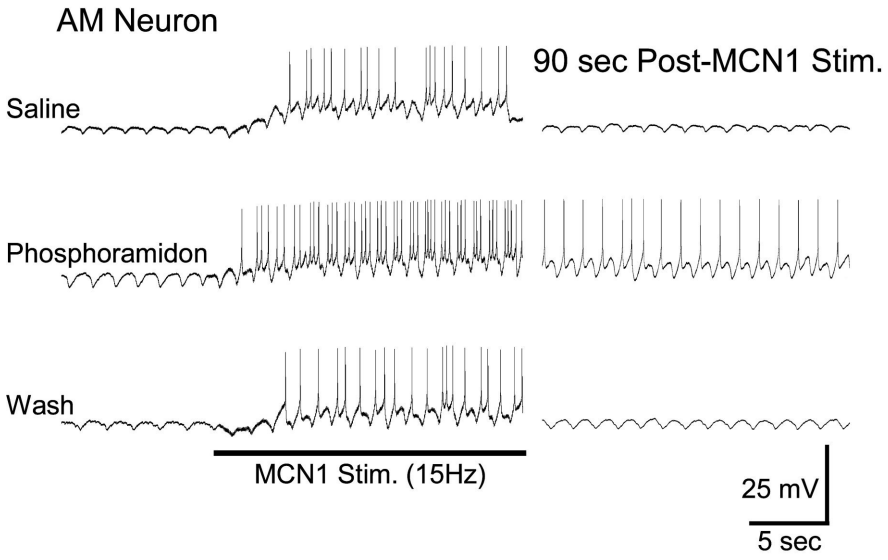

Figure 11. The endopeptidase inhibitor phosphoramidon enhanced and prolonged the AM neuron response to MCN1 stimulation. Before MCN1 stimulation under each condition, the AM neuron was subthreshold but exhibited pyloric-timed hyperpolarizations. During saline superfusion, MCN1 stimulation consistently activated the AM neuron. AM neuron activity subsided soon after the end of MCN1 stimulation. Phosphoramidon (10^{-5} M) superfusion, which enhances the actions of CabTRP Ia but not those of either proctolin or GABA, reversibly strengthened and prolonged the AM response to MCN1 stimulation. Most hyperpolarized Vm: Saline, -60 mV; Phosphoramidon, -57 mV; Saline Wash, -60 mV.

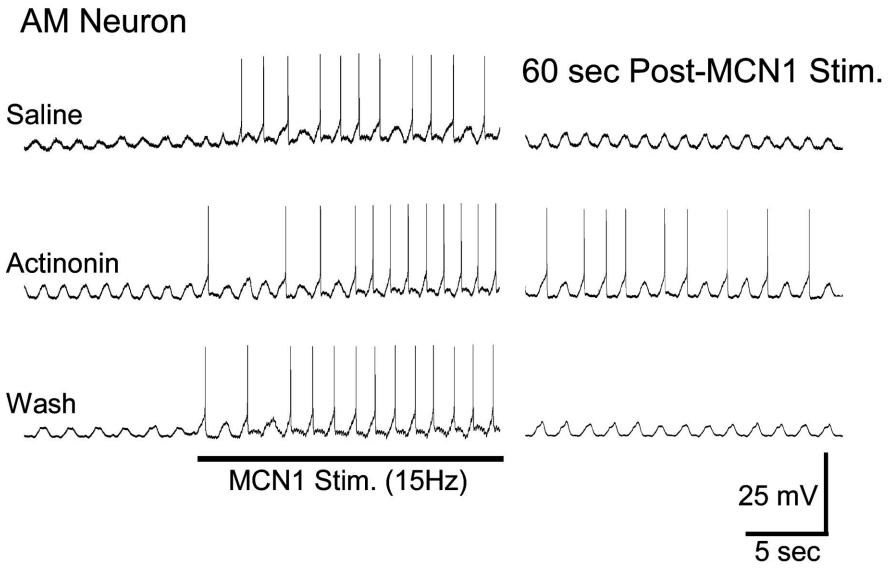

Figure 12. The aminopeptidase inhibitor actinonin prolonged the AM neuron response to MCN1 stimulation. Actinonin (10^{-4} M), which enhances proctolin actions but not those of CabTRP Ia or GABA, reversibly prolonged the AM neuron response to MCN1 stimulation. Most hyperpolarized Vm: Saline, -64 mV; Actinonin, -64 mV; Saline Wash, -57 mV.

protractor neuron GM was also sensitive to both MCN1-released peptides. However, unlike the MCN1 influence on the AM neuron, the ability of these peptidase inhibitors to prolong the MCN1 excitation of GM was only evident at higher MCN1 stimulation frequencies. Specifically, when we used the same modest MCN1 stimulation protocol (5-10 Hz tonic stimulation) that we used for the AM experiments, the duration of the post-stimulus MCN1 excitation of GM was unaffected by either actinonin (pre-actinonin: 23.9 ± 24.4 sec; actinonin: 29.4 ± 27.0 sec; post-actinonin: 22.4 ± 20.4 sec; n=4; $p>0.3$, pre-actinonin vs. actinonin) or phosphoramidon (pre-phospho.: 17.2 ± 13.4 sec; phopho.: 38.0 ± 37.1 sec; post-phospho.: 34.0 ± 30.2 sec; n=4; $p>0.1$, pre-phospho. vs. phospho.). This inability of these peptidase inhibitors to prolong MCN1 excitation of GM was not a consequence of there being a variable effectiveness of peptidase inhibitor action. For example, when we recorded simultaneously from GM and AM, there was the usual approximately 10-fold increase in duration of the AM response to MCN1 stimulation. In contrast, when we increased the MCN1 stimulation frequency (30 Hz tonic stimulation), the duration of the post-stimulus MCN1 excitation of GM was prolonged by actinonin (pre-actinonin: 16.3 ± 16.6 sec; actinonin: 74.2 ± 51.3 sec; post-actinonin: 14.3 ± 5.0 sec; n=5; $p<0.05$, pre-actinonin vs. actinonin). At the increased MCN1 stimulation frequency, phosphoramidon also prolonged the duration of the GM response to MCN1 (pre-phospho.: 14.8 ± 4.5 sec; phospho.: 32.7 ± 11.3 sec; post-phospho.: 8.0 ± 1.6 sec; n=3; $p<0.05$, pre-phospho. vs. phospho.). We did not manipulate the influence of MCN1-released CabTRP Ia and proctolin on the protractor MG

neuron because our direct peptide application experiments indicated that MG only responded directly to CabTRP Ia application (Fig. 8).

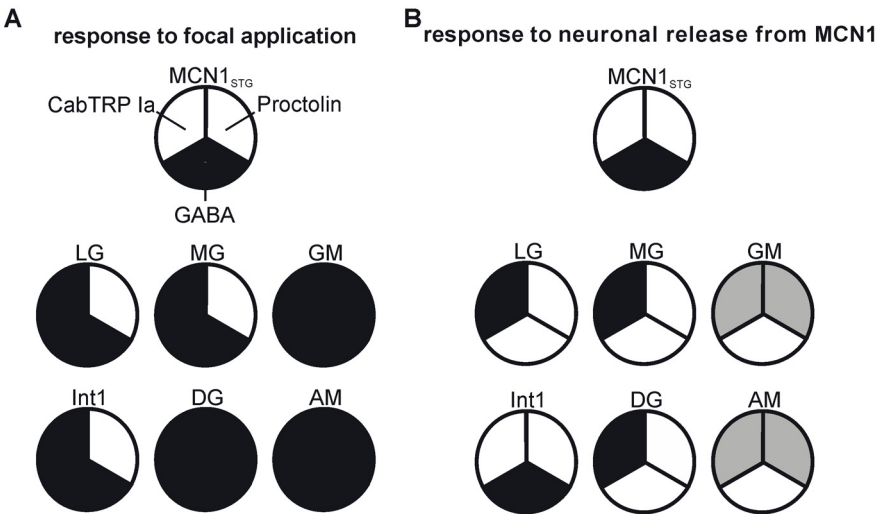

Figure 13. Most gastric mill neurons respond to application of more of the MCN1 cotransmitters than to their release from MCN1. (A) All six of the studied gastric mill neurons respond to focal application of the MCN1 cotransmitters CabTRP Ia and GABA, while only three of these six neurons respond to proctolin application. $MCN1_{STG}$ only responds to GABA application. (B) Four of the six gastric mill neurons, plus $MCN1_{STG}$, are each influenced by only one of the three MCN1-released cotransmitters. MCN1 uses only CabTRP Ia to excite the LG, MG and DG neurons, while it uses only GABA to excite Int1 and inhibit the contralateral $MCN1_{STG}$. The follower motor neurons AM and GM are each excited by both MCN1-released peptides. Labels: white sections, no response to the indicated transmitter; black, positive response to the indicated transmitter; gray, positive response when the neuron is supra-threshold.

DISCUSSION

Divergent cotransmitter actions on gastric mill CPG neurons

Cotransmission is well-established in many species, but there is only limited information available regarding its consequences for neuronal circuit activity (Blitz & Nusbaum, 1999; Nusbaum et al., 2001; Thirumalai & Marder, 2002; Sun et al., 2003). In this paper we have extended previous studies by determining the set of cotransmitters used by an identified projection neuron to drive rhythmic neuronal activity from a defined motor circuit (Fig. 13). Specifically, we have shown that the MCN1 projection neuron directly excites the reciprocally inhibitory CPG neurons LG and Int1 via distinct cotransmitters. MCN1 excitation of Int1 is exclusively GABAergic. The only transmitter-mediated action of MCN1 on LG is a slow, CabTRP Ia-mediated excitation (Wood et al., 2000). MCN1 also selectively influenced the contralateral $MCN1_{STG}$ via GABAergic inhibition. In contrast, MCN1 used both of its peptide transmitters to excite several gastric mill follower motor neurons (Fig. 13B).

There was generally a good correspondence between the gastric mill neurons excited by focally applied CabTRP Ia and/or proctolin and those which responded to the MCN1 release of these peptides (Fig. 13). Among these neurons, only the DG neuron exhibited a response to applied peptide (proctolin) without a corresponding response to MCN1 stimulation. This unmatched DG response to proctolin may be caused by a spatial segregation of its proctolin

receptors, whose function may be to mediate the DG response to MCN7, a second proctolin-containing projection neuron that excites DG (Blitz et al., 1999). Whether the residual DG response to MCN1 stimulation during spantide I application resulted from the lack of a complete suppression of this CabTRP Ia action by spantide or from a PTX-insensitive, GABAergic excitation remains to be determined. It also remains possible that the aminopeptidase inhibitor actinonin enhances MCN1 excitation of the AM and GM neurons because it enables MCN1-released proctolin to extend its diffusion distance and bind with receptors that are normally inaccessible. These receptors might normally act to bind proctolin released from one or both of the other two proctolinergic neurons (MPN, MCN7) that innervate the STG (Blitz et al., 1999). However, neither MPN nor MCN7 appear to influence the GM neuron (Blitz and Nusbaum, 1997; Blitz et al., 1999). It remains to be determined whether the AM neuron responds to either MPN or MCN7. The possibility of a similar scenario underlying the ability of the endopeptidase inhibitor phosphoramidon to enhance the excitation of AM and GM by MCN1-released CabTRP Ia is less likely, because MCN1 is the only source of neuronally released CabTRP Ia in the STG (Blitz et al., 1999). Further supporting the likelihood that these peptidase inhibitors were not in general extending the range of these peptides is that the action of neuronally released peptides is not limited to a synaptic cleft region (Karhunen et al., 2001). Instead, they commonly diffuse considerable distances to reach their postsynaptic receptors (Jan & Jan, 1982; Burnstock, 2004).

There was less of a correspondence between the gastric mill neuron responses to applied GABA and MCN1-released GABA (Fig. 13). For example, the LG neuron responded consistently to focal GABA application but there was no evidence for a GABAergic component to the MCN1 influence on this neuron (Wood et al., 2000; this paper). Similarly, GABA both excited and inhibited Int1, but MCN1 had only excitatory GABAergic actions on Int1. All of the gastric mill follower motor neurons were hyperpolarized by GABA application but none showed an inhibitory component in their response to MCN1 stimulation. Presumably, the GABA receptors on these neurons that were not relevant to the MCN1 actions mediate their responses to other GABAergic neurons (Swensen et al., 2000).

The third MCN1 cotransmitter, proctolin, had no direct influence on the gastric mill CPG. However, it is likely that MCN1 uses proctolin to indirectly influence the gastric mill rhythm because MCN1-released proctolin excites the pyloric rhythm and the pyloric rhythm regulates the speed of the gastric mill rhythm (Bartos et al., 1999; Wood & Nusbaum, 2002).

Functional consequences of divergent cotransmitter actions

The fast GABAergic and slow peptidergic actions of MCN1 on LG and Int1 are pivotal to enabling MCN1 to activate the gastric mill rhythm (Coleman et al., 1995). Having distinct time courses to these two actions is important because

MCN1 cotransmitter release is largely restricted to the retractor phase of the gastric mill rhythm, when Int1 is active and LG is hyperpolarized (Coleman & Nusbaum, 1994; Coleman et al., 1995). The fast excitation of Int1 has an immediate impact on its firing rate. The slow excitation of the LG neuron during the retractor phase plays two roles (Coleman et al., 1995; Bartos et al., 1999; Beenhakker et al., 2005). First, it enables an extended retractor phase duration while eventually enabling LG to escape from Int1-mediated inhibition and initiate a burst of action potentials. Second, its slow decay enables the LG burst to persist for several seconds.

The function of the MCN1 inhibition of the contralateral $MCN1_{STG}$ remains to be determined. However, both MCN1s are activated by the same sensory inputs, suggesting that their mutual inhibition would occur under physiological conditions (Beenhakker et al., 2004; Blitz et al., 2004). At these times, however, these projection neurons effectively drive the gastric mill rhythm, so their mutual presynaptic inhibition may regulate but does not suppress their transmitter release. There is a comparable situation in the *Aplysia* feeding system involving a pair of histaminergic neurons that are reciprocally inhibitory but coactive during the feeding motor pattern (Evans et al., 1999).

It is not clear why MCN1 uses only CabTRP Ia to influence the LG neuron, given that it uses both peptide cotransmitters to excite many gastric mill follower neurons. This same convergence occurs on most pyloric circuit neurons (Swensen & Marder, 2000; Wood et al., 2000; Wood & Nusbaum, 2002).

Moreover, CabTRP Ia and proctolin converge to activate the same voltage-dependent current in all of their pyloric targets (Swensen & Marder, 2000, 2001).

The use of only CabTRP Ia by MCN1 to excite the LG neuron may relate to other constraints on this system. For example, the modulatory proctolin neuron (MPN) and MCN1 share the cotransmitters GABA and proctolin (Nusbaum & Marder, 1989a; Blitz et al., 1999). These two projection neurons also both excite the pyloric rhythm, albeit evoking distinct versions of this rhythm (Blitz et al., 1999; Wood & Nusbaum, 2002). In contrast, whereas MCN1 stimulation elicits the gastric mill rhythm, MPN stimulation suppresses it (Blitz & Nusbaum, 1997). This MPN suppression results largely from its GABAergic inhibition of projection neurons, including MCN1, in the CoGs (Blitz & Nusbaum, 1999). If the LG neuron were excited by proctolin release from MCN1, then MPN would likely have a comparable influence on LG and therefore would activate the gastric mill rhythm instead of suppressing it. This likelihood results from the facts that neuronally-released peptides often diffuse relatively long distances (Jan & Jan, 1982; Burnstock, 2004; Seal & Edwards, 2006) and these two projection neurons share proctolinergic actions on many STG neurons (Nusbaum & Marder, 1989b; Blitz et al., 1999; Wood et al., 2000; Wood & Nusbaum, 2002).

Convergence of cotransmitter actions onto the same postsynaptic target is established in several systems (Jan & Jan, 1982; Jonas et al., 1998; Vilim et al., 2000; Koh et al., 2003; Li et al., 2004; Burnstock, 2004; Koh & Weiss, 2005; Nishimaru et al. 2005). Divergence of cotransmission onto separate targets has

also been reported (Jan & Jan, 1982; Sun et al., 2003; Dugue et al., 2005; Samano et al. 2006). When convergence results from corelease that pairs an ionotropic and metabotropic action, the metabotropic action often causes an initial non-linear alteration of the ionotropic action, after which it persists as a prolonged change in the intrinsic properties of the target neuron (Fox & Lloyd, 2001; Vilim et al., 2000; Koh et al., 2003; Koh & Weiss, 2005). At some synapses with convergent cotransmitter actions, there can also be a functional, firing frequency-dependent divergence when neuropeptide release requires a higher firing frequency than the coreleased small molecule transmitter (Whim & Lloyd, 1989; Peng & Horn, 1991; Vilim et al., 2000). With respect to MCN1 actions on the gastric mill circuit, a firing frequency-dependent divergence of cotransmitter actions is not likely to occur because MCN1 excitation of LG persisted at firing frequencies (2 Hz) below those at which MCN1 initiates the gastric mill rhythm (>5 Hz). This is also the case for the cotransmitter motor neuron B16 in *Aplysia* (Vilim et al., 2000).

The stomatogastric system has been the focus of several previous cotransmission studies. One example of intraganglionic cotransmission involves modulation of the pyloric rhythm by the gastropyloric receptor (GPR) sensory neuron, which uses serotonin and acetylcholine to have convergent and divergent actions on different STG neurons (Katz & Harris-Warrick, 1989, 1990, 1991; Kiehn & Harris-Warrick, 1992). The pyloric rhythm is also modulated by application of peptide cotransmitters, localized to the same projection neuron,

that excite separate pyloric motor neurons (Thirumalai & Marder, 2002).

There are also two examples of inter-ganglionic cotransmitter divergence in the stomatogastric system. First, the paired inferior ventricular nerve (IVN) projection neurons appear to use only histamine in the STG to influence the pyloric and gastric mill rhythms, despite the presence of a peptide cotransmitter (Christie et al., 2004). The peptide cotransmitter is suggested to mediate the IVN neuron activation of CoG projection neurons, including MCN1 (Christie et al., 2004). Second, MPN elicits a proctolin-mediated pyloric rhythm in the STG while having only GABAergic actions on CoG projection neurons (Nusbaum & Marder, 1989a,b; Blitz & Nusbaum, 1999; Wood & Nusbaum, 2002). It is worth noting that, thus far, there is no evidence that the IVN or MPN cotransmitters are segregated to separate ganglia.

The present work extends these previous studies by establishing that cotransmission can be used to enable coreleased transmitters to affect separate CPG targets and to do so via distinct time courses, thereby enabling the activation of a complete motor circuit. It will be interesting to next determine whether these distinct cotransmitter actions on the gastric mill CPG can be regulated separately. This may well be the case insofar as the GPR sensory neuron appears to selectively weaken MCN1 excitation of the LG neuron (Beenhakker et al., 2005). Such situations could thereby enable a single cotransmitter neuron to have altered actions on its target circuit under different conditions.

ABBREVIATIONS

AM, anterior median; CabTRP Ia, *Cancer borealis* tachykinin related peptide Ia; CoGs, commissural ganglia; CPG, central pattern generator; DG, dorsal gastric; GM, gastric mill; GPR, gastropyloric receptor; IC, inferior cardiac; Int1, interneuron 1; *ion*, inferior oesophageal nerve; IV, inferior ventricular; LG, lateral gastric; LP, lateral pyloric; MCN1, modulatory commissural neuron 1; MG, medial gastric; MPN, modulatory proctolin neuron; PD, pyloric dilator; PTX, picrotoxin; STG, stomatogastric ganglion; STNS, stomatogastric nervous system; VD, ventricular dilator.

REFERENCES

Bartos, M. & Nusbaum M.P. (1997) Intercircuit control of motor pattern modulation by presynaptic inhibition. *J. Neurosci.,* **17**, 2247-2256.

Bartos, M., Manor, Y., Nadim, F., Marder, E. & Nusbaum, M.P. (1999) Coordination of fast and slow rhythmic neuronal circuits. *J. Neurosci.*, **19**, 6650-6660.

Beenhakker, M.P. & Nusbaum, M.P. (2004) Mechanosensory activation of a motor circuit by coactivation of two projection neurons. *J. Neurosci.*, **24**, 6741-6750.

Beenhakker, M.P., Blitz, D.M. & Nusbaum, M.P. (2004) Long-lasting activation of rhythmic neuronal activity by a novel mechanosensory system in the crustacean stomatogastric nervous system. *J. Neurophysiol.*, **91**, 78-91.

Beenhakker, M.P., DeLong, N.D., Saideman, S.R., Nadim, F. & Nusbaum, M.P. (2005) Proprioceptor regulation of motor circuit activity by presynaptic inhibition of a modulatory projection neuron. *J. Neurosci.*, **25**, 8794-8806.

Blitz, D.M. & Nusbaum, M.P. (1997) Motor pattern selection via inhibition of parallel pathways. *J. Neurosci.*, **17**, 4965-4975.

Blitz, D.M. & Nusbaum, M.P. (1999) Distinct functions for cotransmitters mediating motor pattern selection. *J. Neurosci.*, **19**, 6774-6783.

Blitz, D.M., Christie, A.E., Coleman, M.J., Norris, B.J., Marder, E. & Nusbaum,

M.P. (1999) Different proctolin neurons elicit distinct motor patterns from a multifunctional neuronal network. *J. Neurosci.*, **19**, 5449-5463.

Blitz, D.M., Beenhakker, M.P. & Nusbaum, M.P. (2004) Different sensory systems share projection neurons but elicit distinct motor patterns. *J. Neurosci.*, **24**, 11381-11390.

Burnstock, G. (2004) Cotransmission. *Curr. Opin. Pharmacol.*, **4**, 47-52.

Cazalis, M., Dayanithi, G. & Nordmann, J.J. (1985) The role of patterned burst and interburst interval on the excitation-coupling mechanism in the isolated rat neural lobe. *J. Physiol.*, **369**, 45-60.

Christie, A.E., Lundquist, C.T., Nassel, D.R. & Nusbaum, M.P. (1997) Two novel tachykinin-related peptides from the nervous system of the crab *Cancer borealis*. *J. Exp. Biol.*, **200**, 2279-2294.

Christie, A..E., Stein, W., Quinlan, J.E., Beenhakker, M.P., Marder, E., Nusbaum, M.P. (2004) Actions of a histaminergic/peptidergic projection neuron on rhythmic motor patterns in the stomatogastric nervous system of the crab *Cancer borealis*. *J. Comp. Neurol.*, **469**, 153-169.

Coleman, M.J., Nusbaum, M.P., Cournil, I. & Claiborne, B.J. (1992) Distribution of modulatory inputs to the stomatogastric ganglion of the crab, *Cancer borealis*. *J. Comp. Neurol.*, **325**, 581-594.

Coleman, M.J., Konstant, P.H., Rothman, B.S. & Nusbaum, M.P. (1994)

Neuropeptide degradation produces functional inactivation in the crustacean nervous system. *J. Neurosci.*, **14**, 6205-6216.

Coleman, M.J. & Nusbaum, M.P. (1994) Functional consequences of compartmentalization of synaptic input. *J. Neurosci.*, **14**, 6544-6552.

Coleman, M.J., Meyrand, P. & Nusbaum, M.P. (1995) A switch between two modes of synaptic transmission mediated by presynaptic inhibition. *Nature*, **378**, 502-505.

Combes, D., Simmers, J. & Moulins, M. (1995) Structural and functional characterization of a muscle tendon proprioceptor in lobster. *J. Comp. Neurol.*, **363**, 221-234.

Dugue, G.P., Dumoulin, A., Triller, A. & Dieudonne, S. (2005) Target-dependent use of coreleased inhibitory transmitters at central synapses. *J. Neurosci.*, **25**, 6490-6498.

Evans, C.G., Alexeeva, V., Rybak, J., Karhunen, T., Weiss, K.R. & Cropper, E.C. (1999) A pair of reciprocally inhibitory histaminergic sensory neurons are activated within the same phase of ingestive motor programs in *Aplysia*. *J. Neurosci.*, **19**, 845-858.

Fox, L.E. & Lloyd, P.E. (2001) Evidence that post-tetanic potentiation is mediated by neuropeptide release in *Aplysia*. *J. Neurophysiol.*, **86**, 2845-2855.

Heinzel, H.G., Weimann, J.M. & Marder, E. (1993) The behavioral repertoire of the gastric mill in the crab, *Cancer pagurus*: an in situ endoscopic and electrophysiological examination. *J. Neurosci.*, **13**, 1793-1803.

Jan, L.Y. & Jan, Y.N. (1982) Peptidergic transmission in sympathetic ganglia of the frog. *J. Physiol.*, **327**, 219-46.

Jonas, P., Bischofberger, J. & Sandkuhler, J. (1998) Corelease of two fast neurotransmitters at a central synapse. *Science*, **281**, 419-424.

Karhunen, T., Vilim, F.S., Alexeeva, V., Weiss, K.R. & Church, P.J. (2001) Targeting of peptidergic vesicles in cotransmitting terminals. *J. Neurosci.*, **21**, RC127.

Katz, P.S. & Harris-Warrick. R.M. (1989) Serotonergic/cholinergic muscle receptor cells in the crab stomatogastric nervous system. II. Rapid nicotinic and prolonged modulatory effects on neurons in the stomatogastric ganglion. *J. Neurophysiol.*, **62**, 571-581.

Katz, P.S. & Harris-Warrick, R.M. (1990) Neuromodulation of the crab pyloric central pattern generator by serotonergic/cholinergic proprioceptive afferents. *J. Neurosci.*, **10**, 1495-1512.

Katz, P.S. & Harris-Warrick, R.M. (1991) Recruitment of crab gastric mill neurons into the pyloric motor pattern by mechanosensory afferent stimulation. *J. Neurophysiol.*, **65**, 1442-1451.

Kiehn, O. & Harris-Warrick, R.M. (1992) Serotonergic stretch receptors induce plateau properties in a crustacean motor neuron by a dual-conductance mechanism. *J. Neurophysiol.*, **68**, 485-495.

Koh, H.Y., Vilim, F.S., Jing, J. & Weiss, K.R. (2003) Two neuropeptides colocalized in a command-like neuron use distinct mechanisms to enhance its fast synaptic connection. *J. Neurophysiol.*, **90**, 2074-2079.

Koh, H.Y. & Weiss, K.R. (2005) Peptidergic contribution to posttetanic potentiation at a central synapse of *Aplysia*. *J. Neurophysiol.*, **94**, 1281-1286.

Li, W.C., Soffe, S.R. & Roberts, A. (2004) Glutamate and acetylcholine corelease at developing synapses. *Proc. Natl. Acad. Sci. (USA)*, **101**, 15488-15493.

Marder, E. & Bucher, D. (2007) Understanding circuit dynamics using the stomatogastric nervous system of lobsters and crabs. *Annu. Rev. Physiol.*, **69**, 291-316.

Nishimaru, H., Restrepo, C.E., Ryge, J., Yanagawa, Y. & Kiehn, O. (2005) Mammalian motor neurons corelease glutamate and acetylcholine at central synapses. *Proc. Natl. Acad. Sci. (USA)*, **102**, 5245-5249.

Norris, B.J., Coleman, M.J. & Nusbaum, M.P. (1996) Pyloric motor pattern modification by a newly identified projection neuron in the crab stomatogastric nervous system. *J. Neurophysiol.*, **75**, 97-108.

Nusbaum, M.P. & Marder, E. (1989a) A modulatory proctolin-containing neuron (MPN). I. Identification and characterization. *J. Neurosci.*, **9**, 1591-1599.

Nusbaum, M.P. & Marder, E. (1989b) A modulatory proctolin-containing neuron (MPN). II. State-dependent modulation of rhythmic motor activity. *J. Neurosci.*, **9**, 1600-1607.

Nusbaum, M.P., Blitz, D.M., Swensen, A.M., Wood, D. & Marder, E. (2001) The roles of co-transmission in neural network modulation. *Trends Neurosci.*, **24**, 46-54.

Nusbaum, M.P. & Beenhakker, M.P. (2002) A small-systems approach to motor pattern generation. *Nature*, **417**, 343-350.

Peng, Y.Y. & Horn, J.P. (1991) Continuous repetitive stimuli are more effective than bursts for evoking LHRH release in bullfrog sympathetic ganglia. *J. Neurosci.*, **11**, 85-95.

Samano, C., Zetina, M.E., Marin, M.A., Cifuentes, F. & Morales, M.A. (2006) Choline acetyl transferase and neuropeptide immunoreactivities are colocalized in somata, but preferentially localized in distinct axon fibers and boutons of cat sympathetic preganglionic neurons. *Synapse*, **60**, 295-306.

Seal, R.P. & Edwards, R.H. (2006) Functional implications of neurotransmitter co-release: glutamate and GABA share the load. *Curr. Opin. Pharmacol.*,

6, 114-119.

Stein, W., Hertzberg, S.R. & Nusbaum, M.P. (2001) Direct and indirect circuit modulation by cotransmitters. Soc. Neurosci. Abstr., 27, 806.

Stein, W., Eberle, C.C. & Hedrich, U.B. (2005) Motor pattern selection by nitric oxide in the stomatogastric nervous system of the crab. *Eur. J. Neurosci.*, **21**, 2767-2781.

Sun, Q.Q., Baraban, S.C., Prince, D.A. & Huguenard, J.R. (2003) Target-specific neuropeptide Y-ergic synaptic inhibition and its network consequences within the mammalian thalamus. *J. Neurosci.*, **23**, 9639-9649.

Swensen, A.M. & Marder, E. (2000) Multiple peptides converge to activate the same voltage-dependent current in a central pattern-generating circuit. *J. Neurosci.*, **20**, 6752-6759.

Swensen, A.M., Golowasch, J., Christie, A.E., Coleman, M.J., Nusbaum, M.P. & Marder, E. (2000) GABA and responses to GABA in the stomatogastric ganglion of the crab *Cancer borealis*. *J. Exp. Biol.*, **203**, 2075-2092.

Swensen, A.M. & Marder, E. (2001) Modulators with convergent cellular actions elicit distinct circuit outputs. *J. Neurosci.*, **21**, 4050-4058.

Thirumalai, V. & Marder, E. (2002) Colocalized neuropeptides activate a central pattern generator by acting on different circuit targets. *J. Neurosci.*, **22**, 1874-1882.

Vilim, F.S., Cropper, E.C., Price, D.A., Kupfermann, I. & Weiss, K.R. (2000) Peptide cotransmitter release from motorneuron B16 in *Aplysia californica*: costorage, corelease, and functional implications. *J. Neurosci.*, **20**, 2036-2042.

Whim, M.D. & Lloyd, P.E. (1989) Frequency-dependent release of peptide cotransmitters from identified cholinergic motor neurons in *Aplysia*. *Proc. Natl. Acad. Sci. (USA)*, **86**, 9034-9038.

Wood, D.E., Stein, W. & Nusbaum, M.P. (2000) Projection neurons with shared cotransmitters elicit different motor patterns from the same neural circuit. *J. Neurosci.*, **20**, 8943-8953.

Wood, D.E. & Nusbaum, M.P. (2002) Extracellular peptidase activity tunes motor pattern modulation. *J. Neurosci.*, **22**, 4185-4195.

Chapter 3

Proprioceptor Regulation of Motor Circuit Activity by Presynaptic Inhibition of a Modulatory Projection Neuron

Mark P. Beenhakker

Nicholas D. DeLong

Shari R. Saideman

Farzan Nadim

Michael P. Nusbaum

Published:

The Journal of Neuroscience, 2005

25: 8794-8806

ABSTRACT

Phasically active sensory systems commonly influence rhythmic motor activity via synaptic actions on the relevant circuit and/or motor neurons. Using the crab stomatogastric nervous system (STNS), we have identified a distinct synaptic action by which an identified proprioceptor, the gastro/pyloric muscle stretch receptor (GPR) neuron, regulates the gastric mill (chewing) motor rhythm. Previous work showed that rhythmically stimulating GPR in a gastric mill-like pattern, in the isolated STNS, elicits the gastric mill rhythm via its activation of two identified projection neurons, MCN1 and CPN2, in the commissural ganglia. Here, we determine how activation of GPR with a behaviorally appropriate pattern (active during each gastric mill retractor phase) influences an ongoing gastric mill rhythm via actions in the stomatogastric ganglion, where the gastric mill circuit is located. Stimulating GPR during each retractor phase selectively prolongs that phase and thereby slows the ongoing rhythm. This selective action on the retractor phase results from two distinct GPR actions. First, GPR presynaptically inhibits the axon terminals of MCN1, reducing MCN1 excitation of all gastric mill neurons. Second, GPR directly excites the retractor phase neurons. Because MCN1 transmitter release occurs during each retractor phase, these parallel GPR actions selectively reduce the buildup of excitatory drive to the protractor phase neurons, delaying each protractor burst. Thus, rhythmic proprioceptor feedback to a motor circuit can result from a global reduction in excitatory drive to that circuit, via presynaptic inhibition, coupled with a phase-specific excitatory input that prolongs the excited phase by delaying onset of the subsequent phase.

INTRODUCTION

Sensory influences on the central pattern generator (CPG) circuits that underlie rhythmic motor behaviors extend from phasic actions that fine-tune motor output to the activation or termination of entire motor programs (Stein et al., 1997; McCrea, 1998; DiPrisco et al., 2000; Perrins et al., 2002; Frost et al., 2003; Pearson, 2004; Shetreat-Klein and Cropper, 2004; Buschges, 2005). The phasic, cycle-specific regulatory actions commonly result from direct synaptic actions on CPG neurons and associated motor neurons. In contrast, sensory activation or termination of CPG activity often results from its influences on upstream projection neurons.

Here, we use the stomatogastric nervous system (STNS) of the crab *Cancer borealis* to document that the same proprioceptor neuron can activate and regulate rhythmic motor activity, via distinct synaptic actions on different regions of the same projection neuron. The STNS includes four ganglia that contain a set of distinct but interacting CPGs controlling various aspects of the ingestion and processing of food by the foregut (Nusbaum and Beenhakker, 2002). The CPGs that generate the chewing (gastric mill circuit) and filtering (pyloric circuit) motor patterns occur in the stomatogastric ganglion (STG), while the projection neurons that regulate their activity are located primarily in the paired commissural (CoGs) ganglia. The gastric mill rhythm can be activated in the isolated STNS without sensory input (Coleman and Nusbaum, 1994), but sensory input does regulate this rhythm (Combes et al., 1999; Beenhakker et al., 2004; Blitz et al., 2004).

One well-defined sensory input to the gastric mill circuit is the gastro/pyloric receptors (GPRs), two pairs of bilaterally symmetric proprioceptor neurons that are activated by stretch of gastric mill protractor muscles (Katz et al., 1989; Katz and Harris-Warrick, 1989). The GPRs modulate the pyloric rhythm and activate the gastric mill rhythm (Katz and Harris-Warrick, 1990; 1991; Blitz et al., 2004). They elicit the gastric mill rhythm by activating modulatory commissural neuron 1 (MCN1) and commissural projection neuron 2 (CPN2), which occur as single copies in each CoG (Blitz et al., 2004).

Blitz et al. (2004) studied the GPR ability to activate the gastric mill rhythm in an 'open-loop' paradigm in the isolated STNS wherein GPR was stimulated in a gastric mill-like pattern. Here we created a closed loop-like situation in the isolated STNS to understand how GPR influences an ongoing gastric mill rhythm activated by either a distinct sensory pathway or direct stimulation of MCN1 (Coleman and Nusbaum, 1994; Beenhakker et al., 2004). During these gastric mill rhythms, GPR was stimulated with its behaviorally-appropriate pattern, during the retractor phase, to close the GPR loop. With this approach, we demonstrate that GPR slows the gastric mill rhythm by selectively prolonging the retractor phase. This results from GPR-mediated presynaptic inhibition of the STG terminals of MCN1 and a parallel excitation of retractor phase neurons. The latter effect appears to enable GPR to replace a subset of the excitatory actions that it removes by its inhibition of MCN1.

Some of these results were published in abstract form (Beenhakker and Nusbaum, 2003).

METHODS

Animals/preparation. Male crabs, *Cancer borealis* (Jonah crabs), were obtained from Commercial Lobster & Seafood Co. (Boston, MA) and the Marine Biological Laboratory (Woods Hole, MA). Crabs were housed in commercial tanks containing chilled, filtered and recirculated artificial seawater (10°C). Before dissection, each crab was anesthetized by packing in ice for at least 30 minutes. The foregut was removed and then transferred to a dissection dish containing saline (10-12°C) to enable dissection of the STNS from the foregut. The isolated STNS (Fig. 1*A*) was then transferred and pinned down in a silicone elastomer (Sylgard 184, KR Anderson, Santa Clara, CA)-lined Petri dish filled with saline (10-12°C).

Solutions. During dissection and experimentation, the STNS was supplied with *C. borealis* saline (mM): 440 NaCl, 26 $MgCl_2$, 11 KCl, 13 $CaCl_2$, 10 Trizma base and 5 maleic acid (pH 7.4-7.6). In some experiments, neuronal interactions were limited to those presumed to be monosynaptic by superfusing the preparation with saline containing 5 times the normal concentration of the divalent salts (high divalent cation saline) (Blitz and Nusbaum, 1999). This saline contained (in mM): 439 NaCl, 130 $MgCl_2$, 11 KCl, 64.5 $CaCl_2$, 10 Trizma base and 5 maleic acid (pH 7.4-7.6). During each experiment the STNS was continuously superfused with saline (7-12 ml/min), via a switching manifold to enable fast solution changes, cooled (10-11°C) with a Peltier device.

Electrophysiology. STNS neurons were identified by their patterns of activity, synaptic interactions with other identified neurons and axonal branching patterns in connecting and peripheral nerves (Beenhakker et al., 2004; Beenhakker and Nusbaum, 2004). Standard intracellular and extracellular recording techniques were used in this study (Beenhakker et al., 2004). Briefly, extracellular recordings of neuronal activity were obtained by electrically isolating individual sections of STNS nerves from the bath by building a petroleum jelly-based cylindrical compartment around a section of nerve. One of two stainless steel electrode wires was placed within this compartment, to record action potentials propagating through the nerve, while the second wire was placed in the bath as a reference electrode. The differential signal was recorded, filtered and amplified, first through an amplifier from AM Systems (Model 1700, Carlsborg, WA) and then through an amplifier from Brownlee Precision (Model 410, Santa Clara, CA). Extracellular stimulation of a nerve was achieved by placing the two extracellular wires into a stimulus isolation unit (Astromed/Grass Instruments, Model SIU5, West Warwick, RI) controlled by a stimulator (Astromed/Grass Instruments, Model S88). Intracellular recordings of STNS somata were obtained with sharp glass microelectrodes (15-30 MΩ) filled with either 4 M potassium acetate (KAc) plus 20 mM potassium chloride (KCl) or 0.6 M K_2SO_4 plus 20 mM KCl. Neurotransmitter release from the STG terminals of projection neurons is suppressed by intra-axonal recordings with KAc-filled electrodes positioned near the entrance to the STG (Coleman et al., 1995). Therefore, to preserve

transmitter release during these intra-axonal recordings, we used an intracellular electrode solution of 1 M KCl (Bartos and Nusbaum, 1997). All intracellular signals were amplified and filtered with Axoclamp 2B amplifiers (Axon Instruments, Foster City, CA), then further amplified with Brownlee Model 410 amplifiers. Intracellular current injections were performed in discontinuous current clamp (DCC) mode with sampling rates of 2-3 KHz.

In these experiments, we primarily worked with the GPR2 stretch receptor, by stimulating the *gpn* nerve through which its axon projects. However, we found that the STNS response to GPR1 stimulation was the same as GPR2 stimulation. As GPR is activated during the retractor phase of the gastric mill rhythm (Katz and Harris-Warrick, 1989), we stimulated the *gpn* during this phase. This stimulation was performed manually by turning the stimulator on at the beginning of the retractor phase. We tested the effect of stimulating GPR for both a fixed duration and by terminating the stimulation at the burst onset time of the lateral gastric (LG) neuron. In the latter case, each stimulation was terminated either by anticipating the onset of the protractor phase (LG neuron burst onset), based on the trajectory of the LG neuron membrane potential, or else waiting until the LG burst began.

Data Acquisition. Data were acquired in parallel onto a chart recorder (MT-95000 or Everest Model, Astromed Corp., West Warwick, RI), and by digitizing (~5 KHz) and storing the data on computer with data acquisition hardware/software (SPIKE2, Cambridge Electronic Design, Cambridge,

England). Digitized data were analyzed with a homemade SPIKE2 program ('The Crab Analyzer', freely available at http://www.neurobiologie.de/). Briefly, the burst duration of a neuron was defined as the elapsed time (sec) between the first and last action potential in an impulse burst. The firing frequency was calculated by dividing the number of action potentials minus one by the burst duration. Gastric mill cycle period was defined by the duration (sec) between the onsets of 2 successive impulse bursts in the LG neuron.

Data are presented as mean ± SD. Statistical analyses were performed with SigmaStat 3.0 (SPSS, Chicago, IL). Figures were made from Spike2 files incorporated in the Adobe Photoshop (Adobe, San Jose, CA) and Powerpoint graphics programs (Microsoft, Seattle, WA).

Dynamic Clamp. We used the dynamic clamp technique (Sharp et al., 1993; Prinz et al., 2004) to inject an artificial ionic or synaptic current into the LG neuron. The dynamic clamp software uses intracellularly recorded membrane potentials (V_m) of biological neurons to calculate an artificial current (I_{dyn}) using a conductance ($g_{dyn}(t)$) that is numerically computed as well as a predetermined reversal potential (E_{rev}). The artificial current is computed in real time, updated in each time step (0.2 ms) according to the new values of recorded membrane potential and injected back into the biological neuron. The intrinsic currents are computed according to the equations below:

$$I_{dyn} = g_{dyn} m^p \cdot h^q \cdot (V_1 - E_{syn})$$

$$\tau_X(V_2)\frac{dX}{dt} = X_\infty(V_2) - X;\ \ X = m, h$$

$$X_\infty(V) = \frac{1}{1 + \exp\left(\frac{V - V_X}{k_X}\right)}$$

$$\tau_X(V) = \tau_{X,Lo} + \frac{\tau_{X,Hi} - \tau_{X,Lo}}{1 + \exp\left(-\frac{V - V_X}{|k_X|}\right)}$$

where V_1 and V_2 both represent the membrane potential V_m. The synaptic currents are computed according to the same equations where V_1 represents V_{Post} and V_2 represents V_{Pre}. The values of parameters used by dynamic clamp in the above equations are given in Table 1.

In the dynamic clamp experiments involving the injection of the interneuron 1 (Int1) inhibitory synaptic current into the LG neuron, we used a model cell to represent Int1. This model cell included a passive leak current and Hodgkin-Huxley-like voltage-dependent inward and outward currents that underlie action potential generation. Consistent with the biological gastric mill circuit (Coleman et al., 1995; Bartos et al., 1999), the model Int1 was inhibited by the pyloric dilator (PD) and LG neurons, ongoing recordings of which were maintained in the biological preparation. The activity of the model Int1 was used to inject a simulated inhibitory current into the LG neuron to mimic the effect of increasing the inhibitory action of the biological Int1 (see Bartos et al., 1999).

In experiments in which the modulatory action of the MCN1 projection neuron on the LG neuron was mimicked with the dynamic clamp software, we

used previously published parameters for the peptide-elicited, voltage-dependent current as characterized in other STG neurons (Golowasch and Marder, 1992; Swensen and Marder, 2000, 2001). In the biological network, the modulatory input from MCN1 to LG decays during each LG burst (Coleman and Nusbaum, 1994; Coleman et al., 1995). To mimic this decay we added an inactivation component to the modeled current (see Table 1 and Results).

These experiments were performed using the version of the dynamic clamp software developed in the Nadim laboratory (available at http://stg.rutgers.edu/software) on a PC running Windows XP and a NI PCI-6070-E data acquisition board (National Instruments, Austin, TX). All intracellular recordings were performed in single-electrode discontinuous current clamp mode.

Gastric Mill Model. We constructed a computational model modified from an existing conductance-based model of the gastric mill circuit (Nadim et al., 1998). The previously published version modeled the LG, Int1, and MCN1 neurons as having multiple compartments separated by an axial resistance, with each compartment possessing intrinsic and/or synaptic conductances. We modified this model only by adding an additional single compartment cell, representing the GPR neuron, and several additional synaptic conductances (Table 2). All other parameters were unmodified from those previously published.

To model the GPR neuron, we added a single compartment cell with a passive leak current plus Hodgkin-Huxley-like voltage-dependent inward and

outward currents to effect action potential generation. Consistent with physiological measurements (see Results), this model neuron made an inhibitory synaptic connection onto a distal compartment of the MCN1 axon terminals (t0 compartment: see Nadim et al., 1998), as well as an excitatory connection onto the Int1 neurite compartment. To mimic the cumulative actions of repeated GPR stimulations, the GPR synapse onto MCN1 was modeled as a slow activating, slow deactivating current. The conductances and other parameters of these currents were chosen to mimic the behavior of the gastric mill circuit in the presence of GPR stimulation (Table 2). In these models we only incorporated each of these two synapses separately, because our aim was to assess their individual contributions to the observed GPR action on the gastric mill rhythm. Finally, to more accurately mimic known mechanisms of gastric mill rhythm generation, we also added an excitatory synaptic connection between MCN1 and Int1 (Coleman et al., 1995).

Simulations were performed on a PC with Windows XP. We used the *Network* simulation software developed in the Nadim laboratory, which was run using the freely available CYGWIN Linux emulation software package. We used a 4th order Runge-Kutta numerical integration method with time steps of 0.05 and 0.01 ms. Results were visualized by plotting outputted data points using the freely available GNUPLOT software package.

Table 1 – Dynamic Clamp Parameters												
Synapses												
Current	Vm (mV)	Km (mV)	TmLo (ms)	TmHi (ms)	P	Vh (mV)	Kh (mV)	ThLo (ms)	ThHi (ms)	Q	Gmax (nS)	Erev (mV)
LG-Int1	-45	-0.1	5	1500	1	n/a	n/a	n/a	n/a	0	30	-120
Int1-LG	-40	-1	5	200	1	n/a	n/a	n/a	n/a	0	100	-80
PD-Int1	-20	-1	5	1000	1	n/a	n/a	n/a	n/a	0	10	-120
Int1 Model Cell Currents												
	Vm	Km	TmLo	TmHi	P	Vh	Kh	ThLo	ThHi	Q	Gmax	Erev
Leak	-40	-5	50	100	0	n/a	n/a	n/a	n/a	0	1	-60
Na	-40	-10	5	5	1	-40	3.0	50	50	1	30	45
K	-40	-10	100	500	1	n/a	n/a	n/a	n/a	0	50	-80
Simulated CabTRP Current in LG												
	Vm	Km	TmLo	TmHi	P	Vh	Kh	ThLo	ThHi	Q	Gmax	Erev
CabTRP	-40	-10	200	50	1	-40	0.5	12000	8000	1	250	0

Table 1: Parameters used in dynamic clamp experiments.

Table 2 – Model Parameters								
Synapses								
Synapse	Gmax (nS)	Erev (mV)	Minf			Mtau		
MCN1-Int1	6	0	$\frac{1}{1+e^{-45(V+70)}}$			1		
GPR-Int1	20	0	$\frac{1}{1+e^{-(V+60)}}$			50		
GPR-MCN1	40	-80	$\frac{1}{1+e^{-(V+60)}}$			$2000+\frac{4000}{1+e^{V+60}}$		
GPR Intrinsic Currents								
Current	Gmax	Erev	p	q	Minf	Mtau	Hinf	Htau
Leak	3	-68	n/a	n/a	n/a	n/a	n/a	n/a
Na	120	50	3	1	$\frac{1}{1+e^{-5(V+62)}}$	Inst	$\frac{1}{1+e^{5(V+64)}}$	$1+\frac{5}{1+e^{-0.24(V+64)}}$
K	36	-77.5	4	n/a	$\frac{1}{1+e^{-5(V+54)}}$	$8+\frac{20}{1+e^{0.24(V+54)}}$	n/a	n/a

Table 2: Parameters used to incorporate GPR synapses into an existing model of the gastric mill rhythm (Nadim et al., 1998). GPR was modeled as a single compartment cell with active and passive properties, and three synaptic currents were added to existing model cells. “Inst” denotes an instantaneous time constant.

RESULTS

GPR prolongs the retractor phase of the VCN-elicited gastric mill rhythm

The gastric mill rhythm is a two-phase motor pattern in which there is a rhythmic repeating alternation in impulse bursts between teeth protraction- and retraction-related neurons (Heinzel et al., 1993). There are eight different gastric mill neurons in *C. borealis*, half of which are active during protraction and half are active during retraction (Beenhakker and Nusbaum, 2004). In this paper, we use LG neuron activity to represent the protractor phase while the retractor phase is represented by the activity of the dorsal gastric (DG) neuron and/or Int1 (Fig. 1*B*). The reciprocally inhibitory neurons LG and Int1 comprise the core of the gastric mill CPG (Coleman et al., 1995; Bartos et al., 1999).

In situ, the GPRs are rhythmically activated during each retraction phase of the gastric mill rhythm. For GPR2, this activity pattern results from its dendrites being embedded in a protractor (gm9a) muscle that is stretched during each DG retractor neuron burst (Katz and Harris-Warrick, 1989) (Fig. 1*B*). The gastric mill rhythm is generally not spontaneously active in vitro, but it can be readily triggered by stimulation of known sensory pathways, including transient stimulation of the VCN mechanosensory neurons (Beenhakker et al., 2004). To determine what, if any, changes occurred in an ongoing gastric mill rhythm as a result of activating GPR at the behaviorally appropriate time, we stimulated GPR during successive DG neuron bursts in an ongoing VCN-elicited gastric mill rhythm (eg, Fig. 2).

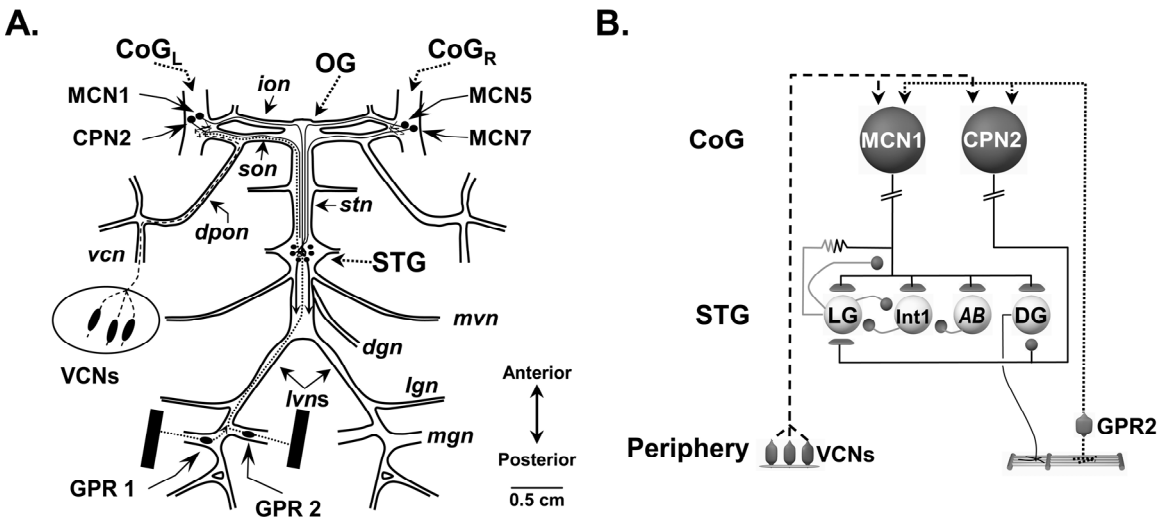

Figure 1. Schematic of the isolated stomatogastric nervous system (STNS) and the pathways by which two identified sensory systems influence the gastric mill circuit. *A.* The STNS consists of the unpaired stomatogastric (STG) and oesophageal (OG) ganglia, the paired commissural (CoG) ganglia, plus the connecting and peripheral nerves. In each CoG there is a single a copy of each identified CoG projection neuron, including MCN1, MCN5, MCN7 and CPN2. The STNS receives sensory information from the proprioceptor neurons GPR1 and 2, and the mechanoreceptor VCNs. *B.* The GPRs and VCNs each elicit the gastric mill rhythm by activating MCN1 and CPN2, which in turn activate the gastric mill circuit. The CPG neurons LG and Int1 have reciprocal inhibitory connections and are influenced by the pyloric pacemaker neuron AB. The dorsal gastric (DG) neuron is a gastric mill retractor motor neuron that innervates the gm4 muscle. Contraction of gm4 stretches the GPR-innervated muscles, thereby activating the GPRs (Katz and Harris-Warrick, 1989). Synapse symbols: t-bars, excitation; filled circles, inhibition; resistor, electrical coupling. **Abbreviations.**

Nerves: *dgn*, dorsal gastric nerve; *dpon*, dorsal posterior oesophageal nerve; *ion*, inferior oesophageal nerve; *lgn*, lateral gastric nerve; *lvn*, lateral ventricular nerve; *mgn*, medial gastric nerve; *mvn*, medial ventricular nerve; *son*, superior oesophageal nerve; *stn*, stomatogastric nerve; *vcn*, ventral cardiac nerve.

Neurons: AB, anterior burster; CPN2, commissural projection neuron 2; GPR, gastropyloric receptor; MCN1,5,7, modulatory projection neuron 1,5,7; VCN, ventral cardiac neuron.

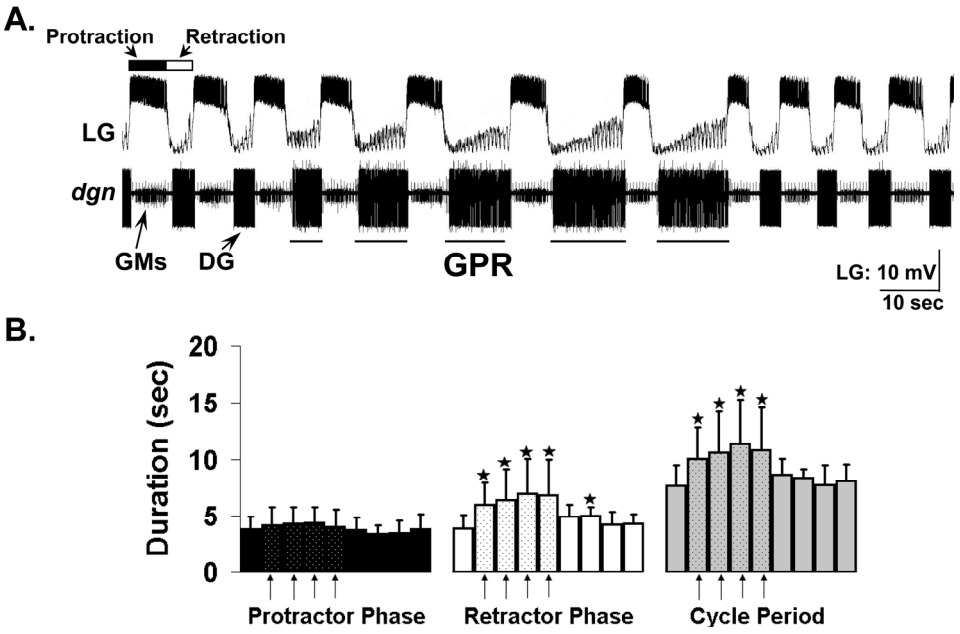

Figure 2. GPR stimulation prolongs the retractor phase of the VCN-elicited gastric mill rhythm. *A,* Stimulating GPR in its behaviorally-relevant pattern during the VCN-elicited gastric mill rhythm in the isolated STNS slows the rhythm by selectively prolonging the retractor phase. *B,* Relative to pre-GPR stimulation levels, during each cycle when GPR was stimulated (arrowheads) there was a significant increase in the duration of the gastric mill retractor phase and the overall speed of the rhythm (cycle period), but there was no change in the protractor phase duration (*$p<0.05$; n=8; One Way Repeated Measures ANOVA, Student-Newman Keuls Test). Each bar represents a single gastric mill cycle, with one cycle shown pre-, 5 cycles during- and 4 cycles post-GPR stimulation. Note the rapid return to control levels after GPR stimulation was terminated.

There were three attractive features of using the VCN mechanosensory system to activate the gastric mill circuit. First, a relatively brief (1-2 min) stimulation of the VCNs triggers a long-lasting (tens of minutes) gastric mill rhythm (Beenhakker et al., 2004). Second, both the VCNs and the GPRs elicit the gastric mill rhythm via the same two CoG projection neurons, MCN1 and CPN2 (Beenhakker & Nusbaum, 2004; Blitz et al., 2004), thereby confining the scope of the pertinent circuitry to a limited number of neurons. The VCN- and GPR-elicited gastric mill rhythms are qualitatively similar but quantitatively distinct (Blitz et al., 2004). Third, the ability of the GPRs to influence MCN1 and CPN2 in the CoGs is suppressed during the VCN-elicited gastric mill rhythm, thereby limiting the likely locus of any persisting GPR actions to the STG (Beenhakker, 2004).

Stimulating GPR during each DG neuron burst slowed the gastric mill rhythm (Cycle Period: pre-GPR, 7.6 ± 1.8 sec; during GPR stim., 10.7 ± 3.4 sec; post-GPR, 8.2 ± 1.1 sec; Repeated Measures ANOVA: $p<0.001$, $n=8$) (Fig. 2). This slowing of the rhythm resulted from a selective increase in retractor phase duration that occurred during every cycle in which GPR was stimulated (Fig. 2*B*). For example, there was a consistent increase in the DG retractor neuron burst duration when GPR was stimulated (pre-GPR: 3.3 ± 1.8 sec; during GPR stim.: 6.6 ± 2.9 sec; post-GPR: 3.2 ± 0.5 sec; Repeated Measures ANOVA: $p<0.05$, $n=4$) (Fig 2*B*). In contrast, GPR stimulation did not alter the duration of the LG protractor neuron (pre-GPR: 3.8 ± 1.1 sec; during GPR stim.: 4.2 ± 1.4 sec; post-

GPR: 3.6 ± 1.0 sec; Repeated Measures ANOVA: $p>0.05$; n=8) (Fig. 2*B*). These GPR actions did not extend far past the final GPR stimulation. For example, DG neuron burst duration was prolonged for one additional cycle while gastric mill cycle period returned to pre-GPR levels as soon as GPR stimulation was terminated (Fig. 2*B*).

The selective increased duration of the gastric mill retractor phase by GPR stimulation also changed the relative fraction of each cycle (duty cycle) devoted to protraction and retraction. Specifically, GPR stimulation reduced the LG neuron duty cycle by causing a phase advance of its burst termination (pre-GPR: 49.6 ± 9%, during GPR stim.: 39.5 ± 9%, post-GPR: 43.3 ± 8%; pre-GPR vs. during GPR: $p<0.05$, n=8), and it increased the DG neuron duty cycle by phase advancing its burst onset (pre-GPR: 63.1 ± 9%, during GPR stim.: 49.7 ± 8%, post-GPR: 64.1 ± 8%; pre-GPR vs. during GPR: $p<0.05$, n=4). Thus, when GPR was active the gastric mill rhythm changed from having a balanced participation of the protractor and retractor neurons in each cycle to one in which there was relatively more retractor phase activity.

GPR prolongs the retractor phase by its synaptic actions in the STG

The GPR and VCN neurons both activate the gastric mill rhythm by eliciting a long-lasting activation of the projection neurons MCN1 and CPN2 (see Fig. 1) (Beenhakker and Nusbaum, 2004; Blitz et al., 2004). These two projection neurons appear to play distinct roles, with MCN1 providing the main

excitatory drive to the gastric mill circuit while CPN2 sculpts the activity patterns of the gastric mill neurons (Norris et al., 1994; Bartos et al., 1999; Beenhakker and Nusbaum, 2004). Surprisingly, during the VCN-elicited gastric mill rhythm, GPR stimulation no longer influences MCN1 or CPN2 in the CoGs as these GPR actions are effectively and reversibly masked by the VCN influence on these projection neurons (Beenhakker, 2004). It therefore appeared likely that the GPR ability to selectively prolong the retractor phase of the VCN-elicited gastric mill rhythm resulted from direct GPR actions within the STG.

We tested this hypothesis by transecting the superior- (*sons*) and inferior oesophageal nerves (*ions*) to eliminate the CoGs and assessing the influence of GPR stimulation on gastric mill rhythms elicited by selective extracellular nerve (*ion*) stimulation of MCN1 (Fig 3*A*). Under these conditions, tonic MCN1 stimulation routinely elicits the gastric mill rhythm (Bartos et al., 1999). Although two STG-projecting neurons, MCN1 and MCN5, project to the STG through the *ion* (Coleman and Nusbaum, 1994; Norris et al., 1996), low stimulus voltages selectively activate MCN1 (Bartos and Nusbaum, 1997; Bartos et al., 1999).

During MCN1-elicited gastric mill rhythms, GPR stimulation during the retractor phase again slowed the rhythm by selectively prolonging the retractor phase (Figs. 3*B*, 4). In fact, all of the GPR actions on the VCN-elicited gastric mill rhythm also occurred when GPR was rhythmically stimulated during the MCN1-elicited gastric mill rhythm with the CoGs removed. For example, these rhythmic GPR stimulations prolonged the gastric mill cycle period (pre-GPR: 5.6

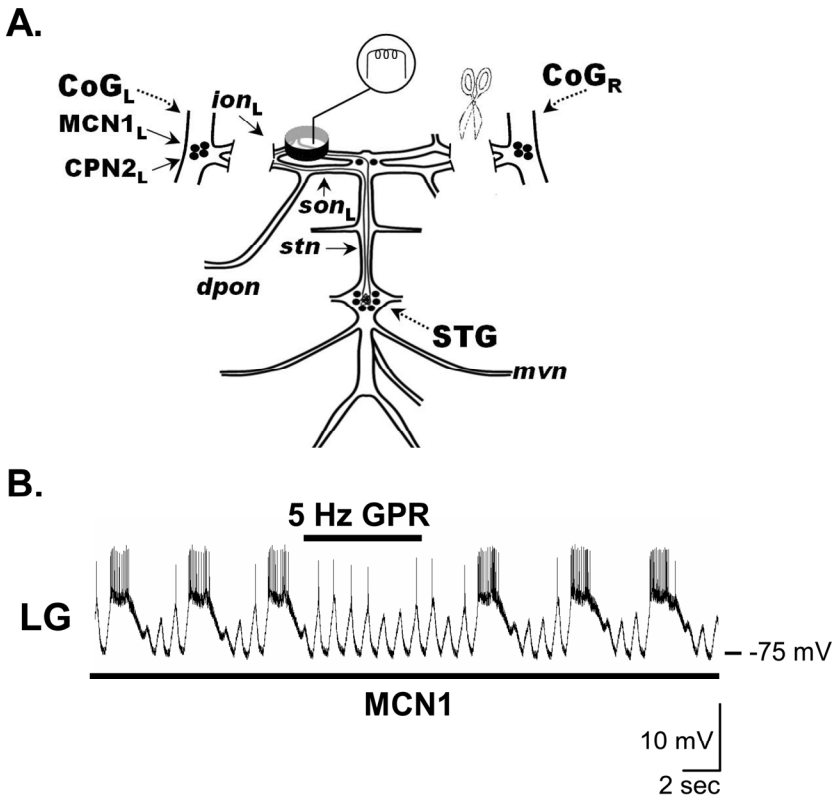

Figure 3. Influence of GPR on the MCN1-elicited gastric mill rhythm. *A.* Preparation used to study the MCN1-elicited gastric mill rhythm. The CoGs were eliminated by transection of the *ions* and *sons*, and selective MCN1 stimulation was accomplished by extracellular stimulation of the *ion* to elicit the gastric mill rhythm (Bartos et al., 1999). *B.* Stimulating GPR during the retractor phase of the MCN1-elicited gastric mill rhythm selectively prolonged that retractor phase. MCN1 stimulation (black bar: 30 Hz tonic) began before the presented recording segment and persisted for the duration of the recording shown.

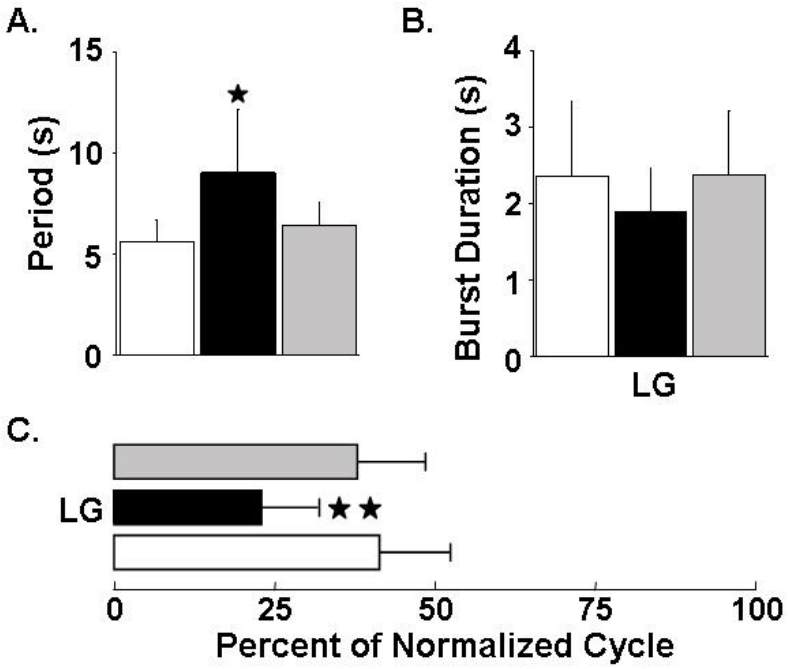

Figure 4. Quantification of the GPR actions on the MCN1-elicited gastric mill rhythm. The pre- (white bars), during- (black bars) and post-GPR stimulation (gray bars) conditions each represent the mean of 5 consecutive gastric mill cycles. *A,* GPR stimulation during the MCN1-elicited gastric mill rhythm reversibly prolonged the gastric mill cycle period by ~60% ($p<0.05$, $n=6$). *B/C,* Stmulating GPR during the MCN1-elicited gastric mill rhythm (B) did not alter the LG neuron burst duration ($p>0.05$, $n=6$) but (C) reduced the fraction of a gastric mill cycle during which LG was active (LG duty cycle) by nearly 20% ($p<0.01$, $n=6$).

± 1 sec; during GPR: 9.0 ± 3 sec; post-GPR: 6.4 ± 1 sec; $p<0.05$, Repeated Measures ANOVA, n=6) (Fig. 4*A*) without changing the LG neuron burst duration (pre-GPR: 2.4 ± 0.9 sec; during GPR: 1.9 ± 0.3 sec; post-GPR: 2.4 ± 0.8 sec; $p>0.05$, Repeated Measures ANOVA, n=6) (Fig. 4*B*). Moreover, as indicated for the VCN-elicited rhythm, by maintaining the same LG neuron burst duration while prolonging the gastric mill cycle period these GPR stimulations reduced LG neuron duty cycle (before GPR: 41.0 ± 11%; during GPR: 22.9 ± 9%; after GPR: 37.5 ± 11%; $p<0.01$, Repeated Measures ANOVA, n=6) (Fig. 4*C*).

GPR does not slow the gastric mill rhythm via its synapses on STG neurons

GPR has numerous synaptic actions within the STG on both gastric mill and pyloric neurons (Katz and Harris-Warrick, 1989, 1990, 1991; see below). Among the GPR targets are several pathways by which GPR could slow the gastric mill rhythm. The first of these pathways consists of the electrically-coupled pyloric pacemaker neurons (AB, PD neurons), whose rhythmic bursting activity is modulated by GPR (Katz and Harris-Warrick, 1990). The pyloric pacemaker neurons regulate the gastric mill cycle period via their rhythmic inhibition of Int1, which in turn provides pyloric-timed removal of Int1 inhibition (disinhibition) to the LG neuron (Nadim et al., 1998; Bartos et al., 1999). These disinhibitions, which are evident during each LG interburst (e.g., Fig. 3*B*), shorten the time to LG neuron burst onset after the preceding LG burst, thereby

increasing the speed of the gastric mill rhythm (Bartos et al., 1999; Wood et al., 2004). Consequently, changing the frequency of these pyloric-timed disinhibitions causes a concomitant change in the speed of the gastric mill rhythm (Bartos et al., 1999). We tested and eliminated this pathway as the means by which GPR regulates the gastric mill cycle period by suppressing the pyloric pacemaker activity with hyperpolarizing current injection during an ongoing MCN1-elicited gastric mill rhythm. Despite the absence of both the pyloric rhythm and the disinhibitions in the LG neuron, there was no change in the GPR ability to slow the ongoing gastric mill rhythm (n=4).

Another means by which GPR could influence the speed of the gastric mill rhythm is by its excitatory action on the DG neuron (Katz and Harris-Warrick, 1989; Kiehn and Harris-Warrick, 1992), because at high firing frequencies the DG neuron can inhibit the LG neuron. However, as was the case when the pyloric pacemaker neurons were silenced, suppression of DG neuron activity by hyperpolarizing current injection did not alter the GPR influence on the gastric mill rhythm (n=3).

A third potential target of GPR that could mediate the slowing of the gastric mill rhythm is the LG neuron. The level of LG neuron activity and its ability to escape from Int1-mediated inhibition is instrumental to gastric mill rhythm generation (Coleman et al., 1995; Bartos et al., 1999). Moreover, previous work showed that GPR stimulation produces an initial, apparently polysynaptic inhibitory response in the LG neuron, followed by an extended

period of enhanced pyloric-timed subthreshold membrane potential oscillations (Katz and Harris-Warrick, 1991). We also noticed the latter response (see Fig. 5*A*). However, we observed no change in the LG neuron membrane potential when GPR was stimulated during either the VCN- or MCN1-elicited gastric mill rhythms. We nonetheless sought to identify the neuron(s) responsible for this previously documented inhibitory action of GPR on the LG neuron because such a neuron could mediate the ability of GPR to prolong the retractor phase (by delaying the protractor phase) and thereby increase the cycle period of ongoing gastric mill rhythms.

We tested the hypothesis that Int1 was responsible for the observed GPR influence on the LG neuron. As mentioned above, the LG neuron and Int1 constitute the pair of reciprocally-inhibitory neurons at the core of the gastric mill CPG, and Int1 is responsible for the subthreshold, pyloric-timed membrane potential oscillations that occur in the LG neuron (Coleman et al., 1994; Bartos et al., 1999). We found that GPR did indeed consistently excite Int1, during which there was an increased hyperpolarization in the LG neuron (n=5) (Fig. 5*A1*). This GPR action appeared to be monosynaptic, because GPR action potentials elicited constant-latency excitatory postsynaptic potentials (EPSPs) in Int1 that persisted in the presence of high divalent cation saline (Fig. 5*A2*).

It was possible that GPR excitation of Int1 also explained the GPR-mediated prolongation of the retractor phase of the gastric mill rhythm. Specifically, if GPR enhanced Int1 activity during the gastric mill rhythm then this

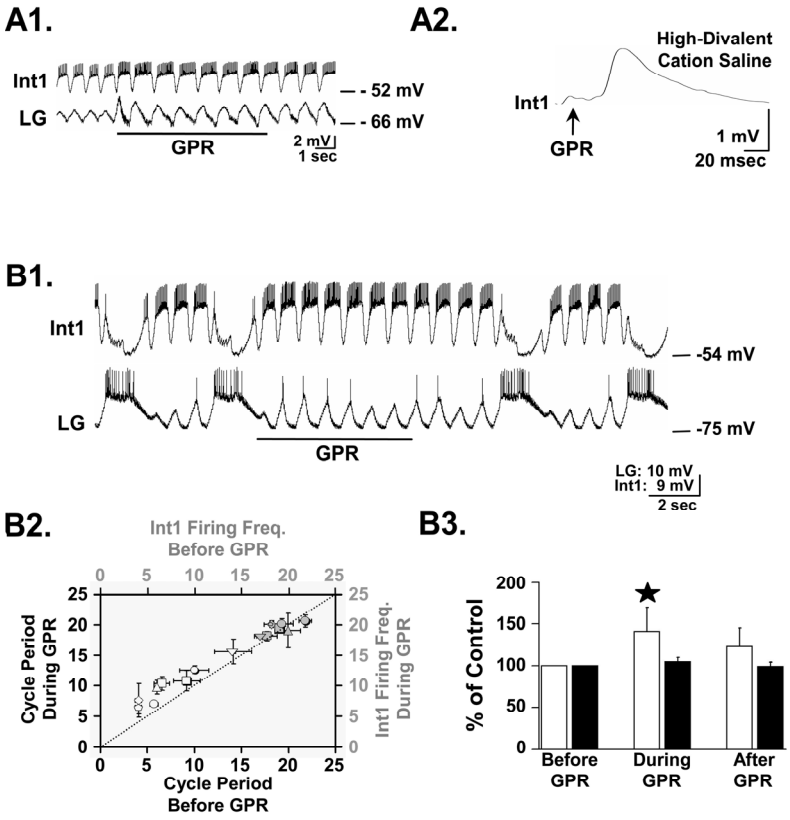

Figure 5. GPR excites Int1 but does not alter Int1 activity during the gastric mill rhythm. *A1.* In the isolated STG with no ongoing gastric mill rhythm, GPR stimulation (5 Hz) excited Int1 and produced a concomitant increase in the amplitude of the subthreshold, pyloric-timed oscillations in the LG neuron. *A2*, Single GPR stimuli evoked constant latency EPSPs in Int1 in high divalent cation saline. EPSP represents the average of 8 Int1 responses to GPR stimulation. The relatively long latency to EPSP onset results from the ~2 cm distance traveled by the GPR-elicited action potentials to reach the STG. *B1*, GPR stimulation (5 Hz) during an ongoing MCN1-elicited gastric mill rhythm prolonged the retractor phase without an evident change in Int1 activity. *B2*, GPR failed to enhance Int1 activity during ongoing gastric mill rhythms at times when it did

prolong the gastric mill cycle period. Shown are the mean (±SD) gastric mill cycle period (white symbols) and corresponding Int1 firing frequency (gray symbols) before and during GPR stimulation for 8 preparations, organized by symbol shape. The dotted line represents no change between the pre- and during-GPR conditions. *B3.* Int1 firing frequency (black bars) and gastric mill cycle period (white bars) data are normalized to pre-control conditions. In the same preparations, GPR stimulation increased the gastric mill cycle period (40.8 ± 28.9%; $p<0.001$, $n=8$) but failed to alter Int1 firing frequency (4.5 ± 5.4%; $p>0.05$; $n=8$).

would likely strengthen Int1 inhibition of the LG neuron, thereby slowing the LG neuron escape from Int1 inhibition and prolonging the retractor phase. It was not possible to directly test this hypothesis by suppressing Int1 activity because its activity is necessary for gastric mill rhythm generation (Bartos et al., 1999). Therefore, as a first step, we determined whether GPR stimulation did indeed increase Int1 activity during the gastric mill rhythm. Surprisingly, GPR stimulation did not increase the Int1 firing frequency during either the VCN- or MCN1-elicited gastric mill rhythms (VCN rhythms: pre-GPR: 19.3 ± 1.4 Hz; during GPR: 19.6 ± 0.9 Hz; $p>0.05$, n=6) (MCN1 rhythms: pre-GPR: 17.6 ± 0.9 Hz; during-GPR: 19.1 ± 1.3 Hz; $p>0.05$, n=2) (Fig. 5*B*). Despite the lack of change in Int1 firing frequency during these GPR stimulations, the gastric mill rhythm was slowed as usual (n=8) (Fig. 5*B*).

There remained two possible mechanisms by which GPR excitation of Int1 could increase Int1 inhibition of the LG neuron. First, GPR might selectively enhance the graded component of Int1 transmitter release. STG circuit neurons exhibit both spike-mediated and graded release (Hartline and Graubard, 1992). The second possibility was that GPR could increase the amount of transmitter release per Int1 action potential.

We assessed the possibility that a GPR-mediated strengthening of the Int1 inhibition of the LG neuron was responsible for the GPR actions on the gastric mill rhythm in two ways. First, we implemented a modified version of our previously developed computational model of the MCN1-elicited gastric mill

rhythm (Nadim et al., 1998; see Methods). Using this model, we found that when the Int1 inhibitory input to the LG neuron was strengthened by GPR excitation of Int1, the gastric mill rhythm was measurably slowed (cycle period: control, ~9s; with GPR stimulation, ~13s) (Fig. 6). However, in contrast to the biological condition, both the retractor and protractor phases of these cycles were prolonged (protractor phase duration: control, ~6s; with GPR stimulation, ~8s; retractor phase duration: control, ~3s; with GPR stimulation, ~6s).

To understand the consequences of increasing the strength of Int1 inhibition of the LG neuron, it is helpful to know the previously documented interactions between MCN1, Int1 and LG. Specifically, each LG neuron burst initiates after a period during which it steadily depolarizes to escape from Int1-mediated inhibition, due to the buildup of excitatory drive that LG receives from MCN1 during this phase of the rhythm (Coleman et al., 1995; Bartos et al., 1999) (Fig. 6). Thus, when Int1 inhibition of LG was strengthened, the LG neuron required more time to build up more excitatory drive from MCN1 to enable it to escape from Int1 inhibition. When the LG burst finally was initiated, it inhibited the STG terminals of MCN1 (as well as Int1) (Coleman and Nusbaum, 1994; Coleman et al., 1995), causing the excitatory drive it had received from MCN1 to decay.

The strengthened Int1 inhibition of LG thus caused an increased LG neuron burst duration for the following two reasons. First, the excitatory drive from MCN1 not only mediates LG escape from Int1 inhibition but is also

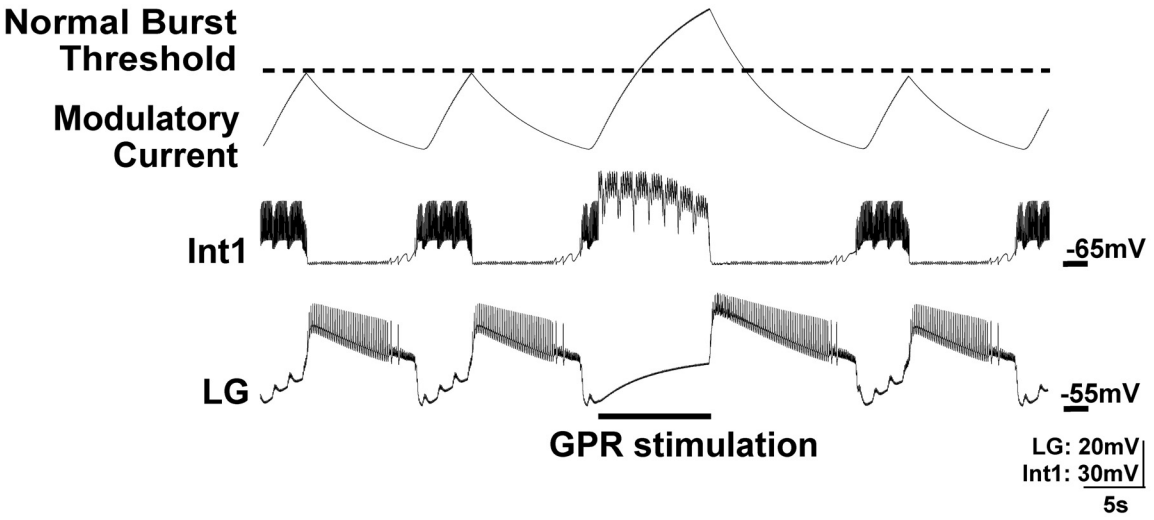

Figure 6. Increasing the strength of Int1 inhibition of the LG neuron during GPR stimulation prolongs both phases of the MCN1-elicited gastric mill rhythm in a computational model. GPR was stimulated during a retractor phase, as occurs in the biological system. In this version of the model, the strength of Int1 inhibition of LG was explicitly enhanced by GPR stimulation. The result was an increase in the duration of that retractor phase (Int1 active) as well as an increase in the subsequent protractor phase (LG active). Note that the rhythm returned to control levels in the next cycle. The modulatory current trace represents the cycle-by-cycle buildup and decay of MCN1 excitation of the LG neuron. When GPR is silent, the LG neuron burst initiates when the level of modulatory current attains the level designated as “normal burst threshold”.

responsible for the LG burst. Consequently, increasing the duration of a constant level of MCN1 input will result in a longer duration LG neuron burst. Second, because the rate of decay from MCN1 excitation was unchanged by strengthening Int1 input, and the level of excitatory drive at the time of burst onset was higher than in the control rhythm, the time needed for this modulatory drive to decay to the LG burst termination point was prolonged (Fig. 6).

To test the predictions of this model, we returned to the biological system and used the dynamic clamp technique to inject an additional Int1-like inhibitory conductance into LG during each Int1 period of activity (ie, during the time when GPR would be active) (see Methods for details; see also Bartos et al., 1999). As a result of this increased inhibitory conductance, there was an increased hyperpolarization in the LG neuron (by –7.8 ± 1.2 mV; n=6). LG nonetheless remained able to escape the combined biological and dynamic clamp-mediated inhibition, and the gastric mill rhythm was maintained (Fig. 7). Under these conditions, the retractor phase was reversibly prolonged (pre-DClamp: 5.6 ± 1.8 sec; DClamp: 12.1 ± 4.7 sec; post-DClamp: 6.9 ± 1.5 sec; Two-way ANOVA $p<0.01$; Tukey pairwise comparison: DClamp vs. Pre. $p<0.01$, DClamp vs. Post, $p<0.05$, Post vs. Pre, $p>0.05$; n=6) as was the gastric mill cycle period (pre-DClamp: 9.7 ± 2.5 sec; DClamp: 18.3 ± 6.0 sec; post-DClamp: 11.2 ± 2.0 sec; Two-way ANOVA $p<0.005$; Tukey pairwise comparison: DClamp vs. Pre, $p<0.005$, DClamp vs. Post, $p<0.05$, Post vs. Pre, $p>0.05$; n=6) (Fig. 7*A*,*B*). Additionally, as predicted by the modeling results, the LG (protractor phase)

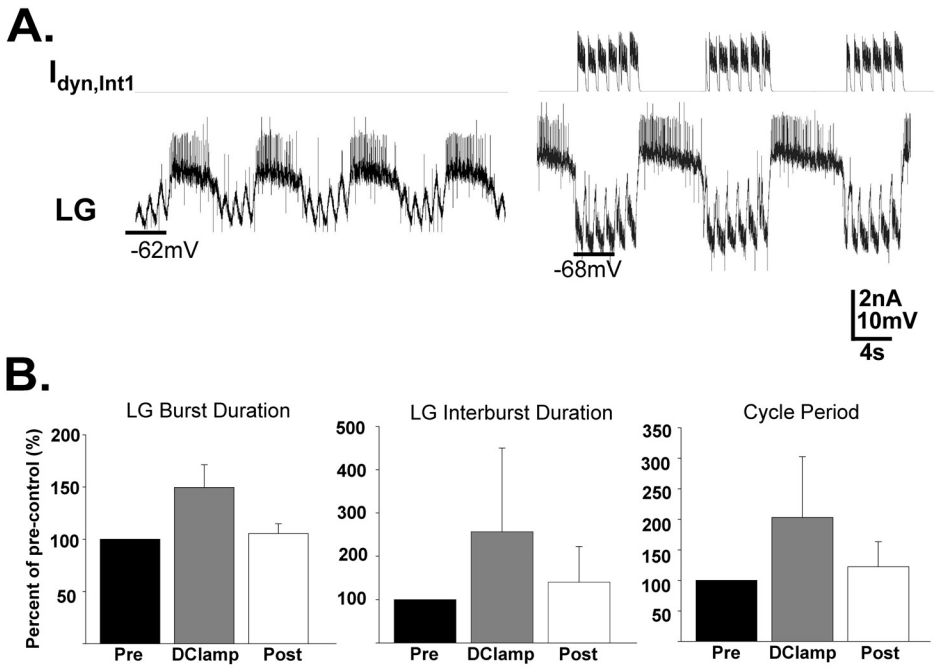

Figure 7. Increasing the strength of Int1 inhibition of the LG neuron with the dynamic clamp, in the biological preparation, slows the gastric mill rhythm by prolonging both phases of the rhythm. *A,* During an ongoing MCN1-elicited gastric mill rhythm, the dynamic clamp was used to increase the strength of Int1 inhibition of the LG neuron. This increased inhibition led to a prolonged retractor phase as well as a longer duration of each subsequent protractor phase. The vertical lines occurring periodically during the LG burst (rising above and below the action potentials) and interburst represent artifacts that occur when recording in discontinuous current clamp-mode while performing nerve (*ion*) stimulation. *B,* Quantitative analysis supporting the result represented in Panel *A*. Under these conditions, GPR stimulation reversibly prolonged the LG burst duration, LG interburst duration and gastric mill cycle period ($p<0.01$, $n=6$).

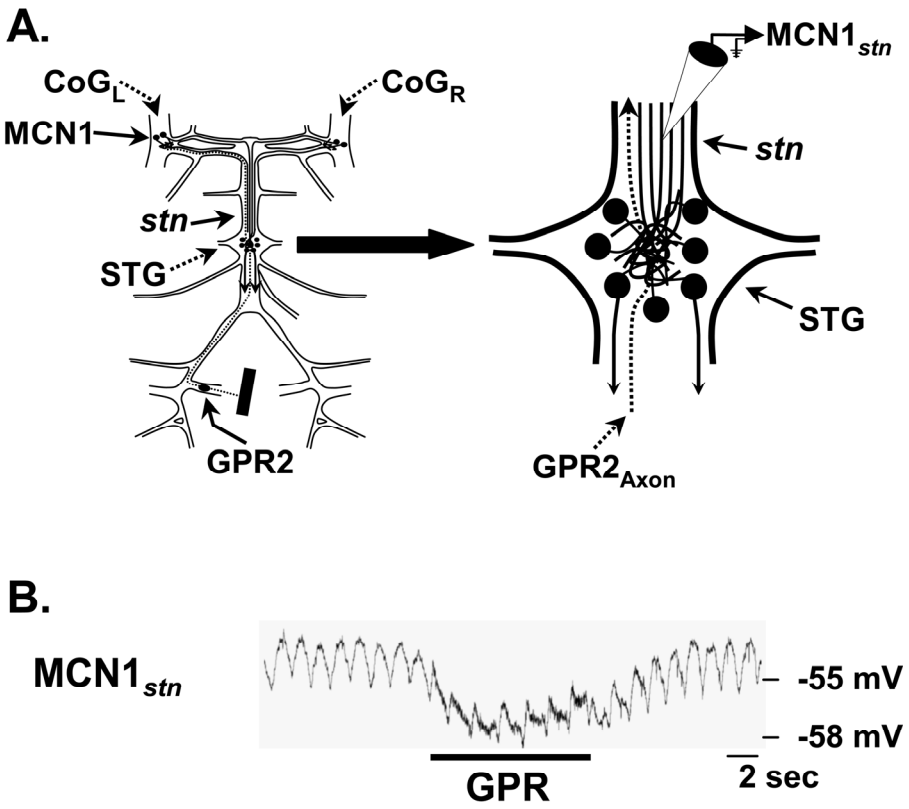

Figure 8. GPR stimulation hyperpolarizes the STG terminals of MCN1. A, Schematic of the isolated STNS (left), with an expanded view of the STG (right) to indicate the location of the intra-axonal recording site for MCN1$_{stn}$. *B.* Intracellular recording of MCN1$_{stn}$ revealed a hyperpolarizing response to GPR stimulation (5 Hz). Note the subthreshold pyloric-timed oscillations in MCN1$_{stn}$. The thickened MCN1$_{stn}$ trace during GPR stimulation represents the stimulus artifact.

neuron burst duration was also reversibly prolonged (pre-DClamp: 4.1 ± 1.2 sec; DClamp: 6.2 ± 2.6 sec; post-DClamp: 4.3 ± 1.5 sec; Two-way ANOVA $p<0.005$; Tukey pairwise comparison: DClamp vs. Pre, $p<0.005$, DClamp vs. Post, $p<0.01$, Post vs. Pre, $p>0.05$; n=6) (Fig. 7*A,B*). These results, combined with the fact that GPR stimulation did not change the Int1 firing frequency during the gastric mill rhythm, led us to conclude that the GPR-mediated selective prolongation of the gastric mill retractor phase and associated slowing of the rhythm was not likely to result, at least exclusively, from its excitation of Int1.

GPR stimulation inhibits the STG terminals of MCN1

We next examined the possibility that the GPR ability to selectively prolong the gastric mill retractor phase resulted from GPR inhibition of the STG terminals of MCN1. Depending on its strength, such a synaptic action would slow or prevent the LG neuron escape from Int1 inhibition. MCN1 drive to the gastric mill circuit, including its slow excitation of the LG neuron, occurs primarily during each retractor phase because its transmitter release is reduced by presynaptic inhibition from the LG neuron during each protractor phase (Coleman and Nusbaum, 1994; Coleman et al., 1995). We therefore tested the hypothesis that the GPR-mediated prolongation of the retractor phase and the associated slowing of the gastric mill rhythm resulted from GPR inhibition of the STG terminals of MCN1. To this end, we recorded intra-axonally from MCN1 in the stomatogastric nerve (*stn*: $MCN1_{stn}$), near the entrance to the STG (see Fig. 8*A*).

This recording site is electrotonically close to the MCN1 terminals in the STG ($MCN1_{STG}$), and electrotonically distant from its arborization and spike initiation zone in the CoG ($MCN1_{CoG}$) (Coleman and Nusbaum, 1994).

GPR stimulation consistently evoked a hyperpolarizing response in $MCN1_{stn}$ (n=5) (Fig. 8*B*). This hyperpolarization was graded in amplitude, correlated with the frequency of GPR stimulation (data not shown). Unlike the LG-mediated presynaptic inhibition of MCN1 (Coleman and Nusbaum, 1994), however, we did not record any unitary IPSPs in $MCN1_{stn}$ in response to GPR stimulation. Instead the GPR-mediated inhibition exhibited a relatively slow rise and decay, taking several seconds to repolarize after GPR stimulation was terminated (Fig. 8*B*). This inhibitory action was likely to occur within the STG neuropil, from where it spread passively to the $MCN1_{stn}$ recording site, as is the case for the LG inhibition of $MCN1_{STG}$ (Coleman and Nusbaum, 1994). This expectation was based on the fact that the GPR-mediated hyperpolarization neither suppressed nor reduced in amplitude or duration the *ion*-elicited action potentials recorded at $MCN1_{stn}$. Instead, as also occurs during LG inhibition of $MCN1_{STG}$ (Coleman and Nusbaum, 1994), these action potentials were either unchanged or increased slightly in amplitude. A comparable increase in the amplitude of *ion*-elicited action potentials occurred at $MCN1_{stn}$ when the MCN1 axon was comparably hyperpolarized by current injection (data not shown).

We could not assess the functional consequences of the GPR-mediated presynaptic inhibition of MCN1 by using an STG target of MCN1 as a reporter

neuron, as we did in characterizing the LG presynaptic inhibition of MCN1 (Coleman and Nusbaum, 1994). This was because every STG target of MCN1 was also a direct and/or indirect target of GPR (Katz and Harris-Warrick, 1990, 1991; this paper). Therefore, we instead used several alternative means to assess the impact of the GPR inhibition on MCN1 transmitter release within the STG. First, to more directly determine whether this GPR-mediated inhibition could effectively influence $MCN1_{STG}$ activity, we took advantage of the fact that injecting depolarizing current into $MCN1_{stn}$ evokes action potentials that are initiated within the STG neuropil (Coleman and Nusbaum, 1994). Consequently, we assessed how GPR stimulation affected MCN1 spike initiation within the STG. To this end, we either injected tonic depolarizing current to elicit tonic MCN1 activity, or else repeatedly (1 Hz) injected 100 msec duration depolarizing current pulses into $MCN1_{stn}$ such that each control pulse elicited several MCN1 action potentials. During tonic $MCN1_{STG}$ stimulation, GPR stimulation reversibly suppressed MCN1 activity (n=3). During rhythmic $MCN1_{STG}$ depolarizations, GPR stimulation consistently and reversibly reduced the number of MCN1 action potentials produced during each depolarizing pulse (pre-GPR: 3.9 ± 0.1 spikes; during GPR: 1.6 ± 1.1 spikes; post-GPR: 3.5 ± 0.1 spikes, $p<0.05$; n=2) (Fig. 9).

Although GPR stimulation effectively inhibited the spike-initiating ability of $MCN1_{STG}$, the GPR influence on incoming MCN1 action potentials was more complex. Specifically, when MCN1 action potentials propagated through the *stn* into the STG during the GPR-mediated hyperpolarization, the electrical EPSPs

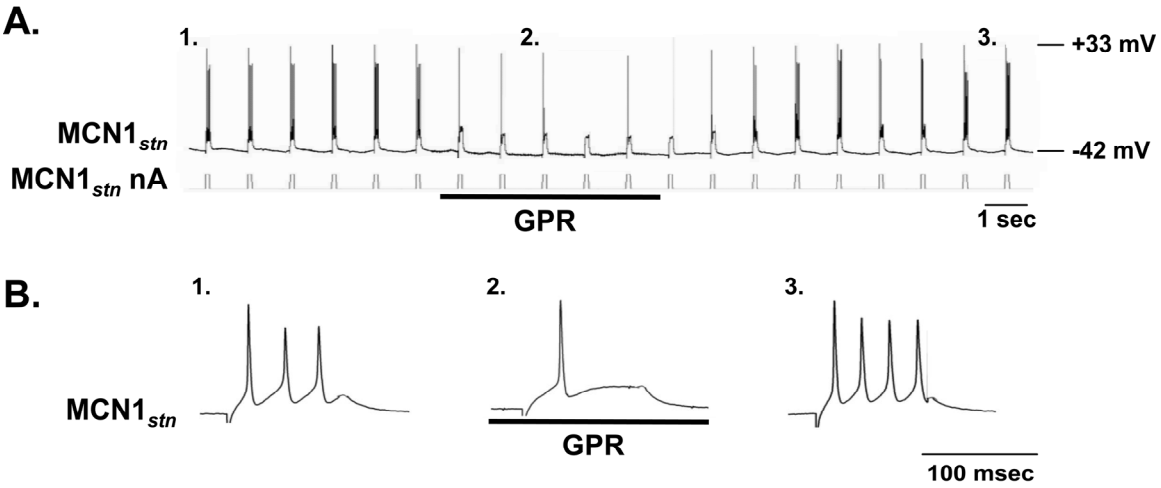

Figure 9. GPR stimulation inhibits MCN1 action potential initiation within the STG neuropil. *A,* Injecting depolarizing current into $MCN1_{stn}$ initiates action potentials within the STG neuropil (Coleman and Nusbaum, 1994). Constant duration (100 msec) and amplitude (+2nA) depolarizing pulses injected into $MCN1_{stn}$ produced a regular number (3-4) of action potentials/pulse. This number was reversibly reduced during GPR stimulation (5 Hz). Note the delay of several seconds after GPR stimulation before the number of MCN1 action potentials/pulse returns to control levels. *B,* Expanded traces from panel *A* of single pulses (1) before, (2) during and (3) after GPR stimulation.

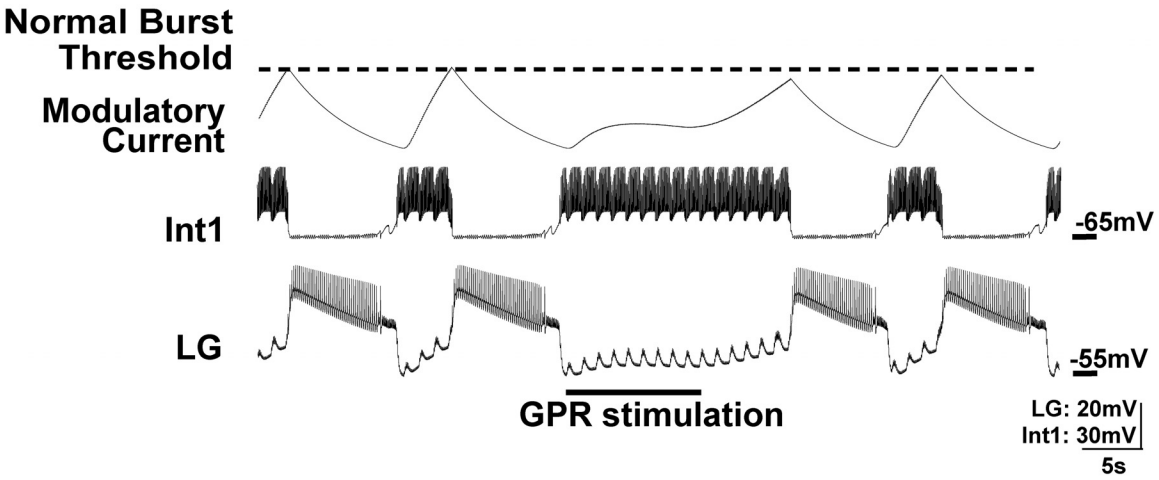

Figure 10. The GPR action on the MCN1-elicited gastric mill rhythm is best mimicked by GPR inhibition of $MCN1_{STG}$ in a computational model of the MCN1-elicited gastric mill rhythm. In this version of the model, GPR stimulation presynaptically inhibited $MCN1_{STG}$, thereby reducing MCN1 actions onto the LG neuron. As a result, the amplitude of the modulatory current induced in LG by MCN1 is reduced during GPR stimulation. This effect persists after GPR stimulation due to the slow time constant of the GPR action. The GPR inhibition of $MCN1_{STG}$ slowed the LG escape from Int1 inhibition, prolonging the retractor phase. Note that, in contrast, the protractor phase duration was not altered.

from MCN1 to LG persisted (not shown). This result left unresolved the issue of whether the GPR inhibition of $MCN1_{STG}$ was ineffective at regulating the influence of MCN1 or, as in the case of the LG inhibition of $MCN1_{STG}$ (Coleman and Nusbaum, 1994; Coleman et al., 1995), this GPR-mediated inhibition affected MCN1 transmitter release without suppressing the electrical synapses made by MCN1.

To address this issue, we returned to our computational model of the gastric mill system and assessed therein the consequences of GPR inhibition of $MCN1_{STG}$ (see Table 2). As shown in Figure 10, this model predicted that within a given range of inhibitory conductances the GPR inhibition of $MCN1_{STG}$ could mimic the actions of GPR on the biological gastric mill rhythm. Specifically, within this conductance range, GPR inhibition of $MCN1_{STG}$ selectively prolonged the gastric mill retractor phase and thereby slowed the rhythm. However, when inhibitory conductances larger than this range were used, LG could not escape from Int1 inhibition and the gastric mill rhythm was terminated.

The results from the model supported the hypothesis that the GPR ability to selectively prolong the gastric mill retractor phase involved its reduction but not elimination of MCN1 transmitter release. This is evident in Figure 10 from the reduced but persisting MCN1 modulation in the LG neuron during GPR stimulation. In this version of the model, we maintained the same level of Int1 inhibition of LG during the rhythm with and without GPR stimulation, to reflect the unchanged Int1 activity level during GPR stimulation in the physiological situation

(Fig. 5*B*). If MCN1 transmitter release was eliminated, the LG neuron would not have been able to escape from Int1 inhibition as long as GPR activity continued. However, when the GPR inhibition of $MCN1_{STG}$ only reduced MCN1 excitation of LG (peak synaptic conductance during GPR ~50% of control peak), then the retractor phase of the model rhythm was prolonged. This extended retractor phase occurred because it took more time to build up the same level of excitatory drive in LG that normally occurs in the absence of GPR activity, which is the amount needed by LG to escape a constant level of Int1 inhibition and generate a burst (Fig. 10). Once that level was attained, the LG neuron fired its burst, inhibiting MCN1 and thereby starting the down-regulation of its own activity. Unlike the situation in which Int1 inhibition of LG was strengthened (Figs. 6, 7), here the same amount of excitatory drive from MCN1 was attained by LG at the time of its burst onset. Thus, the modulatory effect decayed with the same time course as occurred before GPR stimulation, leaving the LG burst duration unchanged.

We then assessed whether the outcomes of the model were likely to reflect the related biological events by using two approaches. First, we tested the model prediction that the rate at which the MCN1 excitation of the LG neuron developed during the retractor phase selectively regulates the retractor phase duration. We did this by tonically stimulating MCN1 at different frequencies and assessing the resulting duration of the retractor and protractor phases. As shown qualitatively by Bartos et al. (1999), the MCN1 firing frequency determines

the speed of the gastric mill rhythm primarily by its control of the retractor phase duration. Our quantitative analysis showed that this is indeed the case. Specifically, the gastric mill cycle period consistently decreased as MCN1 firing frequency increased (Cycle period: MCN1 (6-7 Hz), 14.5 ± 5.3 sec; MCN1 (10 Hz), 10.7 ± 3.5 sec; MCN1 (15 Hz), 9.4 ± 2.7 sec; MCN1 (20 Hz), 7.7 ± 1.9 sec; Two-way ANOVA $p<0.005$; n=7). This change in cycle period was due largely to the parallel change in retractor phase duration (Retractor Phase Duration: MCN1 (6-7 Hz), 9.7 ± 4.8 sec; MCN1 (10 Hz), 5.7 ± 2.4 sec; MCN1 (15 Hz), 3.6 ± 1.2 sec; MCN1 (20 Hz), 3.0 ± 1.0 sec; Two-way ANOVA $p<0.005$; n=7). Under these conditions, the protractor phase duration was unchanged (Protractor Phase Duration: MCN1 (6-7 Hz), 4.8 ± 1.9 sec; MCN1 (10 Hz), 5.0 ± 2.0 sec; MCN1 (15 Hz), 5.8 ± 2.2 sec; MCN1 (20 Hz), 4.7 ± 1.5 sec; Two-way ANOVA, $p>0.05$; n=7).

Second, we used the dynamic clamp to generate a gastric mill-like rhythm by selectively introducing, and manipulating, the likely MCN1-mediated conductance into the LG neuron. For this purpose, we used the peptide-activated current that was first characterized in the *C. borealis* STG to mediate the actions of the peptide proctolin on the pyloric circuit (Golowasch and Marder, 1992) (see Methods). This current, termed the “proctolin current”, was subsequently shown to also mediate the actions of other neuroactive peptides on the pyloric circuit in *C. borealis* (Swensen and Marder, 2000, 2001). One of these peptides is CabTRP Ia, which is the peptide transmitter used by MCN1 to excite the LG neuron (Wood et al., 2000).

For these experiments we used preparations in which the STG remained in communication with the CoGs, to ensure a relatively high rate of spontaneous activity in Int1. As commonly occurs in the isolated STNS, in these preparations Int1 exhibited spontaneous, pyloric-timed activity while the LG neuron was silent (Bartos et al., 1999). Injection of a sufficient level of the proctolin conductance into the LG neuron (see Table 1) enabled LG to escape from Int1 inhibition and fire action potentials. To terminate each LG burst and thereby mimic the gastric mill rhythm-related burst pattern of LG, we added a slow inactivation variable to the proctolin current to mimic the LG presynaptic inhibition of MCN1 that normally regulates that current (Coleman and Nusbaum, 1994; see Methods) (Fig. 11). Consequently, the proctolin current was effectively increasing in amplitude during each LG interburst and decaying during each LG burst.

We then implemented different rates of increase for this modulatory current in order to determine whether this rate could selectively regulate the duration of the retractor phase. To this end, we compared gastric mill-like rhythms with relatively slow (tau=160-320s) and fast (tau=8-16s) rates of rise for this excitatory drive. Consistent with the model predictions, the relatively slowly developing dynamic clamp excitation of LG caused a slower rhythm (cycle period: fast rise, 10.97 ± 4.4s; slow rise, 18.49 ± 5.2s; t-test, $p<0.005$, n=5) with a selectively prolonged retractor phase relative to the faster developing excitation (retractor phase duration: fast rise, 6.62 ± 2.7s; slow rise, 14.19 ± 4.3s; t-test, $p<0.005$, n=5; protractor phase duration: fast rise, 4.36 ± 2.1s; slow rise, 4.30 ±

1.0s; t-test, $p>0.05$, $n=5$) (Fig. 11). These results thus support the hypothesis that the selective prolongation of the retractor phase by GPR stimulation can result from its presynaptic inhibition of $MCN1_{STG}$ slowing the buildup of modulatory excitation from MCN1 to LG during the retractor phase.

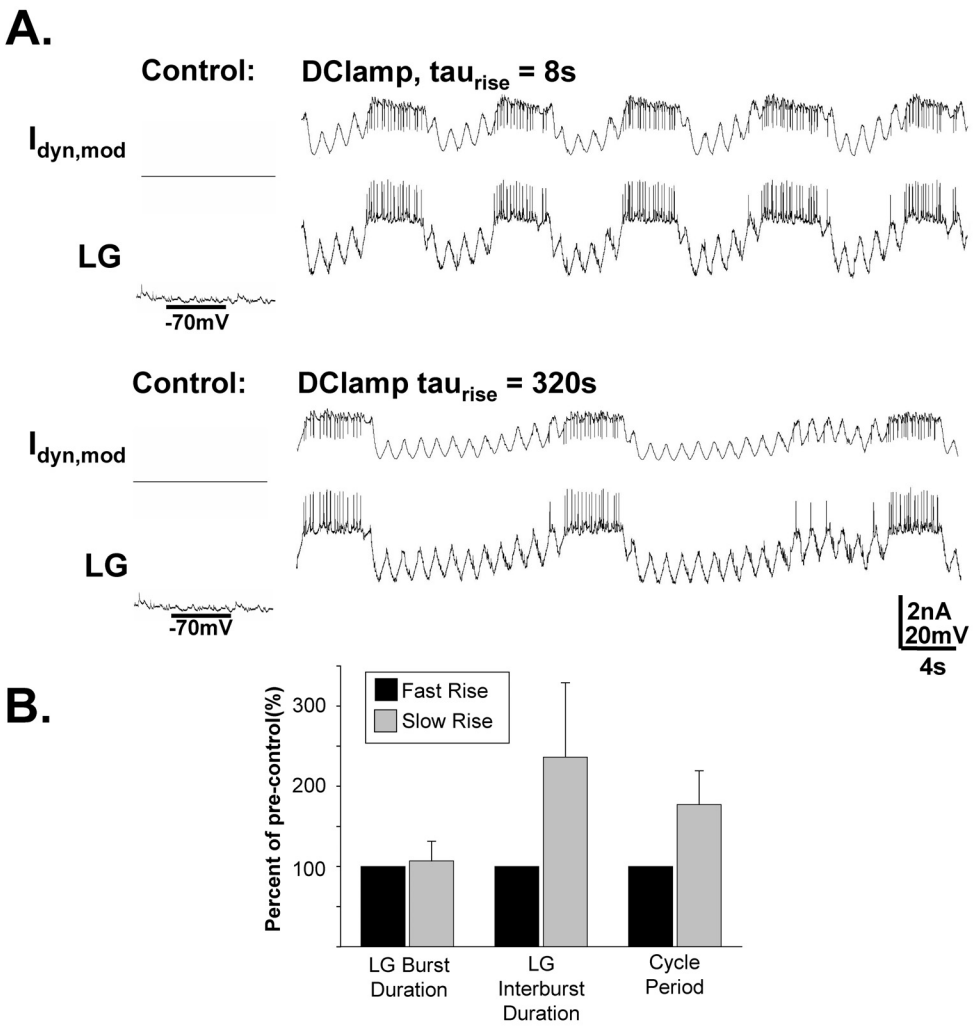

Figure 11. The rate of rise of MCN1-like modulation of the LG neuron selectively regulates the retractor phase duration. *A,* In this experiment, in place of MCN1 stimulation, the biological LG neuron was injected with a dynamic clamp version of the modulatory current that likely represents the current provided by MCN1 (Swensen and Marder, 2000; see Methods). The only parameter that differed during the dynamic clamp current injection in the two traces shown was the rate of rise of the current amplitude during each LG interburst. Note that the slower rate of rise (bottom trace) caused a slower rhythm, which resulted largely from a

selectively prolonged LG interburst (retractor-like phase). Both LG traces are from the same preparation. *B,* Injecting the dynamic clamp version of the modulatory current into LG with a relatively long time constant for its rise in amplitude consistently elicited gastric mill-like activity in LG that was slower, due to a selective increase in LG interburst duration, than that resulting from injection of the same current with a briefer time constant ($p<0.005$, $n=5$).

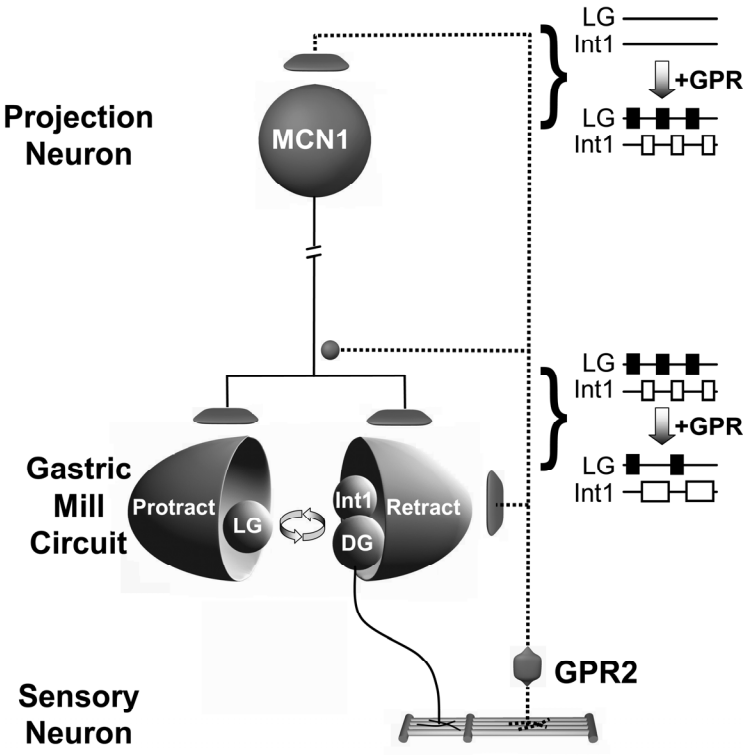

Figure 12. Working model of the GPR actions on the gastric mill system. Gastric mill-like rhythmic GPR stimulation can elicit the gastric mill rhythm (Blitz et al., 2004) by exciting the projection neuron MCN1 (and CPN2) in the commissural ganglia. During the gastric mill rhythm elicited by MCN1 (either directly or via activation of the VCN mechanosensory neurons), stimulating GPR in a behaviorally-appropriate manner (during each retractor DG neuron burst) slows the gastric mill rhythm by selectively prolonging the retractor phase. This latter GPR action results from GPR inhibition of the axon terminals of MCN1 in the stomatogastric ganglion, in concert with its excitation of the retractor neurons Int1 and DG. Synapse symbols: t-bars, excitation; filled circles, inhibition.

DISCUSSION

Sensory inputs shape rhythmic motor activity via direct and indirect actions on the underlying pattern-generating circuits (Pearson, 2004; Buschges, 2005). Although the significance of these inputs to rhythmic motor activity is well documented, the mechanisms through which sensory actions reshape motor output have not been elucidated in most systems. In this paper we show that the phasically-activated muscle stretch receptor neuron GPR regulates the gastric mill rhythm at least partly by presynaptically inhibiting the modulatory projection neuron MCN1 (Fig. 12). In parallel, GPR postsynaptically excites the retractor phase neurons Int1 and DG (Katz and Harris-Warrick, 1989; Kiehn and Harris-Warrick, 1992; this paper) (Fig, 12). The presynaptic inhibition reduces the excitatory drive from MCN1 to all gastric mill neurons, while the postsynaptic excitation appears to function as a replacement for the reduced drive from MCN1 specifically to the retractor neurons. The consequence for the gastric mill rhythm is a selectively prolonged retractor phase and slower cycle period.

GPR regulation of the gastric mill system via presynaptic inhibition of a modulatory projection neuron represents a novel mechanism for phasic sensory regulation of ongoing motor activity. Most previous studies of phasic sensory regulation have instead highlighted CPG and motor neurons as the sensory neuron targets (Hooper and Moulins, 1990; Katz and Harris-Warrick, 1990, 1991; Buschges and el Manira, 1998; Rosen et al., 2000; Shetreat-Klein and Cropper, 2004; Pearson, 2004; Buschges, 2005). However, Combes et al. (1999) have

shown that rhythmic stimulation of the anterior gastric receptor (AGR), a muscle tendon receptor in the lobster STNS, reconfigures an ongoing gastric mill rhythm via synaptic actions on modulatory projection neurons within the CoG.

Sensory regulation of neural circuit activity

To optimize the understanding of how sensory systems influence their targets by manipulating them in the isolated CNS, it is important to implement the biologically appropriate activity pattern for that sensory system. This experimental approach has led to an improved understanding, albeit not yet at the level of identified circuit neurons, of the phasic sensory influence on both intra- and inter-limb coordination during locomotion (Pearson, 2004; Buschges, 2005). We therefore recapitulated a behaviorally-relevant scenario for the GPR neurons by taking advantage of previous studies documenting their response to stretch of the muscles in which their dendrites are embedded (Katz et al., 1989; Katz and Harris-Warrick, 1989; Birmingham et al., 1999, 2003). Our experimental approach is likely to approximate events occurring in the feeding animal because the VCN neurons are thought to be activated during stomach distention (Beenhakker et al., 2004), and the VCN-triggered chewing motor pattern would involve rhythmic stretch of the GPR-innervated muscles.

Acute activation of the GPR neurons at times when there is no gastric mill rhythm evokes a reflex response that includes a relatively long-lasting activation of gastric mill retractor neurons and a modulation of the pyloric rhythm (Katz and

Harris-Warrick, 1989, 1990, 1991). The gastric mill response is a reinforcing reflex because activation of the retractor neuron DG results in stretch of the muscle in which the GPR dendrites are embedded, and GPR in turn evokes a burst of activity in DG (Katz and Harris-Warrick, 1989; Kiehn and Harris-Warrick, 1992). During the gastric mill rhythm, the prolonged reflex response is eventually terminated because the LG neuron escapes from Int1 inhibition and terminates retractor neuron activity (Coleman et al., 1995; this paper).

The GPR effect of prolonging the retractor phase of the gastric mill rhythm is not achieved by directly or indirectly increasing the level of synaptic inhibition in the protractor CPG neuron LG. As elucidated by our computer model and supported by our dynamic clamp experiments, prolonging the retractor phase via any synaptic influence on the LG neuron would increase the duration of the subsequent LG neuron burst, contrary to the GPR actions on the gastric mill rhythm. Thus, to selectively prolong the retractor phase, GPR instead reduces the MCN1 influence on the entire gastric mill circuit to delay the onset of the next protractor phase and, in parallel, helps maintain the retractor phase by substituting its own excitatory drive to the retractor neurons.

It may seem surprising that GPR stimulation did not increase the level of Int1 activity during the gastric mill rhythm, given its ability to directly excite Int1. However, although we did not directly test the effectiveness of this synaptic action during the gastric mill rhythm, GPR is likely to use this synapse to compensate for the reduced MCN1 excitation of Int1 that results from GPR

inhibition of $MCN1_{STG}$. Drawing the conclusion that GPR excitation of Int1 was responsible for the ability of GPR to delay the onset of the protractor phase would have been reasonable given the key role played by the Int1 inhibition of LG in gastric mill rhythm generation (Coleman et al., 1995; Bartos et al., 1999). The fact that this synapse turned out not to be pivotal for the GPR-mediated selective prolongation of the retractor phase provides a valuable lesson in understanding circuit operation. If we had not examined the GPR effect on Int1 activity during the gastric mill rhythm and had not considered the consequences of changing Int1 activity in terms of the buildup of MCN1 excitation of the LG neuron, we might not have searched for GPR influences on $MCN1_{STG}$.

Regulation of circuit activity at multiple sites on the same projection neuron

There are not many systems where it has been possible to document the presence and function of spatially separate synaptic actions by a single neuron onto the same target neuron. Our work with GPR illustrates such an example in that GPR causes a long-lasting excitation of $MCN1_{CoG}$ and a shorter-lasting inhibition of $MCN1_{STG}$ (Blitz et al., 2004; this paper) (Fig. 12). GPR also excites CPN2 in the CoGs, and its co-activation of these two projection neurons initiates the gastric mill rhythm (Blitz et al., 2004). When GPR stimulation elicits the gastric mill rhythm, it also appears to be effectively inhibiting $MCN1_{STG}$ as evidenced by the fact that this version of the gastric mill rhythm is slower than that elicited by the VCN mechanosensory neurons, due to a prolonged retractor

phase (Blitz et al., 2004). It will be instructive to determine whether the opposing GPR actions on $MCN1_{CoG}$ and $MCN1_{STG}$ are mediated by the same or different GPR cotransmitters, which include acetylcholine, serotonin and the peptide allatostatin (Katz and Harris-Warrick, 1989; Skiebe and Schneider, 1994).

The excitatory actions of GPR on MCN1 and CPN2 in the CoG are state-dependent, in that they are absent when these projection neurons have been recently activated by the VCNs (Beenhakker, 2004). This state-dependent excitation of $MCN1_{CoG}$ and $CPN2_{CoG}$ by GPR facilitates the ability of GPR to slow this rhythm via its actions in the STG. Specifically, if GPR continued to excite $MCN1_{CoG}$ during the VCN-elicited gastric mill rhythm, then the increased MCN1 firing frequency would likely result in a reduced effectiveness of the GPR inhibition of $MCN1_{STG}$.

Presynaptic inhibition enables sensory signals to dynamically regulate neural circuit activity

The role of presynaptic inhibition in the context of sensorimotor integration is commonly discussed with regard to the gating in or, more commonly, gating out of sensory information (Nusbaum et al., 1997; Buschges and el Manira, 1998; Evans et al., 2003; Katz, 2004). One frequently documented example of this gating mechanism is the primary afferent depolarization that occurs on sensory axon terminals to reduce sensory input to CPG networks. This has been particularly well-studied for presynaptic inhibition of sensory input to the

locomotor network of both vertebrates and invertebrates (Buschges and el Manira, 1998; Rudomin and Schmidt, 1999; Cattaert et al., 2001; Frost et al., 2003). This presynaptic inhibition can be regulated in a spinal segment-specific manner (Lomeli et al., 1998; Rudomin et al., 2004). Presynaptic inhibition of projection neuron terminals has also been documented at reticulospinal axon terminals relevant to lamprey swimming, but its role in motor pattern generation remains to be elucidated (Svensson et al., 2003). The findings described herein extend these studies by showing that proprioceptor-mediated presynaptic inhibition of a modulatory projection neuron can contribute to phase-specific regulation of rhythmic activity.

The parallel presynaptic and postsynaptic actions of the GPR proprioceptor neuron enable it to simultaneously mediate its reflex function of prolonging teeth retraction without terminating ongoing CPG activity. If GPR instead terminated CPG activity to mediate its reflex function, then once GPR activity ceased it would take several gastric mill cycles until the rhythm was back to its steady-state level (Bartos et al., 1999). Instead, as shown here, the gastric mill rhythm returns to its pre-GPR activity level as soon as GPR activity terminates.

Another level of control in this system is suggested by the fact that the sensitivity of GPR to muscle stretch is itself modulated (Birmingham et al., 1999, 2003; Birmingham, 2001). We therefore anticipate that our appreciation for how sensory signals regulate neural circuit activity will be extended further as we

assess the consequences resulting from modulation of GPR sensitivity for its influence on the gastric mill motor circuit.

REFERENCES

Bartos M, Nusbaum MP (1997) Intercircuit control of motor pattern modulation by presynaptic inhibition. J Neurosci 17:2247-2256.

Bartos M, Manor Y, Nadim F, Marder E, Nusbaum MP (1999) Coordination of fast and slow rhythmic neuronal circuits. J Neurosci 19:6650-6660.

Beenhakker MP (2004) Sensory regulation of rhythmically active neuronal networks. PhD Thesis, University of Pennsylvania.

Beenhakker MP, Nusbaum MP (2003) Sensory regulation of a modulatory projection neuron at two separate locations. Soc Neurosci Abstr 60411.

Beenhakker MP, Nusbaum MP (2004) Mechanosensory activation of a motor circuit by coactivation of two projection neurons. J Neurosci 24: 6741-6750.

Beenhakker MP, Blitz DM, Nusbaum MP (2004) Long-lasting activation of rhythmic neuronal activity by a novel mechanosensory system in the crustacean stomatogastric nervous system. J Neurophysiol 91:78-91.

Birmingham JT (2001) Increasing sensor flexibility through neuromodulation. Biol Bull 200:206-210.

Birmingham JT, Szuts Z, Abbott LF, Marder E (1999) Encoding of muscle movement on two time scales by a sensory neuron that switches between spiking and burst modes. J Neurophysiol 82:2786-2797.

Birmingham JT, Billimoria CP, De Klotz TR, Stewart RA, Marder E (2003) Differential and history-dependent modulation of a stretch receptor in the

stomatogastric system of the crab, *Cancer borealis*. J Neurophysiol 90:3608-3616.

Blitz DM, Beenhakker MP, Nusbaum MP (2004) Different sensory systems share projection neurons but elicit distinct motor patterns. J Neurosci 24: 11381-11390.

Blitz DM, Nusbaum MP (1999) Distinct functions for cotransmitters mediating motor pattern selection. J Neurosci 19:6774-6783.

Buschges A (2005) Sensory control and organization of neural networks mediating coordination of multisegmental organs for locomotion. J Neurophysiol 93:1127-1135.

Buschges A, el Manira AE (1998) Sensory pathways and their modulation in the control of locomotion. Curr Opin Neurobiol 8:733-739.

Cattaert D, Libersat F, El Manira A (2001) Presynaptic inhibition and antidromic spikes in primary afferents of the crayfish: a computational and experimental analysis. J Neurosci 21:1007-1021.

Coleman MJ, Nusbaum MP (1994) Functional consequences of compartmentalization of synaptic input. J Neurosci 14:6544-6552.

Coleman MJ, Meyrand P, Nusbaum MP (1995) A switch between two modes of synaptic transmission mediated by presynaptic inhibition. Nature 378:502-505.

Combes D, Meyrand P, Simmers J (1999) Dynamic restructuring of a rhythmic motor program by a single mechanoreceptor neuron in lobster. J Neurosci 19:3620-3628.

Di Prisco GV, Pearlstein E, Le Ray D, Robitaille R, Dubuc R (2000) A cellular mechanism for the transformation of a sensory input into a motor command. J Neurosci 21:8169-8176.

Evans CG, Jing J, Rosen SC, Cropper EC (2003) Regulation of spike initiation and propagation in an *Aplysia* sensory neuron: gating-in via central depolarization. J Neurosci 23:2920-2931.

Frost WN, Tian L-M, Hoppe TA, Mongeluzi DL, Wang J (2003) A cellular mechanism for prepulse inhibition. Neuron 40:991-1001.

Golowasch J, Marder E (1992) Proctolin activates an inward current whose voltage dependence is modified by extracellular Ca^{2+}. J Neurosci 12:810-817.

Hartline DK, Graubard K (1992) Cellular and synaptic properties in the crustacean stomatogastric nervous system. In: Dynamic Biological Networks: The Stomatogastric Nervous System (Harris-Warrick RM, Marder E, Selverston AI, Moulins M, eds), pp 31-86. Cambridge, MA: MIT Press.

Heinzel H-G, Weimann JM, Marder E (1993) The behavioral repertoire of the gastric mill in the crab, *Cancer pagurus*: an in situ endoscopic and electrophysiological examination. J Neurosci 13:1793-1803.

Hooper SL, Moulins M (1990) Cellular and synaptic mechanisms responsible for a long-lasting restructuring of the lobster pyloric network. J Neurophysiol 64: 1574-1589.

Katz PS (2004) Synaptic gating: the potential to open closed doors. Curr Biol 13:R554-R5565.

Katz PS, Eigg MH, Harris-Warrick RM (1989) Serotonergic/cholinergic muscle receptor cells in the crab stomatogastric nervous system. I. Identification and characterization of the gastropyloric receptor cells. J Neurophysiol 62:558-570.

Katz PS, Harris-Warrick RM (1989) Serotonergic/cholinergic muscle receptor cells in the crab stomatogastric nervous system. II. Rapid nicotinic and prolonged modulatory effects on neurons in the stomatogastric ganglion. J Neurophysiol 62:571-581.

Katz PS, Harris-Warrick RM (1990) Neuromodulation of the crab pyloric central pattern generator by serotonergic/cholinergic proprioceptive afferents. J Neurosci 10:1495-1512.

Katz PS, Harris-Warrick RM (1991) Recruitment of crab gastric mill neurons into the pyloric motor pattern by mechanosensory afferent stimulation. J Neurophysiol 65:1442-1451.

Kiehn O, Harris-Warrick RM (1992) Serotonergic stretch receptors induce plateau properties in a crustacean motor neuron by a dual-conductance mechanism. J Neurophysiol 68:485-495.

Lomeli J, Quevedo J, Linares P, Rudomin P (1998) Local control of information flow in segmental and ascending collaterals of single afferents. Nature 395:600-604.

McCrea DA (1998) Neuronal basis of afferent-evoked enhancement of locomotor activity. Ann N Y Acad Sci 860:216-225.

Nadim F, Manor Y, Nusbaum MP, Marder E (1998) Frequency regulation of a slow rhythm by a fast periodic input. J Neurosci 18:5053-5067.

Norris BJ, Coleman MJ, Nusbaum MP (1994) Recruitment of a projection neuron determines gastric mill motor pattern selection in the stomatogastric nervous system of the crab, *Cancer borealis*. J Neurophysiol. 72:1451-1463.

Norris BJ, Coleman MJ, Nusbaum MP (1996) Pyloric motor pattern modification by a newly identified projection neuron in the crab stomatogastric nervous system. J Neurophysiol. 75:97-108.

Nusbaum MP, Beenhakker MP (2002) A small-systems approach to motor pattern generation. Nature 417:343-350.

Nusbaum MP, El Manira A, Gossard J-P, Rossignol S (1997) Presynaptic mechanisms during rhythmic activity in vertebrates and intervebrates. In: Neurons, Networks and Motor Behavior (Stein PSG, Grillner S, Selverston A, Stuart DG, eds), pp 237-253. Cambridge, MA: MIT Press.

Pearson K (2004) Generating the walking gait: role of sensory feedback. Prog Brain Res 143:123-129.

Perrins R, Walford A, Roberts A (2002) Sensory activation and role of inhibitory reticulospinal neurons that stop swimming in hatchling frog tadpoles. J Neurosci 22:4229-4240.

Prinz AA, Abbott LF, Marder E (2004) The dynamic clamp comes of age. Trends Neurosci 27:218-224.

Rosen SC, Miller MW, Evans CG, Cropper EC, Kupfermann I (2000) Diverse synaptic connections between peptidergic mechanoafferent neurons and neurons in the feeding system of *Aplysia*. J Neurophysiol 83:1605-1620.

Rudomin P, Lomeli J, Quevedo J (2004) Differential modulation of primary afferent depolarization of segmental and ascending intraspinal collaterals of single muscle afferents in the cat spinal cord. Exp Brain Res 156:377-391.

Rudomin P, Schmidt RF (1999) Presynaptic inhibition in the vertebrate spinal cord revisited. Exp Brain Res 129:1-37.

Sharp AA, O'Neil MB, Abbott LF, Marder E (1993) The dynamic clamp: artificial conductances in biological neurons. Trends Neurosci. 16:389-394.

Shetreat-Klein AN, Cropper EC (2004) Afferent-induced changes in rhythmic motor programs in the feeding circuitry of *Aplysia*. J Neurophysiol 92:2312-2322.

Skiebe P, Schneider H (1994) Allatostatin peptides in the crab stomatogastric nervous system: inhibition of the pyloric motor pattern and distribution of allatostatin-like immunoreactivity. J Exp Biol 194:195-208.

Stein PSG, Grillner S, Selverston AI, Stuart DG, eds (1997) Neurons, networks, and motor behavior. Cambridge, MA: The MIT Press.

Svensson E, Wikstrom MA, Hill RH, Grillner S (2003) Endogenous and exogenous dopamine presynaptically inhibits glutamatergic reticulospinal transmission via an action of D2-receptors on N-type Ca2+ channels. Eur J Neurosci 17:447-454.

Swensen AM, Marder E (2000) Multiple peptides converge to activate the same voltage-dependent current in a central pattern-generating circuit. J Neurosci 20:6752-6759.

Swensen AM, Marder E (2001) Modulators with convergent cellular actions elicit distinct circuit outputs. J Neurosci. 21:4050-4058.

Wood DE, Manor Y, Nadim F, Nusbaum MP (2004) Intercircuit control via rhythmic regulation of projection neuron activity. J Neurosci 25: 7455-7463.

Wood DE, Stein W, Nusbaum MP (2000) Projection neurons with shared cotransmitters elicit different motor patterns from the same neural circuit. J Neurosci 20:8943-8953.

Chapter 4

Presynaptic Inhibition Selectively Weakens Peptidergic Cotransmission in a Small Motor System

Nicholas D. DeLong

Mark P. Beenhakker

Michael P. Nusbaum

Submitted:

Nature Neuroscience, 2009

ABSTRACT

Little is known regarding whether presynaptic regulation of multi-transmitter neurons influences all transmission from these neurons. Using the crab stomatogastric ganglion, we determined that the GPR proprioceptor neuron uses presynaptic inhibition to selectively regulate peptidergic cotransmission from the axon terminals of MCN1, a projection neuron that drives the biphasic gastric mill (chewing) rhythm. MCN1 drives this rhythm via fast GABAergic excitation of the retractor neuron Int1 and slow peptidergic excitation of the protractor neuron LG. We demonstrate that GPR inhibition of the MCN1 axon terminals is serotonergic, and this serotonergic inhibition selectively weakens the MCN1 peptidergic excitation of LG. At the circuit level, we show that this selective regulation of MCN1 peptidergic cotransmission is necessary for the normal GPR regulation of the gastric mill rhythm. Thus, presynaptic inhibition can change the balance of cotransmitter actions and thereby enable a multi-transmitter neuron to have distinct, state-dependent actions on its target network.

INTRODUCTION

Cotransmission provides the potential for additional flexibility in neuronal signaling[1]. In general, cotransmission enables the convergence or divergence of co-released transmitters onto the same or separate target cells, respectively[2-8]. At the level of network activity, however, the impact of cotransmission remains largely unexplored[9-11]. Even less well understood is whether presynaptic regulation of synaptic transmission can selectively regulate only a subset of co-released transmitters, thereby providing the opportunity for another level of network flexibility.

Here we examine the synaptic regulation of cotransmission and its impact on rhythmically active motor circuits (central pattern generators: CPG) in the isolated stomatogastric nervous system (STNS) of the crab *Cancer borealis*[12]. The STNS includes the paired commissural ganglia (CoGs), oesophageal ganglion (OG) and stomatogastric ganglion (STG). The STG contains the CPGs for the gastric mill (chewing) and pyloric (filtering of chewed food) rhythms, while most projection neurons that regulate these rhythms originate in the CoGs[12-13]. The gastric mill rhythm driven by the CoG projection neuron called modulatory commissural neuron 1 (MCN1) is well-characterized, as is its regulation by the muscle stretch-sensitive, gastro-pyloric receptor (GPR) sensory neuron[14-16]**.** In brief, during the MCN1-elicited gastric mill rhythm, GPR stimulation selectively prolongs the gastric mill retractor phase by presynaptically inhibiting the STG terminals of MCN1 ($MCN1_{STG}$)[16]. This GPR action results at least partly from

weakening MCN1 peptidergic excitation of LG[16].

Here we determine the relative influence of GPR on the co-released MCN1 transmitters GABA and *Cancer borealis* tachykinin-related peptide Ia (CabTRP Ia) during the MCN1-elicited gastric mill rhythm. We first show that GPR uses only one of its three cotransmitters (serotonin) to presynaptically inhibit $MCN1_{STG}$ and, thus, to selectively prolong the gastric mill retractor phase. These GPR actions are suppressed by the serotonin receptor antagonist methiothepin. We then take advantage of this methiothepin-sensitive serotonergic action to show that the GPR inhibition of $MCN1_{STG}$ selectively weakens the peptidergic action of MCN1 on the gastric mill CPG, leaving its GABAergic action unchanged. At the circuit level, this selective inhibition of peptide cotransmission is necessary for the GPR selective prolongation of the gastric mill retractor phase.

RESULTS

GPR regulates the MCN1-gastric mill rhythm via serotonin

The MCN1-elicited gastric mill rhythm is a two phase motor pattern that includes alternating action potential bursts in protraction- and retraction phase STG neurons (**Fig. 1**)[17]. This rhythmic motor activity drives the protraction and retraction chewing movements of the teeth in the gastric mill stomach compartment[18]. In *C. borealis*, the CPG for this rhythm includes the reciprocally inhibitory retractor phase neuron Int1 and protractor neuron LG, plus $MCN1_{STG}$ (**Fig. 1**)[14-15].

MCN1 drives the gastric mill rhythm via its slow peptidergic (CabTRP Ia) excitation of LG and fast GABAergic excitation of Int1 (**Fig. 1b**)[6,14,19]. These MCN1 actions occur during the retraction phase, because LG inhibits $MCN1_{STG}$ during protraction (**Fig. 1b**)[14,20]. There are also several additional gastric mill motor neurons that are active during the MCN1-gastric mill rhythm, but their activity is not necessary for rhythm generation[15,17].

The GPR neurons are two, bilaterally symmetric pairs of neurons that function as proprioceptors[21]. Each GPR arborizes its dendrites in muscles that are stretched during the retractor phase of the gastric mill rhythm[21-22]. In the isolated STNS, selective extracellular stimulation of either GPR (*gpn* or *mgn* nerves) during the retractor phase of the MCN1-gastric mill rhythm selectively prolongs that phase, due to its presynaptic inhibition of $MCN1_{STG}$ (**Fig. 1b,c**)[16].

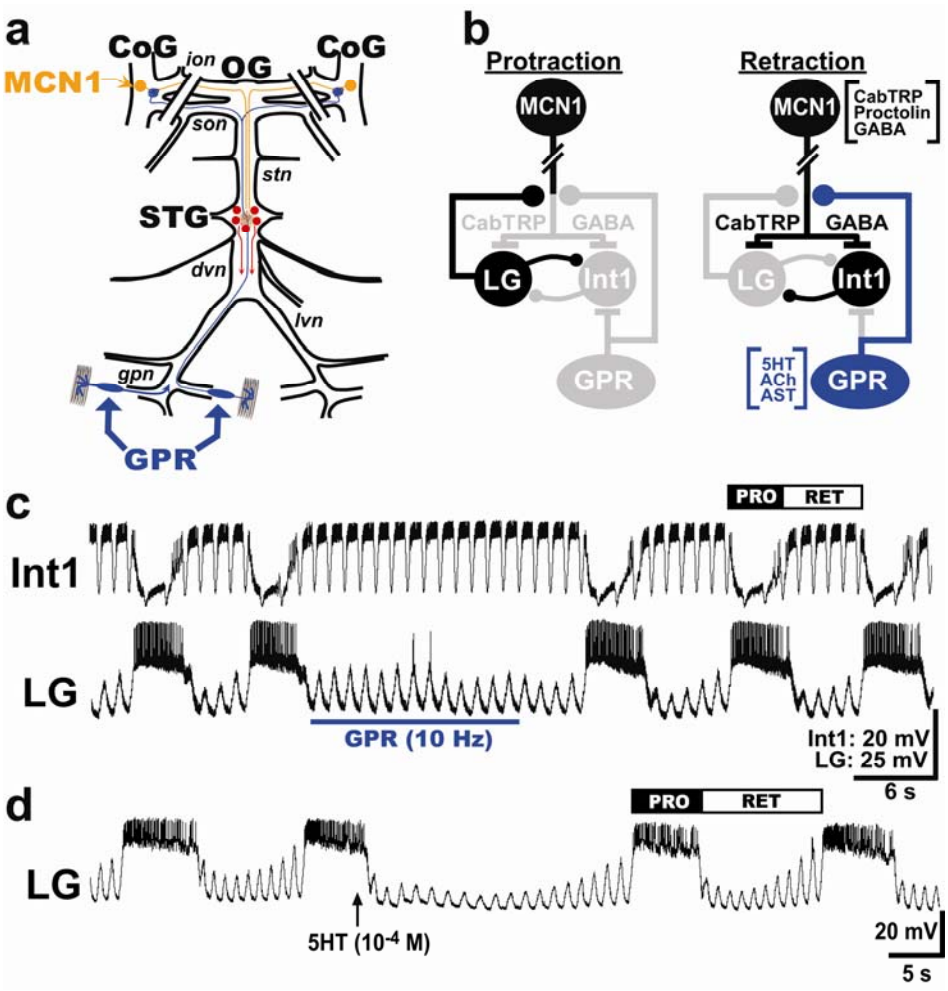

Figure 1. Schematic of the isolated STNS and MCN1-gastric mill rhythm regulation by the proprioceptor neuron GPR. **(a)** In each CoG, there is a single copy of the projection neuron MCN1. MCN1 projects to the STG via the *ion* and *stn* nerves. Each GPR arborizes in the STG and each CoG. The paired diagonal bars through the *sons* and *ions* represent the transection of these nerves at the start of each experiment. Grey rectangles represent protractor muscles in which GPR dendrites arborize. **(b)** Core gastric mill CPG schematic during each phase (protraction, retraction) of the gastric mill rhythm, including its regulation during retraction by GPR. Paired diagonal bars through MCN1 axon

represent additional distance between CoG and STG. All synapses shown are located in the STG neuropil. Gray somata and synapses represent silent neurons/synapses. Synapses drawn on somata or axons actually occur on small branches in the STG neuropil. Note that MCN1 uses only CabTRP Ia to excite LG and only GABA to excite Int1. Symbols: Filled circles, synaptic inhibition; T-bars, synaptic excitation. MCN1 and GPR cotransmitters are listed alongside their somata. **(c)** As shown previously[16], GPR stimulation selectively prolongs the retractor phase of the MCN1-elicited gastric mill rhythm. Most hyperpolarized V_m: Int1, -54 mV; LG, -75 mV. Abbreviations: PRO, protraction; RET, retraction. **(d)** Brief (2 s) 5-HT pressure application (arrow: pipette concentration: 10^{-4} M) onto the desheathed STG neuropil selectively prolonged the gastric mill retractor phase. Most hyperpolarized V_m: LG, -76 mV.

GPR contains the cotransmitters serotonin (5-hyroxytryptamine, 5-HT), acetylcholine (ACh) and allatostatin (AST), and it is the only source of 5-HT within the STG[21,23]. To further elucidate the mechanisms by which GPR regulates the MCN1-gastric mill rhythm, we aimed to determine the role of each GPR cotransmitter in its inhibition of $MCN1_{STG}$.

Relatively brief (1 s), focal application of serotonin (10^{-4} M) onto the desheathed STG neuropil mimicked the GPR action on the gastric mill rhythm (**Fig. 1d**). Specifically, serotonin application reversibly increased the duration of only the immediately subsequent retractor phase (pre-5-HT: 5.9 ± 1.0 s; 5-HT: 21.8 ± 5.8 s; post-5-HT: 7.6 ± 2.4 s; n=7, p=0.009) (**Fig. 1d**). There was no concomitant alteration in the protractor phase duration (pre-5-HT: 5.5 ± 1.4 s; 5-HT: 4.7 ± 1.3 s; post-5-HT: 5.6 ± 1.4 s; n=7, p=0.87). Similar to our previous results[16], GPR stimulation in these same preparations also prolonged the retractor phase (pre-GPR: 4.8 ± 0.4 s; during GPR: 17.1 ± 4.8 s; post-GPR: 4.9 ± 0.2 s; n=4, p=0.022) without altering protraction duration (pre-GPR: 4.2 ± 0.7 s; during GPR: 3.6 ± 0.6 s; post-GPR: 4.0 ± 0.8 s; n=4, p=0.84).

In contrast to these serotonin actions, neither focally applied AST (10^{-5} M: n=3, p=0.94) nor the muscarinic agonist oxotremorine (OXO: 10^{-4} M: n=3, p=0.94) mimicked the GPR actions on the MCN1-gastric mill rhythm (Supplementary **Fig. 1**). Similarly, co-applying AST (10^{-5} M: n=3, p=0.58) or OXO (10^{-4} M: n=3, p=0.14) with serotonin (10^{-4} M) was equivalent to applying serotonin alone in the same preparations (**Supplementary Fig. 1**).

To determine whether serotonin was necessary for mediating the GPR actions on the gastric mill rhythm, we tested the ability of the serotonin receptor antagonist methiothepin (10^{-5} M) to suppress these GPR effects. Methiothepin, which suppresses some serotonergic actions in decapod crustaceans[24], suppressed the GPR influence on the gastric mill rhythm (**Fig. 2a**). During methiothepin application, GPR stimulation did not change the retractor phase duration (pre-GPR: 5.1 ± 1.0 s; GPR: 7.8 ± 1.2 s; post-GPR: 6.6 ± 1.4 s; n=5, p=0.32) or the gastric mill cycle period (pre-GPR: 12.8 ± 2.7 s; GPR: 15.4 ± 3.4 s; post-GPR: 14.0 ± 3.1 s; n=5, p=0.86) (**Fig. 2a**).

In the aforementioned experiments GPR was stimulated only during the behaviorally-relevant retractor phase. Insofar as the retractor phase duration was briefer when GPR was stimulated during methiothepin application, due to the ability of LG to begin its burst sooner, it remained possible that the lack of a GPR-mediated effect during methiothepin application resulted from the relatively brief activation of the GPR pathway and not serotonin receptor blockade. To test this possibility, we took advantage of the fact that GPR has no effect on the gastric mill rhythm when it is stimulated only during the protraction phase (**Supplementary Fig. 2**), and so determined the influence of methiothepin during prolonged, tonic GPR stimulation. During saline superfusion, tonic GPR stimulation still prolonged retraction (Pre-GPR: 4.1 ± 0.4 s; During GPR: 9.3 ± 1.5 s, n=5, p=0.011) without altering protraction duration (Pre-GPR: 5.1 ± 0.9 s; During GPR: 3.6 ± 0.5 s, n=5, p=0.11), whereas during methiothepin application

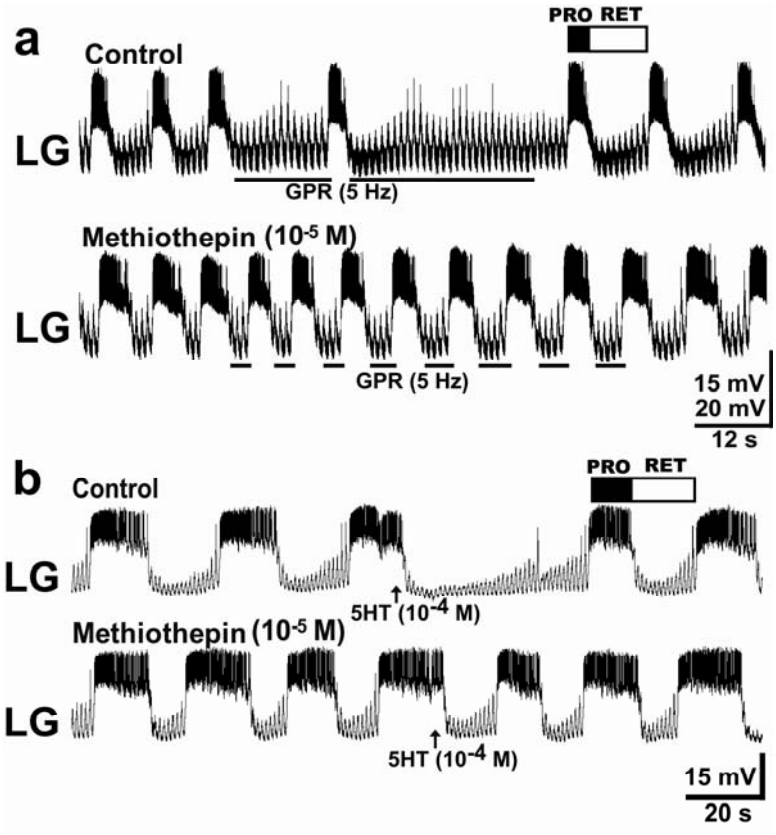

Figure 2. Regulation of the MCN1-elicited gastric mill rhythm by GPR stimulation and 5-HT application is suppressed by the serotonin receptor antagonist methiothepin. **(a)** Bath application of methiothepin suppressed the GPR action on the gastric mill rhythm. **Top:** GPR stimulation (bars) selectively prolonged the retractor phase during normal saline superfusion. **Bottom:** During methiothepin application, GPR stimulation (bars) did not change the retractor phase duration. After a 1.5 hour saline wash, GPR stimulation again prolonged the retractor phase (not shown). Most hyperpolarized V_m: LG, -62 mV (in both panels). **(b)** Bath application of methiothepin suppressed the effect of pressure ejected 5-HT on the gastric mill rhythm. **Top:** During saline superfusion, brief (1 s) pressure ejection of 5-HT (arrow) onto the desheathed STG neuropil

selectively prolonged the gastric mill retractor phase. **Bottom:** During methiothepin superfusion, pressure ejected 5-HT (arrow) did not alter the gastric mill rhythm. After a 1 hr saline wash, 5-HT application again prolonged the retractor phase (not shown). Most hyperpolarized V_m: LG, -63 mV (in both panels). Panels a and b are from separate preparations.

GPR did not alter retraction (Pre-GPR: 5.4 ± 0.7 s; During GPR: 7.2 ± 1.3 s, n=5, p=0.13) or protraction (Pre-GPR: 8.3 ± 1.8 s; During GPR: 7.3 ± 1.7 s, n=5, p=0.34).

To determine whether this methiothepin action resulted from its influence on a serotonin receptor, we tested its ability to influence the action of pressure-applied serotonin on the gastric mill rhythm. Methiothepin did suppress the serotonin influence on the gastric mill retractor phase (pre-5-HT: 8.8 ± 2.1 s; 5-HT: 14.5 ± 6.0 s; post-5-HT: 6.1 ± 1.6 s; n=4, p=0.32) (**Fig. 2b**). These results support the hypothesis that serotonin is pivotal to the GPR regulation of the gastric mill rhythm, with the other GPR cotransmitters playing no apparent role.

GPR regulates the gastric mill rhythm via serotonergic inhibition of $MCN1_{STG}$

We hypothesized that methiothepin eliminated the effects of GPR stimulation on the gastric mill rhythm by blocking GPR-mediated inhibition of $MCN1_{STG}$[16]. To test this hypothesis, we took advantage of the fact that GPR stimulation causes a slow hyperpolarization in $MCN1_{STG}$ that interferes with the ability of $MCN1_{STG}$ to initiate action potentials in response to depolarizing current injection[16]. We used this assay to determine whether GPR inhibited $MCN1_{STG}$ via a methiothepin-sensitive serotonergic synapse.

Pressure applied 5-HT (10^{-4} M) mimicked the GPR effects on $MCN1_{STG}$, causing $MCN1_{STG}$ to hyperpolarize and reducing the number of MCN1 action

potentials elicited by each current pulse (Pre-5-HT: 5.6 ± 1.9 spikes; During 5-HT: 0.6 ± 0.2 spikes; Post-5-HT: 5.3 ± 1.8 spikes; RM-ANOVA p=0.02, n=5) (**Fig. 3a**). In these same preparations, GPR stimulation had the same effect (Pre-GPR: 6.1 ± 2.1 spikes; During GPR: 1.3 ± 0.9 spikes; Post-GPR: 4.3 ± 2.2 spikes; RM-ANOVA p=0.011, n=4) (**Fig. 3b**).

Bath applied methiothepin (10^{-5} M) prevented the GPR inhibition of $MCN1_{STG}$ spiking during depolarizing current injections (Pre-GPR: 11.8 ± 1.7 spikes; During GPR: 8.8 ± 1.5 spikes; Post-GPR: 11.3 ± 1.4 spikes; RM-ANOVA p=0.06, n=4) (**Fig. 3b**). It also prevented the inhibition of $MCN1_{STG}$ spiking by 5-HT application (Pre-5-HT: 8.8 ± 0.7 spikes; During 5-HT: 7.4 ± 1.8 spikes; Post-5-HT: 7.8 ± 0.8 spikes; RM-ANOVA p=0.10, n=5) (**Fig. 3a**). These results thus support the hypothesis that GPR inhibits $MCN1_{STG}$ by a methiothepin-sensitive serotonergic action.

GPR also excites Int1 and inhibits LG, but neither of these actions are methiothepin-sensitive, nor do they appear to contribute to the GPR influence on the MCN1-gastric mill rhythm (**Supplementary Data Note 1, Supplementary Figs. 1-5**). To further test the hypothesis that GPR regulated the gastric mill rhythm exclusively via its inhibition of $MCN1_{STG}$, we assessed the GPR influence on a gastric mill-like rhythm elicited by dynamic clamp current injection. Specifically, in the absence of MCN1 stimulation, we injected into LG a simulated version of the modulator (MCN1-released CabTRP Ia)-activated conductance ($G_{MI\text{-}MCN1}$) that is normally elicited by MCN1 stimulation and is responsible for

driving the gastric mill rhythm. This manipulation elicits a gastric mill-like rhythm in LG (**Fig. 4**), by activating LG in a manner that enables rhythmic reciprocal inhibitory interactions with Int1, which is spontaneously active[16].

When GPR was rhythmically stimulated during the retractor phase (LG interburst) of the dynamic clamp-simulated gastric mill rhythm, it did not influence either the LG interburst (retraction) duration (Pre-GPR: 5.7 ± 0.8 s; During GPR: 7.6 ± 0.7 s; Post-GPR: 7.2 ± 0.8 s; p=0.25, n=5) or burst (protraction) duration (Pre-GPR: 2.6 ± 0.6 s; During GPR: 2.6 ± 0.6 s; Post-GPR: 2.9 ± 0.6 s; p=0.96, n=5) (**Fig. 4**). These data further support the hypothesis that GPR regulates this rhythm exclusively via its serotonergic inhibition of $MCN1_{STG}$.

GPR selectively inhibits the MCN1 peptidergic action on the gastric mill CPG

When GPR is stimulated during an MCN1-elicited gastric mill rhythm, the MCN1 excitation of LG is weakened and its GABAergic excitation of Int1 appears to be unchanged[16]. This suggested that GPR inhibition of $MCN1_{STG}$ reduces CabTRP Ia release but not GABA release, insofar as MCN1 influences LG only via CabTRP Ia and Int1 only via GABA (Fig. 1b)[6,19]. However, it remained possible that the MCN1 firing rate used to elicit the gastric mill rhythm enabled MCN1 to release sufficient GABA to saturate the GABA receptors on Int1. If so, then GPR or 5-HT inhibition of $MCN1_{STG}$ may have been insufficient to reduce GABA levels below those that saturate GABA receptors on Int1. Because 5-HT

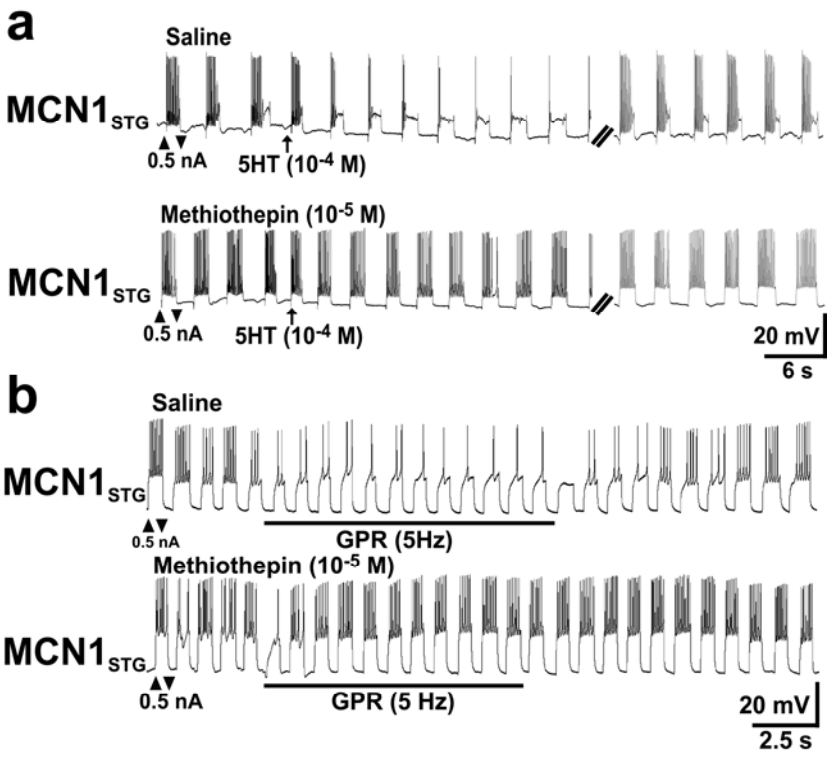

Figure 3. GPR and 5-HT inhibit $MCN1_{STG}$ via a methiothepin-sensitive action. **(a) Top:** The number of $MCN1_{STG}$ spikes elicited by rhythmic depolarizing current injections was reduced by 5-HT application (1 s, arrow) onto the desheathed STG neuropil during saline superfusion (Pre-5-HT: 13.2 ± 0.4 spikes; Steady-state Post-5-HT: 1.0 spike; n=5 cycles). **Bottom:** 5-HT application (1 s, arrow) with methiothepin present had a weaker effect on the $MCN1_{STG}$ response to depolarizing current injections than during saline superfusion (Pre-5-HT: 14.4 ± 1.8 spikes; Steady-state Post-5-HT: 9.4 ± 1.2 spikes; n=5 cycles). Double hashmarks in each panel represent a time break (10-30 s). Most hyperpolarized V_m: $MCN1_{STG}$ (Top) -62 mV; (Bottom) -63 mV. **(b) Top:** During rhythmic depolarizing current injections as above, the number of elicited $MCN1_{STG}$ spikes was reduced or eliminated during and for a brief time after GPR stimulation (Pre-

GPR: 6.2 ± 0.6 spikes; During-GPR: 1.3 ± 0.2 spikes/dep.; n=5 cycles). **Bottom:** GPR stimulation did not alter the $MCN1_{STG}$ response to these current injections during methiothepin superfusion (Pre-GPR: 5.2 ± 1.0 spikes; During-GPR: 6.0 ± 0.4 spikes; n=5 cycles). Most hyperpolarized V_m: $MCN1_{STG}$ (Top) -54 mV; (Bottom) -54 mV.

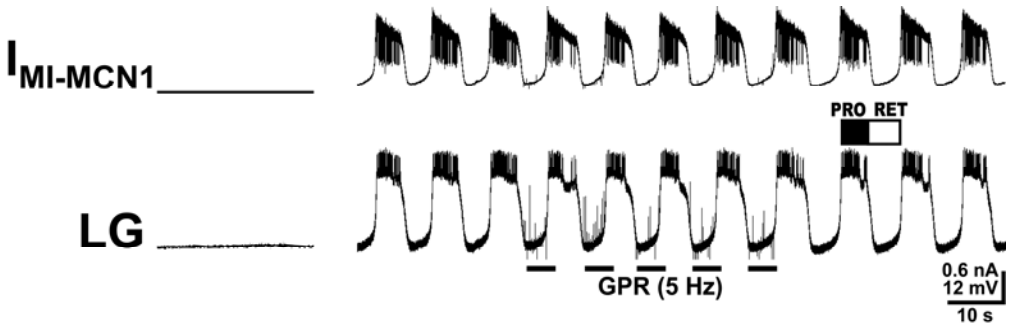

Figure 4. GPR does not influence the dynamic clamp-elicited gastric mill-like rhythm. (**Left**) Prior to activating the dynamic clamp injections, the LG neuron was silent. V_m: -71 mV. (**Right**) Activation of a MCN1-like gastric mill rhythm by dynamic clamp injection of the modulator (MCN1)-activated voltage-dependent inward current ($I_{MI\text{-}MCN1}$) into LG, in the absence of MCN1 stimulation[16]. During this rhythm, GPR stimulation (bars) during a succession of retractor phases did not alter either phase of the MCN1-like gastric mill rhythm. Note that the $I_{MI\text{-}MCN1}$ injections were regulated both by the voltage-dependent characteristics of the current and by LG burst-timed deactivation to mimic the natural LG presynaptic inhibition of $MCN1_{STG}$[16]. The LG-mediated deactivation of $I_{MI\text{-}MCN1}$ is evident by the steadily decreasing $I_{MI\text{-}MCN1}$ amplitude during each LG burst. The fast transient events during the LG interbursts represent *gpn* nerve stimulation artifacts. Most hyperpolarized V_m: -75 mV.

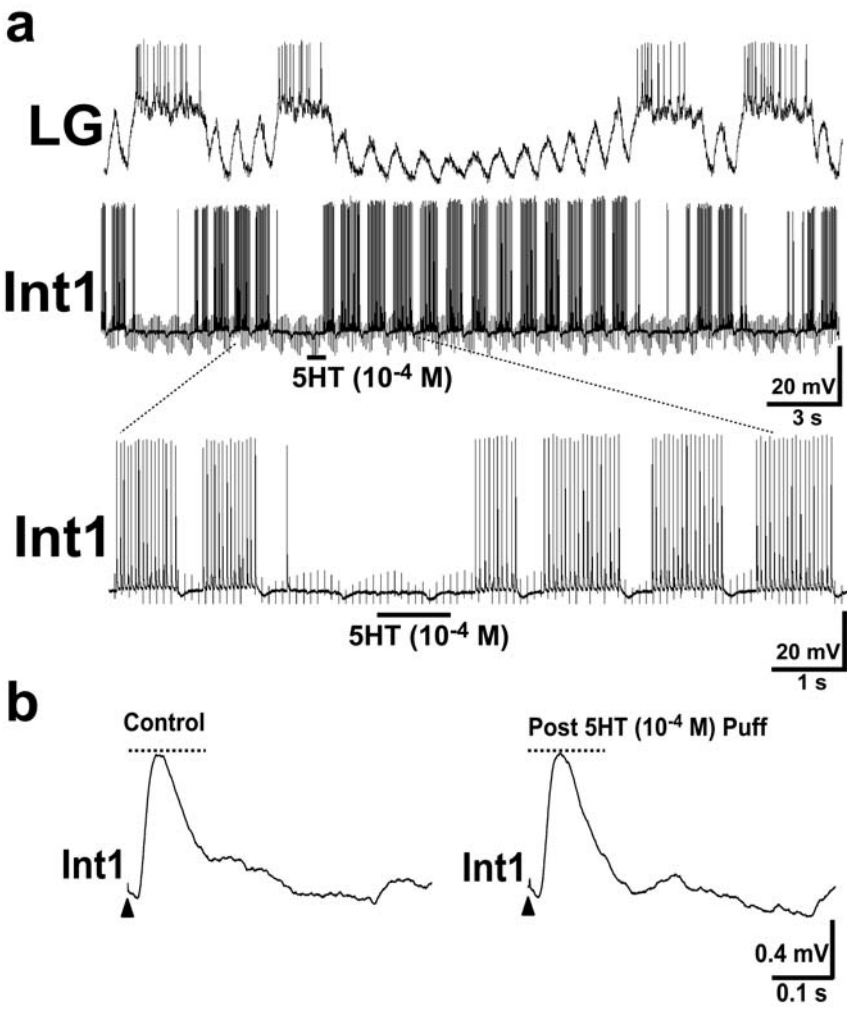

Figure 5. 5-HT application does not alter MCN1 excitation of Int1. **(a)** (**Top**) To determine if GPR stimulation reduced the amount of $MCN1_{STG}$-released GABA, but the effect was masked by stimulating MCN1 at frequencies (15-20 Hz) that saturated the GABA receptors on Int1, 5-HT was pressure-ejected onto the STG neuropil when MCN1 was stimulated at a lower frequency that did not maximally excite Int1. During a gastric mill rhythm elicited by modest MCN1 stimulation (10 Hz), 5-HT application (1 s, bar) did not alter Int1 firing frequency (Pre-5-HT: 18.3 ± 1.4 Hz; Post-5-HT: 17.8 ± 0.2 Hz), despite still selectively prolonging the gastric

mill retractor phase. In this same experiment, increased MCN1 stimulation (20 Hz) elicited a faster Int1 firing rate (21.9 ± 0.3 Hz; $p=1.6 \times 10^{-6}$). (**Bottom**) Expanded time scale of a section from Panel a (dotted lines) showing the unchanged Int1 firing frequency after 5-HT application (bar). The fast transient events in Int1 represent *ion* nerve stimulation artifacts. Most hyperpolarized V_m: Int1, -58 mV; LG, -58 mV. **(b)** 5-HT application does not alter the MCN1-elicited EPSP amplitude in Int1. During low frequency MCN1 stimulation (2 Hz), with no gastric mill rhythm elicited and the pyloric rhythm suppressed, MCN1-elicited EPSPs in Int1 were comparable (**left**) without- and (**right**) with pressure-ejected 5-HT. Dotted line indicates peak of control EPSP. V_{rest} (left, right): -70 mV. Each EPSP is the average of 10 individual EPSPs.

mimicked the GPR effect on $MCN1_{STG}$ while, unlike GPR, it had no direct effect on Int1 (**Supplementary Fig. 3a**), we tested the saturation hypothesis by determining whether 5-HT application could weaken Int1 activity during gastric mill rhythms elicited by a lower MCN1 stimulation frequency that caused a submaximal Int1 firing frequency.

As expected[16], the standard MCN1 stimulation (15-20 Hz) used to drive the gastric mill rhythm increased the Int1 firing rate (Pre-MCN1: 9.9 ± 2.4 Hz; During MCN1: 19.9 ± 1.4 Hz, n=4, p=0.003). Stimulating MCN1 at a lower rate (10 Hz) in these same preparations still elicited the gastric mill rhythm and also increased Int1 activity (Pre-MCN1: 9.9 ± 2.4 Hz; During 10 Hz MCN1 Stim.: 15.9 ± 1.8 Hz; n=4, p=0.007). However, the increase in the Int1 firing rate was smaller than during the faster (15-20 Hz) MCN1 stimulation frequency (n=4, p=0.012). Nonetheless, during weaker MCN1 stimulation (7.5-10 Hz), 5-HT application did not reduce the Int1 firing frequency (Pre-5-HT: 15.4 ± 1.8 Hz, 5-HT: 14.8 ± 1.5 Hz; p=0.39, n=4), despite still selectively prolonging the retractor phase (**Fig. 5a**). Thus, it was unlikely that excess GABA release by MCN1 was masking a reduction of its release during the serotonergic inhibition of $MCN1_{STG}$ by GPR.

The sensitivity of our assay for GABA release was limited by the relatively high activity level in MCN1 and Int1 during the gastric mill- and pyloric rhythms. Therefore, we also assayed the ability of 5-HT to regulate MCN1-mediated GABAergic excitation of Int1 with these rhythms silenced, and with Int1 maintained at a hyperpolarized membrane potential (-70 mV) to suppress its

spontaneous firing. Under these conditions, MCN1 stimulation (2 Hz) did not elicit the gastric mill rhythm but did elicit unitary EPSPs in Int1 (**Fig. 5b**)[14]. Focally applying 5-HT did not alter the amplitude of these EPSPs (Pre-5-HT: 0.74 ± 0.19 mV; During 5-HT: 0.80 ± 0.16 mV, p=0.82, n=4) (**Fig. 5b**). As a positive control for the effectiveness of the 5-HT applications in these preparations, 5-HT was also applied during the MCN1 (15-20 Hz)-elicited gastric mill rhythm, where it prolonged the retractor phase (p=0.026, n=4) without altering the Int1 firing rate (p=0.15, n=4).

Selective inhibition of $MCN1_{STG}$ peptidergic cotransmission is pivotal to GPR regulation of the gastric mill rhythm

We tested whether the inability of GPR to alter Int1 activity was necessary for the GPR influence on the gastric mill rhythm. We first evaluated this hypothesis by employing a previously-described computational model of the GPR-regulated gastric mill rhythm[16]. Specifically, we simulated the gastric mill rhythm generated by a model gastric mill circuit in which MCN1-mediated peptidergic excitation of LG was selectively reduced by GPR (i.e. MCN1-mediated GABAergic excitation of Int1 was not altered by GPR). We then compared the output of this model to the modified version in which GPR concomitantly reduced MCN1 excitation of both LG and Int1 (**Fig. 6**).

Consistent with previous work[16], GPR stimulation prolonged the retractor phase when MCN1-mediated excitation of Int1 persisted (pre-GPR: 7.1 s; GPR:

47.4 s; post-GPR: 9.4 s) without altering the protractor phase duration (pre-GPR: 10.6 s; GPR: 9.8 s; post-GPR: 10.4 s) (**Fig 6a**). The prolonged retractor phase results from GPR inhibition of $MCN1_{STG}$, which reduces the rate of build-up of MCN1 excitation of LG[16]. Due to this reduction, there is an increased duration needed for the CabTRP Ia-activated conductance ($G_{MI\text{-}MCN1}$) to rise to the level needed to overcome Int1 inhibition and enable an LG burst.

We compared the aforementioned model to one in which MCN1 excitation of Int1 was suppressed by GPR inhibition of $MCN1_{STG}$ (Int1 spikes/burst: Pre-gastric mill rhythm, 5 spikes; During gastric mill control cycles, 7 spikes; Gastric mill cycles with GPR stimulation, 5 spikes) (**Fig. 6b**). In this latter model, GPR stimulation produced a 60% increase in retraction duration (Pre-GPR: 5.8 s; GPR: 9.8 s; Post-GPR: 6.3 s). This change is modest when compared to the approximately 5-fold increase observed in the original model and the nearly 4-fold increase observed experimentally.

The weakened GPR effect on retraction duration in the modified model occurred because the reduced rate of build-up of $G_{MI\text{-}MCN1}$ in LG was paralleled by a weaker Int1 inhibition of LG. Because GPR stimulation reduced Int1-to-LG inhibition in this model, the strength of MCN1-to-LG excitation required for LG to reach burst threshold was decreased (**Fig. 6**). Similarly, because the modulator-activated conductance was smaller in magnitude than in control cycles at LG burst onset, less time was needed for this conductance to decay to the level at which the LG burst terminated, thereby reducing the LG burst duration (**Fig. 6**).

We next used the biological preparation to assess the model prediction that selective inhibition of MCN1 peptidergic cotransmission is necessary for the GPR influence on the gastric mill rhythm. To mimic a hypothetical circuit in which GPR reduced MCN1 excitation of Int1 as well as LG, during the period of GPR stimulations Int1 was injected with sufficient constant amplitude hyperpolarizing current (0.3 – 0.8 nA) to modestly reduce its firing frequency (During MCN1: 17.3 ± 0.8 Hz; During MCN1 w/GPR and Int1 hype.: 14.0 ± 1.2 Hz; n=4, paired t-test p=0.012) (**Fig. 7**).

Consistent with the model prediction, reducing Int1 activity while stimulating GPR altered the GPR influence on the gastric mill rhythm. Instead of selectively prolonging retraction, the retractor phase duration was unchanged relative to control cycles (Control: 5.2 ± 2.0 s; GPR Stim. plus Int1 hype.: 6.3 ± 3.1 s; n=4, p=0.38) (**Fig. 7a**). In these same preparations, when Int1 was not hyperpolarized by current injection, retraction was prolonged by GPR stimulation (Control: 5.2 ± 2.0 s; GPR Stim.: 21.7 ± 5.5 s; n=4, p=0.01) (**Fig. 7b**). Combining GPR stimulation with reduced Int1 activity also did not alter the protractor phase duration (Control: 3.5 ± 1.1 s; GPR Stim. plus Int1 hype.: 2.1 ± 0.3 s; n=4, p=0.12), as was also the case, as usual, when GPR was stimulated without manipulating Int1 activity (Control: 3.5 ± 1.1 s; GPR Stim.: 3.5 ± 1.2 s; n=4, p=0.48).

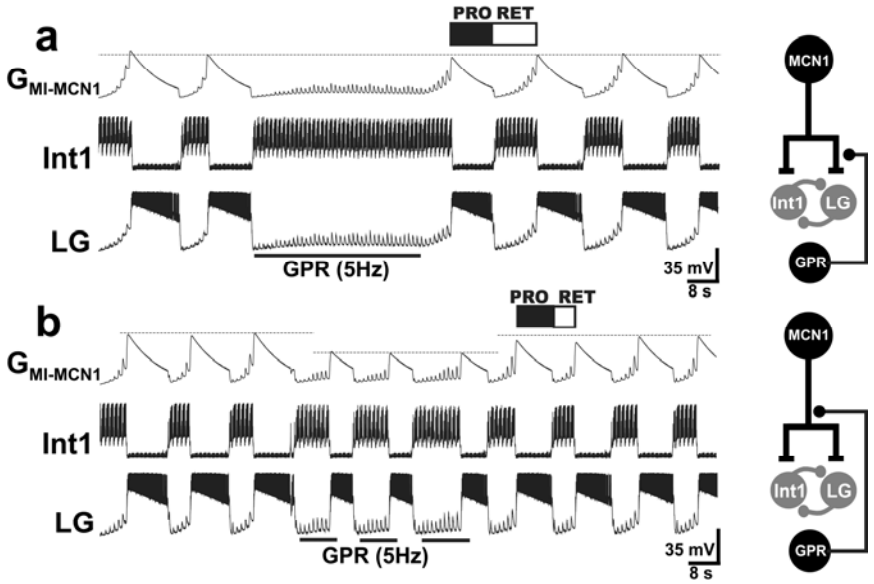

Figure 6. Selective inhibition of MCN1 peptidergic cotransmission by GPR is necessary for the normal GPR regulation of the MCN1-gastric mill rhythm in a computational model. In this model, MCN1 activates $G_{MI-MCN1}$ in the LG neuron[16]. During retraction, $G_{MI-MCN1}$ steadily builds up until it reaches a level sufficient for LG to escape from Int1 inhibition and burst. During protraction, LG inhibition of $MCN1_{STG}$ causes the $G_{MI-MCN1}$ amplitude to decay until the LG burst terminates. **(a) (Left)** In the biologically-realistic model, where GPR inhibition of $MCN1_{STG}$ did not alter MCN1 excitation of Int1, GPR stimulation (bar) selectively prolonged the retractor phase. Because GPR did not alter the Int1 firing frequency, the Int1 inhibition of LG was unaffected by GPR. Thus, the $G_{MI-MCN1}$ amplitude needed to overcome this Int1 inhibition was unchanged. The only difference was that during GPR stimulation more time was needed for $G_{MI-MCN1}$ to reach LG burst threshold (dotted line). **(Right)** Circuit schematic implemented in this model, with the GPR synapse onto $MCN1_{STG}$ being restricted to influencing the MCN1

synapse onto LG. Symbols: t-bars, synaptic excitation; filled circles, synaptic inhibition. **(b) (Left)** In an altered model where GPR inhibition of MCN1 did suppress MCN1 excitation of Int1, GPR stimulation (bars) had a reduced effect on retraction, as well as reducing protraction duration. Note the reduced $G_{MI\text{-}MCN1}$ amplitude that enabled LG burst onset during GPR stimulation (dotted line). **(Right)** Circuit schematic implemented in this model, showing that the GPR synapse onto $MCN1_{STG}$ influenced the MCN1 synapses onto LG and Int1.

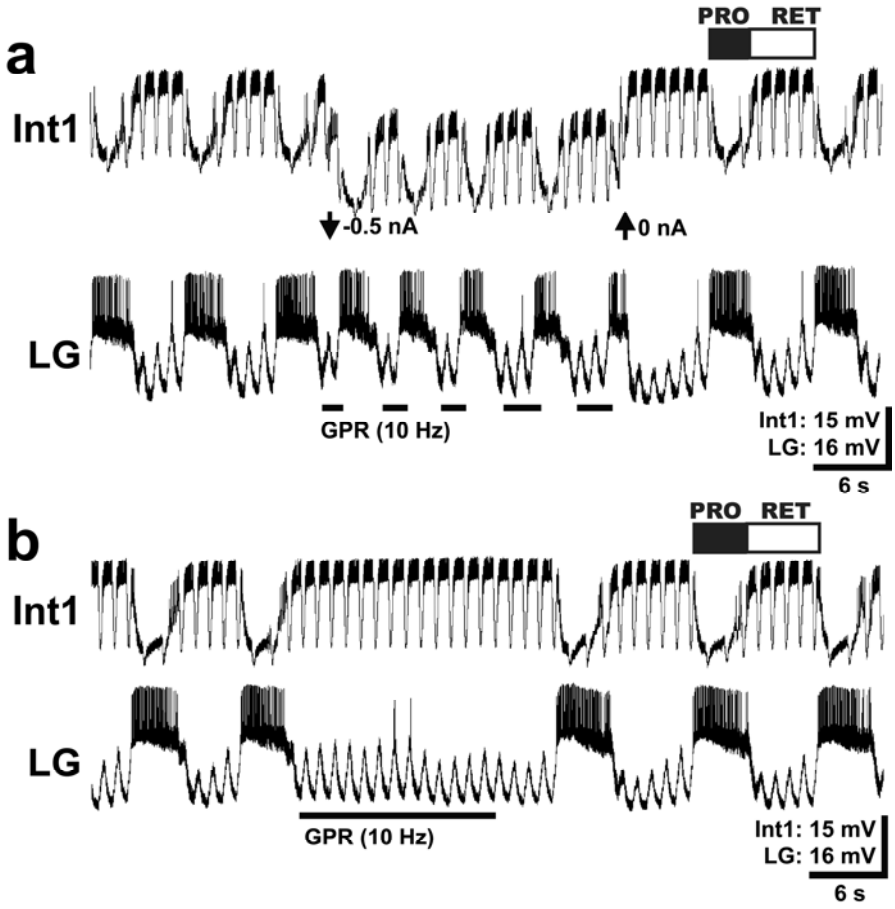

Figure 7. An unchanging Int1 firing frequency is necessary for the normal GPR regulation of the MCN1-gastric mill rhythm in the biological preparation. **(a)** During the gastric mill rhythm, coordinately stimulating GPR (bars) and injecting hyperpolarizing current into Int1 to reduce its firing frequency (Pre-GPR/Int1 hype.: 18.1 ± 0.1 Hz; During GPR/Int1 hype.: 15.8 ± 0.2 Hz, n=5 cycles, p=0.002) did not prolong the retractor phase (Pre-GPR/Int1 hype.: 3.9 ± 0.1 s; During GPR/Int1 hype.: 3.5 ± 0.4 s, n=5 cycles, p=0.19) and reduced the protractor phase duration (Pre-GPR/Int1 hype.: 2.9 ± 0.1 s; During GPR/Int1 hype.: 1.8 ± 0.1 s, n=5 cycles, $p=8.5 \times 10^{-5}$). **(b)** In the same preparation, GPR stimulation (bar) in the absence of current injection into Int1 selectively prolonged the

retractor phase without altering Int1 firing frequency (Pre-GPR: 17.3 ± 0.7 Hz; During GPR: 17.7 ± 0.3 Hz, n=5 cycles, p=0.11). Most hyperpolarized V_m: LG, -65 mV; Int1, -54 mV.

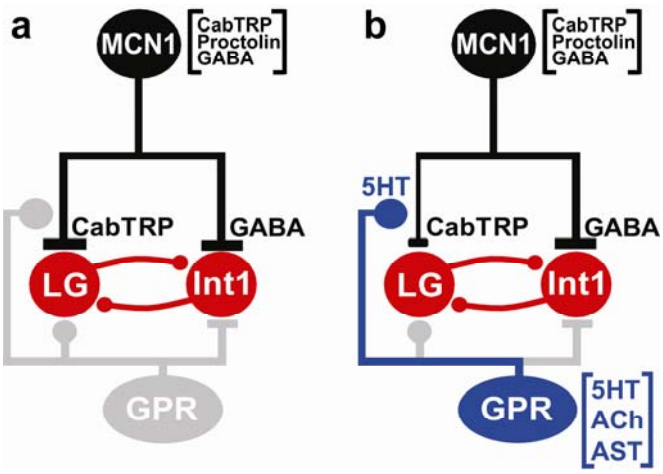

Figure 8. Summary circuit schematics representing the pathway by which an identified stretch-sensitive proprioceptor neuron (GPR) selectively inhibits peptidergic cotransmission from a modulatory projection neuron (MCN1) that drives a rhythmically active motor circuit. **(a)** Circuit schematic representing the MCN1 influence on the gastric mill CPG neurons LG and Int1 in the absence of GPR input. **(b)** Circuit schematic indicating the selectively weakened peptidergic MCN1 synapse onto the LG neuron when GPR is active, as represented by the thinned lines and shortened t-bar for the peptidergic synapse. Additionally, this GPR action is mediated by only one GPR cotransmitter (5-HT). Note that the other two GPR synapses (gray) onto the gastric mill CPG do not influence this circuit during the MCN1-elicited gastric mill rhythm. Separate transmitter release sites for GABA and CabTRP Ia in $MCN1_{STG}$ are shown for diagrammatic purposes only, to represent their separate actions onto Int1 and LG, respectively. There is no available information regarding their sites of release from the $MCN1_{STG}$ terminals. The third MCN1 cotransmitter (proctolin), does not influence on the gastric mill CPG.

DISCUSSION

We have established that presynaptic inhibition can regulate peptidergic (CabTRP Ia) cotransmission without altering cotransmission mediated by a small molecule transmitter (GABA). Additionally, because the cotransmitting neuron uses CabTRP Ia and GABA to excite separate postsynaptic neurons, this presynaptic inhibition changes the balance of excitation to the separate postsynaptic targets (**Fig. 8**). At the circuit level, this regulation of peptidergic cotransmission from the projection neuron MCN1 is necessary for the proprioceptor GPR to selectively prolong the gastric mill retractor phase. Previous pharmacological studies analyzing bulk release from stimulated sympathetic nerves also support the hypothesis that presynaptic receptors can separately regulate co-released transmitters[25].

We established that GPR did not weaken MCN1 GABAergic excitation of Int1 by showing that application of the GPR cotransmitter 5-HT mimicked the ability of GPR stimulation to selectively prolong retraction without altering the Int1 firing frequency. This conclusion was strengthened by our findings that 5-HT application neither directly influenced Int1 nor did it alter the MCN1-elicited EPSP amplitude in Int1. We used this approach because GPR is the only source of 5-HT in the STG[21], and we determined that the GPR action on MCN1 was serotonergic. We found no evidence that the GPR actions on LG and Int1 contribute to its regulation of the MCN1-gastric mill rhythm (**Fig. 8**). These GPR synapses, however, may contribute to its regulation of other versions of this

rhythm, particularly those in which MCN1 does not participate (e.g. Saideman et al., 2007).

Selective regulation of peptidergic cotransmission

The intracellular mechanism by which GPR selectively regulates peptidergic cotransmission by MCN1 remains to be determined, but our results suggest that GPR reduces neuropeptide release from MCN1 while sparing GABA release. However, we did not determine how GPR influences the actions of the other MCN1 peptide cotransmitter, proctolin[26], so it remains possible that the serotonergic inhibition of $MCN1_{STG}$ specifically inhibits CabTRP Ia transmission.

Selective inhibition of neuropeptide release might result from any of several mechanisms. For example, the release sites of GABA and CabTRP Ia may be spatially separated such that the GPR synapse onto $MCN1_{STG}$ affects only peptide release. There is, however, no evidence for spatial segregation of the $MCN1_{STG}$ cotransmitters[26-27]. Alternatively, there may be distinct biochemical regulation of neuropeptide and GABA release in $MCN1_{STG}$. Although the molecular-level details underlying neuropeptide release and its regulation lags relative to available information for small molecule transmitter release, it is clear that there are both shared and distinct aspects to their regulation[28-31]. Neuropeptide and small molecule transmitter release also have different intra-terminal Ca^{2+} requirements, and appear to be regulated in at least some terminals by different types of Ca^{2+} channels[32-34].

Consistent with the possibility of a biochemical regulation is the likelihood that the GPR inhibition of $MCN1_{STG}$ is metabotropic. For example, no unitary IPSPs are recorded in $MCN1_{STG}$ in response to GPR stimulation, and the resulting hyperpolarization outlasts the GPR stimulation[16] (this study). Additionally, GPR has metabotropic 5-HT actions on other STG targets[35], and a G-protein-coupled, methiothepin-sensitive 5-HT receptor has been cloned and characterized in the decapod crustacean nervous system[24].

The ability of axo-axonic synapses to regulate transmitter release is well-documented[36-38], but the effectiveness of these synapses for co-regulating the release of multiple transmitters has yet to be explored in other systems. It may well be the case that at a particular set of axon terminals, some presynaptic inputs co-regulate the release of all cotransmitters while other inputs target the release of only one or a subset of them. For example, $MCN1_{STG}$ receives additional presynaptic inputs, such as from the LG neuron[20]. Hence, it will be informative to learn whether the selective regulation of peptide cotransmitter release is a necessary consequence of the organization of the $MCN1_{STG}$ axon terminals or if distinct presynaptic inputs to $MCN1_{STG}$ regulate peptide and GABA release in a manner distinct from GPR.

A changing balance of cotransmitter actions can also result from changes in the firing frequency of a neuron with peptide and small molecule cotransmitters. Specifically, some cotransmitter neurons have primarily or exclusively small molecule transmitter-mediated ionotropic synaptic actions when

firing at low frequencies, with their metabotropic, peptidergic actions becoming prominent at faster firing frequencies[3,32]. While this may also be the case for MCN1, it does have peptidergic actions at firing frequencies that are below the frequency threshold for activating the gastric mill rhythm[39]. This distinction between the firing frequency threshold for peptide release and the threshold for the behaviorally-relevant firing frequency of a neuron also occurs for at least some other multi-transmitter neurons[3].

Regulation of network activity by cotransmission

The functional consequences of cotransmitter actions are most extensively studied on individual target cells[1-2,7-8,40]. However, cotransmission studies have focused on neuronal circuits in *Aplysia*[11,41], rodent thalamus[10,42], and the STNS[6,9,13,19,26,43-44]. It remains to be determined if presynaptic input selectively regulates peptidergic cotransmission in each of these systems. Where it does occur, its impact is likely to further extend the flexibility already established for neuronal circuits resulting from their modulatory inputs.

Although most cotransmission studies have focused on the convergent actions of co-released transmitters on a target cell[1,7-8,11,40-41], divergent cotransmission has also been documented[4-6,9-10,19,43]. The ability of GPR to use only one cotransmitter (serotonin) to regulate the MCN1-activated gastric mill CPG extends the influence of divergent cotransmission to sensorimotor integration.

In conclusion, the proprioceptor GPR regulates the MCN1-elicited gastric mill rhythm via a single cotransmitter (serotonin) that selectively regulates peptidergic cotransmission by $MCN1_{STG}$. The distinct regulation of co-released transmitters by a presynaptic input provides the opportunity for functional compartmentalization, such that arborizations of the cotransmitting neuron in other regions of the CNS would be unaffected by this local regulation. Additionally, as shown here, the altered balance of cotransmitter actions resulting from presynaptic inhibition can change network output without evident changes in either the firing rate or pattern of the cotransmitting neuron or parallel changes in the modulatory state of the network.

METHODS

Animals/preparation. Male crabs [*C. borealis* (Jonah crabs)] were obtained from Yankee Lobster Co. (Boston, MA) and the Marine Biological Laboratory (Woods Hole, MA), and housed in commercial tanks containing chilled (10° C), filtered, and recirculated artificial seawater. Before dissection, each crab was anesthetized by packing it in ice for at least 30 min. Briefly, the foregut was removed from the animal, bisected along the ventral midline and pinned ventral side down in a silicone elastomer (Sylgard 170: K.R. Anderson, Morgan Hill, CA; World Precision Inc., Sarasota, FL)-coated glass bowl in chilled *C. borealis* saline. The isolated STNS (see Fig. 1a) was then dissected from the foregut, transferred and pinned down in a Sylgard 184-coated (K.R. Anderson) Petri dish filled with saline (10–12° C). During each experiment, the STNS was continuously superfused with saline (7–12 ml/min) via a switching manifold, to enable fast solution changes, and cooled (10–11° C) with a Peltier device. In all experiments, both CoGs were disconnected from the rest of the STNS by bisecting the inferior oesophageal nerves (*ions*) and superior oesophageal nerves (*sons*) (**Fig. 1a**).

Solutions. C. borealis saline included (in mM): 440 NaCl, 26 $MgCl_2$, 13 $CaCl_2$, 11 KCl, 10 Trizma base and 5 maleic acid, pH 7.4–7.6. Solutions of all pharmacological agents were dissolved in saline during the experiment for which

they were used, including methiothepin (Sigma-Aldrich, St. Louis, MO), serotonin (5-hydroxytryptamine, 5-HT: Sigma-Aldrich), oxotremorine sesquifumerate (OXO: Sigma-Aldrich), and allatostatin III (AST: American Peptide Company, Sunnyvale, CA). Methiothepin (10^{-5} M) was applied by superfusion. 5-HT, OXO and AST were applied by pressure-ejection (1-2 s, 4-8 psi) from a microelectrode (1-2 MΩ) place immediately above the desheathed STG neuropil, using a Picospritzer II Microinjector (General Valve Corp., Fairfield, NJ).

Electrophysiology. Standard intracellular and extracellular recording techniques were used in this study[16]. Briefly, extracellular recordings in identified nerves were obtained by electrically isolating sections of nerves from the bath with a petroleum jelly-based cylindrical compartment (Vaseline: Medical Accessories and Supply Headquarters, Alabaster, AL). One of two stainless-steel electrode wires was placed within this compartment to record action potentials propagating through the nerve, and the second wire was placed in the bath as a reference electrode. The differential signal was recorded, filtered and amplified with AM Systems (Carlsborg, WA; model 1700) and Brownlee Precision (Santa Clara, CA; model 410) amplifiers. Extracellular stimulation of a nerve was achieved by placing the two extracellular recording wires into a stimulus isolation unit (model SIU5; Astromed/Grass Instruments, West Warwick, RI) controlled by a stimulator (model S88; Astromed/Grass Instruments).

Intracellular recordings of STNS somata and axons were obtained with

sharp glass microelectrodes (15–30 MΩ) filled with 0.6 M K_2SO_4 plus 20 mM KCl. All intracellular signals were amplified and filtered with Axoclamp 2B amplifiers (Molecular Devices, Sunnyvale, CA), and then further amplified with Brownlee model 410 amplifiers. Intracellular current injections were performed in discontinuous current-clamp (DCC) mode with sampling rates of 2–3 kHz. To facilitate intracellular recordings, the STG was desheathed and viewed with light transmitted through a darkfield condenser (Nikon, Tokyo, Japan).

All STNS neurons were identified by their patterns of activity, synaptic interactions with other identified neurons, and axonal branching patterns in connecting and peripheral nerves[16-17]. The gastric mill rhythm was elicited by tonic, extracellular stimulation of the *ion* on the STG side of the bisected nerve[14]. This nerve contains only two projection neurons that innervate the STG (MCN1, MCN5), and low intensity *ion* stimulation can selectively activate MCN1[14].

GPR stimulation was accomplished by extracellular stimulation of the gastropyloric nerve (*gpn*), through which the GPR2 axon projects[21]. GPR is present as a pair of bilaterally symmetric neurons (GPR1 and GPR2) that project through different peripheral nerve branches, but their actions on the gastric mill rhythm are equivalent[16]. In most experiments, we stimulated the *gpn* during the retractor phase of the gastric mill rhythm to mimic its likely *in vivo* activity pattern[16]. This stimulation was performed manually by turning the stimulator on at the beginning of the retractor phase and terminating the stimulation immediately after the burst onset time of the LG neuron. LG burst onset marks

the end of the retractor phase and the start of the protractor phase.

Data acquisition and analysis. Data were acquired in parallel onto a chart recorder (Everest model; Astromed) and by digitizing (~5 kHz) and storing the data on computer with data acquisition hardware/software (Spike2; Cambridge Electronic Design, Cambridge, UK). Digitized data were analyzed with a homemade Spike2 program ("The Crab Analyzer," freely available at http://www.uni-ulm.de/~wstein/spike2/index.html). In brief, the burst duration of a neuron was defined as the elapsed time (in seconds) between the first and last action potential in an impulse burst. The intraburst firing frequency was calculated by determining the number of action potentials in a burst minus 1, and then dividing it by the burst duration. The gastric mill cycle period was defined by the duration (in seconds) between the onset of two successive impulse bursts in the LG neuron. All analyses involved determining the mean ± SE for the parameter of interest from at least 5 consecutive gastric mill cycles in each experiment.

Statistical analyses were performed with SigmaStat 3.0 (SPSS, Chicago, IL) or Microsoft Excel (Microsoft Corp., Seattle, WA). Statistical tests employed included the paired Student's *t*-test and repeated measures ANOVA (RM-ANOVA). In any case where only two groups were compared, a paired *t*-test was used and the p-value is reported. Except where noted, all *t*-tests performed were one-tailed. In all other cases, and where noted in the text, an ANOVA was used

to compare the pre-control, manipulation (GPR stimulation or neurotransmitter application) and post-control groups. For each case, the SigmaStat software was first used to verify a normal distribution (Kolmogorov-Smirnov test). In any case where the ANOVA reported a statistical difference between the compared groups, the Student-Newman-Keuls post-hoc test was used, and the reported p-value represents the post-hoc comparison of the pre-control and manipulation groups. In all such experiments, the effect of the manipulation was reversible, and there was no significant difference between the pre-control and post-control groups. Figures were made from Spike2 files incorporated into Adobe Illustrator and Photoshop (Adobe, San Jose, CA).

Dynamic clamp. We used the dynamic clamp technique[45] to inject a simulated version of a biological conductance into the LG neuron. Specifically, as in previously published work[16], we elicited a gastric mill-like rhythm by injecting into LG a simulated version of the CabTRP Ia-activated conductance. The resulting, voltage-dependent current in LG enables the generation of rhythmic alternating bursts between LG and Int1 that is comparable to those occurring during the MCN1-elicited gastric mill rhythm. These experiments were performed using the version of the dynamic clamp software developed in the Nadim laboratory (Rutgers Univ. and New Jersey Institute of Technology; available at http://stg.rutgers.edu/software/) on a personal computer (PC) running Windows XP and a NI PCI-6070-E data acquisition board (National Instruments, Austin,

TX). All dynamic clamp-implemented current injections were performed with intracellular recordings in single-electrode DCC mode.

Gastric Mill Model. We implemented a computational model modified as indicated below from an existing conductance-based model of the gastric mill circuit[16,46]. We retained all aspects of the model implemented by Beenhakker et al.[16], including modeled versions of the LG, Int1, MCN1 and GPR neurons. The only parameter that was altered from the model version presented in Beenhakker et al.[16] was the presynaptic voltage dependence of the MCN1 synapse onto Int1. This synapse was modified to increase its sensitivity to GPR inhibition of MCN1, and the results were compared to the original version as published in Beenhakker et al.[16]. In the modified version, the activation parameter (m) for this synapse was modeled as follows: $m = \frac{1}{1 + e^{-(V+50)}}$

In the above equation, m is the activation parameter and V is the membrane potential of the MCN1 axon terminal compartment.

REFERENCES

1. Seal, R.P. & Edwards, R.H. Functional implications of neurotransmitter co-release: glutamate and GABA share the load. *Curr. Opin. Pharmacol.* **6**, 114-119 (2006).
2. Jan, L.Y. & Jan, Y.N. Peptidergic transmission in sympathetic ganglia of the frog. *J. Physiol.* **327**, 219-246 (1982).
3. Vilim, F.S., Cropper, E.C., Price, D.A., Kupfermann, I. & Weiss, K.R. Peptide cotransmitter release from motorneuron B16 in *Aplysia californica*: costorage, corelease, and functional implications. *J. Neurosci.* **20**, 2036-2042 (2000).
4. Dugue, G.P., Dumoulin, A., Triller, A. & Dieudonne, S. Target-dependent use of co-released inhibitory transmitters at central synapses. *J. Neurosci.* **25**, 6490-6498 (2005).
5. Nishimaru, H., Restrepo, C.E., Ryge, J., Yanagawa, Y. & Kiehn, O. Mammalian motor neurons corelease glutamate and acetylcholine at central synapses. *Proc. Natl. Acad. Sci. (U.S.A.)* **102**, 5245-5249 (2005).
6. Stein, W., DeLong, N.D., Wood, D.E.& Nusbaum, M.P. Divergent co-transmitter actions underlie motor pattern activation by a modulatory projection neuron. *Eur. J. Neurosci.* **26**, 1148-1165 (2007).
7. Lu, T., Rubio, M.E. & Trussell, L.O. Glycinergic transmission shaped by the corelease of GABA in a mammalian auditory synapse. *Neuron* **57**, 524-535 (2008).

8. Maher, B.J. & Westbrook, G.L. Co-transmission of dopamine and GABA in periglomerular cells. *J. Neurophysiol.* **99**, 1559-1564 (2008).

9. Blitz, D.M. & Nusbaum, M.P. Distinct functions for cotransmitters mediating motor pattern selection. *J. Neurosci.* **19**, 6774-6783 (1999).

10. Sun, Q.Q., Baraban, S.C., Prince, D.A. & Huguenard, J.R. Target-specific neuropeptide Y-ergic synaptic inhibition and its network consequences within the mammalian thalamus. *J. Neurosci.* **23**, 9639-9649 (2003).

11. Koh, H.Y. & Weiss, K.R. Activity-dependent peptidergic modulation of the plateau-generating neuron B64 in the feeding network of *Aplysia*. *J. Neurophysiol.* **97**, 1862-1867 (2007).

12. Marder, E. & Bucher, D. Understanding circuit dynamics using the stomatogastric nervous system of lobsters and crabs. *Annu. Rev. Physiol.* **69**, 291-316 (2007).

13. Nusbaum, M.P., Blitz, D.M., Swensen, A.M., Wood, D. & Marder, E. The roles of co-transmission in neural network modulation. *Trends Neurosci.* **24**, 146-154 (2001).

14. Coleman, M.J., Meyrand, P. & Nusbaum, M.P. A switch between two modes of synaptic transmission mediated by presynaptic inhibition. *Nature* **378**, 502-505 (1995).

15. Bartos, M., Manor, Y., Nadim, F., Marder, E. & Nusbaum, M.P. Coordination of fast and slow rhythmic neuronal circuits. *J. Neurosci.* **19**, 6650-6660 (1999).

16. Beenhakker, M.P., DeLong, N.D., Saideman, S.R., Nadim, F. & Nusbaum, M.P. Proprioceptor regulation of motor circuit activity by presynaptic inhibition of a modulatory projection neuron. *J. Neurosci.* **25**, 8794-8806 (2005).

17. Saideman, S.R., Blitz, D.M. & Nusbaum, M.P. Convergent motor patterns from divergent circuits. *J. Neurosci.* **27**, 6664-6674 (2007).

18. Heinzel, H.G., Weimann, J.M. & Marder, E. The behavioral repertoire of the gastric mill in the crab, *Cancer pagurus*: an in situ endoscopic and electrophysiological examination. *J. Neurosci.* **13**, 1793-1803 (1993).

19. Wood, D.E., Stein, W. & Nusbaum, M.P. Projection neurons with shared cotransmitters elicit different motor patterns from the same neural circuit. *J. Neurosci.* 20, 8943-8953 (2000).

20. Coleman, M.J. & Nusbaum, M.P. Functional consequences of compartmentalization of synaptic input. *J. Neurosci.* **14**, 6544-6552 (1994).

21. Katz, P.S., Eigg, M.H. & Harris-Warrick, R.M. Serotonergic/cholinergic muscle receptor cells in the crab stomatogastric nervous system. I. Identification and characterization of the gastropyloric receptor cells. *J. Neurophysiol.* **62**, 558-570 (1989).

22. Birmingham, J.T., Szuts, Z.B., Abbott, L.F. & Marder, E. Encoding of muscle movement on two time scales by a sensory neuron that switches between spiking and bursting modes. *J. Neurophysiol.* **82**, 2786-2797 (1999).

23. Skiebe, P. & Schneider, H. Allatostatin peptides in the crab stomatogastric nervous system: inhibition of the pyloric motor pattern and distribution of allatostatin-like immunoreactivity. *J. Exp. Biol.* **194**, 195-208 (1994).

24. Spitzer, N., Edwards, D.H. & Baro, D.J. Conservation of structure, signaling and pharmacology between two serotonin receptor subtypes from decapod crustaceans, *Panulirus interruptus* and *Procambarus clarkii*. *J. Exp. Biol.* **211**, 92-105 (2008).

25. Donoso, M.V., Aedo, F. & Huidobro-Toro, J.P. The role of adenosine A_{2A} and A_3 receptors on the differential modulation of norepinephrine and neuropeptide Y release from peripheral sympathetic nerve terminals. *J. Neurochem.* **96**, 1680-1695 (2006).

26. Blitz, D.M., Christie, A.E., Coleman, M.J., Norris, B.J., Marder, E. & Nusbaum, M.P. Different proctolin neurons elicit distinct motor patterns from a multifunctional neuronal network. *J. Neurosci.* **19**, 5449-5463 (1999).

27. Kilman, V.L. & Marder, E. Ultrastructure of the stomatogastric ganglion neuropil of the crab, *Cancer borealis*. *J. Comp. Neurol.* **374**, 362-375 (1996).

28. Gracheva, E.O., Burdina, A.O., Touroutine, D., Berthelot-Grosjean, M., Parekh, H. & Richmond, J.E. Tomosyn negatively regulates both synaptic transmitter and neuropeptide release at the *C. elegans* neuromuscular junction. *J. Physiol.* **585**, 705-709 (2007).

29. Sieburth, D., Madison, J.M. & Kaplan, J.M. PKC-1 regulates secretion of neuropeptides. *Nat. Neurosci.* **10**, 49-57 (2007).

30. Speese, S., Petrie, M., Schuske, K., Ailion, M., Ann, K., Iwasaki, K., Jorgensen, E.M. & Martin, T.F. UNC-31 (CAPS) is required for dense-core vesicle but not synaptic vesicle exocytosis in *Caenorhabditis elegans*. *J. Neurosci.* **27**, 6150-6162 (2007).

31. Hammarlund, M., Watanabe, S., Schuske, K. & Jorgensen, E.M. CAPS and syntaxin dock dense core vesicles to the plasma membrane in neurons. *J. Cell Biol.* **180**, 483-491 (2008).

32. Peng, Y.Y. & Zucker, R.S. Release of LHRH is linearly related to the time integral of presynaptic Ca^{2+} elevation above a threshold level in bullfrog sympathetic ganglia. *Neuron* **10**, 465-473 (1993).

33. Ohnuma, K., Whim, M.D., Fetter, R.D., Kaczmarek, L.K. & Zucker, R.S. Presynaptic target of Ca^{2+} action on neuropeptide and acetylcholine release in *Aplysia californica*. *J. Physiol.* **535**, 647-662 (2001).

34. Ghijsen, W.E. & Leenders, A.G. Differential signaling in presynaptic neurotransmitter release. *Cell Mol. Life Sci.* **62**, 937-954 (2005).

35. Kiehn, O. & Harris-Warrick, R.M. Serotonergic stretch receptors induce plateau properties in a crustacean motor neuron by a dual-conductance mechanism. *J. Neurophysiol.* **68**, 485-495 (1992).

36. Watson, A., Le Bon-Jego, M. & Cattaert, D. Central inhibitory microcircuits controlling spike propagation into sensory terminals. *J. Comp. Neurol.*

484, 234-248 (2005).

37. Fink, K.B. & Gothert, M. 5-HT receptor regulation of neurotransmitter release. *Pharmacol. Rev.* **59**, 360-417 (2007).

38. Rudomin, P. In search of lost presynaptic inhibition. *Exp. Brain Res.* **196**, 139-151 (2009).

39. Kirby, M.S. & Nusbaum, M.P. Peptide hormone modulation of a neuronally modulated motor circuit. *J. Neurophysiol.* **98**, 3206-3220 (2007).

40. Lamotte d'Incamps, B. & Ascher, P. Four excitatory postsynaptic ionotropic receptors coactivated at the motoneuron-Renshaw cell synapse. *J. Neurosci.* **28**, 14121-14131 (2008).

41. Koh, H.Y., Vilim, F.S., Jing, J. & Weiss, K.R. Two neuropeptides colocalized in a command-like neuron use distinct mechanisms to enhance its fast synaptic connection. *J. Neurophysiol.* **90**, 2074-2079 (2003).

42. Brill, J., Kwakye, G. & Huguenard, J.R. NPY signaling through Y1 receptors modulates thalamic oscillations. *Peptides* **28**, 250-256 (2007).

43. Thirumalai, V. & Marder, E. Colocalized neuropeptides activate a central pattern generator by acting on different circuit targets. *J. Neurosci.* **22**, 1874-1882 (2002).

44. Wood, D.E. & Nusbaum, M.P. Extracellular peptidase activity tunes motor pattern modulation. *J. Neurosci.* **22**, 4185-4195 (2002).

45. Sharp, A.A., O'Neil, M.B., Abbott, L.F. & Marder, E. The dynamic clamp: artificial conductances in biological neurons. *Trends Neurosci.* **16**, 389-

394 (1993).

46. Nadim, F., Manor, Y., Nusbaum, M.P. & Marder, E. Frequency regulation of a slow rhythm by a fast periodic input. *J. Neurosci.* **18**, 5053-5067 (1998).

Supplementary Data

Supplementary Note 1. The GPR actions on Int1 and LG are methiothepin-insensitive

Int1: Even though Int1 was not 5-HT-responsive, it was possible that methiothepin altered the Int1 response to GPR stimulation by a non-specific action. This possibility, however, was not supported by the fact that the previously documented GPR excitation of Int1 that occurs in the absence of MCN1 stimulation[2] remained effective in the presence of methiothepin (Pre-GPR: 1.4 ± 1.0 Hz; During GPR: 9.5 ± 1.2 Hz; n=5, $p=4.1 \times 10^{-4}$) (Supplementary Fig. 4a).

LG: The LG neuron is generally inactive when there is no gastric mill rhythm. At these times its resting potential was not altered by either GPR stimulation (Pre-GPR: -63.4 ± 6.1 mV; During GPR: -63.7 ± 6.5 mV; two-tailed t-test, p=0.28, n=5) or 5-HT application (Pre-5-HT: -59.7 ± 8.5 mV; 5-HT: -60.9 ± 9.3 mV; two-tailed t-test, p=0.10, n=3). However, in the absence of MCN1 stimulation, the number of LG spikes per depolarizing current pulse was reversibly reduced by both GPR stimulation and 5-HT application (Supplementary Fig. 3c,d). This GPR action on LG must be mediated by a distinct 5-HT receptor, however, because it persisted in the presence of methiothepin (n=3, p=0.036) (Supplementary Fig. 4b). Additionally, as shown above, this GPR action on LG was ineffective during the gastric mill rhythm

(Supplementary Fig. 2).

A previous study also documented both a GPR-elicited EPSP in LG and a post-GPR stimulation increase in the pyloric-timed LG oscillations[3]. However, we observed these EPSPs in only 2 of more than 50 preparations, and did not observe the increased pyloric-timed oscillations (n>50). Presumably, the distinction between the earlier and current experiments was the conditions under which the recordings were made. In the earlier work there was minimal background activity in LG, and the LG input resistance was presumably relatively high due to reduced synaptic input, because input from the CoGs and OG was blocked and no projection neurons were stimulated or modulators applied. Under these conditions, the LG membrane potential was generally flat or exhibited small amplitude pyloric-timed oscillations, because there was no gastric mill rhythm and the pyloric rhythm was silent or cycling slowly[3]. In contrast, during our recordings LG received considerable input from synapses and/or current injection, and exhibited relatively large amplitude pyloric- and gastric mill-timed oscillations which presumably reduced its input resistance and could have shunted the relatively small amplitude EPSPs and obscured the modest pyloric-timed oscillations. Whether these events were present and not observed or not present in our experiments, they did not have an impact on the results of our GPR stimulations insofar as eliminating the GPR influence on $MCN1_{STG}$ was sufficient to account for the GPR influence on the gastric mill rhythm.

SUPPLEMENTARY FIGURES.

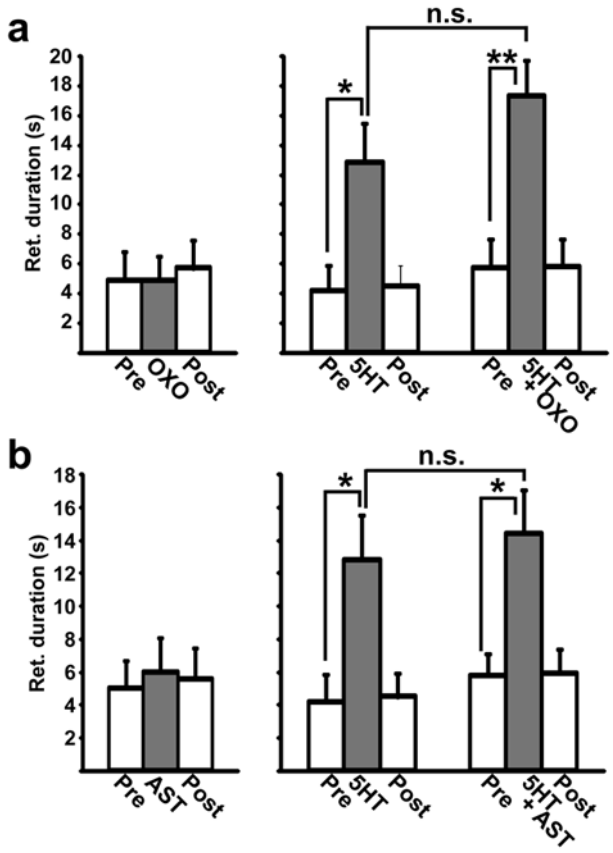

Supplementary Figure 1. Serotonin is the only GPR cotransmitter to mimic the ability of GPR stimulation to prolong the retractor phase of the MCN1-elicited gastric mill rhythm. (**a) (Left)** Pressure application of the muscarinic agonist oxotremorine (OXO: pipette concentration, 10^{-4} M) to the desheathed STG neuropil did not alter the gastric mill retractor phase duration relative to the retraction phase duration pre- and post-application (n=3, RM-ANOVA: p=0.94). **(Right)** Co-applying 5-HT and OXO prolonged the retractor phase (n=3, RM-ANOVA: p=0.01) to the same extent as applying 5-HT alone in the same

preparations (n=3, p=0.15). Symbols: n.s., not significant; *p<0.05; **p<0.01. Analysis: one way ANOVA across all groups compared, Student-Newman-Keuls post-hoc test for all pairwise comparisons. (**b) (Left)** Pressure application of the neuropeptide allatostatin (AST: pipette concentration, 10^{-5} M) did not alter the gastric mill retractor phase duration relative to the retraction phase duration pre- and post-application (n=3, RM-ANOVA: p=0.94). Application of a higher AST concentration (10^{-4} M) terminated the gastric mill rhythm for ~1 minute (n=2, data not shown), during which many gastric mill neurons hyperpolarized, as shown previously for the pyloric rhythm response to AST[2]. **(Right)** Co-applying 5-HT and AST also prolonged the retractor phase (n=3, RM-ANOVA: p=0.021) to the same extent as 5-HT alone in the same preparations (n=3, RM-ANOVA: p=0.58).

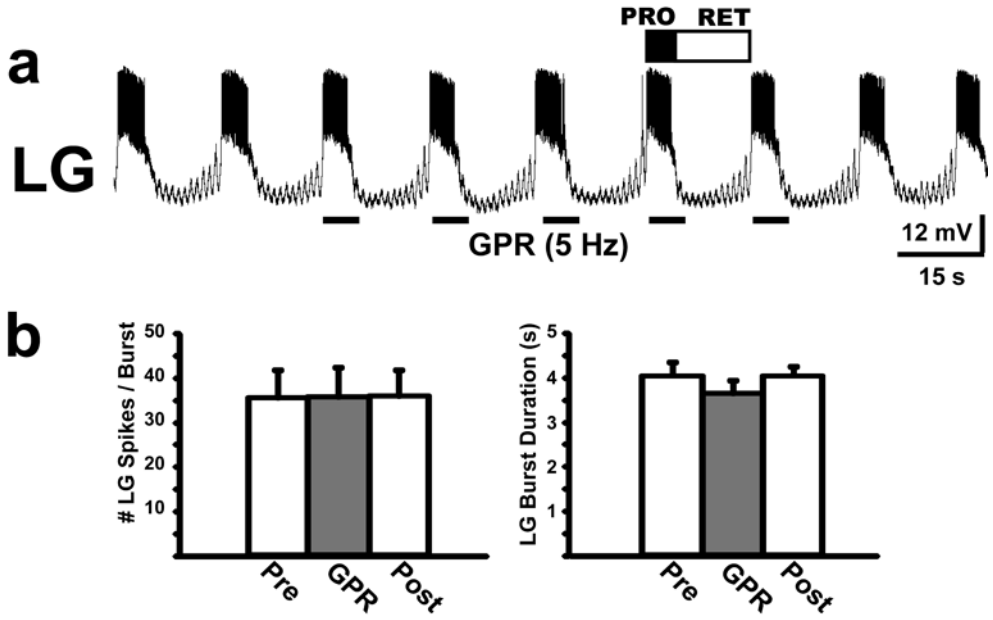

Supplementary Figure 2. GPR stimulation during the gastric mill protractor phase did not alter LG activity. GPR stimulation during the gastric mill retractor phase does not alter the protractor phase activity of the CPG neuron LG during the MCN1-gastric mill rhythm[3]. Here, we tested the possible influence of GPR on LG activity by rhythmically stimulating GPR during the protractor (LG burst) phase. Most hyperpolarized Vm: -61 mV. **(a)** Rhythmic GPR stimulation (bars) during protraction did not alter either phase of the MCN1-elicited gastric mill rhythm. **(b)** Across preparations, rhythmic GPR stimulation during protraction did not alter either the number of LG spikes/burst (n=4, p=0.99) or its burst duration (n=4, p=0.49).

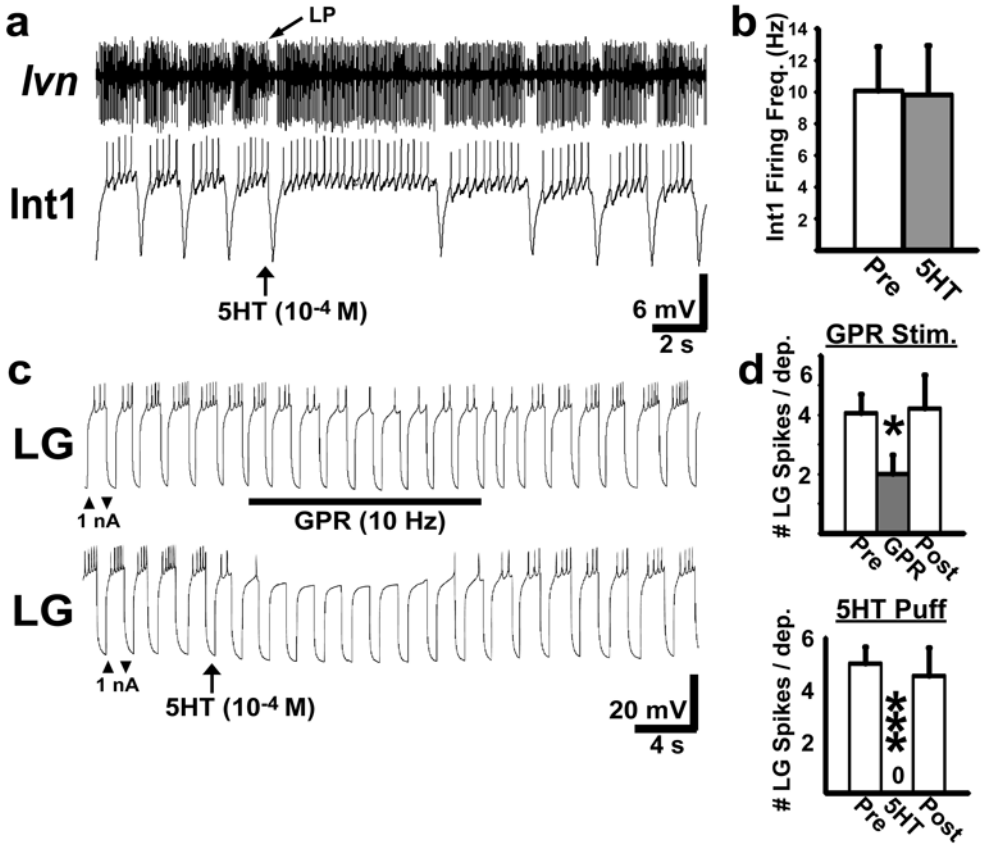

Supplementary Figure 3. Focal 5-HT application does not alter Int1 activity but it does inhibit LG activity. **(a)** In the absence of a gastric mill rhythm, pressure ejected 5-HT (1 s, bar) onto the desheathed STG neuropil did not alter the pyloric rhythm-timed intraburst firing frequency of Int1 (Pre-5-HT: 4.3 ± 0.1 Hz, n=5 cycles; 5-HT: 3.9 Hz, n=1 cycle; Post-5-HT: 5.1 ± 0.2 Hz, n=5 cycles). The 5-HT application was effective in that it prolonged the pyloric cycle period (note increased duration of the first lateral pyloric (LP) neuron burst after the 5-HT application). The pyloric rhythm is recorded in the *lvn* [large unit: LP neuron; small unit: pyloric dilator (PD) neuron]. Most hyperpolarized V_m: -58 mV. **(b)** 5-HT application did not alter spontaneous Int1 activity across preparations (n=4,

p=0.42). **(c)** Both GPR stimulation and 5-HT application inhibited LG activity driven by rhythmic depolarizing current pulses in LG. (**Top)** Spikes in LG from each current injection were inhibited by GPR stimulation (Pre-GPR: 5.3 ± 0.3 spikes; During GPR: 1.4 ± 0.2 spikes). (**Bottom)** Depolarization-elicited LG spikes were inhibited by focally applied 5-HT (Pre-5-HT: 4.4 ± 0.3 spikes; Post-5-HT: 0 spikes). Most hyperpolarized V_m: (Both panels) -60 mV. **(d)** LG activity was inhibited across preparations by both GPR stimulation (RM-ANOVA: p=0.035, n=3) and 5-HT application (RM-ANOVA: p=0.002, n=3).

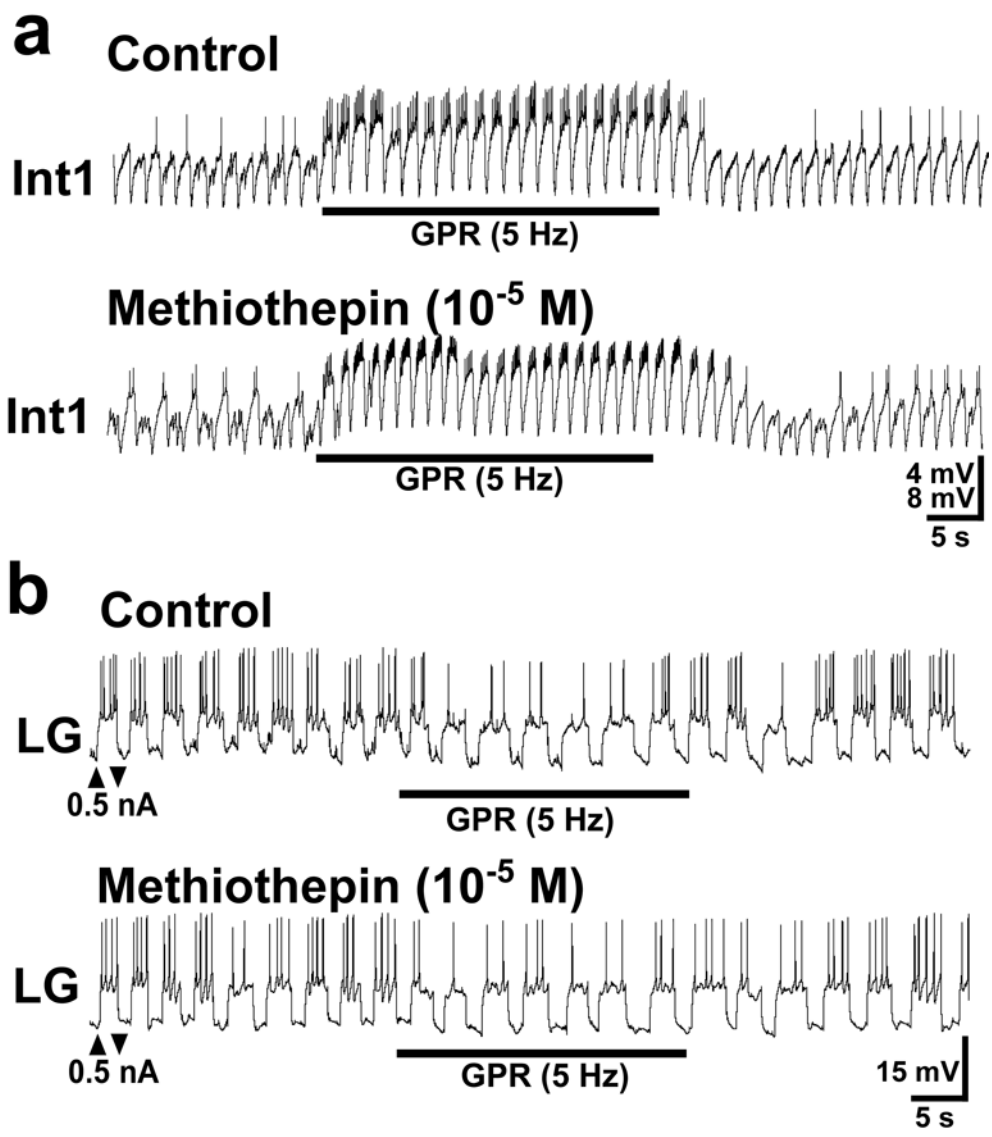

Supplementary Figure 4. Methiothepin does not alter the GPR actions on Int1 or LG. **(a) (Top)** In the absence of a gastric mill rhythm, GPR stimulation increased the pyloric rhythm-timed activity of Int1 during saline superfusion. (**Bottom)** Methiothepin superfusion did not interfere with the ability of GPR stimulation to excite Int1. Most hyperpolarized V_m (both panels): -54 mV. **(b) (Top)** Injection of periodic depolarizing current into LG during saline superfusion

elicited bursts of action potentials that were inhibited during GPR stimulation. (**Bottom)** Methiothepin superfusion did not interfere with the ability of GPR stimulation to inhibit the depolarizing current-elicited action potentials in LG. Most hyperpolarized V_m (both panels): -56 mV.

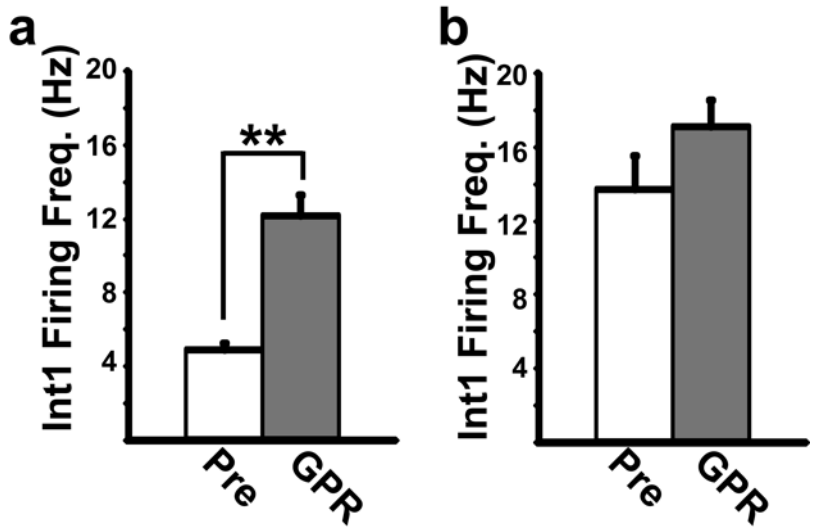

Supplementary Figure 5. A ceiling effect limits Int1 responsiveness to GPR stimulation during the gastric mill rhythm. **(a)** GPR consistently increased the intra-burst firing rate of the spontaneously active Int1 (n=4, p=0.002). **(b)** In these same preparations, the same level of GPR stimulation did not alter the Int1 firing rate when Int1 activity was first elevated by depolarizing current to mimic its response to MCN1 stimulation (n=4, p=0.11).

SUPPLEMENTARY REFERENCES

1. Katz, P.S. & Harris-Warrick, R.M. Recruitment of crab gastric mill neurons into the pyloric motor pattern by mechanosensory afferent stimulation. *J. Neurophysiol.* **65**, 1442-1451 (1991).
2. Skiebe, P. & Schneider, H. Allatostatin peptides in the crab stomatogastric nervous system: inhibition of the pyloric motor pattern and distribution of allatostatin-like immunoreactivity. *J. Exp. Biol.* **194**, 195-208 (1994).
3. Beenhakker, M.P., DeLong, N.D., Saideman, S.R., Nadim, F. & Nusbaum, M.P. Proprioceptor regulation of motor circuit activity by presynaptic inhibition of a modulatory projection neuron. *J. Neurosci.* **25**, 8794-8806 (2005).

Chapter 5

Parallel Regulation of a Modulator-Activated Current via Distinct Dynamics Underlies Co-Modulation of Motor Circuit Output

Nicholas D. DeLong

Matthew S. Kirby

Dawn M. Blitz

Michael P. Nusbaum

In Press:

The Journal of Neuroscience, 2009

ABSTRACT

The cellular mechanisms underlying co-modulation of neuronal networks are not elucidated in most systems. We are addressing this issue by determining the mechanism by which a peptide hormone, crustacean cardioactive peptide (CCAP), modulates the biphasic (protraction/retraction) gastric mill (chewing) rhythm driven by the projection neuron MCN1 in the crab stomatogastric ganglion. MCN1 activates this rhythm by slow peptidergic (CabTRP Ia) and fast GABAergic excitation of the reciprocally inhibitory central pattern generator neurons LG (protraction) and Int1 (retraction), respectively. MCN1 synaptic transmission is limited to the retraction phase, because LG inhibits MCN1 during protraction. Bath-applied CCAP also excites both LG and Int1, but selectively prolongs protraction. Here, we use computational modeling and dynamic clamp manipulations to establish that CCAP prolongs the gastric mill protractor (LG) phase and maintains the retractor (Int1) phase duration by activating the same modulator-activated inward current (I_{MI}) in LG as MCN1-released CabTRP Ia. However, the CCAP-activated current ($I_{MI\text{-}CCAP}$) and MCN1-activated current ($I_{MI\text{-}MCN1}$) exhibit distinct time courses in LG during protraction. This distinction results from $I_{MI\text{-}CCAP}$ being regulated only by postsynaptic voltage, whereas $I_{MI\text{-}MCN1}$ is also regulated by LG presynaptic inhibition of MCN1. Hence, without CCAP, retraction and protraction duration are determined by the time course of $I_{MI\text{-}MCN1}$ build-up and feedback inhibition-mediated decay, respectively, in LG. With $I_{MI\text{-}CCAP}$ continually present, the impact of the feedback inhibition is reduced, prolonging protraction and maintaining retraction duration. Thus, co-modulation of rhythmic motor activity can result from convergent activation, via distinct dynamics, of a single voltage-dependent current.

INTRODUCTION

The parallel influence of distinct modulatory inputs is likely a common occurrence in the CNS, yet its impact on neuronal network output is described in only a few systems (Dickinson et al., 1997; Svensson et al., 2001; McLean and Sillar, 2004; Crisp and Mesce, 2006; Kirby and Nusbaum, 2007). Such parallel inputs might target the same, overlapping or distinct sets of network neurons, and they could act via convergent or distinct mechanisms. This level of mechanistic detail regarding co-modulation, however, is unavailable for most networks, though it is partly established for the motor network output onto motor neurons in some spinal locomotor systems (Svensson et al., 2001; McLean and Sillar, 2004).

We are studying the mechanisms underlying co-modulation of motor pattern generation using the stomatogastric nervous system (STNS) of the crab *Cancer borealis* (Nusbaum and Beenhakker, 2002; Marder and Bucher, 2007). Within the STNS, the stomatogastric ganglion (STG) contains the central pattern generator (CPG) circuits for the gastric mill (chewing) and pyloric (filtering of chewed food) rhythms. Modulatory projection neurons that regulate these CPGs are located primarily in the commissural ganglia (CoGs) (Coleman et al., 1992; Nusbaum et al., 2001).

The peptide hormone crustacean cardioactive peptide (CCAP) modulates the biphasic gastric mill rhythm driven by the projection neuron modulatory commissural neuron 1 (MCN1), by selectively prolonging the gastric mill protractor phase (Kirby and Nusbaum, 2007). MCN1 activates the gastric mill CPG via slow, peptidergic (CabTRP Ia) excitation of the protractor CPG neuron

lateral gastric (LG) and fast, ionotropic (GABA) excitation of the retractor CPG neuron interneuron 1 (Int1) (Wood et al., 2000; Stein et al., 2007). MCN1 cotransmitter release occurs primarily during retraction, due to feedback inhibition from LG during protraction (Coleman et al., 1995). CCAP also excites LG and Int1 (Kirby and Nusbaum, 2007). Additionally, CCAP and CabTRP Ia activate the same modulator-activated, voltage-dependent inward current (I_{MI}) in pyloric neurons (Swensen and Marder, 2000, 2001), suggesting a comparable convergence in gastric mill neurons.

Here we test and confirm the hypothesis that CCAP co-modulates the MCN1-gastric mill rhythm by convergent activation of an ionic current (I_{MI}) in the LG neuron. Also pivotal is that, unlike MCN1-activated I_{MI} ($I_{MI\text{-}MCN1}$), the CCAP-activated I_{MI} ($I_{MI\text{-}CCAP}$) is independent of LG synaptic control. The latter distinction results in the two I_{MI} components exhibiting different dynamics during protraction, including a sustained $I_{MI\text{-}CCAP}$ amplitude and a declining $I_{MI\text{-}MCN1}$ amplitude. By manipulating $I_{MI\text{-}CCAP}$ in LG during the MCN1-gastric mill rhythm, we show that $I_{MI\text{-}CCAP}$ is necessary and sufficient for enabling CCAP to prolong protraction and maintain retraction duration. Specifically, protraction is prolonged by $I_{MI\text{-}CCAP}$ summing with $I_{MI\text{-}MCN1}$ to maintain LG suprathreshold for a longer duration. With protraction prolonged, however, $I_{MI\text{-}MCN1}$ decays further. Without compensation, this result would prolong retraction, because it would take longer for $I_{MI\text{-}MCN1}$ to build-up sufficiently for LG to burst. However, $I_{MI\text{-}CCAP}$ sums with $I_{MI\text{-}MCN1}$ during retraction to prevent a change in retraction duration. Thus, co-modulation of CPG activity can result from convergent ionic current activation, acting in part via distinct time courses.

METHODS

Animals. Male Jonah crabs (*Cancer borealis*) were obtained from commercial suppliers (Yankee Lobster Co., Boston, MA; Marine Biological Laboratory, Woods Hole, MA). Crabs were housed in commercial tanks containing recirculating, aerated, artificial seawater (10-12º C). Before dissection, the crabs were cold-anesthetized by packing them in ice for at least 30 minutes. The foregut was then removed and maintained in chilled physiological saline while the STNS was dissected from it and pinned down in a saline-filled silicone elastomer-lined Petri dish (Sylgard 184, KR Anderson, Santa Clara, CA).

Solutions. The isolated STNS was maintained in *C. borealis* saline containing (in mM): 439 NaCl, 26 $MgCl_2$, 13 $CaCl_2$, 11 KCl, 10 Trizma base and 5 maleic acid (pH 7.4-7.6). During experimentation, the preparation was continuously superfused with this solution (7-12 ml/min, 10-12º C). For voltage clamp experiments, TTX (10^{-7} M, Sigma Chemical Co., St. Louis, MO), picrotoxin (10^{-5} M, Sigma), TEACl (10^{-2} M, Sigma) and $CdCl_2$ (2 X 10^{-4} M, Fluka Chemical Corp., Milwaukee, WI) were added to *C. borealis* saline. These pharmacological agents were used to suppress sodium currents (TTX), glutamatergic inhibitory synaptic transmission (picrotoxin), a subset of potassium currents (TEACl) and a subset of calcium currents ($CdCl_2$) (Marder and Eisen, 1984; Golowasch and Marder, 1992a). CCAP (Bachem Americas Inc., Torrance, CA) and CabTRP Ia (Biotechnology Center, University of Wisconsin, Madison, WI) were diluted from stock solutions into normal *C. borealis* saline or the voltage clamp saline

immediately prior to use.

Electrophysiology. All experiments were conducted using the isolated STNS, from which the CoGs were removed by transecting the superior- (*sons*) and inferior oesophageal nerves (*ions*) (Fig. 1*A*). Intracellular and extracellular recordings of gastric mill neurons were made using routine methods for the STNS (Beenhakker and Nusbaum, 2004). Sharp glass microelectrodes (Current clamp:15-30 MΩ; Voltage clamp: 15-20 MΩ), filled with 4 M K-acetate plus 20 mM KCl or 0.6 M K_2SO_4 plus 10 mM KCl, were used for intracellular recordings. Intracellular recordings were made with Axoclamp 2 and 900A amplifiers (Molecular Devices, Sunnyvale, CA), and intracellular current clamp injections were performed in single electrode discontinuous current clamp (DCC) mode with sample rates of 2-5 kHz. Discontinuous single electrode voltage clamp (dSEVC) recordings were performed with sampling rates of 5-15 kHz. To facilitate intracellular recordings, the STG was desheathed and visualized with light transmitted through a dark-field condenser (Nikon, Tokyo, Japan).

For dSEVC recordings made from the LG primary neurite within the STG neuropil, LG was first filled with Alexa 568 (Invitrogen, Carlsbad, CA) using an intra-somatic recording. The LG neuropil arborization was then visualized with a TXR filter set on a MZ16F epifluorescence microscope (Leica, Bannockburn, IL) to enable impalement of the primary LG neurite with a second microelectrode, which was then used to perform dSEVC recordings of total cell currents. The somatic impalement was maintained to verify that the correct neurite was being

recorded once action potentials were eliminated with TTX. Voltage ramps (-90 to 0 mV at a rate of 75 mV/s) and steps (-90 to 0 mV in 5 or 10 mV increments, 500 ms duration) were applied and currents were recorded using PClamp (V. 9.2; Molecular Devices) and Digidata 1322A (Molecular Devices). In some experiments, as noted, CabTRP Ia was applied via pressure ejection (10 psi, 5 s duration) from a microelectrode positioned slightly above the STG neuropil using a Picospritzer II (Parker Hannifin Corp, Cleveland, OH).

Each extracellular nerve recording was made using a pair of stainless steel wire electrodes (reference and recording), the ends of which were pressed into the Sylgard-coated dish. A differential AC amplifier (Model 1700: AM Systems, Carlsborg, WA) amplified the voltage difference between the reference wire, placed in the bath, and the recording wire, placed near an individual nerve and isolated from the bath by petroleum jelly (Vaseline, Lab Safety Supply Inc., Janesville, WI). This signal was then further amplified and filtered (Model 410 Amplifier: Brownlee Precision, Santa Clara, CA). Extracellular nerve stimulation was accomplished by placing the pair of wires used to record nerve activity into a stimulus isolation unit (SIU 5: Astromed/Grass Instruments, West Warwick, RI) that was connected to a stimulator (Model S88: Astromed/Grass Instruments).

To elicit the gastric mill rhythm in the isolated STG, we selectively activated MCN1 by tonic extracellular stimulation of one or both of the transected *ions*, on the STG side of the transection (Fig. 1) (Bartos and Nusbaum, 1997; Bartos et al., 1999). Individual STNS neurons were identified by their axonal pathways, activity patterns and interactions with other neurons (Weimann et al.,

1991; Blitz et al., 1999; Beenhakker and Nusbaum, 2004). During the MCN1-gastric mill rhythm, the LG burst defines the protractor phase while its interburst duration, which is equivalent to the duration of Int1 activity, defines the retractor phase (Coleman et al., 1995; Bartos et al., 1999; Kirby and Nusbaum, 2007).

Dynamic Clamp. We used the dynamic clamp to inject an artificial version of an ionic current (I_{MI}) into the LG neuron (Sharp et al, 1993; Bartos et al., 1999; Prinz et al, 2004; Beenhakker et al., 2005; Goaillard and Marder, 2006). The dynamic clamp software uses the intracellularly recorded membrane potential of a biological neuron to calculate an artificial current (I_{dyn}) using a conductance [$g_{dyn}(t)$] that is numerically computed, as well as a predetermined reversal potential (E_{rev}). The injected current is based upon real time computations, updated in each time step (0.2 ms) according to the new values of recorded membrane potential, and injected back into the biological neuron. The intrinsic currents are computed according to the following equations:

$$I_{dyn} = g_{dyn} m^p h^q (V_1 - E_{rev})$$

$$\tau_X(V_2)\frac{dX}{dt} = X_\infty(V_2) - X; X = m, h$$

$$X_\infty(V) = \frac{1}{1 + \exp\left(\frac{V - V_X}{k_X}\right)}$$

$$\tau_X(V) = \tau_{X,Lo} + \frac{\tau_{X,Hi} - \tau_{X,Lo}}{1 + \exp\left(-\frac{V - V_X}{|k_X|}\right)},$$

where V_1 and V_2 both represent the membrane potential, and X stands for either

m or h for calculations involving activation or inactivation, respectively.

In our dynamic clamp experiments we modeled I_{MI} using parameters both previously determined (Golowasch and Marder 1992; Swensen and Marder, 2000, 2001) and determined during the voltage clamp experiments in the LG neuron (see Results). Specifically, we set the half-maximum voltage of the activation curve (V_m) at -45 mV, with the peak current occurring at -37 mV. We set the reversal potential (E_{rev}) to 0 mV, consistent with our findings and previous voltage clamp results for I_{MI} (Golowasch and Marder, 1992). I_{MI} shows a voltage-dependence to its activation (Golowasch and Marder, 1992a; Swensen and Marder 2000, 2001). Therefore, the integer power of the activation variable *m* (abbreviated 'p' above) was set to a value of 1. The slope of the activation sigmoid at half-maximum (K_m) was -5.0 mV, the time constant of activation at membrane potentials below V_m ($\tau_{m,Lo}$) was 50.0 ms and the activation time constant at membrane voltages above V_m ($\tau_{m,Hi}$) was 100.0 ms. I_{MI} does not inactivate, so the integer power of the inactivation variable *h* (abbreviated 'q' above) was set to 0. Therefore, no values were needed for K_h, $\tau_{h,Lo}$, and $\tau_{h,Hi}$, all of which are used to calculate the inactivation of the current. The conductance value at maximum activation (G_{max}) varied between 5 and 30 nS, depending on the experiment. In all of our dynamic clamp experiments, the maximum current injected into the LG neuron never exceeded 1 nA (see Results).

We used a version of the dynamic clamp developed in the Nadim laboratory (Rutgers University, Newark, NJ; available at

http://stg.rutgers.edu/software/) to run on a personal computer (PC) running Windows XP and a NI PCI-6070-E data acquisition board (National Instruments, Austin, TX). As above, all dynamic clamp current injections were performed while recording in single-electrode, DCC mode (sample rates 2-5 kHz).

Data Analysis. Data analysis was facilitated by a custom-written program (The Crab Analyzer) for Spike2 (Cambridge Electronic Design, Cambridge, England) that determines the activity levels and burst relationships of individual neurons (freely available at http://www.uni-ulm.de/~wstein/spike2/index.html). Unless otherwise stated, each datum in a data set was derived by determining the average of ten consecutive gastric mill-timed impulse bursts in the biological preparation, or the average of three consecutive cycles for the computational modeling studies. In all experiments, the burst duration was defined as the duration (s) between the onset of the first and last action potential in an impulse burst. The average firing rate was determined by the number of action potentials minus one divided by the burst duration. Protractor phase duration was equivalent to LG burst duration, and retractor phase duration was equivalent to the LG interburst duration (time between the last action potential in one LG burst and the first action potential in the next LG burst). The cycle period of the gastric mill rhythm was determined by calculating the duration from the onset of successive LG neuron bursts.

Voltage-clamp data analysis was performed using PClamp software. Total cell currents were determined either by averaging 2-3 sets of 10 ramps or

5-10 sets of steps in each condition and subtracting the control from the experimental condition. The voltage-dependent inward current originally described by Golowasch and Marder (1992) was identified as a proctolin-activated current and thus designated I_{proct}. However, it is now known that many modulators activate this current (Swensen and Marder 2000, 2001). Consequently, this current is now designated as the modulator-activated inward current (I_{MI}) (Grashow et al., 2009).

Data were collected onto a chart recorder (Models MT 95000 and Everest: Astromed Corp., West Warwick, RI) and simultaneously onto a PC computer using data acquisition/analysis tools (Spike2; digitized at ~5 kHz). Figures were made from Spike2 or PClamp files incorporated into Adobe Illustrator (Adobe, San Jose, CA) or Igor Pro (Wavemetrics, Lake Oswego, OR) and CorelDraw (Corel Corporation, Ottawa, Ontario, Canada). Statistical analyses were performed with SigmaStat 3.0 and SigmaPlot 8.0 (SPSS Inc., Chicago, IL). All comparisons were made using the paired Student's t-test, except where noted. Data are expressed as the mean ± standard error (SE).

Gastric Mill Model. We constructed a computational model modified from an existing conductance-based model of the gastric mill circuit (Nadim et al., 1998; Beenhakker et al., 2005). The previously published version modeled the LG, Int1, and MCN1 neurons as having multiple compartments separated by an axial resistance, with each compartment possessing intrinsic and/or synaptic conductances. To more realistically mimic the biological system, in this version

of the model we modified the MCN1-activated synaptic conductance ($G_{MI\text{-}MCN1}$) in the dendrite compartment of the LG neuron to include a postsynaptic voltage dependence (Table 1). The parameters of this model current were based on both a previously published voltage-clamp analysis of this current in the pyloric LP neuron and on the LG neuron voltage clamp results obtained in this paper (Golowasch and Marder, 1992a; Swensen and Marder, 2000, 2001; see Results). To mimic the effects of CCAP bath application to the biological system, we also added to the LG neuron dendrite compartment an intrinsic (non-synaptically activated) current ($I_{MI\text{-}CCAP}$) with the same voltage dependence as $I_{MI\text{-}MCN1}$ (Table 1). This approach was based on the fact that CCAP and MCN1-released CabTRP Ia both excite LG (Wood et al., 2000; Kirby and Nusbaum, 2007; Stein et al., 2007), and activate I_{MI} in STG pyloric neurons (Swensen and Marder, 2000, 2001), as well as LG (this paper).

Simulations were performed on a PC with Windows XP. We used the Network simulation software developed in the Nadim laboratory (http://stg.rutgers.edu/software/network.htm), which was run using the freely available CYGWIN Linux emulation software package. We used a fourth-order Runge–Kutta numerical integration method with time steps of 0.05 and 0.01 ms. Results were visualized by plotting outputted data points using the freely available Gnuplot software package (www.gnuplot.info). In most figures showing the model output, we present $G_{MI\text{-}MCN1}$ and/or $G_{MI\text{-}CCAP}$ instead of their associated I_{MI} to more clearly display their trajectory during the gastric mill retractor and protractor phases. G_{MI} parallels I_{MI} except for the fast I_{MI} transient that occurs

during each LG action potential (see Fig. 3). The fast transients result from the voltage-sensitivity of I_{MI}, which is not shared by G_{MI}. It is also noteworthy that the presentation of I_{MI} in the model and dynamic clamp figures represents different conventions. Specifically, the model output directly reports actual current flow in the model neuron and so uses the standard voltage clamp convention, whereas the dynamic clamp output represents the current injected into the neuron and hence uses the standard current clamp convention. Consequently, I_{MI} is represented as an inward (downward trajectory) current in the model output figures but is represented as a depolarizing (upward trajectory) current in the dynamic clamp output figures.

Table 1: Gastric Mill Rhythm Model Parameters for $I_{MI-MCN1}$ and $I_{MI-CCAP}$							
Current	**G_{max}**	**E_{rev}**	**m_{inf}**	**m_{tau}**	**$m_{postinf}$**	**$m_{posttau}$**	**m_{power}**
$I_{MI-MCN1}$	10	0	$\frac{1}{1+e^{-2(V_{MCN1}+68)}}$	$8000+\frac{9000}{1+e^{-2(V_{MCN1}+68)}}$	$\frac{1}{1+e^{-0.1(V_{LG}+50)}}$	50	n/a
$I_{MI-CCAP}$	0.2	0	$\frac{1}{1+e^{-0.1(V_{LG}+50)}}$	50	n/a	n/a	1

Table 1. The values used for $I_{MI-MCN1}$ and $I_{MI-CCAP}$ in the computational model of the MCN1-elicited gastric mill rhythm. The other model parameters were unchanged from previous studies (Nadim et al., 1998; Beenhakker et al., 2005). Abbreviations: G_{max}, conductance value at maximum activation; E_{rev}, reversal potential; m_{inf}, steady-state activation curve; m_{tau}, activation time constant; $m_{postinf,}$ steady-state activation curve for the post-synaptic voltage dependence; $m_{posttau}$, activation time contstant for the post-synaptic voltage dependence; m_{power}, integer power of the activation variable m; n/a, not relevant to computation. Parameter names are derived from the nomenclature used in the Network modeling software, which was used to perform all simulations (http://stg.rutgers.edu/software/network.htm).

RESULTS

The gastric mill system in *C. borealis*

The gastric mill rhythm (cycle period 5-20 s) controls the rhythmic protraction and retraction chewing movements of the teeth in the gastric mill stomach compartment (Heinzel et al., 1993). This rhythm is thus composed of alternating impulse bursts in protractor and retractor motor neurons, plus a single retractor phase interneuron (Int1) (Fig. 1*B*) (Kirby and Nusbaum, 2007). Several gastric mill neurons coincidentally exhibit faster rhythmic impulse bursts that are time-locked to the pyloric rhythm (cycle period 0.5-2 s) (Weimann et al. 1991; Kirby and Nusbaum, 2007). The pyloric rhythm controls the filtering of chewed food in the pylorus, which is the stomach compartment immediately posterior to the gastric mill. Int1 is one of the neurons exhibiting this dual rhythmic firing pattern during the MCN1-elicited gastric mill rhythm (Fig. 1*B*) (Bartos et al., 1999). Both LG and Int1 are present as single neurons in the *C. borealis* STG.

The core CPG underlying the MCN1-gastric mill rhythm includes the reciprocally inhibitory protractor phase neuron LG and retractor phase neuron Int1, plus the STG terminals of MCN1 ($MCN1_{STG}$) (Fig. 1*C*) (Coleman et al. 1995; Bartos et al. 1999). The gastric mill cycle period is also regulated by the pyloric pacemaker neurons, via an inhibitory synapse from the anterior burster (AB) neuron onto Int1 (Bartos et al., 1999). During retraction, the slow MCN1 excitation of LG builds up until LG escapes from Int1-mediated inhibition and initiates an action potential burst that starts the protractor phase. During protraction, the LG burst inhibits Int1 and also inhibits $MCN1_{STG}$ transmitter

release, thereby reducing or removing further MCN1 excitation of LG (Fig. 1*C*). Hence, the LG burst persists only until the slowly decaying effects of the peptidergic excitation from MCN1 no longer maintain LG at a sufficiently depolarized membrane potential, at which point the protractor phase terminates and retraction resumes.

Superfusing CCAP (≥10^{-10} M) to the isolated STG slows the MCN1-gastric mill rhythm by selectively prolonging the protractor phase (Fig. 1*D*) (Kirby and Nusbaum, 2007). This response occurs despite the fact that CCAP directly excites both LG and Int1, while having no effect on $MCN1_{STG}$ (Kirby and Nusbaum, 2007). Hence, during the CCAP-modulated gastric mill rhythm, LG exhibits prolonged bursts with an increased firing frequency, but Int1 activity is unchanged (Kirby and Nusbaum, 2007). Additionally, despite its lack of effect on $MCN1_{STG}$, CCAP lowers the threshold MCN1 firing frequency necessary to elicit the gastric mill rhythm (Kirby and Nusbaum, 2007). Here, our goal was to determine the mechanism(s) by which CCAP selectively prolongs the protractor phase of the MCN1-gastric mill rhythm and facilitates the ability of MCN1 to activate this rhythm.

CCAP and CabTRP Ia both activate I_{MI} in the LG neuron

To determine the mechanism whereby CCAP modulates the MCN1-gastric mill rhythm, we first identified the ionic currents in LG that were influenced by MCN1 and CCAP using dSEVC recordings from the LG primary neurite (see Methods). To obtain voltage clamp of sufficient quality, we conducted these

experiments with action potentials suppressed, which prevented us from identifying the MCN1-activated current(s) via MCN1 stimulation. However, because CabTRP Ia is the sole cotransmitter by which MCN1 influences LG (Wood et al., 2000; Stein et al., 2007), we bath applied CabTRP Ia and CCAP to identify the ionic current(s) affected by these two pathways.

Bath applied CCAP (10^{-7} M) and CabTRP Ia (10^{-6} M) each caused an inward shift in the holding current at a holding potential of -60 mV (Saline: -1.8 ± 1.0 nA, CCAP: -2.6 ± 1.2 nA, n=4, p=0.05; Saline: -1.6 ± 0.7 nA, CabTRP Ia: -2.0 ± 0.7 nA; n=4, p=0.003). Subtraction of the control total current from the total current during CCAP or CabTRP Ia application revealed a voltage-dependent inward difference current (Fig. 2*A,B*). The peak current amplitude (CCAP: -2.6 ± 0.4 nA, n=4; CabTRP Ia: -0.8 ± 0.2 nA, n=4) occurred at -36.3 ± 2.4 mV in CCAP (10^{-7} M: n=4) and -36.7 ± 6.2 mV in CabTRP Ia (10^{-6} M: n=4). The half-maximal current occurred at -51.1 ± 6.3 mV in CCAP (n=4) and at -60.9 ± 4.2 mV in CabTRP Ia (n=4).

The voltage dependence of these peptide-elicited currents was comparable to one another and to that previously reported for I_{MI} in pyloric neurons (Golowasch and Marder, 1992a; Swensen and Marder, 2000). To further test whether CCAP and CabTRP Ia converged to activate the same current (I_{MI}) in the LG neuron, we performed occlusion experiments. Specifically, CabTRP Ia (10^{-4} M) was pressure applied to the desheathed STG neuropil in control conditions, then CCAP (10^{-6} M) was bath-applied during which the influence of CabTRP Ia (10^{-4} M) was again assayed. Pressure-ejected CabTRP

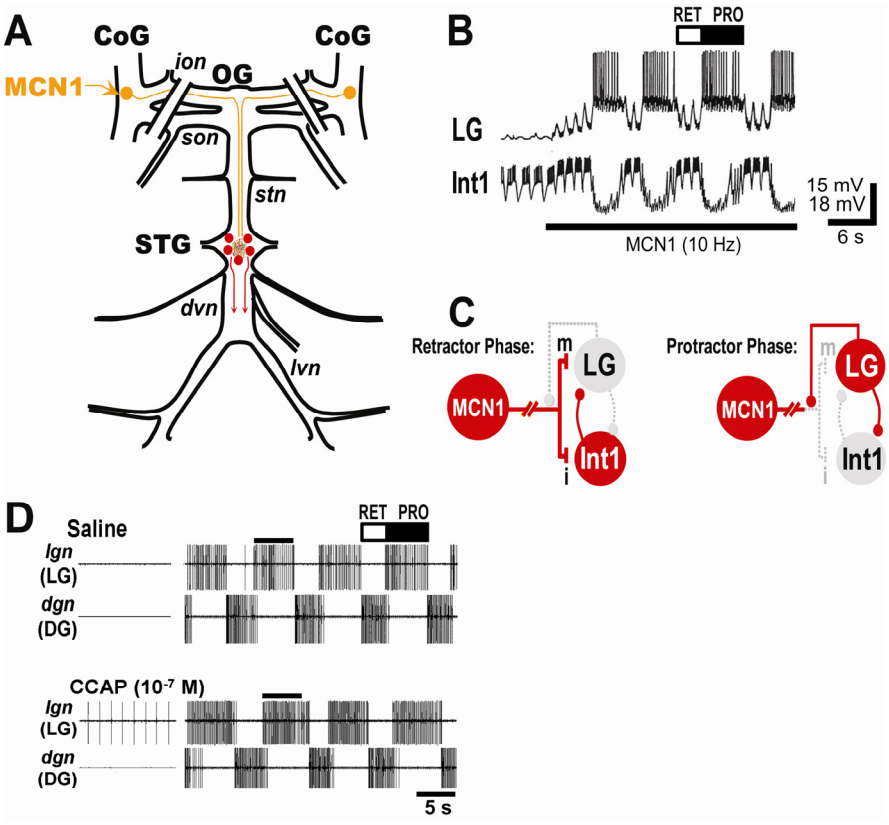

Figure 1. Schematics of the isolated stomatogastric nervous system and the core CPG circuit for the MCN1-elicited gastric mill rhythm, plus examples of the MCN1-elicited gastric mill rhythm and the influence of the peptide hormone CCAP on this rhythm. *A,* The STNS consists of the unpaired STG and OG plus the paired CoGs. There is a single MCN1 in each CoG. The paired lines crossing the *ions* and *sons* indicate that these nerves were transected at the start of each experiment, isolating the STG from the CoGs. Abbreviations: Nerves- *dvn*, dorsal ventricular nerve; *ion*, inferior oesophogeal nerve; *lvn*, lateral ventricular nerve; *son*, superior oesophageal nerve; *stn*, stomatogastric nerve. *B*, MCN1 stimulation activates the gastric mill rhythm. Before MCN1 stimulation, LG was silent and Int1 exhibited pyloric rhythm-timed activity. At the start of

MCN1 stimulation, the retractor phase was initiated with a fast increase in Int1 activity while LG slowly depolarized. The pyloric-timed depolarizations in LG resulted from the rhythmic inhibitory input to Int1 from the pyloric pacemaker neuron AB (Bartos et al., 1999). When LG reached burst threshold, it inhibited Int1 (and $MCN1_{STG}$) and protraction commenced. *C*, Schematic of the core CPG for the MCN1-elicited gastric mill rhythm during each phase of this rhythm. Despite the schematic representation of synapses onto somata, all synapses are located on small neuronal branches in the STG neuropil. Active neurons have red-filled somata, while inactive neurons have gray-filled somata. Symbols: small filled circles represent synaptic inhibition, while t-bars represent synaptic excitation; m, metabotropic; i, ionotropic. Based on Coleman et al. (1995) and Bartos et al. (1999). *D*, As shown by Kirby and Nusbaum (2007), bath-applied CCAP selectively prolongs the protractor phase of the MCN1-elicited gastric mill rhythm. Note that CCAP did not activate the gastric mill rhythm prior to MCN1 stimulation. Retraction is represented by the dorsal gastric (DG) retractor motor neuron. Bar on top of second LG burst in each panel represents the LG burst duration in saline, to show that the LG burst is prolonged by CCAP.

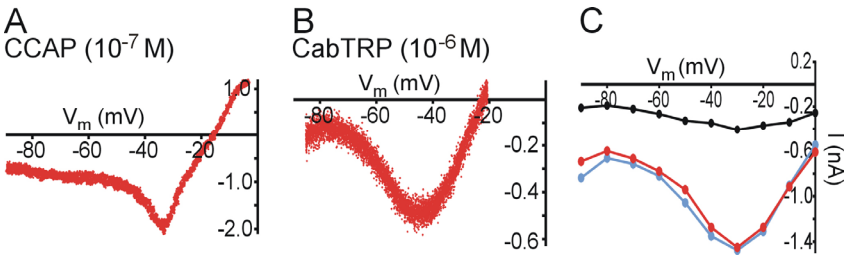

Figure 2. The peptides CCAP and CabTRP Ia activate the same voltage-dependent inward current in the LG neuron. *A,B,* Subtracting the total average current elicited by voltage ramps (-90 to 0 mV, 75 mV/s) in control conditions from the total current elicited in 10^{-7} M CCAP (*A*) or 10^{-6} M CabTRP Ia (*B)* revealed a voltage-dependent inward current. The currents plotted are the difference currents resulting from subtracting the average of 20 (*A*) or 30 (*B*) ramp trials in each condition. *C*, Voltage steps (-90 to 0 mV, 10 mV increments, 500 ms duration) were used to measure the currents activated by pressure applied CabTRP Ia (10^{-4} M; 10 psi, 5 s; black line and symbols), CCAP (10^{-6} M; bath application; red line and symbols) and CabTRP Ia in the presence of CCAP (blue line and symbols). In each case, the control current was subtracted from the experimental condition and the difference currents are plotted. In this example, the I_{Peak} for CabTRP Ia alone was ~0.4 nA, but with CCAP present the I_{Peak} added by CabTRP Ia was ~0.02 nA. Each plot is the mean steady state current (last 200 ms of a step) at each voltage, from the average of 5 sets of steps. The different E_{rev} in panels A/B and C reflects the variability in measured E_{rev} for I_{MI} in this and previous work (Golowasch and Marder, 1992a). This variability is likely due to the relatively large leak- and voltage-dependent outward currents in STG neurons at depolarized voltages (Golwasch and Marder, 1992b;

Khorkova and Golowasch, 2007). However, within each experiment, E_{rev} for $I_{MI\text{-}CabTRP\ Ia}$ and $I_{MI\text{-}CCAP}$ was similar and in all experiments the measured E_{rev} was comparable to those previously reported (Golowasch and Marder 1992). Panels A-C were different preparations.

Ia activated the aforementioned voltage-dependent inward current in the control condition (Peak current: -0.9 ± 0.2 nA, n=4) (Fig. 2*C*). Subsequent bath-applied CCAP also activated a voltage-dependent inward current. However, pressured-ejected CabTRP Ia in the presence of CCAP elicited little to no additional current compared to CCAP alone (CCAP: -1.9 ± 0.2 nA; CCAP + CabTRP Ia: -2.1 ± 0.2 nA, n=4; CCAP vs CCAP + CabTRP Ia: p=0.16; CabTRP Ia alone vs CCAP + CabTRP Ia: p<0.001, One Way RM ANOVA followed by Student-Newman Keuls test) (Fig. 2*C*). After CCAP washout, CabTRP Ia again elicited a current comparable to the pre-CCAP condition (-1.0 ± 0.1 nA, n=3; Wash vs Control: p=0.91; One Way RM ANOVA followed by Student-Newman Keuls test). This reversible occlusion result indicated convergence of the two peptides on the same voltage-dependent inward current. Given the similar properties of this current to those of the previously identified I_{MI} (Golowash and Marder 1992; Swensen and Marder, 2000), and the fact that CCAP and CabTRP Ia activate this current in pyloric neurons, we conclude that these peptides also activate I_{MI} in LG.

CCAP actions in a computational model mimic its actions on the biological gastric mill rhythm

We next examined the role of $I_{MI\text{-}CCAP}$ in LG for mediating the selective prolongation of the gastric mill protractor phase by bath-applied CCAP, using our previously developed computational model of the MCN1-gastric mill rhythm (Nadim et al., 1998; Beenhakker et al., 2005). We modeled I_{MI} based on values

obtained in our LG voltage clamp experiments (see above) as well as previously determined values (Golowasch and Marder, 1992a; Swensen and Marder, 2000) (Table I). Further, we assumed that the CCAP influence was at a steady-state, comparable to its continued presence during bath application of the peptide in the biological experiments (Kirby and Nusbaum, 2007), and so the $I_{MI\text{-}CCAP}$ amplitude and its associated $G_{MI\text{-}CCAP}$ were sensitive only to changes in the LG membrane potential.

The trajectory of the model $G_{MI\text{-}MCN1}$ in the LG neuron steadily increased in amplitude during retraction due to continual MCN1 release of CabTRP Ia, and decayed during protraction due to feedback inhibition from LG onto $MCN1_{STG}$ (Figs. 1*C*, 3*A,B*) (Coleman and Nusbaum, 1994; Coleman et al., 1995; Beenhakker et al., 2005). As is evident in Figure 3, the $G_{MI\text{-}MCN1}$ peak amplitude occurred at LG burst onset, from which point it decayed until it could no longer sustain the LG burst. The trajectory of the $G_{MI\text{-}CCAP}$ amplitude in LG during retraction was similar to that of $G_{MI\text{-}MCN1}$, but was distinct during protraction where it exhibited a sustained maximal amplitude (Fig. 3*B*). The model I_{MI} trajectory in LG tracked that of G_{MI} for both MCN1 and CCAP, except at LG burst onset where I_{MI} amplitude diminished because the LG membrane potential approached E_{rev} for I_{MI}.

We used this model to test whether we could mimic the CCAP-mediated selective increase in protractor phase duration by adding $I_{MI\text{-}CCAP}$ to (a) Int1 and LG, (b) Int1 alone or (c) LG alone. We did not document the presence of $I_{MI\text{-}CCAP}$ in the biological Int1, but for use in the model we assumed it to be the current

responsible for the CCAP excitation of Int1. This assumption was based on the fact that it is the relevant current in all CCAP-responsive pyloric circuit neurons as well as LG (Swensen and Marder 2000; this study).

In the model, adding $I_{MI\text{-}CCAP}$ to both Int1 and LG prolonged the protractor phase relative to the control gastric mill rhythm (Control: 11.0 ± 0.4 sec; CCAP: 14.0 ± 0.3 sec; n=3 cycles, $p<0.05$) without altering the retractor phase duration (Control: 7.0 ± 0.2 sec; CCAP: 7.3 ± 0.3 sec; n=3 cycles, $p=0.39$). When instead $I_{MI\text{-}CCAP}$ was added only to Int1, there was no change in the protractor phase duration (Control: 11.0 ± 0.4 sec; CCAP: 10.4 ± 0.2 sec; n=3 cycles, $p=0.15$) or retractor phase duration (Control: 7.0 ± 0.2 sec; CCAP: 7.3 ± 0.5 sec; n=3 cycles, $p=0.21$). Despite the lack of effect on the gastric mill rhythm, the CCAP-activated conductance was effective at increasing the Int1 intraburst firing frequency in the absence of a gastric mill rhythm (Control: 6.9 ± 0.04 Hz; CCAP: 9.2 ± 0.08 Hz, n=3 cycles, $p<0.001$), similar to what was previously observed with biological CCAP superfusion (Kirby and Nusbaum, 2007). Lastly, providing $I_{MI\text{-}CCAP}$ only to LG was comparable to adding this current to both Int1 and LG. Specifically, the gastric mill protractor phase was prolonged (Control: 11.0 ± 0.4 sec; CCAP: 13.8 ± 0.3 sec; n=3 cycles, $p<0.05$), without altering the retractor phase duration (control: 7.0 ± 0.2 sec; CCAP: 6.8 ± 0.1 sec; n=3 cycles, $p=0.27$) (Fig. 3).

In both models that exhibited an increased protractor phase duration with CCAP present, there was no change in the summed peak I_{MI} amplitude in LG despite the parallel activation of this current by MCN1 and CCAP. For example, in the model where $I_{MI\text{-}CCAP}$ was added only to LG, the summed peak I_{MI}

amplitude was unchanged at both the start (MCN1: -48.3 ± 1.4 pA; MCN1 plus CCAP: -47.4 ± 0.7 pA; n=3 cycles, p=0.35) and end MCN1: -15.2 ± 0.5 pA; MCN1 plus CCAP: -16.2 ± 0.4 pA; n=3 cycles, p=0.14) of each LG burst (Fig. 4). Consequently, the membrane potential at which the LG burst terminated was the same whether or not $I_{MI\text{-}CCAP}$ was present (MCN1: -31.1 ± 1.28 mV; MCN1 plus CCAP: -29.78 ± 1.14 mV, n=4 cycles, p=0.15). Despite the fact that the total peak I_{MI} was unchanged, the component contributed by MCN1 ($I_{MI\text{-}MCN1}$) was decreased at LG burst onset (w/o CCAP: -48.3 ± 1.4 pA; w/CCAP: -41.6 ± 0.6 pA; n=3 cycles, $p<0.05$) and offset (w/o CCAP: -15.2 ± 0.5 pA; w/CCAP: -9.4 ± 0.3 pA; n=3 cycles, $p<0.05$), although the net decrease of $I_{MI\text{-}MCN1}$ was essentially unchanged (~32 pA). The decreased contribution from MCN1 is shown for G_{MI} levels in Figure 4.

The $I_{MI\text{-}CCAP}$ amplitude was roughly constant across the duration of the LG burst and so appeared responsible for the prolonged LG burst in CCAP (Fig. 3). This $I_{MI\text{-}CCAP}$ effect resulted from its replacing a portion of the decaying $I_{MI\text{-}MCN1}$ during the LG burst with a non-decaying I_{MI} component (Figs. 3, 4). In the CCAP condition, the total I_{MI} amplitude (i.e. $I_{MI\text{-}MCN1}$ plus $I_{MI\text{-}CCAP}$) was equal to the $I_{MI\text{-}MCN1}$ amplitude without CCAP at both LG burst onset and offset (Fig. 4). However, the presence of the non-decaying $I_{MI\text{-}CCAP}$ component reduced the overall decay rate of I_{MI}, and thus prolonged the LG burst (Fig. 4*C*). Furthermore, because some $I_{MI\text{-}MCN1}$ was replaced by $I_{MI\text{-}CCAP}$, the $I_{MI\text{-}MCN1}$ amplitude at LG burst offset in the CCAP condition was reduced compared with the control condition (Figs. 3, 4*C*).

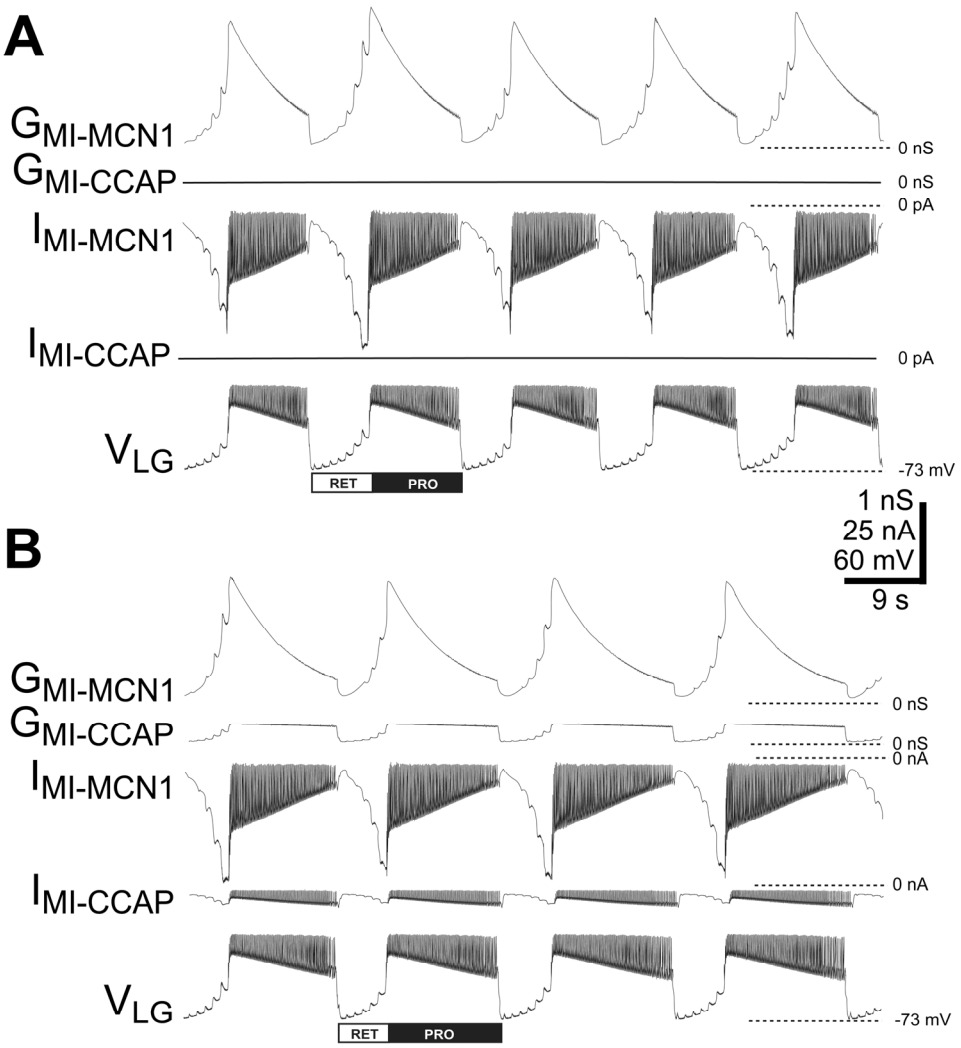

Figure 3. Distinct dynamics of the CCAP- and MCN1-activated I_{MI} in LG underlie the selective prolongation of the gastric mill protractor phase by CCAP in a computational model. *A,* The gastric mill rhythm driven only by MCN1. Note the pyloric-timed build-up of $I_{MI\text{-}MCN1}$ and its underlying conductance ($G_{MI\text{-}MCN1}$) in LG, during each retractor phase and decay during protraction. $I_{MI\text{-}MCN1}$ was regulated by its voltage-sensitivity, the proximity of the LG membrane potential to E_{rev} for I_{MI} ("driving force"), and the inhibitory feedback synapse from LG to $MCN1_{STG}$. G_{MI} was unaffected by the driving force. *B,* The gastric mill rhythm driven by both

MCN1 stimulation and CCAP. As in the biological preparation, the LG burst (protraction) is prolonged while its interburst (retraction) is unchanged in duration. Note the distinct dynamics of $G_{MI\text{-}CCAP}$ and $G_{MI\text{-}MCN1}$ during protraction. In this model, $I_{MI\text{-}CCAP}$ was added only to LG.

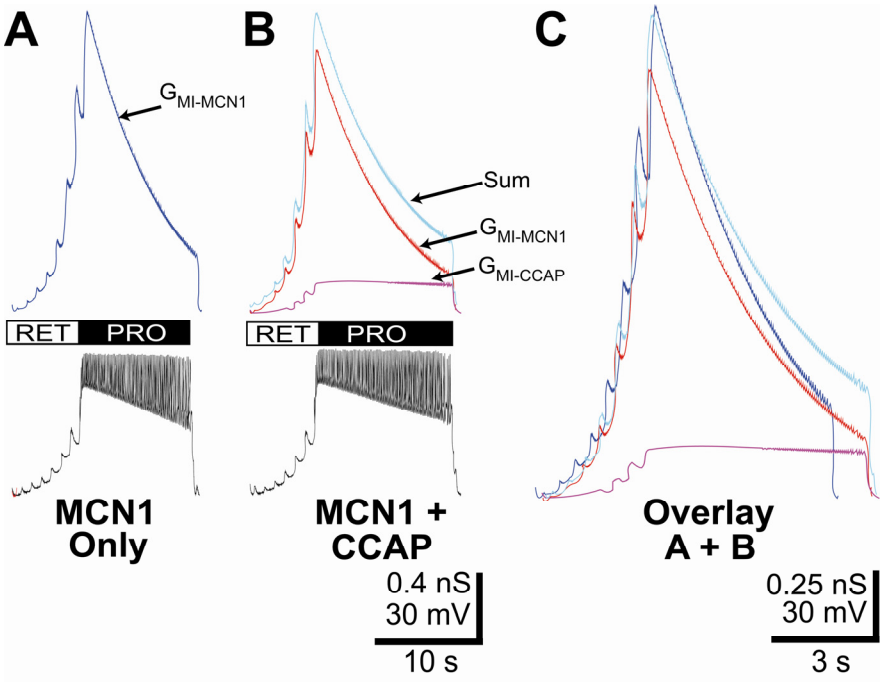

Figure 4. MCN1- and CCAP-activated G_{MI} exhibit different dynamics during the MCN1-gastric mill rhythm, but the total peak G_{MI} activated during this rhythm is the same when MCN1 is stimulated in saline and with CCAP present. Using the computational model, the G_{MI} trajectory and amplitude during a single cycle of the gastric mill rhythm are shown when MCN1 is stimulated (*A*) without CCAP and (*B*) with CCAP present. "Sum" represents the summation of $G_{MI\text{-}MCN1}$ and $G_{MI\text{-}CCAP}$. *C,* Overlay of Panels A and B indicate that the summed peak G_{MI} in Panel B is the same as $G_{MI\text{-}MCN1}$ from Panel A.

The unchanged retractor phase duration in the versions of the model with CCAP present in either LG and Int1 or LG alone was also consistent with our previous results from the biological preparation, in which CCAP selectively prolonged the protractor phase (Kirby and Nusbaum, 2007). In these models, the $I_{MI\text{-}MCN1}$ amplitude was smaller at LG burst offset with CCAP present (Figs. 3, 4). However, the continued presence of $I_{MI\text{-}CCAP}$ throughout the retractor phase apparently compensated for the reduced $I_{MI\text{-}MCN1}$ amplitude, resulting in the retractor phase remaining unaltered by the presence of CCAP (Figs. 3, 4).

Injecting artificial $I_{MI\text{-}CCAP}$ into LG selectively prolongs protractor phase activity

We used the dynamic clamp to inject artificial $I_{MI\text{-}CCAP}$ selectively into the biological LG neuron and thereby test the prediction from our computational model that the CCAP action on LG is pivotal for its influence on the gastric mill rhythm. During the MCN1-gastric mill rhythm, injecting artificial $I_{MI\text{-}CCAP}$ into LG over a range of conductance values (10-30 nS) elicited a CCAP-like selective prolongation of the protractor phase. For example, using a 20 nS conductance value, this current injection consistently increased the duration of the gastric mill cycle period (Control: 9.6 ± 1.0 sec; $I_{MI\text{-}CCAP}$: 12.2 ± 1.4 sec, n=10, p=0.003) (Fig. 5). This slowing of the rhythm resulted from a selective increase in the protractor phase (LG burst) duration (Control: 4.9 ± 0.5 sec; $I_{MI\text{-}CCAP}$: 6.8 ± 0.8 sec; n=10, p=0.001), insofar as there was no change in the retractor phase duration (n=10, p=0.09) (Fig. 5). Artificial $I_{MI\text{-}CCAP}$ injections also selectively prolonged the

protractor phase at lower (10 nS: protraction, p=0.02; retraction, p=0.22, n=5) and higher (30 nS: protraction, p=0.01; retraction, p=0.28, n=5) conductance values. When we injected $I_{MI\text{-}CCAP}$ into LG at 5 nS, there was no consistent change across preparations in either phase of the rhythm (protraction, p=0.07; retraction, p=0.14, n=5). The maximal amplitude of these CCAP-like I_{MI} injections (range: 0.3 – 1.0 nA, mean: 0.64 ± 0.05 nA, n=16) was less than the maximal $I_{MI\text{-}CCAP}$ amplitude determined in voltage clamp experiments in both pyloric neurons and the LG neuron (Golowasch and Marder, 1992a; Swensen and Marder, 2000; this study). They were also comparable to previous dynamic clamp I_{MI} injections used to study neuropeptide actions on the pyloric circuit (Swensen and Marder, 2001) and those injected into LG to drive a MCN1-like gastric mill rhythm (Beenhakker et al., 2005).

The increased LG neuron burst duration resulting from $I_{MI\text{-}CCAP}$ injection presumably resulted from the associated increased depolarizing current, which was largest at the depolarized membrane potential that occurs during the LG burst (Fig. 5*B*). The LG burst nonetheless still terminated, despite the presence of the additional drive from $I_{MI\text{-}CCAP}$. As shown above in the computational model, LG burst termination presumably resulted from the fact that despite $I_{MI\text{-}CCAP}$ prolonging the LG burst, it did not prevent the continued decay of $I_{MI\text{-}MCN1}$ during each LG burst to the point where LG could no longer sustain its activity (Fig. 4) (Coleman et al., 1995; Beenhakker et al., 2005).

To test whether $I_{MI\text{-}CCAP}$ alone was sufficient to elicit a LG burst, we used the dynamic clamp to inject the same simulated CCAP conductance described

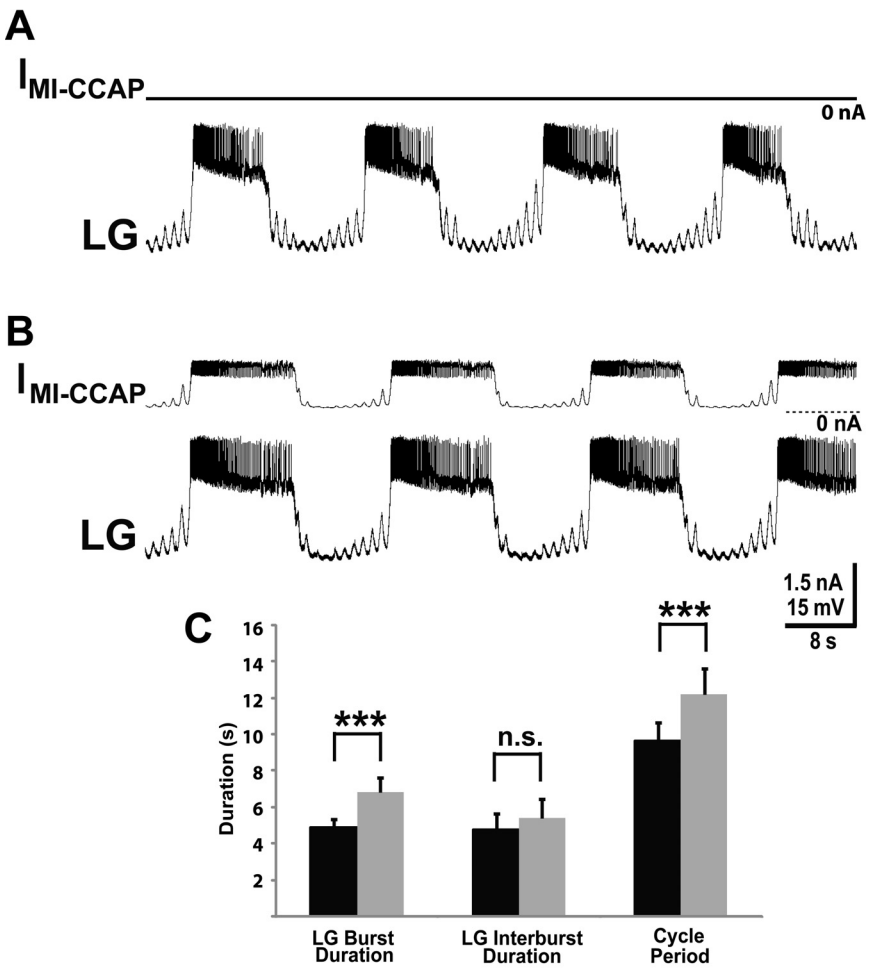

Figure 5. Injection of an artificial $I_{MI\text{-}CCAP}$ into LG mimics the influence of bath-applied CCAP on the biological MCN1-gastric mill rhythm. *A,* A control gastric mill rhythm, represented by an intracellular LG recording, driven by tonic MCN1 stimulation (15 Hz) with no dynamic clamp-mediated $I_{MI\text{-}CCAP}$ injected into LG. Most hyperpolarized V_m: LG, -65 mV. *B,* In the same LG recording as Panel A, injection of an artificial $I_{MI\text{-}CCAP}$ into LG with the dynamic clamp selectively prolonged the gastric mill protraction phase. MCN1 stimulation was the same as in Panel A. Note the relatively constant amplitude of the artificial $I_{MI\text{-}CCAP}$ during each LG burst. Most hyperpolarized V_m: LG, -66 mV. *C,* Dynamic clamp-

mediated injection of artificial $I_{MI\text{-}CCAP}$ into LG consistently prolonged the LG burst without altering the retraction duration, and thereby increased the gastric mill cycle period. Data are from 10 preparations. Symbols: Black bars, MCN1 stimulation only; Gray bars, MCN1 plus artificial $I_{MI\text{-}CCAP}$; ***$p<0.005$; n.s., not significant.

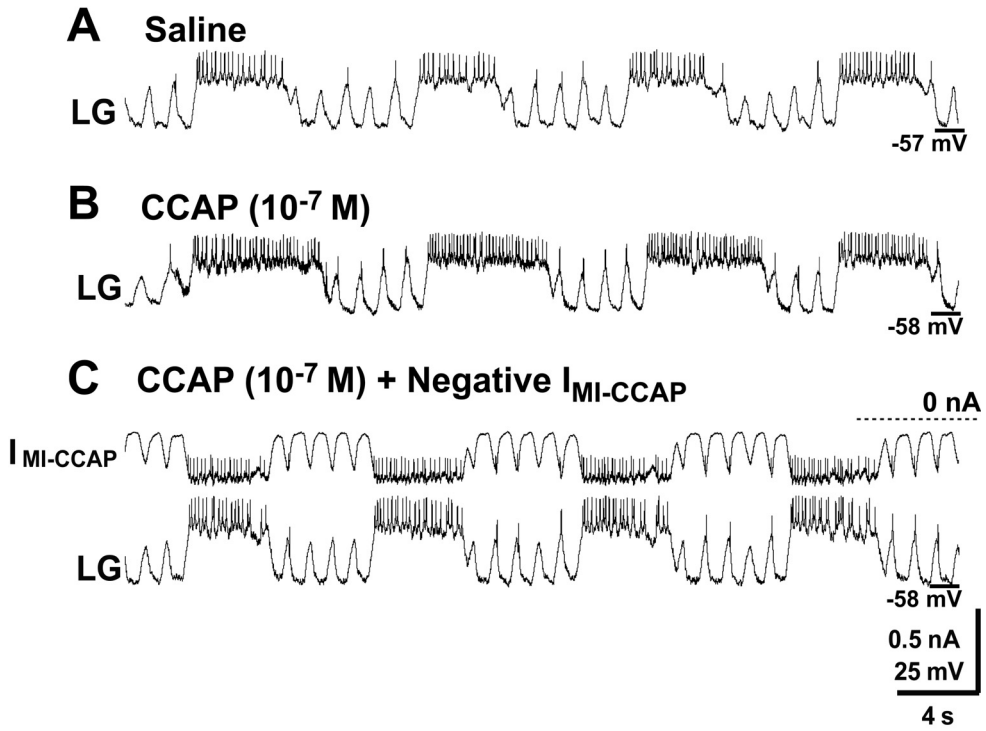

Figure 6. Dynamic clamp-mediated subtraction of $I_{MI\text{-}CCAP}$ in LG during bath application of CCAP eliminates the CCAP prolongation of the gastric mill protractor phase. *A,* The MCN1-gastric mill rhythm without CCAP application. *B,* Bath applied CCAP selectively prolonged the gastric mill protractor phase. *C,* Injection of a negative conductance version of $I_{MI\text{-}CCAP}$ into LG during CCAP application eliminated the prolongation of the protractor phase by CCAP without altering the retractor phase duration. All 3 panels are from the same intracellular LG recording.

above into the LG neuron without MCN1 stimulation. Under this condition, injecting $I_{MI\text{-}CCAP}$ did not activate spiking in LG or change its membrane potential (Control: -61.9 ± 2.3 mV; I_{MI}: -59.0 ± 3.6 mV; n=3, p=0.09). The lack of an evident LG response to $I_{MI\text{-}CCAP}$ injection presumably resulted from the relatively small amplitude of this voltage-dependent current near the resting potential (Golowasch and Marder, 1992a; Swensen and Marder, 2000; see above). Thus, $I_{MI\text{-}CCAP}$ alone was not sufficient to elicit a LG burst.

Injecting artificial $I_{MI\text{-}CCAP}$ into LG (G_{MI} 20 nS) during the gastric mill rhythm also increased the number of action potentials during the LG burst (Control, 33.7 ± 4.5 spikes; I_{MI}: 51.2 ± 8.5 spikes; n=10, p=0.002) as well as its intra-burst firing frequency (Control: 6.6 ± 0.5 Hz; I_{MI}: 9.6 ± 1.7 Hz; n=10, p<0.05) (Fig. 5*A,B*). These changes in LG activity were comparable to those observed during CCAP bath application (Kirby and Nusbaum, 2007).

Subtracting I_{MI} in LG eliminates CCAP prolongation of the protractor phase

We further tested the hypothesis that the CCAP-mediated selective prolongation of the gastric mill protractor phase resulted from CCAP activation of I_{MI} in the LG neuron by selectively subtracting this current in LG during CCAP bath application. Specifically, during bath applied CCAP (10^{-7} M), we reversed the sign of the artificial $I_{MI\text{-}CCAP}$ conductance (i.e., from +20 nS to -20 nS) injected into LG while leaving all other dynamic clamp parameters unchanged.

Injecting the negative conductance version of $I_{MI\text{-}CCAP}$ into LG during CCAP application eliminated the CCAP prolongation of the gastric mill protractor phase

(Control: 3.8 ± 0.6 sec; CCAP: 5.2 ± 0.3 sec; CCAP plus Neg. I_{MI}: 4.3 ± 0.3 sec, n=4; one-way ANOVA, $p<0.05$; Holm-Sidak post-hoc test: CCAP vs. Control, $p<0.05$; All other pairwise comparisons, $p>0.05$) (Fig. 6). These injections had no unexpected effects on the motor pattern. For example, there was no concomitant change in the retractor phase duration (Control: 5.2 ± 1.0 sec; CCAP: 4.7 ± 0.5 sec; CCAP plus Neg. I_{MI}: 6.6 ± 1.3 sec, n=4, $p=0.13$). This result also confirmed the prediction of our computational model that $I_{MI\text{-}CCAP}$ in LG alone is sufficient to mimic the influence of bath-applied CCAP on the gastric mill rhythm. If the influence of $I_{MI\text{-}CCAP}$ was necessary in both LG and Int1, then selectively eliminating $I_{MI\text{-}CCAP}$ in LG alone would not have returned the gastric mill rhythm to the control condition.

$I_{MI\text{-}CCAP}$ in LG maintains a constant retractor phase duration

It was initially surprising to learn that bath-applied CCAP did not alter the retractor phase duration (Kirby and Nusbaum, 2007). Our expectation was that, despite the fact that the $I_{MI\text{-}CCAP}$ amplitude in LG was likely to be relatively small during retraction, it would still summate with the MCN1-activated current. We anticipated that this summation would result in the burst threshold onset for LG occurring sooner, thereby reducing the duration of this phase. Both our model and dynamic clamp injections did show that $I_{MI\text{-}CCAP}$ was indeed activated during retraction, but was smaller in amplitude than the parallel build-up of $I_{MI\text{-}MCN1}$. The model, however, also suggested that the retractor phase duration was unchanged by CCAP because the $I_{MI\text{-}CCAP}$ compensated for the reduced level of

$I_{MI\text{-}MCN1}$ during retraction when CCAP was present (Fig. 4). It thus remained to be determined whether the relatively small amplitude of $I_{MI\text{-}CCAP}$ during retraction was nonetheless sufficient to influence the retractor phase duration.

We first used our computational model to test the hypothesis that the presence of $I_{MI\text{-}CCAP}$ only during protraction was sufficient to mimic the ability of bath-applied CCAP to selectively prolong protraction. To this end, we compared simulations of the MCN1-gastric mill rhythm with $I_{MI\text{-}CCAP}$ in LG being absent or continually present vs. being present only during protraction (Fig. 7). In contrast to the ability of continually present $I_{MI\text{-}CCAP}$ to selectively prolong protraction (Fig. 7*A,B*), simulations where $I_{MI\text{-}CCAP}$ was present only during the protractor phase still prolonged protraction (Control: 11.0 ± 0.4 sec; CCAP during Protraction: 14.5 ± 0.3 sec; n=3 cycles, $p<0.05$) but it also increased the retractor phase duration (Control: 7.0 ± 0.2 sec; CCAP during Protraction: 8.1 ± 0.1 sec; n=3 cycles, $p<0.05$) (Fig. 7*C,D*).

The retractor phase was prolonged when CCAP was absent during retraction because, during the CCAP-prolonged protractor phase, $I_{MI\text{-}MCN1}$ decayed to a lower level relative to rhythms without any CCAP (Control: -15.2 ± 0.5 pA; CCAP during Protraction: -9.7 ± 0.5 pA; n=3 cycles, $p<0.05$) (Fig. 7*A,C*). Thus, when there was no CCAP present during retraction, it took the MCN1-activated current longer to build up to the point needed to initiate the next LG burst (Fig. 7*A*-*C*). When CCAP was present continuously, the additional CCAP conductance during the retractor phase offset this effect (see above). Thus, although continuous application of the CCAP conductance to LG in our model

selectively changed the protractor phase duration, its presence during retraction was also necessary for maintaining the control retractor phase duration (Fig. 7*D*).

We next used dynamic clamp injections of $I_{MI\text{-}CCAP}$ to test the computational model prediction that $I_{MI\text{-}CCAP}$ during retraction was also necessary to enable CCAP to maintain the retraction duration unchanged from the control condition. Specifically, we injected $I_{MI\text{-}CCAP}$ (G_{MI}: 20 nS) either continuously or selectively during the protraction phase of the MCN1-gastric mill rhythm (Fig. 8*A-C*). The protraction-specific injections reproducibly prolonged the protractor phase (Control: 7.4 ± 1.3 sec; Protraction-only $I_{MI\text{-}CCAP}$: 12.7 ± 2.2 sec; n=5, p=0.006) (Fig. 8). As predicted by the model, injecting $I_{MI\text{-}CCAP}$ only during protraction also prolonged the retractor phase (Control: 6.3 ± 1.0 sec; Protraction-only $I_{MI\text{-}CCAP}$: 8.7 ± 1.3 sec; n=5, p=0.007). Hence, the gastric mill cycle period was increased (Control: 13.7 ± 2.0 sec; Protraction-only $I_{MI\text{-}CCAP}$: 21.3 ± 3.2 sec; n=5, p=0.002) (Fig. 8). Concomitant with these manipulations, there was a significant increase in the number of LG action potentials per burst (Control: 58.1 ± 13.1 spikes; Protraction-only $I_{MI\text{-}CCAP}$: 119.5 ± 24.1 spikes; n=5, p=0.003).

Artificial $I_{MI\text{-}CCAP}$ injection into LG reduces the MCN1 firing frequency threshold for gastric mill rhythm initiation

CCAP superfusion also reduces the threshold MCN1 firing frequency necessary to elicit the gastric mill rhythm (Kirby and Nusbaum, 2007). The magnitude of this action ranged from ~25% at higher CCAP concentrations (10^{-7}

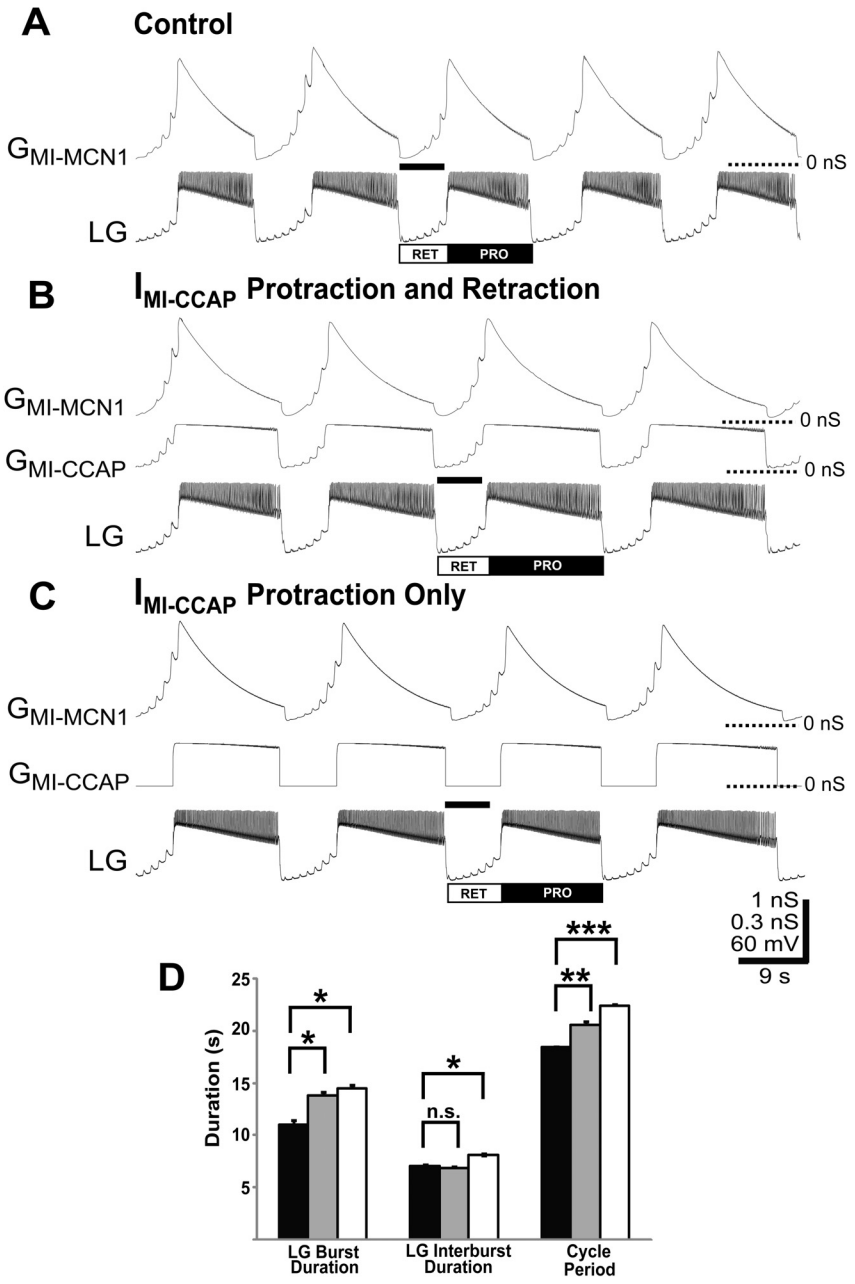

Figure 7. Limiting the influence of $I_{MI\text{-}CCAP}$ in LG to the protractor phase does not mimic the action of bath-applied CCAP on the gastric mill rhythm in a computational model. *A,* Gastric mill rhythm, driven only by MCN1 stimulation. Black bar represents the retractor phase duration. *B,* Gastric mill rhythm resulting from MCN1 stimulation during the continually-present influence of

CCAP. Note the prolongation of the LG burst (protraction) and unchanged duration of the LG interburst (retraction) relative to Panel A. Black bar represents the retractor phase duration in Panel A. *C,* Selectively providing $I_{MI\text{-}CCAP}$ to the gastric mill protractor phase changed the CCAP influence on the MCN1-gastric mill rhythm by prolonging retraction as well as protraction. Note that the retractor phase is prolonged relative to the black bar that represents the retractor phase duration in the control conditions. Most hyperpolarized V_m (*A*-*C*): LG, -73 mV. *D,* Providing $I_{MI\text{-}CCAP}$ during protraction consistently prolongs both gastric mill phases, causing an increased gastric mill cycle period relative to the saline and continually present $I_{MI\text{-}CCAP}$ conditions. Symbols: black bars, saline condition; gray bars, continually present $I_{MI\text{-}CCAP}$; white bars, $I_{MI\text{-}CCAP}$ present during protraction only; *p<0.05, **p<0.01, ***p<0.005; n.s., not significant.

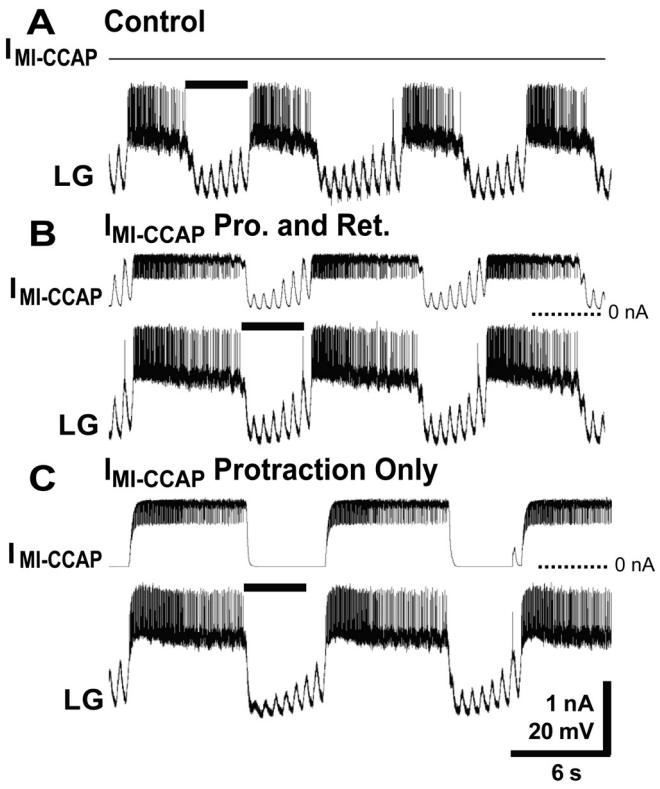

Figure 8. Limiting the influence of artificial $I_{MI-CCAP}$ in LG to the protractor phase does not mimic the action of bath-applied CCAP on the gastric mill rhythm in the biological preparation. *A,* The MCN1-gastric mill rhythm during saline superfusion. Black bar represents the retractor phase duration. *B,* Continual injection of artificial $I_{MI-CCAP}$ into LG via the dynamic clamp selectively prolonged the protractor phase. Black bar represents the retraction duration during saline superfusion. *C,* Protraction-only injection of artificial $I_{MI-CCAP}$ into LG prolonged both phases of the gastric mill rhythm. Note prolonged retractor phase, evident by comparison to the black bar, which indicates the control duration of retraction. All panels are from the same LG recording. Most hyperpolarized V_m: LG, -68 mV.

M – 10^{-8} M) to ~20% at lower CCAP concentrations (10^{-9} M – 10^{-10} M) (Kirby and Nusbaum, 2007). This effect occurred despite the fact that $MCN1_{STG}$ is not CCAP-responsive (Kirby and Nusbaum, 2007). We were therefore interested to learn if the addition of $I_{MI\text{-}CCAP}$ in LG was not only pivotal for altering the gastric mill motor pattern but also tuned the ability of MCN1 to activate this rhythm. Thus, we tested, first in the computational model and then in the biological preparation, whether the reduced MCN1 firing rate threshold resulted from $I_{MI\text{-}CCAP}$ in LG.

We first used our computational model to test whether the presence of $I_{MI\text{-}CCAP}$ in the LG neuron was sufficient to reduce the threshold of MCN1 stimulation needed to elicit the gastric mill rhythm. Adding $I_{MI\text{-}CCAP}$ to LG did reduce the MCN1 stimulation threshold by 25% (Fig. 9). Specifically, when CCAP was absent, the minimum effective MCN1 stimulation rate was 8 Hz for eliciting the gastric mill rhythm, while under the same conditions 6 Hz stimulation produced no gastric mill rhythm. However, when $I_{MI\text{-}CCAP}$ was added to LG, 6 Hz MCN1 stimulation did elicit the gastric mill rhythm (Fig 9).

In the biological preparation, when MCN1 was stimulated in the absence of the dynamic clamp injections and at subthreshold frequency levels for activating the gastric mill rhythm, it still effectively elicited electrical coupling EPSPs (Coleman et al., 1995) and occasional action potentials in LG (Fig. 10*A*). In contrast, stimulating MCN1 either at a faster frequency or at the previously subthreshold frequency with $I_{MI\text{-}CCAP}$ injected into the LG neuron activated the gastric mill rhythm (Fig. 10*B,C*).

Injecting the artificial $I_{MI\text{-}CCAP}$ (G_{MI}: 20 nS) into LG consistently reduced the MCN1 threshold firing frequency for eliciting the gastric mill rhythm. As shown previously (Kirby and Nusbaum, 2007), under control conditions the minimum MCN1 firing frequency at which the gastric mill rhythm was elicited was 6.1 ± 1.1 Hz (n=8). $I_{MI\text{-}CCAP}$ injection into LG reduced this minimum frequency value by ~20% (5.1 ± 1.1 Hz; n=8, $p<0.001$). To control for the possibility of time-dependent changes in the effectiveness of MCN1 stimulation at near-threshold firing levels, we performed a parallel set of experiments in which we determined the threshold MCN1 firing frequency for gastric mill rhythm activation at successive time points that were equivalent to those used in the dynamic clamp experiments. There was no change in the threshold MCN1 firing frequency value in these control experiments (n=9, $p=0.20$).

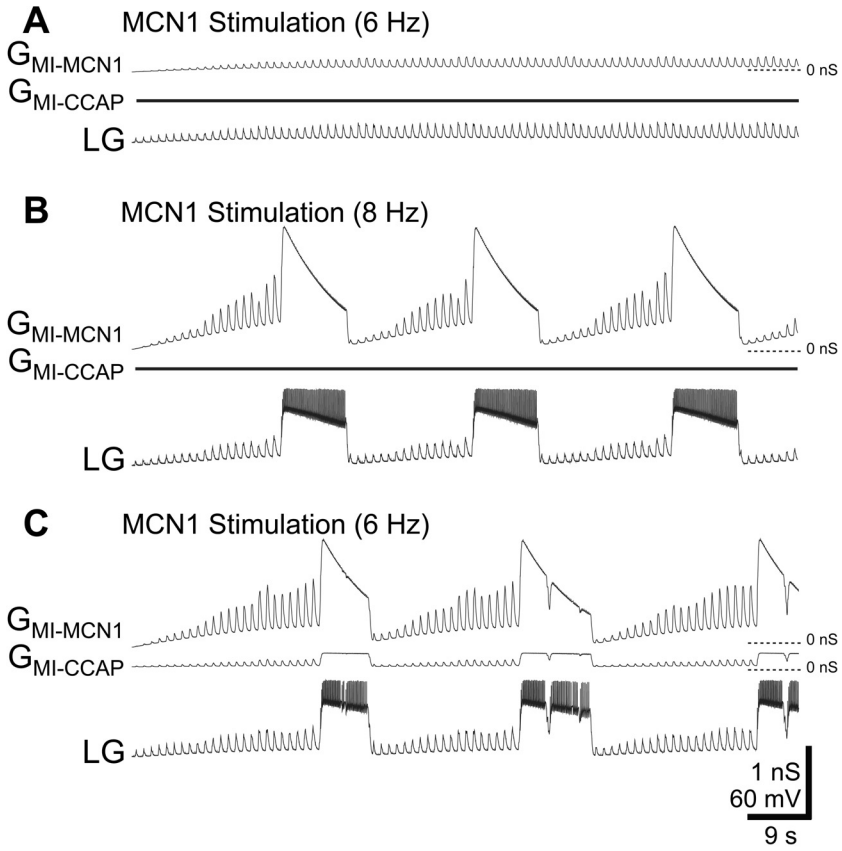

Figure 9. The presence of $I_{MI\text{-}CCAP}$ in LG lowers the threshold MCN1 firing frequency for activating the gastric mill rhythm in a computational model. *A,* Modest MCN1 stimulation in the absence of CCAP did not activate the gastric mill rhythm. Note the small effect of $G_{MI\text{-}MCN1}$ on the LG membrane potential. *B,* A slightly faster MCN1 stimulation frequency, without CCAP present, did elicit the gastric mill rhythm. *C,* The previously sub-threshold MCN1 stimulation frequency did drive the gastric mill rhythm when $I_{MI\text{-}CCAP}$ was present in LG. Most hyperpolarized V_m (*A*-*C*): LG, -73 mV.

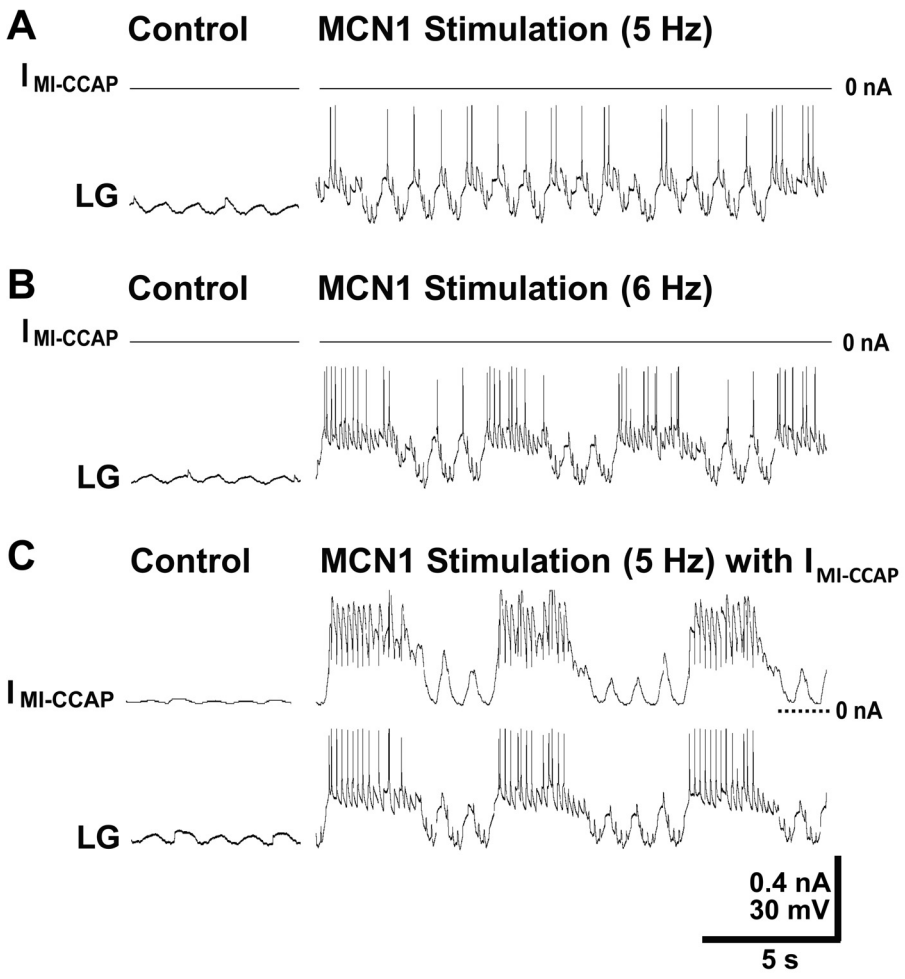

Figure 10. Injection of artificial $I_{MI\text{-}CCAP}$ into LG lowers the threshold MCN1 firing frequency for activating the gastric mill rhythm in the biological preparation. *A,* Modest MCN1 stimulation in the absence of $I_{MI\text{-}CCAP}$ did not activate the gastric mill rhythm, but did elicit unitary EPSPs and action potentials in LG. Most hyperpolarized V_m: LG, -60 mV. *B,* A slightly faster MCN1 stimulation frequency, without $I_{MI\text{-}CCAP}$ injection, did elicit the gastric mill rhythm. Most hyperpolarized V_m: LG, -64 mV. *C,* The previously sub-threshold MCN1 stimulation frequency did drive the gastric mill rhythm when artificial $I_{MI\text{-}CCAP}$ was injected into LG. Most hyperpolarized V_m: LG, -64 mV.

DISCUSSION

We have established that peptide hormone modulation of a neuronally modulated motor circuit results from the convergent hormonal and neuronal activation of the same ionic current, albeit with distinct dynamics, in a single CPG neuron. These results provide a novel mechanism by which co-modulation regulates the activity of both a single neuron and its associated circuit. At the circuit level, the convergent activation of I_{MI} in the LG neuron enabled the peptide hormone CCAP to buoy the decaying influence of $I_{MI\text{-}MCN1}$ during the LG burst and thereby prolong the protractor phase of the MCN1-elicited gastric mill rhythm. It was surprising to discover that the continual presence of $I_{MI\text{-}CCAP}$ was also necessary and sufficient for preventing a change in the retractor phase duration, and that the same mechanism, addition of $I_{MI\text{-}CCAP}$ to the LG neuron, played the distinct role of reducing the threshold firing rate at which MCN1 activates the gastric mill rhythm.

Based on our computational model, the presence of $I_{MI\text{-}CCAP}$ during retraction was necessary due to the reduced $I_{MI\text{-}MCN1}$ amplitude at the start of retraction (i.e., LG burst offset) in the presence of CCAP, relative to the control condition (Fig. 4). Without compensation from CCAP, a reduced amount of $I_{MI\text{-}MCN1}$ at the start of retraction would prolong that phase. This is because more time would be needed to build-up sufficient $I_{MI\text{-}MCN1}$ to enable LG to escape from Int1 inhibition and initiate its burst, as we verified by providing dynamic clamp-injected $I_{MI\text{-}CCAP}$ only during protraction.

It was anticipated from previous studies that $I_{MI\text{-}CCAP}$ would be regulated

only by voltage whereas $I_{MI\text{-}MCN1}$ would also be regulated by rhythmic feedback inhibition (Golowasch and Marder, 1992a; Swensen and Marder 2000, 2001; Beenhakker et al., 2005). However, circuit dynamics are often non-intuitive, and it was our computational modeling results that led us to appreciate the potential role of these distinct dynamics specifically in the LG neuron for regulating the gastric mill rhythm, and for developing the testable predictions that we subsequently verified with our dynamic clamp manipulations.

The necessity and sufficiency of the CCAP action in LG for regulating the gastric mill rhythm was not a foregone conclusion, because CCAP also excites other gastric mill neurons, including Int1 (Kirby and Nusbaum, 2007). CCAP actions appear to be tuned for selectively prolonging the gastric mill protractor phase, insofar as this action occurs across at least four orders of magnitude for bath-applied CCAP (10^{-10} – 10^{-6} M: Kirby and Nusbaum, 2007) and across at least a 3-fold range of dynamic clamp injected CCAP-like G_{MI} (10 – 30 nS: this paper).

Thus far, the motor circuit response to the simultaneous action of different neuromodulators is documented in only a few systems (Dickinson et al., 1997; Katz and Edwards, 1999; Svensson et al., 2001; McLean and Sillar, 2004; Crisp and Mesce, 2006; Koh and Weiss, 2007). However, many and perhaps all neural systems receive multiple modulatory inputs, suggesting that co-modulation is a prevalent mode of network regulation (Proekt et al., 2005; Grillner, 2006; Huguenard and McCormick, 2007; Jing et al., 2007; Marder and Bucher, 2007; Doi and Ramirez, 2008; Jordan et al., 2008).

At the single neuron level, Swensen and Marder (2000) showed that co-applying two peptide modulators with convergent actions on the same ionic current has an additive effect on that current, similar to the convergent MCN1 and CCAP action in the LG neuron. Unlike the latter case, though, both modulators were bath-applied and hence their individual actions on the shared target current were co-regulated solely by the membrane potential of the target neurons (Swensen and Marder, 2000). The convergent postsynaptic action of two inputs onto an intrinsic current via distinct dynamics also suggests a mechanistic explanation for the observation that the same modulatory substance is often present as both a circulating hormone and locally released modulator (Kristan et al., 2005; Marder and Bucher, 2007; Israel et al., 2008). Specifically, in addition to these two modes of delivery likely resulting in overlapping but distinct access to their shared receptors and their acting via different concentrations, these two delivery modes could enable a single modulator to evoke the same type of differential dynamics that we found for the convergent actions of hormonal CCAP and neuronally-released CabTRP Ia.

Non-targets of a neuromodulator can play key roles in the neuronal circuit response to that modulator, while strongly affected targets sometimes play minimal roles (Hooper and Marder, 1987; Ayali and Harris-Warrick, 1999; Thirumalai et al., 2006). Similarly, two CCAP actions appeared to have little impact on the gastric mill rhythm. First, the excitation of the retractor CPG neuron Int1 by CCAP did not alter either Int1 activity during this rhythm or the retractor phase duration in either the biological preparation (Kirby and Nusbaum,

2007) or our computational model (this paper). This result was supported by the ability of our dynamic clamp subtraction of $I_{MI\text{-}CCAP}$ in LG during bath-applied CCAP to return the gastric mill rhythm to the control condition. Presumably the CCAP excitation of Int1 becomes effective under other conditions, such as other versions of the gastric mill rhythm (Beenhakker et al., 2004; Blitz et al., 2004; Saideman et al., 2007; Blitz et al., 2008).

Second, as discussed above, CCAP appeared to have no effect on the retraction phase, but in fact it was necessary to prevent a change in the duration of this phase (Fig. 4). Without our computational model and dynamic clamp manipulations, we would have concluded that CCAP did not influence this phase of the rhythm. The influence of $I_{MI\text{-}CCAP}$ on the retractor phase duration may well have an explicit consequence in the presence of parallel inputs to the gastric mill CPG. For example, the GPR proprioceptor neuron selectively prolongs the gastric mill retractor phase during saline superfusion (Beenhakker et al., 2005). It may be that the presence of CCAP will alter the influence of this sensory feedback system.

It was surprising that adding $I_{MI\text{-}CCAP}$ in LG was also sufficient to mimic the ability of bath-applied CCAP to lower the threshold MCN1 firing frequency for activating the gastric mill rhythm. In general, the ability of neuromodulation to influence a synaptic action could result from a presynaptic and/or postsynaptic site of action (LeBeau et al., 2005; Brill et al., 2007; Marder and Bucher, 2007; McDonald et al., 2008; Doi and Ramirez, 2008). For example, presynaptically, modulation can alter neuronal firing rate, action potential duration and/or the

amount of transmitter released per action potential. Postsynaptically, modulation can alter the response to a synaptic action by changing intrinsic conductances and/or the responsiveness or availability of neurotransmitter receptors. Our results indicate that modulation can also alter neuronal responsiveness, and consequently circuit responsiveness, via a postsynaptic convergent activation of an ionic current. This result also further supports the hypothesis that I_{MI} activation exclusively in LG is pivotal for MCN1 activation of the gastric mill rhythm.

The ability of hormonal CCAP levels to lower the MCN1 firing threshold for gastric mill rhythm activation also has a potential behavioral correlate. First, even in the absence of a recent feeding episode, the steady-state level of CCAP in the hemolymph is likely to be at or above-threshold for the CCAP modulation of the gastric mill rhythm (Phlippen et al., 2000; Kirby and Nusbaum, 2007). Additionally, recent work by Chen et al. (2009) suggests that several identified peptides, including CCAP, are present in the *C. borealis* hemolymph at higher levels in hungry than recently fed crabs. This observation supports the hypothesis that, in hungry crabs, what would normally be too low a MCN1 firing rate would be sufficient to initiate chewing. One source of long-term activation of MCN1 is the ventral cardiac neurons (VCNs), which are mechanosensory neurons embedded in the internal epithelium of the cardiac sac stomach compartment (Beenhakker et al., 2004). The cardiac sac is a food storage compartment just anterior to the gastric mill. This leads to the possibility that, in hungry crabs, modest activation of the VCNs by residual food in the cardiac sac

could trigger sufficient MCN1 activity to initiate an episode of chewing. Thus, co-modulation via convergence onto a single ionic conductance, as we demonstrate here, could serve as a cellular mechanism for altering a behavioral threshold.

In conclusion, the peptide hormone CCAP influences the MCN1-elicited gastric mill rhythm by its convergent activation, with MCN1-released CabTRP Ia, of a voltage-dependent inward current (I_{MI}) in a single CPG neuron (LG neuron). The distinct dynamics of I_{MI} activation and decay by these parallel inputs is pivotal to the resulting motor pattern. Paradoxically, in the presence of CCAP, the amplitude of the MCN1-activated I_{MI} in LG is reduced relative to saline controls (Fig. 4), yet the CCAP contribution enables the same MCN1 activity to elicit prolonged LG bursts. Lastly, although the gastric mill protractor phase is selectively altered by CCAP, in reality CCAP-activated I_{MI} is also necessary for the fact that the retractor duration is not altered. Future experiments will determine whether the presence of this peptide hormone alters the sensitivity of the gastric mill CPG to inputs that influence the apparently unchanged retractor phase.

REFERENCES

Ayali A, Harris-Warrick RM (1999) Monoamine control of the pacemaker kernel and cycle frequency in the lobster pyloric network. J Neurosci 19:6712-6722.

Bartos M, Manor Y, Nadim F, Marder E, Nusbaum MP (1999) Coordination of fast and slow rhythmic neuronal circuits. J Neurosci 19:6650-6660.

Bartos M, Nusbaum MP (1997) Intercircuit control of motor pattern modulation by presynaptic inhibition. J Neurosci 17:2247-2256.

Beenhakker MP, Nusbaum MP (2004) Mechanosensory activation of a motor circuit by coactivation of two projection neurons. J Neurosci 24:6741-6750.

Beenhakker MP, Blitz DM, Nusbaum MP (2004) Long-lasting activation of rhythmic neuronal activity by a novel mechanosensory system in the crustacean stomatogastric nervous system. J Neurophysiol 91:78-91.

Beenhakker MP, DeLong ND, Saideman SR, Nadim F, Nusbaum MP (2005) Proprioceptor regulation of motor circuit activity by presynaptic inhibition of a modulatory projection neuron. J Neurosci 25:8794-8806.

Blitz DM, Christie AE, Coleman MJ, Norris BJ, Marder E, Nusbaum MP (1999) Different proctolin neurons elicit distinct motor patterns from a multifunctional neuronal network. J Neurosci 19:5449-5463.

Blitz DM, Beenhakker MP, Nusbaum MP (2004) Different sensory systems share projection neurons but elicit distinct motor patterns. J Neurosci 24:11381-11390.

Blitz DM, White RS, Saideman SR, Cook A, Christie AE, Nadim F, Nusbaum MP (2008) A newly identified extrinsic input triggers a distinct gastric mill rhythm via activation of modulatory projection neurons. J Exp Biol 211:1000-1011.

Brill J, Kwakye G, Huguenard JR (2007) NPY signaling through Y1 receptors modulates thalamic oscillations. Peptides 28:250-256.

Chen R, Ma M, Hui L, Zhang J, Li L (2009) Measurement of neuropeptides in crustacean hemolymph via MALDI mass spectrometry. J Am Soc Mass Spectrom 20:708-718.

Coleman MJ, Meyrand P, Nusbaum MP (1995) A switch between two modes of synaptic transmission mediated by presynaptic inhibition. Nature 378:502-505.

Coleman MJ, Nusbaum MP, Cournil I and Claiborne BJ (1992) Distribution of modulatory inputs to the stomatogastric ganglion of the crab, *Cancer borealis*. J Comp Neurol 325:581-594.

Coleman MJ, Nusbaum MP (1994) Functional consequences of compartmentalization of synaptic input. J Neurosci 14:6544-6552.

Crisp KM, Mesce KA (2006) Beyond the central pattern generator: amine modulation of decision-making neural pathways descending from the brain of the medicinal leech. J Exp Biol 209:1746-1756.

Dickinson PS, Fairfield WP, Hetling JR, Hauptman J (1997) Neurotransmitter interactions in the stomatogastric system of the spiny lobster: one peptide alters the response of a central pattern generator to a second peptide. J

Neurophysiol 77:599-610.

Doi A, Ramirez JM (2008) Neuromodulation and the orchestration of the respiratory rhythm. Respir Physiol Neurobiol 164:96-104.

Goaillard JM, Marder E (2006) Dynamic clamp analyses of cardiac, endocrine, and neural function. Physiol (Bethesda) 21:197-207.

Golowasch J, Marder E (1992a) Proctolin activates an inward current whose voltage dependence is modified by extracellular Ca^{2+}. J Neurosci 12:810-817.

Golowasch J, Marder E (1992b) Ionic currents of the lateral pyloric neuron of the stomatogastric ganglion of the crab. J Neurophysiol 67:318-331.

Grashow R, Brookings T, Marder E (2009) Reliable neuromodulation from circuits with variable underlying structure. Proc Natl Acad Sci (USA)106:11742-11746.

Grillner S (2006) Biological pattern generation: the cellular and computational logic of networks in motion. Neuron 52:751-766.

Heinzel HG, Weimann JM, Marder E (1993) The behavioral repertoire of the gastric mill in the crab, *Cancer pagurus*: an in situ endoscopic and electrophysiological examination. J Neurosci 13:1793-1803.

Hooper SL, Marder E (1987) Modulation of the lobster pyloric rhythm by the peptide proctolin. J Neurosci 7:2097-2112.

Huguenard JR, McCormick DA (2007) Thalamic synchrony and dynamic regulation of global forebrain oscillations. Trends Neurosci 30:350-356.

Israel JM, Poulain DA, Oliet SH (2008) Oxytocin-induced postinhibitory rebound

firing facilitates bursting activity in oxytocin neurons. J Neurosci 28:385-394.

Jing J, Vilim FS, Horn CC, Alexeeva V, Hatcher NG, Sasaki K, Yashina I, Zhurov Y, Kupfermann I, Sweedler JV, Weiss KR (2007) From hunger to satiety: reconfiguration of a feeding network by *Aplysia* neuropeptide Y. J Neurosci 27:3490-3502.

Jordan LM, Liu J, Hedlund PB, Akay T, Pearson KG (2008) Descending command systems for the initiation of locomotion in mammals. Brain Res Rev 57:183-191.

Katz PS, Edwards DH (1999) Metamodulation: the control and modulation of neuromodulation. In: Beyond neurotransmission: neuromodulation and its importance for information processing (ed. Katz PS). New York: Oxford University Press.

Khorkova O, Golowasch J (2007) Neuromodulators, not activity, control coordinated expression of ionic currents. J Neurosci 27:8709-8718.

Kirby MS, Nusbaum MP (2007) Peptide hormone modulation of a neuronally modulated motor circuit. J Neurophysiol 98:3206-3220.

Koh HY, Weiss KR (2007) Activity-dependent peptidergic modulation of the plateau-generating neuron B64 in the feeding network of *Aplysia*. J Neurophysiol 94:1281-1286.

Kristan WB, Calabrese RL, Friesen WO (2005) Neuronal control of leech behavior. Prog Neurobiol 76:279-327.

LeBeau FE, El Manira A, Griller S (2005) Tuning the network: modulation of

neuronal microcircuits in the spinal cord and hippocampus. Trends Neurosci 28:552-561.

Marder E, Bucher D (2007) Understanding circuit dynamics using the stomatogastric nervous system of lobsters and crabs. Annu Rev Physiol 69:291-316.

Marder E, Eisen JS (1984) Transmitter identification of pyloric neurons: electrically coupled neurons use different transmitters. J Neurophysiol, 51:1345-1361.

McDonald NA, Kuzmiski JB, Naderi N, Schwab Y, Pittman QJ (2008) Endogenous modulators of synaptic transmission: cannabinoid regulation in the supraoptic nucleus. Prog Brain Res 170:129-136.

McLean DL, Sillar KT (2004) Metamodulation of a spinal locomotor network by nitric oxide. J Neurosci 24:9561-9571.

Nadim F, Manor Y, Nusbaum MP, Marder E (1998) Frequency regulation of a slow rhythm by a fast periodic input. J Neurosci 18:5053-5067.

Nusbaum MP, Beenhakker MP (2002) A small-systems approach to motor pattern generation. Nature 417:343-350.

Nusbaum MP, Blitz DM, Swensen AM, Wood D, Marder E (2001) The roles of co-transmission in neural network modulation. Trends Neurosci 24:146-154.

Phlippen MK, Webster SG, Chung JS, Dircksen H (2000) Ecdysis of decapod crustaceans is associated with a dramatic release of crustacean cardioactive peptide into the haemolymph. J Exp Biol 203:521-536.

Proekt A, Vilim FS, Alexeeva V, Brezina V, Friedman A, Jing J, Li L, Zhurov Y, Sweedler JV, Weiss KR (2005) Identification of a new neuropeptide precursor reveals a novel source of extrinsic modulation in the feeding system of *Aplysia*. J Neurosci 25:9637-9648.

Prinz AA, Abbott LF, Marder E (2004) The dynamic clamp comes of age. Trends Neurosci 27:218-224.

Saideman SR, Blitz DM, Nusbaum MP (2007) Convergent motor patterns from divergent circuits. J Neurosci 27:6664-6674.

Sharp AA, O'Neil MB, Abbott LF, Marder E (1993) The dynamic clamp: artificial conductances in biological neurons. Trends Neurosci 16:389-394.

Stein W, DeLong ND, Wood DE, Nusbaum MP (2007) Divergent co-transmitter actions underlie motor pattern activation by a modulatory projection neuron. Eur J Neurosci 26:1148-1165.

Svensson E, Grillner S, Parker D (2001) Gating and braking of short- and long-term modulatory effects by interactions between colocalized neuromodulators. J Neurosci 21:5984-5992.

Swensen AM, Marder E (2000) Multiple peptides converge to activate the same voltage-dependent current in a central pattern-generating circuit. J Neurosci 20:6752-6759.

Swensen AM, Marder E (2001) Modulators with convergent cellular actions elicit distinct circuit outputs. J Neurosci 21:4050-4058.

Thirumalai V, Prinz AA, Johnson CD, Marder E (2006) Red pigment concentrating hormone strongly enhances the strength of feedback to the

pyloric rhythm oscillator but has little effect on pyloric rhythm period. J Neurophysiol 95:1762-1770.

Weimann JM, Meyrand P, Marder E (1991) Neurons that form multiple pattern generators: identification and multiple activity patterns of gastric/pyloric neurons in the crab stomatogastric system. J Neurophysiol 65:111-122.

Wood DE, Stein W, Nusbaum MP (2000) Projection neurons with shared cotransmitters elicit different motor patterns from the same neural circuit. J Neurosci 20:8943-8953.

Chapter 6

Hormonal Modulation of Sensorimotor Integration

Nicholas D. DeLong

Michael P. Nusbaum

ABSTRACT

The parallel influence of hormonal modulation and sensory feedback on motor circuit activity, although likely a common occurrence, is yet to be elucidated in most systems. To this end, we are examining how the hormone crustacean cardioactive peptide (CCAP) modulates the influence of the gastropyloric receptor (GPR) proprioceptor neuron on the gastric mill (chewing) rhythm in the crab stomatogastric ganglion. GPR stimulation selectively prolongs the gastric mill retractor phase, via presynaptic inhibition of modulatory commissural neuron 1 (MCN1), a projection neuron that drives the gastric mill rhythm. Bath-applied CCAP selectively albeit modestly prolongs the gastric mill protractor phase, by activating the same modulator-activated conductance (G_{MI}) in the gastric mill circuit neuron lateral gastric (LG) that is activated by MCN1. Here we show, using computational modeling and dynamic clamp manipulations, that CCAP weakens the GPR regulation of the gastric mill rhythm. This CCAP action results from the ability of CCAP-activated G_{MI} to substitute for the MCN1-activated G_{MI} in LG. Because GPR prolongs retraction duration by weakening MCN1 activation of G_{MI} in LG, the parallel activation of G_{MI} by CCAP reduces the ability of GPR to regulate G_{MI} activation and hence to regulate the gastric mill rhythm. CCAP thereby regulates the GPR-mediated feedback without directly influencing GPR or its synaptic target MCN1. Thus, despite CCAP having only a modest influence on the isolated gastric mill rhythm, its underlying mechanism of action on this rhythm enables it to effectively weaken sensory feedback to that circuit.

INTRODUCTION

Rhythmically active motor circuits generate multiple distinct motor patterns, due to the inputs they receive from descending, ascending and hormonal sources (Marder et al., 2005; Dickinson, 2006; Rossignol et al., 2006; Buschges et al., 2008; Doi and Ramirez, 2008). In most cases, however, these inputs have been studied individually, despite the fact that multiple parallel inputs to a circuit are likely commonly co-active in the intact system (Dickinson, 2006; Marder and Bucher, 2007; Doi and Ramirez, 2008; Pearson, 2008). Co-activating parallel inputs will not necessarily result in a simple summation of their individual actions, due to circuit interactions and because there can be interactions between these inputs (McLean and Sillar, 2004; Beenhakker et al., 2007; Blitz and Nusbaum, 2007; Buschges et al., 2008).

We are studying the hormonal modulation of sensory feedback to a central pattern generator (CPG) circuit, using the isolated stomatogastric nervous system (STNS) of the crab *Cancer borealis* (Nusbaum and Beenhakker, 2002; Marder and Bucher, 2007). The STNS contains several distinct but interacting CPGs whose outputs are regulated by identified projection neurons, sensory neurons and hormones (Marder and Bucher, 2007). The gastric mill (chewing) CPG, located in the stomatogastric ganglion (STG), is driven by the projection neuron modulatory commissural neuron 1 (MCN1) (Nusbaum et al., 2001). This CPG includes the reciprocally inhibitory protractor phase neuron LG (lateral gastric) and retractor phase neuron Int1 (interneuron 1), plus the STG axon terminals of MCN1 ($MCN1_{STG}$) (Coleman et al., 1995; Bartos et al., 1999). MCN1

drives this rhythm via slow, peptidergic excitation of LG and fast, GABAergic excitation of Int1 (Wood et al., 2000; Stein et al., 2007). Both actions occur during retraction, due to LG inhibition of $MCN1_{STG}$ during protraction (Coleman et al., 1995). MCN1 excites LG via a modulator-activated inward current (I_{MI}) (DeLong et al., 2009b).

The MCN1-gastric mill rhythm is altered by the peptide hormone crustacean cardioactive peptide (CCAP) and the gastropyloric receptor (GPR) neuron (Beenhakker et al., 2005; Kirby and Nusbaum, 2007; DeLong et al., 2009a,b). GPR selectively prolongs the retractor phase, by presynaptically inhibiting $MCN1_{STG}$ and thereby reducing activation of the MCN1-elicited I_{MI} ($I_{MI\text{-}MCN1}$) in LG (Beenhakker et al., 2005; DeLong et al., 2009a). Bath-applied CCAP selectively prolongs the protractor phase, by providing a parallel activation of I_{MI} ($I_{MI\text{-}CCAP}$) in LG (DeLong et al., 2009b).

Here, we investigate how CCAP modulates GPR regulation of this gastric mill rhythm. Our computational model predicted that adding $I_{MI\text{-}CCAP}$ to LG is sufficient to weaken GPR regulation of this rhythm, by reducing GPR control I_{MI} in LG. Support for this prediction came from finding that bath-applied CCAP to the biological STG weakened GPR regulation of the gastric mill rhythm. Furthermore, as directly predicted by our model, dynamic clamp injected $I_{MI\text{-}CCAP}$ into LG mimicked this CCAP action, indicating that LG is the site for CCAP gating of the GPR action. These results provide a novel mechanism for modulation of sensorimotor integration, which does not involve a direct modulation of either the sensory neuron or its synaptic target.

METHODS

Animals. Male Jonah crabs (*Cancer borealis*) were obtained from commercial suppliers (Yankee Lobster Co., Boston, MA; Marine Biological Laboratory, Woods Hole, MA). Crabs were housed in commercial tanks containing recirculating, aerated, artificial seawater (10-12° C). Before dissection, the crabs were cold-anesthetized by packing them in ice for at least 30 minutes. The foregut was then removed and maintained in chilled physiological saline while the STNS was dissected from it and pinned down in a saline-filled silicone elastomer-lined Petri dish (Sylgard 184, KR Anderson, Santa Clara, CA).

Solutions. The isolated STNS was maintained in *C. borealis* saline containing (in mM): 439 NaCl, 26 $MgCl_2$, 13 $CaCl_2$, 11 KCl, 10 Trizma base and 5 maleic acid (pH 7.4-7.6). During experimentation, the preparation was continuously superfused (7-12 ml/min, 10-12° C) with *C. borealis* saline via a switching manifold, to enable fast solution changes. CCAP was diluted from stock solutions into saline immediately prior to use.

Electrophysiology. All experiments were conducted using the isolated STNS, from which the CoGs were removed by transecting the superior- (*sons*) and inferior oesophageal nerves (*ions*) (Fig. 1). Intracellular and extracellular recordings of gastric mill neurons were made using routine methods for the STNS (Beenhakker and Nusbaum, 2004). Sharp glass microelectrodes (15-30 MΩ), filled with 0.6 M K_2SO_4 plus 10 mM KCl, were used for intracellular

recordings. Intracellular recordings were made with Axoclamp 2 amplifiers (Molecular Devices, Sunnyvale, CA), and intracellular current clamp injections were performed in single electrode discontinuous current clamp (DCC) mode with sample rates of 2-5 kHz. To facilitate intracellular recordings, the STG was desheathed and visualized with light transmitted through a dark-field condenser (Nikon, Tokyo, Japan).

Each extracellular nerve recording was made using a pair of stainless steel wire electrodes (reference and recording), the ends of which were pressed into the Sylgard-coated dish. A differential AC amplifier (Model 1700: AM Systems, Carlsborg, WA) amplified the voltage difference between the reference wire, placed in the bath, and the recording wire, placed near an individual nerve and isolated from the bath by petroleum jelly (Vaseline, Lab Safety Supply Inc., Janesville, WI). This signal was then further amplified and filtered (Model 410 Amplifier: Brownlee Precision, Santa Clara, CA). Extracellular nerve stimulation was accomplished by placing the pair of wires used to record nerve activity into a stimulus isolation unit (SIU 5: Astromed/Grass Instruments, West Warwick, RI) that was connected to a stimulator (Model S88: Astromed/Grass Instruments).

To elicit the gastric mill rhythm in the isolated STG, MCN1 was selectively activated by tonic extracellular stimulation of one or both of the transected *ions* (10-15 Hz), on the STG side of the transection (Fig. 1) (Coleman et al., 1995; Bartos and Nusbaum, 1997). Individual STNS neurons were identified by their axonal pathways, activity patterns and interactions with other neurons (Weimann et al., 1991; Blitz et al., 1999; Beenhakker and Nusbaum, 2004).

Dynamic Clamp. We used the dynamic clamp to inject an artificial version of an ionic current (I_{MI}) into the LG neuron (Sharp et al., 1993; Bartos et al., 1999; Prinz et al., 2004; Beenhakker et al., 2005; DeLong et al., 2009b). The dynamic clamp software uses the intracellularly recorded membrane potential of a biological neuron to calculate an artificial current (I_{dyn}) using a conductance [$g_{dyn}(t)$] that is numerically computed, as well as a predetermined reversal potential (E_{rev}). The artificial current is computed in real time, updated in each time step (0.2 ms) according to the new values of recorded membrane potential, and injected back into the biological neuron.

For these experiments, we used a version of the dynamic clamp developed in the Nadim laboratory (Rutgers University, Newark, NJ; available at http://stg.rutgers.edu/software/) to run on a personal computer (PC) running Windows XP and a NI PCI-6070-E data acquisition board (National Instruments, Austin, TX). As above, all dynamic clamp current injections were performed while recording in single-electrode, DCC mode (sample rates 2-5 kHz).

Data Analysis. Data analysis was facilitated by a custom-written program (The Crab Analyzer) for Spike2 (Cambridge Electronic Design, Cambridge, England) that determines the activity levels and burst relationships of individual neurons (freely available at http://www.uni-ulm.de/~wstein/spike2/index.html). Unless otherwise stated, each datum in a data set was derived by determining the average of 7-10 consecutive gastric mill-timed LG bursts, except during GPR stimulations when the average was taken for the duration of the GPR stimulation

(1-5 cycles). In all experiments, the burst duration was defined as the duration (seconds, s) between the onset of the first and last action potential in an impulse burst. The firing rate was determined by the number of action potentials minus one divided by the burst duration. The cycle period of the gastric mill rhythm was determined by calculating the duration from the onset of two successive LG neuron bursts.

Data were collected onto a chart recorder (Models MT 95000 and Everest: Astromed Corp., West Warwick, RI) and simultaneously onto a PC computer using data acquisition/analysis tools (Spike2; digitized at ~5kHz). Figures were made from Spike2 files incorporated into Adobe Illustrator (Adobe, San Jose, CA). Statistical analyses were performed with Microsoft Excel (Microsoft, Redmond, WA) and SigmaStat 3.0 (SPSS Inc., Chicago, IL). All comparisons were made using the paired Student's *t*-test. Data are expressed as the mean ± standard error (SE).

Gastric Mill Model. We constructed a computational model modified from an existing conductance-based model of the gastric mill circuit (Nadim et al., 1998; Beenhakker et al., 2005; DeLong et al., 2009b). The previously published version modeled the LG, Int1, and MCN1 neurons as having multiple compartments separated by an axial resistance, with each compartment possessing intrinsic and/or synaptic conductances. We combined our previously published models including GPR (Beenhakker et al., 2005) and CCAP (DeLong et al., 2009b), but we did not add or modify any synaptic or intrinsic

conductances beyond those already published.

Simulations were performed on a PC with Windows XP. We used the Network simulation software developed in the Nadim laboratory (http://stg.rutgers.edu/software/network.htm), which was run using the freely available CYGWIN Linux emulation software package. We used a fourth-order Runge–Kutta numerical integration method with time steps of 0.05 and 0.01 ms. Results were visualized by plotting outputted data points using the freely available Gnuplot software package (www.gnuplot.info).

RESULTS

CCAP gates the GPR regulation of the gastric mill rhythm in a computational model

When manipulated separately, both CCAP and GPR influence the MCN1-elicited gastric mill rhythm. CCAP gains access to the STG as a circulating hormone (Christie et al., 1995; Li et al., 2003; Chen et al., 2009). It selectively prolongs the gastric mill protractor phase (Fig. 1*B*) (Kirby and Nusbaum, 2007), by activating I_{MI} in LG (DeLong et al., 2009b). MCN1 also excites LG by activating I_{MI} (DeLong et al., 2009b). $I_{MI\text{-}CCAP}$ sums with $I_{MI\text{-}MCN1}$ in LG, but only $I_{MI\text{-}MCN1}$ is synaptically regulated by LG. Hence, during protraction, $I_{MI\text{-}CCAP}$ maintains a relatively constant amplitude while $I_{MI\text{-}MCN1}$ decays due to the inhibitory synapse from LG to $MCN1_{STG}$. The maintained $I_{MI\text{-}CCAP}$ amplitude sums with the decaying $I_{MI\text{-}MCN1}$ to keep LG suprathreshold for a longer duration, prolonging its burst (Fig. 1*B*). By summing with $I_{MI\text{-}MCN1}$, $I_{MI\text{-}CCAP}$ also acts to prevent a change in the gastric mill retractor phase duration (DeLong et al., 2009b).

GPR selectively prolongs the gastric mill retractor phase by its presynaptic inhibition of $MCN1_{STG}$ (Fig. 1*C,D*) (Beenhakker et al., 2005; DeLong et al., 2009a). Mechanistically, this GPR action reduces the rate of CabTRP Ia (*Cancer borealis* tachykinin-related peptide Ia) release from MCN1 and hence its activation of $I_{MI\text{-}MCN1}$ in LG (Beenhakker et al., 2005). This action slows the ability of LG to escape from Int1 inhibition and reach burst threshold (Fig. 1*D*).

Insofar as GPR regulates the gastric mill rhythm by influencing the ability

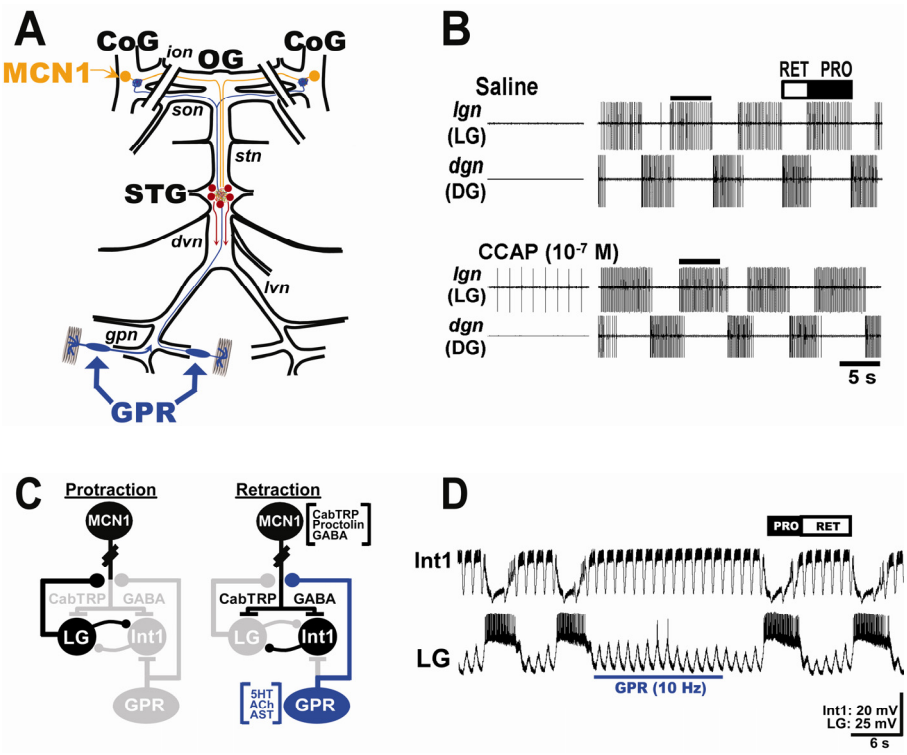

Figure 1: Schematic of the isolated STNS and the MCN1-gastric mill rhythm, as well as its regulation by CCAP and GPR. *A*, In each CoG, there is a single copy of the projection neuron MCN1. MCN1 projects to the STG via the *ion* and *stn* nerves. Each GPR arborizes in the STG and each CoG. The paired diagonal bars through the *sons* and *ions* represent the transection of these nerves at the start of each experiment. Grey rectangles represent protractor muscles in which GPR dendrites arborize. Abbreviations: Ganglia- CoG, commissural ganglion; OG, oesophageal ganglion; STG, stomatogastric ganglion. Neurons- MCN1, modulatory commissural neuron 1; GPR, gastropyloric receptor. Nerves- *dvn*, dorsal ventricular nerve; *gpn*, gastropyloric n.; *ion*, inferior oesophageal n.; *lvn*, lateral ventricular n.; *son*, superior oesophageal n.; *stn*, stomatogastric n. *B*, As shown by Kirby and Nusbaum (2007), bath-applied CCAP selectively prolongs

the protractor phase of the MCN1-elicited gastric mill rhythm. Note that CCAP did not activate the gastric mill rhythm prior to MCN1 stimulation. Retraction (RET) phase is represented by the dorsal gastric (DG) retractor motor neuron. Protraction (PRO) phase is represented by the lateral gastric (LG) protractor CPG/motor neuron. Bar on top of second LG burst in each panel represents the LG burst duration in saline, to show that the LG burst is prolonged by CCAP. *C*, Core gastric mill CPG schematic during each phase (protraction, retraction) of the gastric mill rhythm. Paired diagonal bars through MCN1 axon represent additional distance between CoG and STG. All synapses shown are located in the STG neuropil. Gray somata and synapses represent silent neurons/synapses. Synapses drawn on somata or axons actually occur on small branches in the STG neuropil. Transmitters in brackets next to MCN1 and GPR somata are their identified cotransmitters. Note that MCN1 uses only CabTRP Ia to excite LG and only GABA to excite Int1. Symbols: Filled circles, synaptic inhibition; T-bars, synaptic excitation. *D*, GPR stimulation during retraction, to mimic its *in vivo* activity, selectively prolongs the gastric mill retractor phase. Note that the duration of the retractor (LG silent, Int1 active) phase during GPR stimulation is longer than the same phase in the cycles immediately before and after GPR stimulation.

of MCN1 to activate I_{MI} in LG, and CCAP directly activates I_{MI} in LG, we investigated whether the presence of CCAP influenced the ability of GPR to regulate the gastric mill rhythm. To this end, we combined two previously published versions of our computational model of the MCN1-gastric mill circuit. Specifically, we modified our existing model of the gastric mill CPG plus GPR (Beenhakker et al., 2005; DeLong et al., 2009a) by adding $G_{MI\text{-}CCAP}$ to LG, using previously published parameters (DeLong et al., 2009b). As shown previously, in the version of the model in which $I_{MI\text{-}CCAP}$ was absent from LG, GPR stimulation prolonged the retractor phase (Pre-GPR: 7.5 s; During GPR: 34.4 s) without altering the protractor phase (Pre-GPR: 7.7 s; During GPR: 7.4 s) (Fig. 2*A*) (Beenhakker et al., 2005).

Adding $G_{MI\text{-}CCAP}$ to LG in our model, in the absence of GPR activation, modestly prolonged the protractor phase (Control: 7.7 s; CCAP: 10.7 s) without altering the retractor phase duration (Control: 7.5 s; CCAP: 7.1 s) (Fig. 2*B*) (Kirby and Nusbaum, 2007). When GPR was stimulated while $I_{MI\text{-}CCAP}$ was present in LG, the GPR prolongation of retraction was reduced from >400% to ~40% of the control value (Pre-GPR: 7.1 s; During GPR: 10.0 s), while the protractor phase duration remained unchanged (Pre-GPR: 10.7 s; During GPR: 10.6 s) **(**Fig. 2*B***)**.

The apparent reason for the weakened GPR effect in the model that included $G_{MI\text{-}CCAP}$ in LG was that the addition of this conductance provided an alternative source of G_{MI} that was not subject to GPR regulation (Fig. 3*A,B*). As stated above, GPR regulates $G_{MI\text{-}MCN1}$ in LG by inhibiting $MCN1_{STG}$ (Beenhakker et al., 2005; DeLong et al., 2009a). In illustration of this point, in control cycles

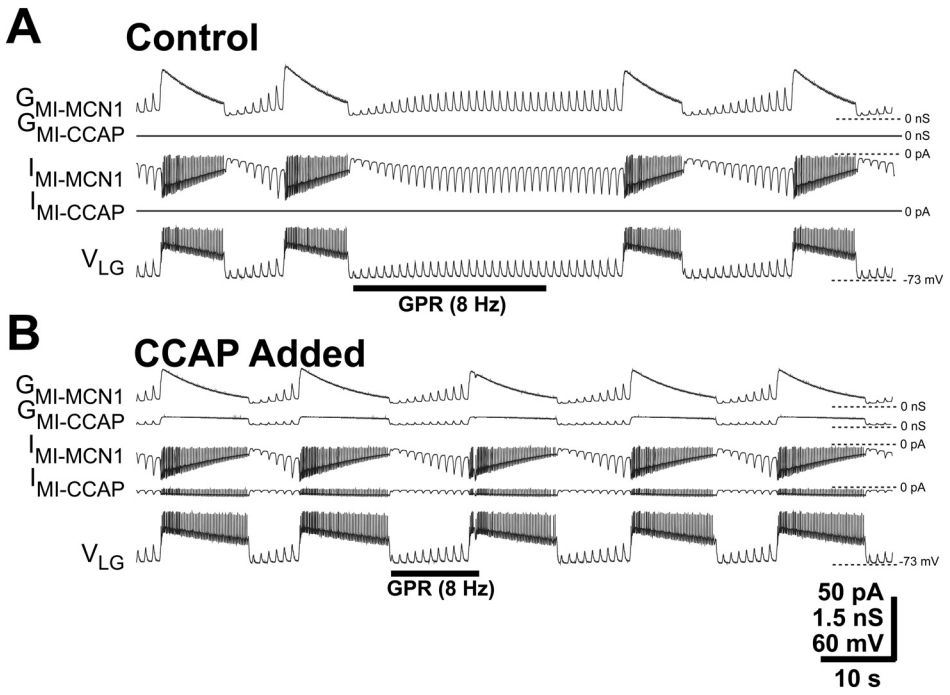

Figure 2: GPR regulation of the gastric mill retractor phase is weakened by the presence of CCAP in a computational model. *A*, GPR regulation of the MCN1-elicited gastric mill rhythm in the absence of CCAP (Control). Under control conditions, the MCN1-elicited current ($I_{MI\text{-}MCN1}$) and conductance ($G_{MI\text{-}MCN1}$) grow in amplitude during each retractor (LG silent) phase, and decay during each protractor (LG active) phase due to the LG presynaptic inhibition of $MCN1_{STG}$ (see Fig. 1*C*). As in the biological preparation, GPR stimulation during the retractor phase selectively prolonged the retractor phase duration (Beenhakker et al., 2005). *B*, Adding the CCAP-activated conductance ($G_{MI\text{-}CCAP}$) to LG reduces the ability of GPR to prolong retraction. As in panel *A*, GPR stimulation was limited to the duration of a single retractor phase, and ceased when the protractor phase (LG burst) was initiated. Due to the presence of $G_{MI\text{-}CCAP}$, this stimulation was less effective in prolonging the retractor phase relative to the

control condition. Note also that, as reported previously (Kirby and Nusbaum, 2007; DeLong et al., 2009b), the presence of $I_{MI\text{-}CCAP}$ in LG selectively prolonged the protractor phase (LG burst).

(i.e., no GPR stimulation) at the point immediately preceding LG burst onset, the peak I_{MI} amplitude was similar when CCAP was either absent or present (CCAP absent: -21.2 pA; CCAP present -20.2 pA). Thus, $I_{MI\text{-}MCN1}$ and $I_{MI\text{-}CCAP}$ summed to the same level as $I_{MI\text{-}MCN1}$ in the absence of CCAP (DeLong et al., 2009b).

During GPR stimulation in the presence of CCAP, LG burst onset was only slightly delayed relative to the preceding and subsequent cycles (10 seconds in duration) (Fig. 2*B*), and again the peak I_{MI} amplitude immediately before LG burst onset (-19.5 pA) was similar to control cycles. As above, this peak I_{MI} was the summed result of its activation by both MCN1 and CCAP ($I_{MI\text{-}MCN1}$: -16.5 pA; $I_{MI\text{-}CCAP}$: -3.0 pA). In contrast, when the peak I_{MI} was measured during GPR stimulation in the absence of CCAP at the the same time point (10 seconds into retraction), it was -17.2 pA (Fig. 3*C*). This was only slightly larger than the $I_{MI\text{-}MCN1}$ component in the presence of CCAP, and smaller than the peak I_{MI} needed for LG to reach burst threshold. Under these conditions, LG burst onset did not occur for another ~25 seconds. Thus, the presence of the additional, GPR-independent $I_{MI\text{-}CCAP}$ reduced the time needed for I_{MI} to bring LG to burst threshold, and thereby reduced the effectiveness of GPR relative to when CCAP was absent. This result predicted, therefore, that CCAP would reduce the ability of GPR to prolong the gastric mill retractor phase.

CCAP modulates the GPR influence on the biological gastric mill rhythm

To begin testing the prediction of the above modeling study, we assayed whether CCAP superfusion in the biological preparation comparably modulated

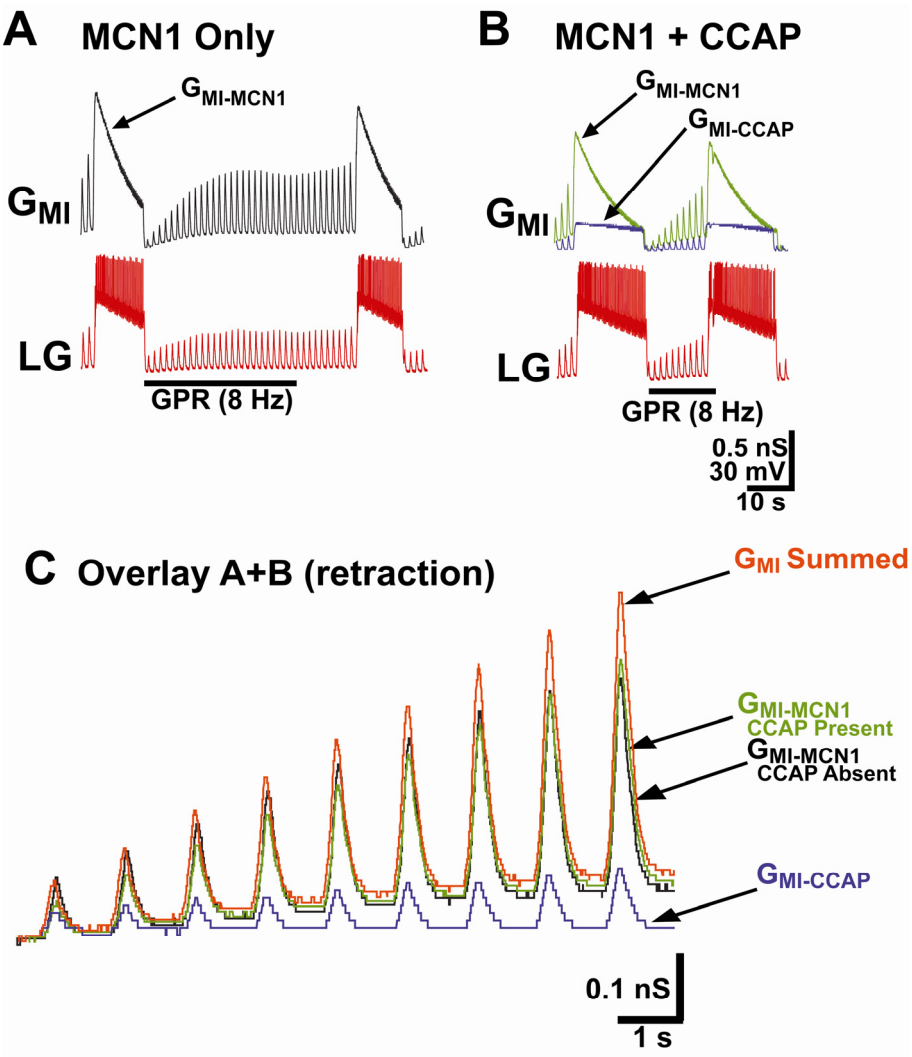

Figure 3: The altered dynamics of G_{MI} when CCAP is present reduces the GPR effectiveness in prolonging the gastric mill retractor phase in a computational model. *A*, During the control gastric mill rhythm, G_{MI} was entirely due to LG input from MCN1 ($G_{MI-MCN1}$). Under these conditions, GPR stimulation prolonged the retractor phase (see Fig. 2*A*) by reducing the rate of build-up of $G_{MI-MCN1}$ due to the GPR presynaptic inhibition of MCN1 (Beenhakker et al., 2005; DeLong et al., 2009a). *B*, When CCAP is present, G_{MI} consists of the summed components contributed by MCN1 ($G_{MI-MCN1}$) and CCAP ($G_{MI-CCAP}$). Under these conditions,

GPR stimulation is less effective in prolonging retraction. *C*, Overlay of the G_{MI} traces from panels *A* and *B*, for durations that were equivalent to the retractor phase duration during GPR stimulation in panel *B*. The traces were all taken from the first ~10 seconds of the retractor phase during which GPR was stimulated in both panels. With CCAP both present and absent, the amplitude of $G_{MI\text{-}MCN1}$ grew steadily during retraction (green and black traces). However, the presence of CCAP produced a summed peak G_{MI} (orange trace) that grew at a faster rate, because it was partially composed of the GPR independent $G_{MI\text{-}CCAP}$, and hence reached LG burst threshold sooner.

the GPR actions on the MCN1-gastric mill rhythm. Specifically, we compared the gastric mill rhythm response to GPR stimulation in control (saline) conditions and in the presence of superfused CCAP.

CCAP superfusion (10^{-7} M) consistently eliminated the GPR prolongation of the gastric mill retractor phase (Fig. 4*A,B*). In normal saline, GPR stimulation (5 Hz) during each retractor phase prolonged retraction (Pre-GPR: 5.3 ± 0.7 s; During GPR: 19.0 ± 5.0 s; n=5, $p<0.05$) without altering the protractor phase duration (Pre-GPR: 4.8 ± 1.8 s; During GPR: 5.8 ± 1.5 s; n=5, p=0.30) (Fig. 4*A,B*). In contrast, during CCAP superfusion, the same GPR stimulation protocol did not alter retraction duration (Pre-GPR: 6.2 ± 1.8 s; During GPR: 9.4 ± 2.5 s; n=5, p=0.17) or protraction duration (Pre-GPR: 6.9 ± 0.9 s; During GPR: 6.8 ± 1.2 s; n=5, p=0.50) (Fig. 4*A,B*). These results were consistent with our model prediction that CCAP gates out the GPR effect on the MCN1-elicited gastric mill rhythm.

To further assess the effectiveness of this CCAP action, we determined whether a stronger GPR stimulation would rescue its influence on the rhythm. Under control conditions, a stronger (10-15 Hz) and more prolonged (30 s) GPR stimulation consistently maintained the retractor phase until after the stimulation was terminated (n=3/3). In contrast, in the presence of CCAP (10^{-7} M), LG consistently escaped during the ongoing GPR stimulation and fired a burst before 30 seconds of GPR stimulation was completed (n=3/3) (Fig. 4*A,B*). However, despite the LG ability to initiate its next burst during GPR stimulation in the latter condition, this higher frequency GPR stimulation did prolong the retractor phase

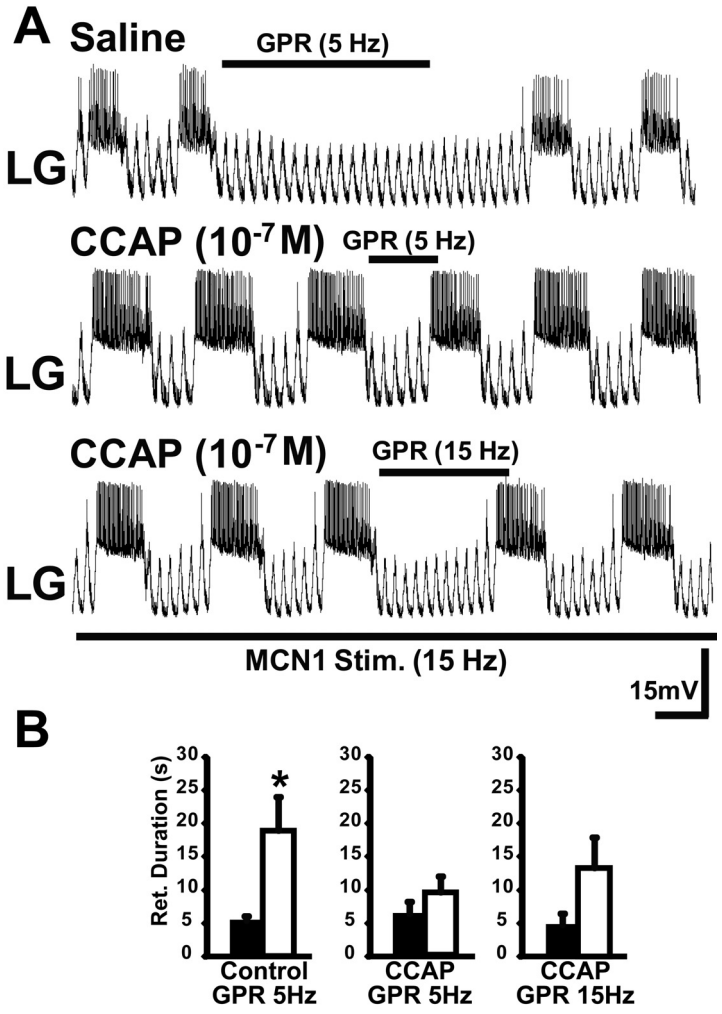

Figure 4: CCAP superfusion reduces the effectiveness of GPR on the MCN1-elicited gastric mill rhythm in the biological preparation. *A*, **(Top)** GPR stimulation selectively prolonged retraction under control conditions. Note the increased retractor phase (LG silent) duration during the cycle in which GPR was stimulated relative to the preceding and subsequent cycles. **(Middle)** In the presence of CCAP, the same level of GPR stimulation barely prolonged retraction. **(Bottom)** In the presence of CCAP, a stronger GPR stimulation (15 Hz) still failed to prolong retraction to the same extent as the weaker GPR

stimulation in the absence of CCAP. *B*, The GPR regulation of retractor phase duration is removed in the presence of CCAP. Black bars represent control gastric mill rhythms, white bars represent GPR stimulation. Number of experiments: Control- 5; CCAP (GPR 5 Hz)- 5; CCAP (GPR 15 Hz)- 3. Symbol: *$p<0.05$.

in 2 of 3 preparations, albeit not to the same extent as slower GPR stimulation in control conditions (Fig. 4*A,B*).

The above experiments were done by stimulating GPR during each retractor phase to mimic the likely GPR *in vivo* activity pattern (Katz et al., 1989). However, because CCAP reduced the ability of GPR to prolong retraction, the total time during which GPR was stimulated was less in CCAP than in control conditions. To eliminate this potential confound, we also tested the ability of a 30 second tonic GPR stimulation (5 Hz) to regulate the gastric mill rhythm under both conditions. This approach did not introduce a confound by extending GPR stimulation through the protractor phase, because stimulating GPR during protraction does not alter the gastric mill rhythm (DeLong et al., 2009a). Using this stimulation protocol in normal saline, GPR again prolonged the retractor phase (Pre-GPR: 5.8 ± 1.3 s; During GPR: 15.7 ± 1.8 s; n=2, $p<0.05$) without altering the protractor phase duration (Pre-GPR: 3.9 ± 1.9 s; During GPR: 3.3 ± 1.2 s; n=2, p=0.30). Using the same stimulation in the presence of CCAP (10^{-7} M), neither the retractor phase (Pre-GPR: 8.4 ± 4.9 s; During GPR: 11.2 ± 7.4 s; n=2, p=0.23) nor the protractor phase (Pre-GPR: 6.5 ± 1.6 s; During GPR: 6.3 ± 2.5 s; n=2, p = 0.44) were altered by GPR stimulation. These results confirmed our model prediction that CCAP gates out the GPR regulation of the gastric mill rhythm.

CCAP gates out the GPR regulation of the gastric mill rhythm by activating $G_{MI\text{-}CCAP}$ in LG

CCAP has actions on several neurons in the STG in addition to LG, including the gastric mill CPG neuron Int1 (Kirby and Nusbaum, 2007). Therefore, although our model predicted that the induction of $G_{MI\text{-}CCAP}$ in LG was responsible for the gating of the GPR effect on the gastric mill rhythm, it remained possible that one or more other CCAP actions contributed to this effect. Consequently, we tested the hypothesis that the CCAP-activated G_{MI} in LG was responsible for gating the GPR effect. To this end, we tested the ability of a simulated version of $G_{MI\text{-}CCAP}$, injected into LG using the dynamic clamp, to mimic the actions of superfused CCAP. For these experiments, we used the same dynamic clamp conductance used in our previously published work, which was based on voltage clamp recordings of $I_{MI\text{-}CCAP}$ in LG (DeLong et al., 2009b).

We compared the effect of GPR stimulation (5 Hz) under control conditions to the same stimulation during dynamic clamp injection of $I_{MI\text{-}CCAP}$ in LG. As described above, under control conditions, GPR stimulation prolonged retraction (Pre-GPR: 6.3 ± 1.0 s; During GPR: 18.6 ± 4.7 s; n=5, $p<0.05$) without altering protraction (Pre-GPR: 5.8 ± 1.3 s; During GPR: 6.7 ± 1.2 s; n=5, p=0.30) (Fig. 5*A*). When the same stimulation was performed with dynamic clamp $I_{MI\text{-}CCAP}$ (20 nS) injected into LG, there was no change in the duration of either retraction (Pre-GPR: 7.9 ± 1.5 s; During GPR: 11.0 ± 2.6 s; n=5, p=0.17) or protraction (Pre-GPR: 8.6 ± 2.2 s; During GPR: 9.0 ± 2.0 s; n=5, p=0.45) (Fig. 5*B*).

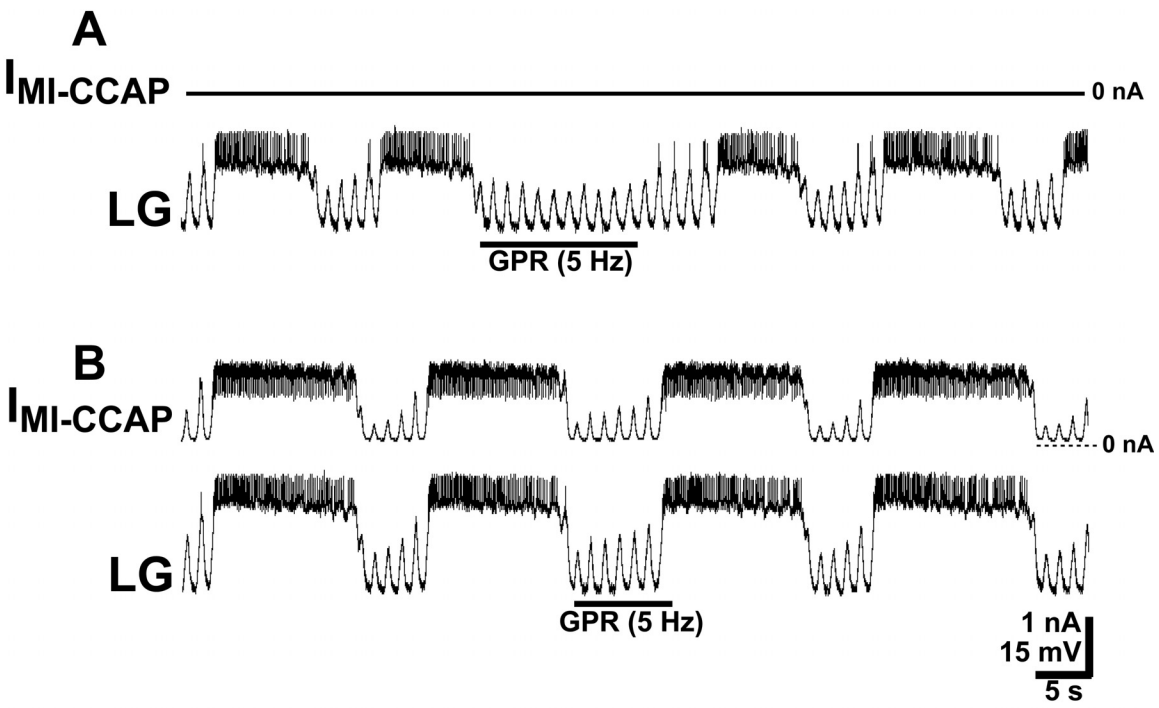

Figure 5: Dynamic clamp injection of the CCAP-activated current ($I_{MI\text{-}CCAP}$) into LG is sufficient to mimic the effect of CCAP superfusion on the MCN1-elicited gastric mill rhythm. *A*, In the absence of the dynamic clamp injection, GPR stimulation during the gastric mill retractor phase selectively prolonged that phase. Note that the amplitude of the injected current ($I_{MI\text{-}CCAP}$) was zero throughout the recording. *B*, Dynamic clamp injection of $I_{MI\text{-}CCAP}$ into LG mimicked the ability of bath-applied CCAP to weaken GPR regulation of the gastric mill rhythm. While $I_{MI\text{-}CCAP}$ was being injected into LG, GPR stimulation barely prolonged the retractor phase. The downward deflections in $I_{MI\text{-}CCAP}$ during each LG action potential resulted from the reduction in driving force as the LG membrane potential approached the reversal potential for I_{MI} (DeLong et al., 2009b). Note the increased LG burst duration during $I_{MI\text{-}CCAP}$ injection, as also occurs during CCAP bath application (Kirby and Nusbaum, 2007).

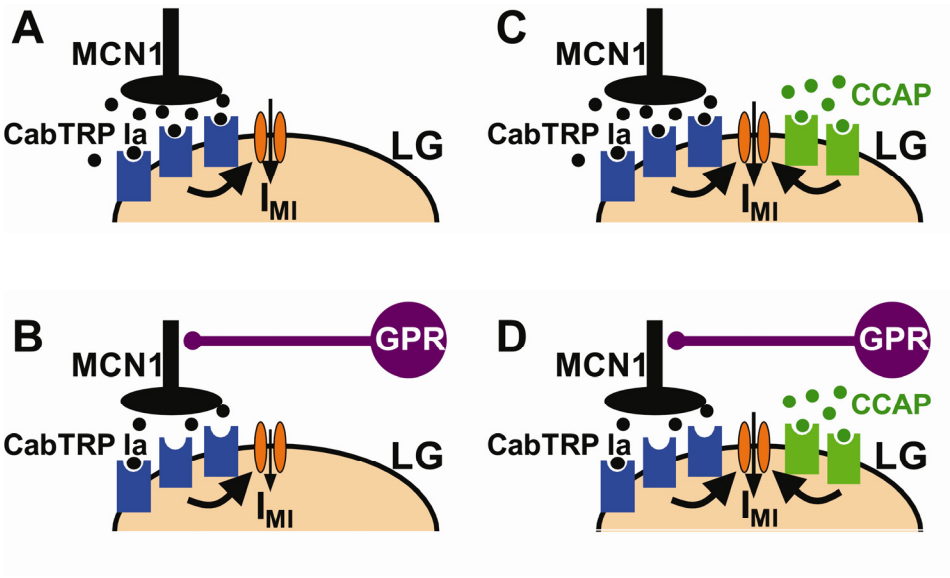

Figure 6: Summary of the mechanism by which CCAP gates out the GPR regulation of the gastric mill rhythm. *A*, During the normal gastric mill rhythm retractor phase, with no CCAP present, MCN1 released CabTRP Ia (filled black circles) binds to receptors on LG (blue geometric shapes) to activate I_{MI}. Downward pointing arrow depicts activated I_{MI}. *B*, During GPR stimulation with no CCAP present, CabTRP Ia release from MCN1 is reduced, resulting in a reduced activation of I_{MI} (note smaller size of I_{MI}-associated arrow). *C*, During the gastric mill rhythm in the presence of CCAP (filled green circles), I_{MI} in LG is activated by both MCN1-released CabTRP Ia and bath-applied CCAP. *D*, During GPR stimulation in CCAP, GPR still reduces the release of CabTRP Ia by MCN1. However, because $I_{MI\text{-}CCAP}$ in LG is not regulated by GPR activity and can compensate for the reduced amount of $I_{MI\text{-}MCN1}$, the GPR effect on I_{MI}, and hence on the gastric mill retractor phase, is reduced.

DISCUSSION

We have elucidated a mechanism by which a circulating hormone gates the effects of sensory feedback to a motor circuit. Previous work has shown that the proprioceptor neuron GPR selectively regulates the gastric mill retractor phase by reducing MCN1 release of CabTRP Ia, thereby reducing the activation of $I_{MI\text{-}MCN1}$ during retraction (Fig. 6*A,B*) (Beenhakker et al., 2005; DeLong et al., 2009a). By merging our previous computational models that explored the separate impact of GPR and CCAP on the MCN1-gastric mill rhythm, the new version of this model predicted that CCAP gates out the GPR effect on the gastric mill rhythm by providing a parallel pathway for activating I_{MI} which is MCN1-independent, and therefore not regulated by GPR. We verified this prediction of the model by demonstrating that either bath-application of CCAP or selective, dynamic clamp injection of $I_{MI\text{-}CCAP}$ into the biological LG gated out the GPR action on the gastric mill rhythm (Fig. 6).

Modulation of sensory input to a motor circuit

Sensory pathways that feed back to regulate motor circuits are modulated at the level of their transduction apparatus and/or near their CNS transmitter release sites (Rossignol et al., 2006; Blitz and Nusbaum, 2007). In some cases, the source of the presynaptic modulation is a retrograde messenger from the postsynaptic target (Glanzman, 2008). The influence of these sensory pathways is also altered by modulatory actions in the postsynaptic targets of these sensory

neurons that strengthen or weaken the sensory input (Edwards et al., 2002; Le Bon-Jego et al., 2006; Glanzman, 2008). Here we have elucidated a novel mechanism by which the influence of a sensory input is modulated. Specifically, we have demonstrated that the peptide hormone CCAP gates out the effect of the proprioceptor neuron GPR, not by a direct action on GPR or on the postsynaptic target (MCN1) by which GPR alters gastric mill CPG output, but by a circuit action downstream of the relevant GPR target. It remains possible that CCAP additionally modulates this sensorimotor pathway by influencing GPR sensitivity to muscle stretch or spike initiation, as do several other neuromodulators (Birmingham et al., 2003).

Modulating circuit dynamics to alter its sensitivity to sensory feedback

Modulation commonly causes considerable change in motor circuit output (Marder et al., 2005; Marder and Bucher, 2007; Doi and Ramirez, 2008). In contrast, the effect of CCAP on the gastric mill rhythm is modest, resulting in a 20-25% increase in protractor phase duration and no change in retractor phase duration, even when applied at high concentrations (Kirby and Nusbaum, 2007). Despite this modest effect, the same CCAP concentration markedly weakens the gastric mill circuit responsiveness to a sensory input (GPR). This illustrates the principle that the modulatory state of a motor circuit can be altered without causing a substantial change in the motor pattern generated. The resulting, latent changes in circuit configuration can nonetheless mediate altered responsiveness to extrinsic inputs.

More broadly, this study serves as a cautionary example against inferring conserved circuit dynamics on the basis of motor output. Previous studies have demonstrated that different circuit dynamics can produce similar motor outputs (Prinz et al., 2004; Saideman et al., 2007b; Grashow et al., 2009) . This study extends this concept to include sensorimotor integration. Although the versions of the gastric mill rhythm in the presence and absence of CCAP are qualitatively similar, they are mediated by different circuit dynamics which cause them to respond differently to input from GPR. Thus the similarity of two motor patterns can conceal different underlying circuit dynamics that cause them to respond differently to extrinsic influences.

REFERENCES

Bartos M, Manor Y, Nadim F, Marder E, Nusbaum MP (1999) Coordination of fast and slow rhythmic neuronal circuits. J Neurosci 19:6650-60.

Bartos M, Nusbaum MP (1997) Intercircuit control of motor pattern modulation by presynaptic inhibition. J Neurosci 17:2247-2256.

Beenhakker MP, DeLong ND, Saideman SR, Nadim F, Nusbaum MP (2005) Proprioceptor regulation of motor circuit activity by presynaptic inhibition of a modulatory projection neuron. J Neurosci 25:8794-806.

Beenhakker MP, Kirby MS, Nusbaum MP (2007) Mechanosensory gating of proprioceptor input to modulatory projection neurons. J Neurosci 27:14308-16.

Beenhakker MP, Nusbaum MP (2004) Mechanosensory activation of a motor circuit by coactivation of two projection neurons. J Neurosci 24:6741-50.

Blitz DM, Christie AE, Coleman MJ, Norris BJ, Marder E, Nusbaum MP (1999) Different proctolin neurons elicit distinct motor patterns from a multifunctional neuronal network. J Neurosci 19:5449-63.

Blitz DM, Nusbaum MP (2007) Mechanosensory regulation of invertebrate motor systems. In: Invertebrate Neurobiology (eds: G. North and G. R.J.), pps 185-208. Cold Spring Harbor Laboratory Press: NY.

Buschges A, Akay T, Gabriel JP, Schmidt J (2008) Organizing network action for locomotion: insights from studying insect walking. Brain Res Rev 57:162-71.

Chen R, Ma M, Hui L, Zhang J, Li L (2009) Measurement of neuropeptides in crustacean hemolymph via MALDI mass spectrometry. J Am Soc Mass Spectrom 20:708-18.

Christie A, Baldwin D, Turrigiano G, Graubard K, Marder E (1995) Immunocytochemical localization of multiple cholecystokinin-like peptides in the stomastogastric nervous system of the crab Cancer borealis. J Exp Biol 198:263-71.

Coleman MJ, Meyrand P, Nusbaum MP (1995) A switch between two modes of synaptic transmission mediated by presynaptic inhibition. Nature 378:502-5.

DeLong ND, Beenhakker MP, Nusbaum MP (2009a) Selective Inhibition of Peptidergic Cotransmission Underlies Sensorimotor Integration in a Small Motor System. Submitted.

DeLong ND, Kirby MS, Blitz DM, Nusbaum MP (2009b) Parallel Regulation of a Modulator-Activated Current Underlies Metamodulation of Motor Circuit Output. J Neurosci, In Press.

Dickinson PS (2006) Neuromodulation of central pattern generators in invertebrates and vertebrates. Curr Opin Neurobiol 16:604-14.

Doi A, Ramirez JM (2008) Neuromodulation and the orchestration of the respiratory rhythm. Respir Physiol Neurobiol 164:96-104.

Edwards DH, Yeh SR, Musolf BE, Antonsen BL, Krasne FB (2002) Metamodulation of the crayfish escape circuit. Brain Behav Evol 60:360-9.

Glanzman DL (2008) New tricks for an old slug: the critical role of postsynaptic mechanisms in learning and memory in Aplysia. Prog Brain Res 169:277-92.

Grashow R, Brookings T, Marder E (2009) Reliable neuromodulation from circuits with variable underlying structure. Proc Natl Acad Sci U S A 106:11742-6.

Katz PS, Eigg MH, Harris-Warrick RM (1989) Serotonergic/cholinergic muscle receptor cells in the crab stomatogastric nervous system. I. Identification and characterization of the gastropyloric receptor cells. J Neurophysiol 62:558-70.

Kirby MS, Nusbaum MP (2007) Peptide hormone modulation of a neuronally modulated motor circuit. J Neurophysiol 98:3206-20.

Le Bon-Jego M, Masante-Roca I, Cattaert D (2006) State-dependent regulation of sensory-motor transmission: role of muscarinic receptors in sensory-motor integration in the crayfish walking system. Eur J Neurosci 23:1283-300.

Li L, Kelley WP, Billimoria CP, Christie AE, Pulver SR, Sweedler JV, Marder E (2003) Mass spectrometric investigation of the neuropeptide complement and release in the pericardial organs of the crab, Cancer borealis. J Neurochem 87:642-56.

Marder E, Bucher D (2007) Understanding circuit dynamics using the stomatogastric nervous system of lobsters and crabs. Annu Rev Physiol. 69:291-316.

Marder E, Bucher D, Schulz DJ, Taylor AL (2005) Invertebrate central pattern generation moves along. Curr Biol 15:R685-99.

McLean DL, Sillar KT (2004) Metamodulation of a spinal locomotor network by nitric oxide. J Neurosci 24:9561-71.

Nadim F, Manor Y, Nusbaum MP, Marder E (1998) Frequency regulation of a slow rhythm by a fast periodic input. J Neurosci 18:5053-67.

Nusbaum MP, Beenhakker MP (2002) A small-systems approach to motor pattern generation. Nature 417:343-50.

Pearson KG (2008) Role of sensory feedback in the control of stance duration in walking cats. Brain Res Rev 57:222-7.

Prinz AA, Bucher D, Marder E (2004) Similar network activity from disparate circuit parameters. Nat Neurosci 7:1345-52.

Rossignol S, Dubuc R, Gossard JP (2006) Dynamic sensorimotor interactions in locomotion. Physiol Rev 86:89-154.

Saideman SR, Blitz DM, Nusbaum MP (2007b) Convergent motor patterns from divergent circuits. J Neurosci 27:6664-74.

Sharp AA, O'Neil MB, Abbott LF, Marder E (1993) The dynamic clamp: artificial conductances in biological neurons. Trends Neurosci 16:389-94.

Weimann JM, Meyrand P, Marder E (1991) Neurons that form multiple pattern generators: identification and multiple activity patterns of gastric/pyloric neurons in the crab stomatogastric system. J Neurophysiol 65:111-22.

Chapter 7

Conclusion

My thesis work has focused on characterizing the mechanisms by which sensory input can be integrated into an ongoing rhythmic motor pattern. Specifically, I have used the gastric mill CPG for this work because of the many experimental advantages available in this system. I used a combination of computational modeling, dynamic clamp and more traditional electrophysiology techniques to investigate the mechanism by which a sensory input (GPR) regulates gastric mill output. As a result, I have uncovered several novel cellular-level mechanisms of sensorimotor integration, as well as furthering the understanding of the dynamics which underlie the generation and regulation of the gastric mill rhythm in particular and CPGs in general.

Taken together, the first three chapters of my thesis elucidate the core mechanism by which GPR regulates the gastric mill rhythm. GPR is a muscle stretch receptor which is phasically active (retractor phase) during an ongoing gastric mill rhythm (Katz et al., 1989). GPR activation during the retractor phase selectively prolongs this phase. Because the regulation of motor pattern timing by muscle-embedded proprioceptors is common in CPG-driven systems (Clarac and Cattaert, 1999; Pearson, 2004; Buschges, 2005), but the cellular mechanisms underlying the actions of such reflex loops is often not well understood, I chose to exploit the accessibility of the gastric mill system to

investigate the mechanism by which GPR regulates gastric mill output. The conclusion of these three chapters is ultimately that this regulation is accomplished by the GPR presynaptic inhibition of the projection neuron which drives the gastric mill rhythm (MCN1), and that this presynaptic inhibition selectively regulates peptidergic cotransmission while sparing the actions of the small molecule cotransmitter (GABA).

In Chapter 2 of my thesis, I participated in a collaboration to investigate the cotransmitter mechanisms by which MCN1 affects its targets in the gastric mill circuit. MCN1 elicits the gastric mill rhythm by exciting LG and Int1, the reciprocally inhibitory pair that comprise the core of the gastric mill CPG (Coleman et al., 1995). For the purposes of understanding the GPR regulation of the rhythm, the most important conclusion from this chapter was that, although MCN1 contains three cotransmitters (GABA, the peptides proctolin and CabTRP Ia) (Blitz et al., 1999), it uses only CabTRP Ia to excite the LG neuron and only GABA to excite Int1.

In Chapter 3 I undertook a series of modeling studies to determine the most likely theoretical mechanism by which GPR accomplishes its selective regulation of the gastric mill retractor phase. The models in this study predicted that GPR presynaptic inhibition of MCN1 was the most likely mechanism by which the retractor phase was selectively prolonged. I also conducted a series of dynamic clamp manipulations that supported these model predictions. In Chapter 4, I continued this work by investigating the cotransmission mechanisms

used by GPR to regulate the gastric mill rhythm, demonstrating that GPR uses a serotonergic synapse to inhibit MCN1 and regulate the gastric mill rhythm. By showing that blocking this specific serotonergic action with a 5HT receptor antagonist abolishes the GPR regulation of the gastric mill rhythm, I more firmly verified the theoretical predictions of the model from Chapter 3, which suggested that the presynaptic inhibition of MCN1 was the key GPR action for regulating the rhythm.

Given the strong evidence that GPR regulates the gastric mill retractor phase by presynaptically inhibiting MCN1, as well as the observation that MCN1 uses divergent cotransmitter mechanisms to affect its gastric mill targets, I next asked whether the GPR action on MCN1 reduced all or only a subset of the MCN1 cotransmitter actions. In the second half of Chapter 4, therefore, I investigated this issue and determined that GPR selectively reduces the MCN1 CabTRP Ia actions on LG, while sparing the MCN1 GABAergic excitation of Int1. Furthermore, this selective regulation of cotransmission was critical to the GPR regulation of the gastric mill rhythm, since experiments in both our computational model and the biological preparation showed that a GPR reduction in MCN1 excitation of Int1 would prevent the normal GPR effect on the rhythm.

Once the core mechanism of the GPR action on the gastric mill rhythm was determined, I next asked how the actions of GPR could be modulated. There are numerous examples in the literature of the modulation of the actions of a sensory input to a CPG (Buschges and El Manira, 1998; Clarac and Cattaert,

1999), but as above, a cellular-level understanding of the mechanisms involved is often absent. Therefore, in Chapters 5 and 6, I investigated the mechanism by which a peptide hormone (CCAP) modulates the gastric mill rhythm, and then extended that work to determine the mechanism by which the same hormone gates the actions of GPR on the gastric mill rhythm.

CCAP, which reaches STG as a circulating hormone and is therefore present at a constant concentration during the gastric mill rhythm, was shown previously to selectively prolong the protractor (LG burst) phase of the gastric mill rhythm (Kirby and Nusbaum, 2007). In Chapter 5, I investigated the mechanism of this action. The findings from this chapter were that CCAP converges to activate the same inward current in LG (I_{MI}) that is activated by MCN1-released CabTRP Ia. During the normal gastric mill rhythm, the amplitude of the MCN1-activated I_{MI} ($I_{MI\text{-}MCN1}$) in LG decays during the protraction (LG burst) phase, due to the LG presynaptic inhibition of MCN1 and the subsequent reduction in CabTRP Ia released onto LG (Coleman et al., 1995; Beenhakker et al., 2005). The CCAP-activated I_{MI} ($I_{MI\text{-}CCAP}$), on the other hand, was not subject to the same decay because it was independent of synaptic regulation by LG. As a result, a portion of the total I_{MI} did not decay during the LG burst, effectively reducing the efficacy of the LG presynaptic inhibition and increasing the protractor phase duration.

Given the above result, and the fact that the GPR regulation of the gastric mill rhythm relies on presynaptic regulation of CabTRP Ia release from MCN1, I

wondered whether CCAP might influence the GPR action on the gastric mill rhythm. In Chapter 6, I investigated this possibility and found that GPR was much less effective at prolonging the gastric mill retractor phase in the presence of CCAP. Furthermore, I used computational modeling and dynamic clamp experiments to show that, as above, this effect resulted from the convergent effect of CCAP and MCN1-released CabTRP Ia in activating I_{MI} in LG. This result provides a novel mechanism for the modulation of a sensory input to a motor circuit that does not involve any direct effects on either the sensory neuron itself or on the synaptic target by which it regulates the CPG.

These results have uncovered several novel mechanisms by which sensory regulation of CPG output can take place. In the first part of my thesis, I demonstrated a role for presynaptic inhibition of a projection neuron (MCN1) which drives CPG output in the selective regulation of one phase of a motor pattern. At the functional level, many phasic sensory inputs to CPGs participate in the control of phase duration, though the exact mechanism of that effect is often not understood (Clarac and Cattaert, 1999; Pearson, 2004; Shetreat-Klein and Cropper, 2004; Buschges, 2005). Given the ubiquity of a reciprocally inhibitory pair of neurons (half-center oscillator) driven by an external excitatory input as a mechanism for rhythm generation, other systems may well use a similar mechanism of presynaptic inhibition to selectively regulate the duration of a particular phase.

Furthermore, the revelation that such a presynaptic sensory input can

selectively regulate the release of a subset of cotransmitters by its synaptic target suggests additional degrees of freedom that are available to neural circuits during the integration of sensory information. Cotransmission is a common feature of neurons (Nusbaum et al., 2001; Seal and Edwards, 2006), and such selective regulation of cotransmission might well provide a mechanism by which sensory (and other) pathways achieve specificity in other systems as well.

Finally, the second part of my thesis describes a novel mechanism by which both the output of a CPG and the regulation of that CPG by sensory input can be modulated. In addition to describing such modulation at the cellular level, this example also demonstrates that the effect of a modulator can sometimes be partially or completely masked under some circumstances, while having a large effect under others. CCAP only modestly (~20%) prolongs the protractor phase of the gastric mill rhythm, and so has only a small effect on the timing of the rhythm overall. GPR stimulation in the presence of CCAP, however, reveals an underlying alteration in the circuit dynamics which has a large effect on the sensitivity of the rhythm to sensory input. This result supports previous studies which have suggested that varying the underlying circuit dynamics can produce similar motor outputs (Prinz et al., 2004; Saideman et al., 2007b), although these altered network states may render the system differently responsive to external stimuli.

Future Directions

To extend the above findings regarding the CCAP modulation of GPR input to the gastric mill CPG, it would be interesting to learn how other neuromodulators influence sensorimotor integration in this system. There are several other modulators that activate the same current (I_{MI}) as CCAP and CabTRP Ia (Swensen and Marder, 2000). Our results so far would predict that these substances, if they act on the LG neuron, would also alter the GPR regulation of the gastric mill rhythm. However, the nature of their effects will depend on the timing of their influence and the concentration in which they are present during the GPR-regulated rhythm. For example, if these modulators are released rhythmically by projection neurons in contrast to the tonic, hormonal presence of CCAP, they might evoke a different response from both the core gastric mill rhythm and its regulation by GPR. It might also be the case that, unlike CCAP, one or more of these other modulators strongly influences Int1 as well as or instead of LG.

Along similar lines, it would be worthwhile to explore the GPR regulation of different versions of the gastric mill rhythm. In particular, the application of *Cancer borealis* pyrokinin (CabPK) peptide to the STG elicits a version of the gastric mill rhythm that is very similar to the MCN1-elicited version, but via a distinct underlying circuit which lacks MCN1 involvement (Saideman et al., 2007b). Preliminary unpublished results from our lab show that GPR regulates this version of the gastric mill rhythm in a similar fashion to the MCN1-elicited version. Specifically, it selectively prolongs the retractor phase of the CabPK-

elicited gastric mill rhythm. It is likely, however, that this regulation relies on a distinct mechanism because the CabPK-rhythm does not involve MCN1 activation, and the GPR regulation of the MCN1-version occurs exclusively via inhibition of MCN1.

Furthermore, unlike CCAP and CabTRP Ia, the CabPK peptide does not appear to activate I_{MI} (DM Blitz, MP Nusbaum, unpublished). Therefore, it is currently unknown how modulators such as CCAP modulate the GPR effect on the CabPK-elicited gastric mill rhythm. Because my work so far has suggested that the convergence of modulators onto I_{MI} is the crucial factor for gating the GPR effect on gastric mill output, it may be that the same gating effect would not be present in the CabPK-version of the rhythm. If this hypothesis is verified, then it would present an interesting scenario in which two similar versions of a motor pattern, generated by distinct mechanisms, would be similarly regulated by sensory feedback, but by distinct circuit mechanisms that were differently susceptible to modulation.

Literature Cited

Beenhakker MP, DeLong ND, Saideman SR, Nadim F, Nusbaum MP (2005) Proprioceptor regulation of motor circuit activity by presynaptic inhibition of a modulatory projection neuron. J Neurosci 25:8794-806.

Blitz DM, Christie AE, Coleman MJ, Norris BJ, Marder E, Nusbaum MP (1999) Different proctolin neurons elicit distinct motor patterns from a multifunctional neuronal network. J Neurosci 19:5449-63.

Buschges A (2005) Sensory control and organization of neural networks mediating coordination of multisegmental organs for locomotion. J Neurophysiol 93:1127-35.

Buschges A, El Manira A (1998) Sensory pathways and their modulation in the control of locomotion. Curr Opin Neurobiol 8:733-9.

Clarac F, Cattaert D (1999) Functional multimodality of axonal tree in invertebrate neurons. J Physiol Paris 93:319-27.

Coleman MJ, Meyrand P, Nusbaum MP (1995) A switch between two modes of synaptic transmission mediated by presynaptic inhibition. Nature 378:502-5.

Katz PS, Eigg MH, Harris-Warrick RM (1989) Serotonergic/cholinergic muscle receptor cells in the crab stomatogastric nervous system. I. Identification and characterization of the gastropyloric receptor cells. J Neurophysiol 62:558-70.

Kirby MS, Nusbaum MP (2007) Peptide hormone modulation of a neuronally modulated motor circuit. J Neurophysiol 98:3206-20.

Nusbaum MP, Blitz DM, Swensen AM, Wood D, Marder E (2001) The roles of co-transmission in neural network modulation. Trends Neurosci 24:146-54.

Pearson KG (2004) Generating the walking gait: role of sensory feedback. Prog Brain Res 143:123-9.

Prinz AA, Bucher D, Marder E (2004) Similar network activity from disparate circuit parameters. Nat Neurosci 7:1345-52.

Saideman SR, Blitz DM, Nusbaum MP (2007b) Convergent motor patterns from divergent circuits. J Neurosci 27:6664-74.

Seal RP, Edwards RH (2006) Functional implications of neurotransmitter co-release: glutamate and GABA share the load. Curr Opin Pharmacol 6:114-9.

Shetreat-Klein AN, Cropper EC (2004) Afferent-induced changes in rhythmic motor programs in the feeding circuitry of aplysia. J Neurophysiol 92:2312-22.

Swensen AM, Marder E (2000) Multiple peptides converge to activate the same voltage-dependent current in a central pattern-generating circuit. J Neurosci 20:6752-9.